A Quantitative Analysis of the Contribution of Costimulation to T Cell Activation by the T cell Receptor and Chimeric Antigen Receptors



Ashna B. Patel

Dunn School of Pathology

University of Oxford

This dissertation is submitted for the degree of

Doctor of Philosophy

Balliol College

April 2023

For my grandparents,

Jashodaben, Bhailalbhai, Ghanshyambhai & Vimlaben,

who bravely crossed oceans for their families.

For my parents,

Bharat & Kalpana,

whose sacrifices meant I could freely pursue my own interests,

and for my brother,

Salil,

who always encouraged me to be curious about the world around me.

Acknowledgements

I am deeply grateful for the support that has made my DPhil journey such a fulfilling and rewarding experience, despite the many challenges encountered along the way.

First and foremost I would like to thank my supervisor, Omer Dushek, for his invaluable support, encouragement and expertise. Omer's patient guidance and mentorship have not only enriched my scientific knowledge and skillset but also instilled in me the confidence to navigate through the complex world of molecular immunology. His generosity with his time, diligence in providing feedback, and empathy shown towards his students has fostered an incredibly supportive research group.

I am also thankful to all members of the Dushek and Van de Merwe research groups for their invaluable contributions and insightful discussions over the years.
Johannes first helped familiarise me with the laboratory skills used in this thesis, whilst Mike helped manage the lab during the challenges of various COVID-19 lockdowns, and Misha (Mikhail) generously lent his biochemistry expertise for protein production and purification. Violaine provided admirable levels of optimism and reassurance despite my many experimental mishaps, Jake was always ready for a supportive chat over a cup of tea, and Anna has been a valuable, fellow coffee enthusiast, whose scientific rigour I admire, and whose continued friendship I am grateful for.

This work would not be possible without the funding and support provided by the BBSRC Interdisciplinary Bioscience DTP. I am also grateful to the Sir William Dunn School of Pathology who provided support through the many challenges posed by the pandemic, and all the administration staff that enabled research to continue throughout.

In addition, thank you to Anton Van der Merwe for generously sharing his immunology expertise over many lab meetings and journal clubs, my second supervisor Mike Dustin, who provided invaluable scientific feedback (especially for the CombiCell project), and my DPhil examiners Prof. Gilian Griffiths and Prof. Simon Davies for agreeing to assess this thesis.

To all my friends who have made my time at Oxford such an enjoyable experience. Xanita, Mae, Frances, Laura, Ellie and Juba - thank you for the many coffees, walks, chats and meals that have helped me through this degree. To Luke, I am so grateful for your patience and support during the final stages of writing.

Lastly, to my family, thank you for your unwavering encouragement and sacrifices throughout all stages of my education, that has ultimately culminated in this work.

Contributions

Like all scientific research, this work is a highly collaborative effort that would not have been possible without the valuable contributions of numerous individuals. The Dushek lab has offered me incredible support throughout my DPhil, allowing me to develop my own approach to scientific inquiry, as well helping out practically with all the tasks associated with primary T cell culture including isolation, transduction and maintenance. Specific data contributions include **Eleanor Denham** who designed and initially expressed all SpyCatcher constructs on CHO cells and produced SpyTag-mCLOVER3. **Johannes Pettmann** who conducted the ICAM-1 CRISPR knockout and subsequent SpyCatcher transduction and selection of CHO cells. **Mikhail Kutuzov** purified all the ligands used, and generated pMHC refolds. **Alexander Mørch** conducted Fluorescence Correlation Spectroscopy of SpyCatcher with the help of the Wolfson Imaging Center at the MRC Weatherall Institute of Molecular Medicine, University of Oxford. **Michael Barton** who helped produce SpyTag-ligands and **Jake Burton** who helped with production and use of CAR constructs.

Abstract

T cells are important immune cells that become activated to respond when they recognise antigen. T cell activation can be initiated by the engagement of the T cell receptor (TCR) with antigens presented by major histocompatibility complex (pMHC) molecules on antigen-presenting cells (APCs). In addition to the TCR, T cells express an array of costimulatory receptors that deliver activatory signals upon engagement with their ligands expressed on APCs. Despite extensive molecular studies highlighting their structural and signalling diversity, it remains unclear whether these receptors are functionally redundant or exhibit unique roles in shaping T cell responses. In this study, we systematically assess the quantitative impact of three well-established costimulatory receptors, CD2, LFA-1, and CD28, on specific T cell phenotypes: antigen adaptation, antigen efficacy, and antigen sensitivity. Given the implementation of costimulation in clinically relevant Chimeric Antigen Receptors (CARs), we also assess the impact of these costimulatory receptors within CAR-T cells. Using primary $CD8^+$ T cells presented with antigen and purified ligands against these costimulatory receptors, we find that CD2 and LFA-1 can prevent T cells from adapting to antigen over time, and that CARs, incorporating an intrinsic CD28 costimulatory domain can override adaptation, independent of extrinsic costimulation. We also find that CD2 and LFA-1 are able to enhance the sensitivity of T cells to antigen by~250-fold, whilst CD28 has minimal impact on antigen

sensitivity. Notably, these conclusions are reproduced in a novel experimental platform, CombiCell, that enables the titration of purified, folded ligand directly onto the surface of cells. Taken together, our results demonstrate that CD2, LFA-1 and CD28 exhibit distinct quantitative impacts on $CD8^+$ T cell and CAR-T cell activation, and these findings have important implications for the effective implementation of costimulation in CAR-T cell immunotherapy.

Contents

1 Introduction **1**

1.1 The Immune System 2

1.2 The Adaptive Immune System 2

1.3 The T Cell Receptor 7

1.4 Functional Outcomes of T Cell Activation 13

1.5 T Cell Costimulatory Receptors 16

1.6 Therapeutic Importance of Costimulation 31

1.7 Chimeric Antigen Receptors 31

1.8 Quantitative Phenotypes 39

1.9 This Thesis 41

2 The Impact of Costimulation on Antigen Adaptation by TCRs & CARs **43**

2.1 Introduction 44

2.2 Results 49

2.3 Discussion 70

3 The Effect of Costimulatory Receptors on T Cell Sensitivity to Antigen 77

3.1 Introduction 78

3.2 Results 81

3.3 Discussion 92

4 A Cellular System to study T Cell-APC Interactions using SpyCatcher / SpyTag 97

4.1 Introduction 98

4.2 Results 101

4.3 Discussion 155

5 Discussion 163

5.1 Summary 164

5.2 Implications of Findings 166

5.3 Future Directions 170

5.4 Conclusions 172

6 Materials & Methods 175

6.1 Reagents 176

6.2 Experimental Methods 181

6.3 Sequences 191

6.4 Data Analysis 195

Bibliography 197

Chapter 1

Introduction

1.1 The Immune System

Every day, we encounter numerous microorganisms that have the potential to harm us, posing a continuous threat of infection. In response our immune system has evolved an intricate set of defense mechanisms to safeguard us from persistent pathogenic challenge. These mechanisms range from physical barriers like the skin, to the innate immune system that offers rapid protection against conserved structures of pathogens and finally, to the adaptive immune system that has evolved in vertebrates to confer a specific response to pathogens [1].

1.2 The Adaptive Immune System

When the initial innate immune responses are inadequate in preventing infection, the adaptive immune system is triggered, orchestrating a more specific host response that offers enduring protection. Remarkably, the adaptive immune system is able to identify and respond specifically to unknown pathogens, for which it has not evolved prior recognition. Unlike the innate immune system that can be rapidly activated within minutes, our adaptive immune system requires several days to develop, but provides a distinct advantage by directing specific immune responses towards invading pathogens whilst also importantly providing durable protection. Indeed, upon subsequent encounters with the same antigen (any substance that elicits an adaptive immune response), immune cells can be reactivated to rapidly carry out effector functions. This elicits a more effective immune response against specific pathogens upon re-challenge, with immunological memory lasting decades after initial exposure and often resulting in life-long protection [2].

1.2.1 B Cells & T Cells: Orchestrators of Adaptive Immunity

The adaptive immune response is orchestrated by two distinct immune cells - B lymphocytes (B cells), which initiate antibody-mediated responses, and T lymphocytes (T cells), which provide B cells with support and can directly neutralize (kill) infected cells. Both branches of adaptive immunity generate antigen-specific responses through specialized receptors, called the B-cell Receptor (BCR) and the T-cell Receptor (TCR) [2]. B cells recognize antigens and stimulate the production of antibodies that can bind directly to antigens, triggering various effector responses, including direct compromise of the target surface (via complement), and activation of antibody-dependent cellular cytotoxicity (ADCC) through innate immune cells like macrophages and neutrophils.

T cells undergo maturation in the thymus after their development in the bone marrow. T cells are unable to directly recognize antigens. Instead, they detect short peptide fragments, derived from proteolytic processing of antigens, that are bound to major histocompatibility complex (MHC) molecules. These peptide-MHC (pMHC) complexes are subsequently transported to the cell surface where they mediate recognition by T cells. This process of antigen presentation by pMHC molecules takes place in nearly all cells in the body and cells capable of presenting antigen to T cells are referred to as Antigen Presenting Cells (APCs). T cells employ their surface T cell receptors (TCRs) to specifically bind and recognize pMHC antigens thereby activating their effector functions. This recognition is critical as it enables T cells to identify and eliminate pathogenic microorganisms that predominantly reside within the intracellular environment and cannot be targeted by antibodies produced by B cells.

Dendritic cells (DCs) are specialized antigen-presenting cells (APCs) that are widely distributed throughout various tissues. They perform the vital role of capturing antigens and presenting them on MHC (major histocompatibility complex) molecules for recognition by T cells. Specifically, $CD8^+$ T cells recognize antigens presented on MHC Class I complexes on DCs, along with costimulatory ligands, leading to their activation and differentiation into effector cells. Similarly, $CD4^+$ T cells differentiate into T helper cells that mediate the activation of various other immune cells such as macrophages, B cells, and $CD8^+$ T cells through the release of cytokines. These activated effector cells exhibit robust cytotoxic activity, enabling them to selectively target and eliminate infected or cancerous cells.

1.2.2 Major T cell Subsets

The human immune system contains two distinct types of T cells, which are classified based on their expression of the CD4 or CD8 co-receptor [3]. These T cells recognise different major histocompatibility complex (MHC) molecules, which are important for presenting antigens to the immune system.

$CD4^+$ T cells recognise exogenous peptides that have been processed and presented on MHC class II proteins, which are expressed on the surface of antigen-presenting cells such as dendritic cells, macrophages, and B cells. In contrast, $CD8^+$ T cells recognise endogenous peptides that are produced within the cell and presented on MHC class I proteins, expressed on the surface of most cells.

These two distinct T cell subsets are therefore associated with different functional profiles. $CD4^+$ T cells play a ”helper” role in the immune response, stimulating and regulating the activities of other immune cells, such as B cells, macrophages and

$CD8^+$ T cells. In contrast, $CD8^+$ T cells have ”effector” functions and are capable of directly killing infected or cancerous cells. Importantly, MHC class I is expressed on all nucleated cells, allowing $CD8^+$ T cells to target any cell that has become infected or transformed into a cancerous cell [4, 5]. On the other hand, $CD4^+$ T cells target extracellular pathogens through MHC class II molecules. The immune system can therefore utilise these different T cell subsets to tailor immune responses against different malignancies according to their specific molecular and cellular characteristics.

1.2.3 $CD8^+$ T Cells

Upon intial antigen encounter of pMHC on APCs, naïve $CD8^+$ T cells undergo clonal expansion and differentiation into cytotoxic T lymphocytes (CTLs) that possess the ability to directly kill infected cells via the release of perforin and granzymes. Additionally, these CTLs produce pro-inflammatory cytokines such as interferon gamma (IFN-γ), tumor necrosis factor alpha (TNF-α), and interleukin 2 (IL-2), which play important roles in coordinating and amplifying the immune response. [6].

Depending on the extent of stimulation during initial antigen encounter, naïve T cells can also differentiate into memory T cells; long-lived cells that retain the capacity to recognize and respond to the same antigen upon re-exposure [7]. After the clearance of an infection, a subset of CTLs mature into memory $CD8^+$ T cells. Upon subsequent infection by the same pathogen, these cells can proliferate and differentiate into secondary effector $CD8^+$ T cells. This immunological memory equips T cells with an accelerated and more potent immune response, providing enhanced protection against future infections [8].

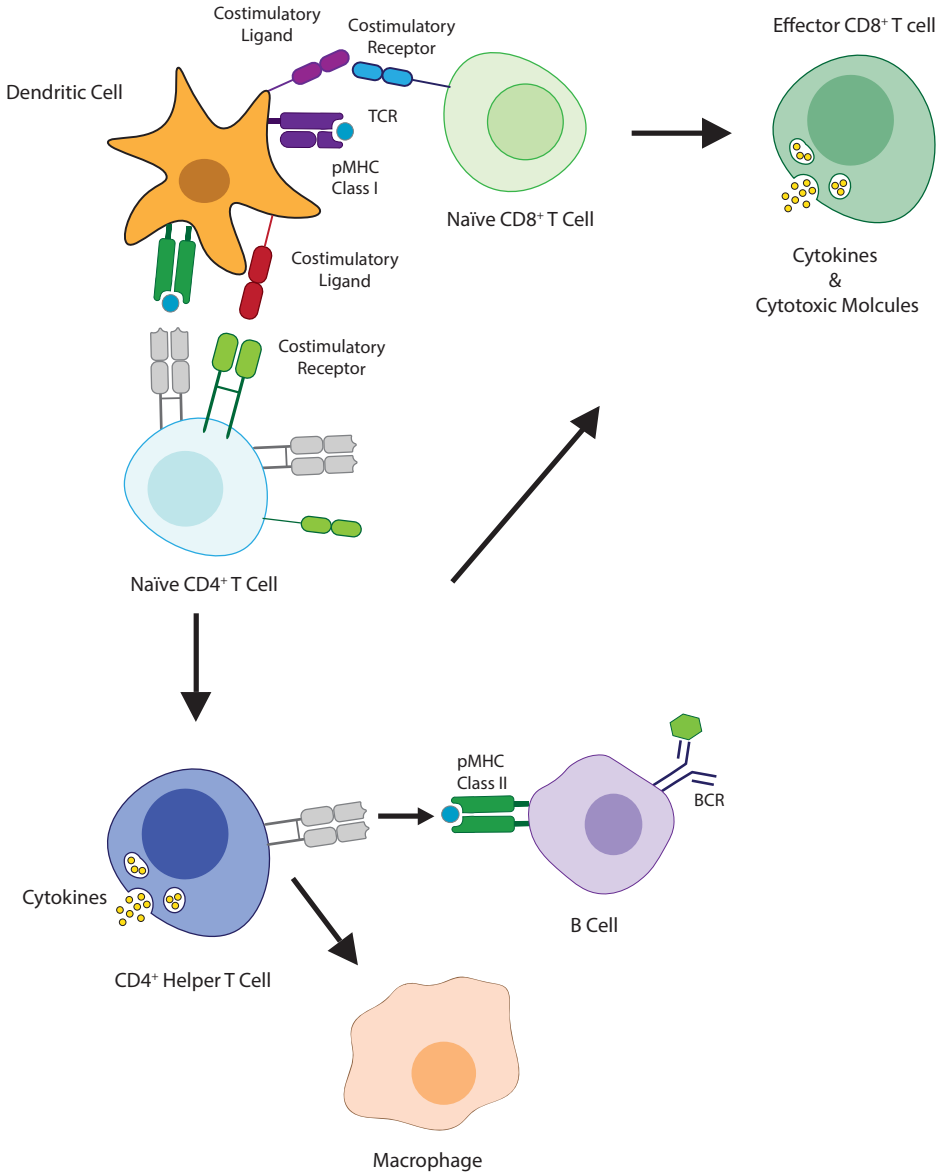


Figure 1.1: Cells of the Adaptive Immune System Collectively Mediate Anti-Viral Activity Antigen presented as pMHC on Dendritic Cells (DCs) are recognised by $CD4^+$ and $CD8^+$ T cells. Specifically, naïve $CD8^+$ T cells recognize antigens presented on MHC Class I complexes on DCs, in conjunction with costimulatory ligands, leading to their activation and differentiation into effector cells. Naïve $CD4^+$ T cells differentiate into T helper cells, which facilitates the activation of various immune cells such as macrophages, B cells, and $CD8^+$ T cells, whilst also secreting cytokines.

1.3 The T Cell Receptor

1.3.1 TCR Diversity

Each T cell expresses a clonotypic T cell receptor (TCR) on its surface, which is generated during T cell development in the thymus. The TCR consists of two chains: the alpha chain and the beta chain, which are each composed of variable (V), diversity (D) and joining (J) gene segments that undergo somatic recombination during T cell development. This process generates a diverse array of TCRs that can recognise a wide range of antigens.

Due to the random nature of TCR generation, the number of unique TCRs within a single human has been estimated to be on the order of 10^8 [9]. This vast diversity of TCRs is thought to be critical in allowing the T cell repertoire to collectively recognise the universe of potential pathogen-derived pMHC molecules.

This high degree of TCR diversity enables the immune system to mount effective responses against a vast array of pathogens and to rapidly adapt to new and emerging infectious agents. Additionally, the diversity of TCRs allows the immune system to discriminate between self and non-self antigens, preventing the activation of autoreactive T cells and the development of autoimmune diseases. The ability of the immune system to generate such a large and diverse repertoire of TCRs underscores the remarkable complexity and sophistication of the human immune system.

1.3.2 TCR Structure

The TCR is composed of a heterodimer of two polypeptide chains linked via a disulphide bridge. In humans most TCRs include an α chain and β chain (conventional $\alpha\beta$ T cells), with a subset of T cells expressing $\gamma\delta$ TCRs. Both chains of the TCR form the antigen binding site that is responsible for antigen specificity. As a result of somatic rearrangement coupled to random insertions and deletions at the $\alpha\beta$ locus during T cell development, the TCR exhibits hypervariability at the antigen binding site. This process means the number of α and β chains that a T cell could produce far exceeds the number of genes found in humans. [1].

The TCR$\alpha\beta$ heterodimer itself has no signalling capacity and is associated with 6 signalling chains at the cell surface: a dimer of a CD3γ and CD3ϵ chain and a dimer of CD3δ and CD3ϵ (collectively referred to as CD3), with an additional, separately encoded intracellular signalling homodimer called ζ chain (sometimes referred to as CD247) [10]. The CD3 chains each have negatively charged acidic residues in their transmembrane regions that interact with the positively charged $\alpha\beta$ heterodimer, stabilising the complex. In addition, the $\alpha\beta$ TCR heterodimer cannot be expressed without CD3, with the ζ chain conferring optimal expression and signalling. Therefore, the TCR consists of the assembly of eight membrane-associated proteins, that collectively enable the TCR to be expressed, recognise antigen and induce subsequent intracellular signalling upon antigen recognition.

1.3.3 TCR Signalling

TCR signalling through the CD3 complex and ζ chains originates from immunoreceptor tyrosine-based activation motifs (ITAMs) situated in their intracellular tails.

The tyrosine residues within ITAMs are phosphorylated upon antigen recognition by Src-family kinases Lck and Fyn, creating binding sites for zeta-chain-associated protein kinase 70 (ZAP-70) [11]. Once bound to the TCR ITAMs,ZAP-70 is phosphorylated on four tyrosines [12], which enhances the protein's catalytic activity. This highly active form of membrane-recruited ZAP-70 phosphorylates multiple tyrosines on the membrane adaptor, Linker for activation of T cells (LAT) and SLP-76. LAT is a scaffold protein that provides docking sites for a variety of adaptor and signalling proteins. In this way the LAT signalosome acts as an amplifier of initial TCR proximal signalling, resulting in the eventual activation of several transcription factors: NFAT (nuclear factor of activated T cells), NFκB (nuclear factor κ) and AP-1 (activating protein 1). These molecules are key orchestraters of T cell effector functions [13], coupling TCR proximal signalling to changes in gene expression. NFAT, NFκB and AP-1 activation results in a broad range of phenotypic changes in the expression of cell surface molecules like CD69, that retains T cells within lymph nodes and 4-1BB, that makes T cells receptive to costimulation, inducing cellular proliferation, producing inflammatory cytokines [11] and potentially enhanced cytotoxic function [14], directing the outcome of the immune response. The precise functional outcome of T cell signalling depends on various factors including the T cell subset, cytokine environment and costimulatory signals (see section 1.5).

TCR signalling is rapidly reversed upon antigen dissociation from the TCR, as recently demonstrated by optogentic studies that allow direct control over receptor-ligand binding half life [15, 16]. The reversibility of TCR signalling is consistent with the activity of membrane phosphatases, such as CD45, which are consituitively active and are known to remove phosphate groups from TCR signalling molecules.

CD45 dephosphorylates the C-terminal tail of Lck, which is normally in a closed conformation that inhibits its activity. This CD45-mediated dephosphorylation results in the active, open conformation of Lck. Conversely, Csk opposes the activity of CD45 by stabilizing the closed, inactive conformation of Lck. The activity of Lck is tightly regulated, with mature T cells having a basal level of active Lck that phosphorylates CD3ζ, setting a threshold for T cell activation [13].

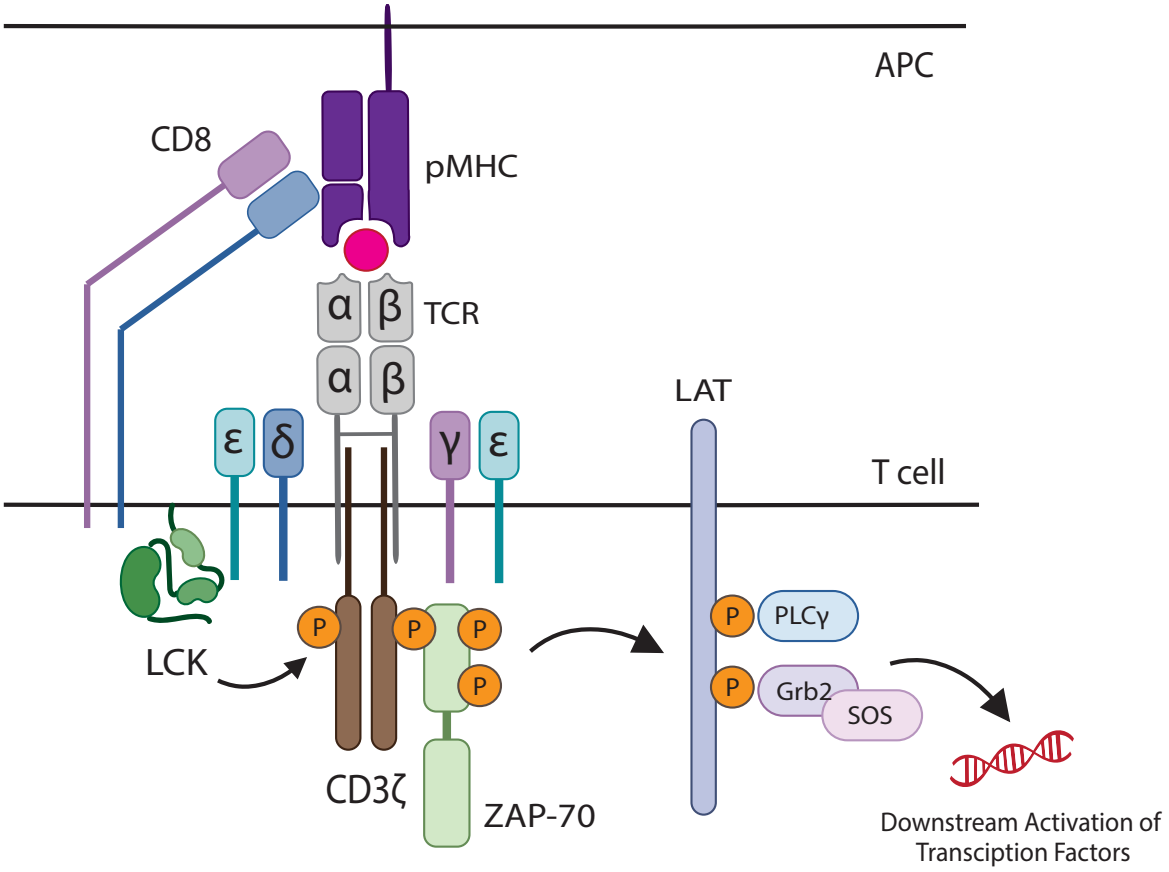


Figure 1.2: TCR Structure and Signal Initiation The $\alpha\beta$ TCR comprises of a $\alpha\beta$ heterodimer associated with 6 CD3 signalling chains; a $\epsilon\delta$ dimer and a $\gamma\epsilon$ dimer and a CD3ζ homodimer. Furthermore, $CD8^+$ T cells express the CD8 heterodimeric coreceptor that binds MHC class I molecules. Upon engagement of the $\alpha\beta$ heterodimer with the peptide-MHC complex expressed on APCs, ITAMs located on the cytoplasmic domain of the ζ chain are phosphorylated by proximal Lck. ZAP-70 can then bind the TCR ITAMS, which then is activated and phosphoralytes the LAT scaffold protein. this creates docking sites for a number of adaptor and signalling molecules such as PLCγ, Grb2 and SOS, that propagate TCR signalling, leading to the eventual activation of transcriptional programs.

1.3.4 TCR Triggering

How exactly the TCR is able to convert pMHC binding into ITAM phosphorylation and subsequent signalling remains unclear. Several models have been proposed to explain TCR triggering at the molecular level.

1. Conformational Change

As other receptors such as G-Protein coupled receptors exhibit structural changes upon ligand binding, that induce different conformations or stabilise one equilibrium state leading to downstream signalling, the TCR has been proposed to elicit signalling in the same way. However, a recently resolved structure of the complete TCR/CD3 structure provided evidence against this model of TCR triggering as no conformational change was observed when the structure was compared to that when pMHC is bound [17], with a subsequent cryo-EM study of a fully assembled, pMHC-bound TCR complex showing the receptor is largely unchanged upon ligand binding [18].

Structural work, however, cannot rule out conformational changes that would be induced by molecular forces. There is experimental evidence that T cells generate forces during the process of antigen recognition [19] and therefore it is conceivable that molecular forces are necessary to induce a conformational change necessary for TCR triggering. However, T cell activation through the TCR has been observed to take place without any detectable forces [20] and even without ligands [21].

3. Receptor Aggregation

Given that crosslinking of the TCR can induce TCR signalling, aggregation of the TCR has been suggested to be the triggering mechanism. However, it is difficult to

understand how few (or even a single) pMHC can activate T cells [22] in the context of receptor aggregation.

4. Kinetic Segregation

Kinetic Segregation explains TCR triggering on the basis of changes in the relative kinase and phosphatase activities that regulate TCR phosphorylation.

In a resting T cell with unligated TCRs, membrane-associated kinases such as Lck, and phosphatases such as CD45, are active and constitutively phosphorylate and dephosphorylate ITAMs on the TCR. The net phosphorylation resulting from these activities on the TCR remains below a threshold needed for signalling to be initiated.

Upon T cell contact with an APC, an area of close-contact is formed between the cell membranes that is stabilised by short receptor/ligand interactions (e.g. the adhesion receptor CD2 on T cells binding the ligand CD58 on the target cell). Larger molecules such as CD45 are excluded from these close contacts. Given that the close contact is required for TCR to bind its pMHC ligand, bound TCR are found only within these regions of the cell membrane and TCRs that do not bind ligand diffuse out of these regions where they are rapidly dephosphorylated. As a result of the exclusion of CD45 from these regions, the bound TCR experiences an increase in the net kinase activity which induces phosphorylation and downstream signalling through the activation and recruitment of ZAP-70 kinase. This segregation of the TCRs into distinct regions of the cell membrane, with differential kinase and phosphatase activities leads to the regulation of TCR phosphorylation and signalling [23].

1.4 Functional Outcomes of T Cell Activation

Following the triggering of the TCR by pMHC binding, a number of signalling pathways are initiated that culminate in a variety of different T cell responses. Collectively, these responses allow T cells to initiate, maintain and regulate immunity that can ultimately clear pathogens.

1.4.1 Cytokines

Upon activation $CD8^+$ T cells produce cytokines such as IL-2, IFN-γ and TNF-α. These collectively contribute to the execution of the cytotoxic functions of $CD8^+$ T cells, albeit through functionally distinct mechanisms.

IFN-γ

In the context of $CD8^+$ T cell activation, IFN-γ has several important functions. IFN-γ can enhance target cell recognition by upregulating components of the MHC Class I presentation pathway, increasing the number and diversity of pMHC that can be presented and by extension, the detection of infected cells by cytotoxic T cells, as well as the recruitment of other immune cells such as macrophages to sites of infection. In addition IFN-γ can also increase the expression of cytotoxic molecules such as perforin and granzymes that can induce apoptosis in target cells and enhance survival of $CD8^+$ T cells [24].

Consistent with these observations at the cellular level, *in vivo* and *in vitro* studies have shown that IFN-γ plays an important role in anti-viral and anti-tumour

immune responses. For example, *in vitro* treatment with IFN-γ can inhibit the replication of herpes simplex virus (HSV), human papillomavirus (HPV), hepatitis C virus (HCV) and human immunodeficiency virus (HIV) [25], whilst IFN-γ can also directly induce apoptosis in tumor cells [26]. Furthermore, mice deficient in IFN-γ are more susceptible to viral infection and more prone to tumor development [27, 24].

TNF-α

Like IFN-γ, TNF-α is important in mediating anti-viral responses by $CD8^+$ T cells. TNF-α can activate and promote $CD8^+$ T cell differentiation into effector T cells, enhance the expression of cytotoxic molecules and directly induce apoptosis on target cells. Furthermore, TNF-α can inhibit replication in a variety of viral contexts [28, 29]. Originally identified for its ability to directly kill tumor cells, the anti-tumor activity of TNF-α at the cellular level has been supported by the cytokine's capacity to induce immune responses, directly kill tumor cells via apoptosis and disrupt tumor vasculature [30].

IL-2

IL-2 was the first cytokine to be identified by it's function as a T cell growth factor. Upon stimulation naïve $CD8^+$ T cells undergo clonal expansion to generate large numbers of cytotoxic T cells to exert control over infection through effector functions such as IFN-γ and TNF-α production. Activated T cells also produce IL-2 themselves that acts in an autocrine fashion, sustaining their own proliferation and survival. Through numerous *in vitro* and *in vivo* studies it is clear that IL-2 is critical for

driving the expansion of both $CD4^+$ and $CD8^+$ T cells. As IL-2 is produced and consumed by T cells, it has been suggested to scale T cell responses [31, 32]. Overall, although unlike IFN-γ and TNF-α, IL-2 lacks direct cytotoxic function, it is critical in promoting and sustaining the proliferation and activity of cytotoxic T cells, thereby in amplifying effector responses [33].

Surface Protein Expression

CD69 is a lectin protein that is expressed upon T cell activation. It controls the migration and lymph-node retention patterns of T cells [34]. 4-1BB (or CD137), a member of the tumor necrosis factor receptor superfamily (TNFSRF), is a costimulatory receptor (see Section 1.5.1) induced on T cells upon activation. Upon binding the ligand 4-1BBL on the surface of other cells, 4-1BB induces a signal transduction pathway that primarily activates the transcription factor NF-κB [35]. As a result, 4-1BB can functionally amplify T cell responses induced by the TCR, such as cytokine production. Given that it requires TCR signalling for this amplification, it is known as a costimulatory receptor.

The surface expression of CD69 and 4-1BB are often used as a proxy for T cell activation. Gene expression of CD69 can be detected 30-60 minutes after T cell activation, with protein expression detected as early as 2-3 hours after stimulation [34]. On the other hand, 4-1BB surface expression peaks between 8 and 16 hours on primary human $CD8^+$ T cells [36].

1.5 T Cell Costimulatory Receptors

1.5.1 Costimulation

Although TCR engagement with pMHC is critical for T cell activation, the quality and strength of T cell responses is influenced by an array of additional receptors expressed by T cells, termed accessory receptors, that interact with their corresponding ligands on APCs. They can be broadly classified depending on whether they deliver activatory signals (costimulatory) or inhibitory signals (coinhibitory) to T cells. Costimulatory receptors can enhance T cell proliferation, cytokine secretion, cytotoxic function, memory formation or survival [35], promoting a robust and effective immune response. In contrast, coinhibitory receptors dampen T cell responses to antigen, balancing excessive immune responses.

Costimulation has historically been used to explain a cornerstone of adaptive immunity; that T cells are only activated under specific circumstances, in which non-self-antigens are detected. Although this central tolerance is developed in the thymus through the interaction with thymic APCs, as naïve T cells circulate in the peripheral lymphoid organs they may encounter self-antigens that were absent during development. Therefore, additional layers of regulation are needed to ensure T cells only react to non-self antigens in the periphery and avoid eliciting an immune response against self antigens. The "2-Signal Model" of lymphocyte activation posits that in addition to signalling via the TCR, an additional signal is provided by APCs, without which activation cannot proceed [37, 38] and induced T cells to enter an unresponsive state termed 'anergy' [39]. Professional APCs (specifically dendritic cells) therefore provide context for naïve T cell priming, via costimulatory molecules that are upregulated upon infection. This ensures immune responses under appropriate

conditions are initiated [40]. CD28 was the first molecule to be identified capable of providing this second signal. However, numerous additional costimulatory receptors have since been identified that modulate TCR signalling qualitatively and quantitatively, with limited stimulatory capacity alone. Therefore, our definition of costimulation has expanded since the identification of CD28, encompassing any receptor that modifies TCR signalling to enhance T cell activation, beyond initial antigen recognition [41–43].

Furthermore, much of our initial understanding of costimulation has been developed within the context of naïve $CD4^+$ T cells that have not experienced antigen before. In contrast, naïve $CD8^+$ T cells do not require costimulation to become activated [44] but costimulatory receptors have been found to be important in conferring optimal immune responses against viruses [45] and cancer [46] within these T cell subpopulations.

1.5.2 Costimulatory Receptor Diversity

Accessory receptors expressed by T cells are highly diverse in terms of their structure, function and expression patterns, even amongst those that deliver the same outcome upon T cell activation [47, 48]. Despite these differences, accessory receptors are often simply categorized as either being costimulatory or coinhibitory based upon their impact on T cell activation. For example, CD28, CD2 and LFA-1 are all well-established costimulatory receptors that belong to different protein families with different signalling pathways (see Table 1.1). This raises the question of whether costimulatory receptors have overlapping or possibly redundant functions, or whether individual receptors play unique roles in shaping the T cell response. Our understanding of how costimulatory receptors function is further complicated

by different interpretations as to what exactly constitutes costimulation. For example, costimulation has been described to lower T cell triggering thresholds, sustain TCR-antigen engagements, amplify TCR signalling, prolong T-cell-APC contact and shorten the time it takes for T cells to commit to activation [49]. It follows that the precise quantitative contribution of each accessory receptor to T cell responses may be different. Overall, the diversity of accessory receptors highlights the complexity of T cell costimulation and the need for further investigation to better understand their unique roles in T cell activation.

1.5.3 The CD2 Costimulatory Receptor

CD2 Structure & Ligand Binding

CD2 is a ~40kDa transmembrane protein belonging to the immunoglobulin superfamily (IgSF) of proteins and is constitutively expressed on the surface of T cells and Natural Killer (NK) cells. CD2 is also particularly enriched on memory T cells relative to naïve T cells [50]. Structurally, CD2 consists of two Ig-domains linked to a proline-rich cytoplasmic tail that is highly conserved across mammals [51].

In humans CD2 primarily binds the structurally similar CD58 (LFA-3) that also belongs to the IgSF [52] and is broadly expressed on hematopoietic and nonhematopoietic cells, including lymphocytes, endothelial cells and erythrocytes [53]. Furthermore, CD58 exist in two isoforms [54], a GPI-achored form that is localised to membrane lipid rafts and a transmembrane form that resides predominantly outside raft domains [55].

CD2-CD58 Binding

CD2 binds CD58 with a relatively low affinity (K_D = 9-22 μM), attributed to a fast off-rate [56], resulting in highly dynamic interactions that enables the TCR to 'scan' the APC surface and engage with multiple pMHC molecules. However, the presence of thousands of interacting CD2/CD58 molecules at the cell surface means that CD2 has been suggested to significantly contribute to cell-cell avidity. Notably, the surface density of CD2 on peripheral T cells has been found to be 100–190 molecules /μm^2 [57] and T cell activation has been found to enhance CD2's avidity through increases in expression and affinity [58, 59]. Taken together this means that despite low affinity, significant binding is expected to occur between CD2 and CD58. Furthermore, the GPI-anchored form of CD58, with enhanced lateral mobility, may facilitate binding in the context of low affinities by promoting accumulation of molecules at the interacting interface [23, 60], as well as permitting highly dynamic sampling of pMHCs at close contact regions, supporting antigen recognition by the T cell [56].

Functional Role of CD2 in T Cell Activation

Despite being one of the earliest T cell surface molecules to be identified, the exact role of CD2 in T cell activation is still unclear. Identified initially as a T cell adhesion molecule [61, 62], mounting evidence supports CD2's ability to facilitate T cell-APC interactions. At the molecular level, CD2/CD58 bring the T-Cell-APC membranes together prior to TCR/pMHC engagement. This intermembrane distance promotes TCR-pMHC binding, as a consequence of similar intermembrane distances between CD2/CD58 and TCR/pMHC [63]. Indeed, CD2 has been found to co-localise with the TCR in the immunological synapse [64, 65], and with other molecules, such as CD28,

that span similar distances with their ligands. Consistent with this role, elongation of the mouse ligand for CD2, CD48 (that spans the same length as CD58), reduces binding and inhibits T cell activation [66].

In addition to functioning as an adhesion molecule, CD2 also elicits intracellular signalling that enhances T cell activation. Early studies described CD2 as a costimulatory receptor based upon results showing that the crosslinking of CD2 with monoclonal antibodies enhanced TCR signalling and these changes were dependent upon CD2's highly conserved, proline-rich cytoplasmic tail [61, 67–72]. Later studies using physiological human ligand (membrane-bound CD58), found that CD2 engagement induced T cell signalling [73]. Although the cytoplasmic tail of CD2 has no intrinsic enzymatic activity, it's proline rich regions are associated with the Lck and Fyn kinases [70], CD2AP [74] CD2BP1, [75], CD2BP2 and CD2BP3 [76] adaptor proteins to propagate intracellular signalling. Furthermore CD2 signalling has been shown to be partly dependent on the CD3ζ chain [77, 78]. Participants of CD2 signalling include CD3ζ [77, 79, 80], Lck [81], Fyn [82] and LAT [73, 83], ultimately leading to the downstream activation of MAPK-Erk pathway [83, 84]. More recent analysis of the CD2 signalling phosphoproteome has validated the participation of these molecules in $CD8^+$ T cell activation and cytolytic activity [85]. Furthermore, CD58 signalling augments effector function of cytotoxic $CD8^+$ T cells, that includes secretion of IL-2, TNF-α, IFN-γ, proliferation and cytotoxicity, with cytokine secretion being notably higher than when $CD4^+$ T cells were costimulated via CD58 [86]. Taken together, CD2 is an established costimulatory receptor with adhesion and signal amplification roles that can increase T cell activation.

The Function of CD2 in Murine Models

Despite the fundamental role proposed for CD2 in T cell activation, *in vivo* studies using knock-out mice [87–89] or blocking antibodies [90] found only a subtle impact on T cell activation. However, it was subsequently reported that differences between CD2's ligand in mice and humans make it challenging to extrapolate rodent findings to human immune function. In particular, CD48 binds to CD2 with an approximately 5-fold lower affinity than human CD58 (K_D = 60-90μM [56]), and it's expression is restricted to fewer tissues [51, 91]. Together, these results suggest that CD2 may be less important in mice compared to human T cells. Additionally, it is difficult to discern the individual role of molecules on cellular function with *in vivo* studies, as many costimulatory receptor/ligand pairs may be interacting at any given time, potentially masking any deleterious effects from gene knockout experiments.

Furthermore, CD2 is a highly conserved molecule across mammals, meaning it has undergone substantial selective pressure since divergence from a common ancestor. Therefore true redundancy is evolutionarily unlikely [92] and that the degree of conservation suggests an important role in mammalian immunity. Overall progress on understanding CD2 function in humans has been complicated by *in vivo* mice findings, but there is mounting evidence to suggest an important role of CD2 in human immunity.

The Function of CD2 in Human Cells

The CD2/CD58 axis has been found to be important in a range of biological contexts in humans. Human cytomegalovirus (HCMV) is a human virus which has recently been shown to specifically downregulate CD58 on the infected cell. This downregu-

lation has been found to impair the ability of human $CD8^+$ T cells to kill infected cells [93]. Similarly, loss of CD58 confers resistance against T cell-mediated cytolysis in tumour cells from a range of cancer types [94, 95] with genome-wide CRISPR-CAS mutagenesis screens confirming CD58 as essential for T cell effector function in tumour cells [96–98]. Additionally, CD28 is often downregulated in tumor infiltrating lymphocytes, with CD2 exhibiting strong effects on cytokine production and cytotoxicity in this context [99]. It is therefore clear that CD2 plays an important role in human immunity.

1.5.4 The LFA-1 Costimulatory Receptor

LFA-1(CD11a/CD18) is a ~120kDa heterodimeric integrin consisting of the CD11a and CD18 subunits. Although integrins are widely expressed proteins, LFA-1 is restricted to leukocytes, where it is constitutively expressed and has been proposed to exist in 3 different allosteric states, each associated with different ligand binding capacities: low, intermediate and high affinity states. Following T cell activation, low affinity LFA-1 on resting T cells can transition into the intermediate affinity state through 'inside-out' signalling by the TCR, whereby intracellular signals exert extracellular changes in LFA-1 from the low/intermediate states to the high affinity state [100]. Several ligands from the IgSF for LFA-1 have been identified, including ICAM-1, 2, 3, 4, 5 and JAM-A, however LFA-1 primarily interacts with and has the highest affinity for ICAM-1 (CD54) on activated T cells [101, 102]. ICAM-1 is a 60-114 kDa protein constitutively expressed in endothelial cells and immune cells at a low level, and is rapidly upregulated in the presence of inflammatory cytokines. LFA-1 initially has a low affinity for ICAM-1 (K_D = > 1 mM), however upon T cell activation and subsequent ligand binding this increases (to a K_D = ~0.2μM) [103, 104].

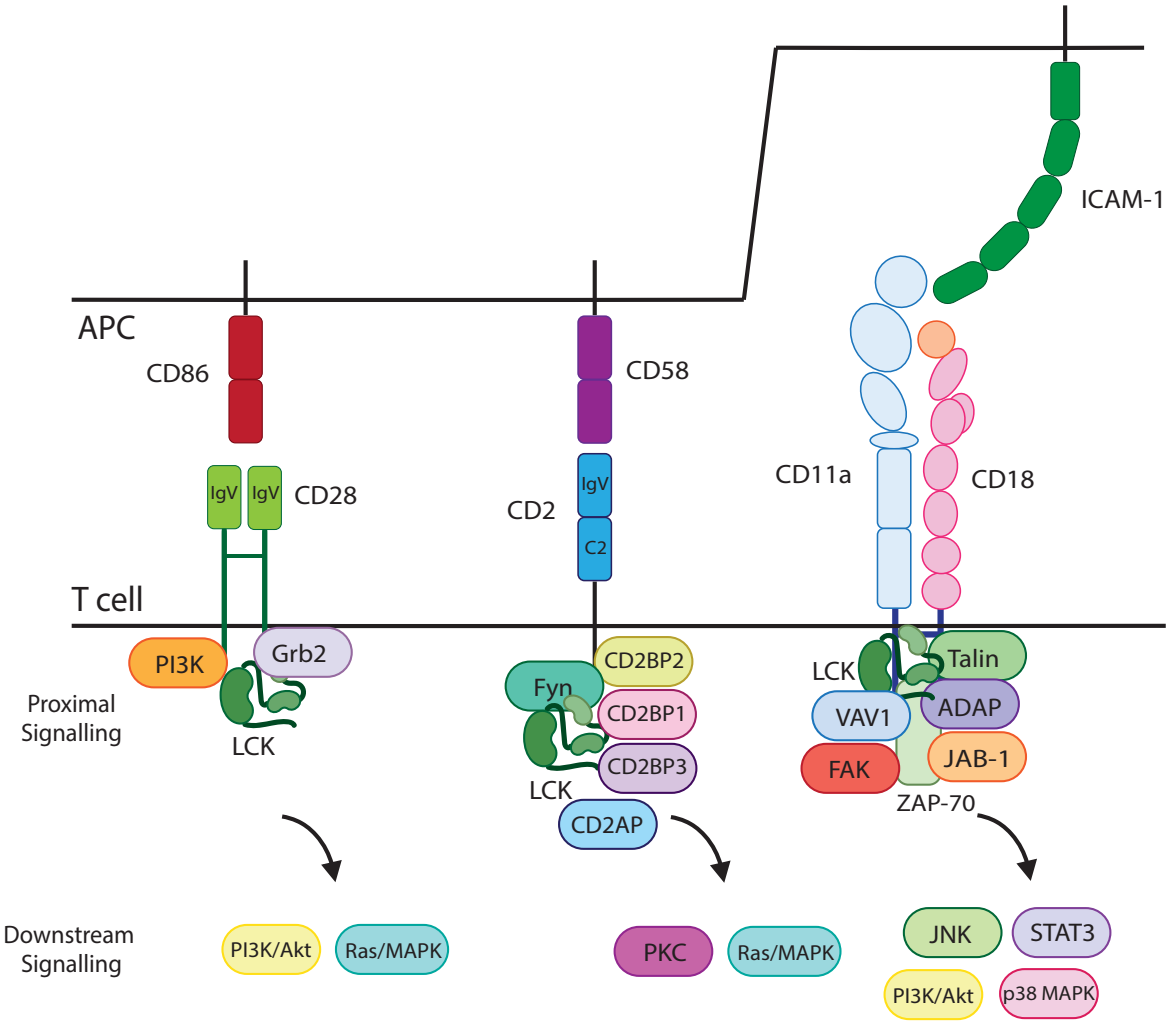


Figure 1.3: Engagement of CD2, LFA-1 and CD28 Induces Different Intracellular Signalling Pathways

A) CD28 is expressed as a homodimer of immunoglobulin variable domains (IgV), linked by a disulphide bond. Upon engagement with either CD80 or CD86 (here CD86 is shown), the cytoplasmic tail of CD28 is phosphorylated by kinases such as Lck, that then allows proteins such as PI3K and Grb2 to bind CD28. This leads to the downstream activation of the PI3K/AKT and Ras/MAPK pathways.

B) CD2 is composed of 2 Ig domains (IgV and IgC2), linked to a proline-rich cytoplasmic tail and binds CD58. CD2's cytoplasmic tail has no intrinsic enzymatic activity but interacts with Lck, Fyn, CD2BP1, CD2BP2, CD2BP3 and CD2ADAP, leading to the downstream activation of MAPK/ERK and PKC pathways.

C) LFA-1 is a heterodimeric integrin composed of a alpha (CD11a) subunit and beta (CD18) subunit. Upon binding ICAM-1, LFA-1 initiates 'outside-in' signalling that involves phophorylation by kinases such as ZAP-70 and Lck. The cytoplasmic tail of LFA-1 also binds a host of adaptor proteins, including talin1, ADAP (adhesion and degranulation-promoting adapter protein), VAV-1, JAB-1 and FAK (focal adhesion kinase) that propagate proximal signalling leading to the downstream activation of JNK, STAT3 and p38 MAPK signalling pathways.

LFA-1 Adhesion

Like CD2, LFA-1 was initially identified as an adhesion molecule, promoting T cell-APC interactions. LFA-1 adhesion is induced by TCR signalling through a combination of conformational changes, LFA-1 clustering and enhanced avidity [105–108]. However in contrast to CD2-CD58, LFA-1-ICAM-1 extends out from the cell membrane at a greater distance of 40nm [43] and is segregated away from CD2, CD28 and the TCR at the immune synapse [74, 109]. Consequently, it has been proposed that ICAM-1 promotes cell-cell interactions by allowing close contact zones to form, thereby promoting proximal TCR signalling [110].

LFA-1 Signalling

In addition to participating in "inside-out" signalling, LFA-1 itself induces intracellular signalling upon changes in it's external environment (such as cytokines and/or TCR/pMHC binding), like CD2 and CD28, termed "outside-in" signalling. LFA-1 has two cytoplasmic tails that lack intrinsic enzymatic activity but bind kinases Lck and ZAP-70 [111], and act as docking sites for several signalling molecules that include LAT, JAB-1 (Jun activating protein 1), talin1, VAV1 (vav guanine nucleotide exchange factor 1), FAK (focal adhesion kinase) and ADAP (adhesion and degranulation-promoting adapter protein). This in turn activates downstream signaling by STAT3, JNK, p38 MAPK and PI3K [112]. *In vitro* studies have reported LFA-1 engagement with ICAM-1 can enhance T cell activation and functional responses such as IL-2 expression [113–115], and that LFA-1 knockout T cells exhibit reduced IL-2 and IFN-γ production [116], whilst LFA-1 stimulation can deliver distinct signals for cytolytic activity of CTLs [117].

Biochemical studies have identified signalling components distinct from TCR signalling upon LFA-1 engagement [118] and the downstream activation of the Erk1/2 MAPK [119] and Ras MAPK signalling pathways [120]. However it remains unclear whether these distinct intracellular molecules have additional costimulatory functions, or if they ultimately aid LFA-1's adhesive function in promoting TCR engagement. Furthermore, *in vivo* studies have shown that LFA-1 lowers the threshold for antigen activation of $CD4^+$ T cells [121] and is required for optimal $CD4^+$ T cell responses [122].

Biological Importance of LFA-1

It has become increasingly clear that LFA-1 function has important biological implications. Indeed, a pathology resulting from defects in the gene encoding the CD18 subunit of LFA-1, termed LAD (leukocyte adhesion deficiency), results in severe immunodeficiencies in humans [123]. Moreover LFA-1 blockade with monoclonal antibodies (MAbs) increases risk of patients developing a fatal CNS infection called progressive multifocal leukoencephalopathy (PML) [124]. However due to LFA-1's broad expression profile and wide-ranging role mediating leukocyte trafficking, T cell development and T cell activation, it is difficult to discern the exact underlying mechanisms behind these pathological phenotypes. Mouse studies have revealed that LFA-1 is important for $CD8^+$ T cell mediated anti-tumor responses [125], viral clearance [126], and human T cells have been found to rely on LFA-1 contact for effective cytolytic activity [127].

1.5.5 The CD28 Costimulatory Receptor

CD28 is a 44kDa member of the Ig Superfamily. It was the first identified costimulatory receptor, providing an important basis for the two-signal model of lymphocyte activation [128–130]. As a result CD28 is the most extensively studied accessory receptor [11]. Constitutively expressed on T cells, CD28 expression decreases with age [131]. Existing as a homodimer at the cell membrane, CD28 binds to monomeric CD86 (B7-2) and dimeric CD80 (B7-1) expressed primarily on professional APCs [132]. Dendritic cells exhibit the highest expression levels of CD80/CD86 [133]. CD28 binds CD86 with a K_D of $\sim 20\mu$M, and CD80 with a K_D of $\sim 4\mu$M [134].

CD28 Ligands: CD86 & CD80

Although structurally similar, the ligands for CD28 exhibit different expression profiles on monocytes, memory B cells, DCs and T cells [135]. Furthermore, CD86 is constitutively expressed and rapidly upregulated upon activation, whereas CD80 expression is induced at later points during an immune response [136, 137]. Both ligands also bind CTLA-4, a coinhibitory receptor expressed by T cells that opposes costimulation provided by CD28 through various mechanisms, including a cell-extrinsic pathway in which CD80 and CD86 are physically captured and subsequently removed from the surface of APCs in a process called transendocytosis [138]. This reduces the availability of CD80 and CD86 to T cells for CD28 dependent costimulation. CTLA-4 shares significant structural homology with CD28 and binds to CD80/CD86 with a higher affinity than CD28 (CD86-CTLA4: $K_D \sim 2\mu$M, CD80-CTLA4: $K_D \sim 0.2\mu$M), preferentially binding to dimeric CD80 over CD86 [134].

The low binding affinity of CD28 for its ligands has been proposed to allow the dynamic formation and disruption of contacts between T cells and APCs, allowing TCRs and pMHCs to laterally diffuse through the immunological synapse [134]. Additionally, CD28-CD86/80 engagement stabilises an intermembrane gap between T cells and APCs, that matches the length of CD2/CD58 and TCR/pMHC interactions, allowing CD28 to colocalise with these molecules [139] and aid the recruitment of signalling molecules via it's cytoplasmic tail.

CD28 Signalling

Upon ligand binding, highly conserved tyrosine motifs within the cytoplasmic tail of CD28 are phosphorylated by kinases such as Lck and Fyn [140–142]. Phosphorylation of a membrane proximal tyrosine allows the lipid kinase phosphatidyl-inositol 3-kinase (PI3K) to bind CD28. PI3K activity leads to the activation of PKCθ (Protein kinase C theta), a critical downstream effector of CD28, which mediates signaling events leading to the activation of the NF-κB, AP-1 and NF-AT transcription factors [48]. One of the main outcomes of CD28 costimulation is the production of IL-2, that is enhanced through both transcriptional and post-transcriptional mechanisms [143]. In addition, CD28 also increases the production of IFN-γ in both $CD4^+$ and $CD8^+$ T cells [144].

An ongoing question surrounding CD28 costimulation is delineating whether CD28 has a qualitative or quantitative impact on TCR signalling. Overall, it is likely CD28 costimulation impacts in both ways as CD28 has been reported to amplify existing TCR signalling and generate unique signals. However, due to CD28's multiple binding partners, the expression of many additional interacting receptor/ligand pairs on T Cells/APCs and non-physiological experimental conditions [145] it has been

challenging to identify the exact contribution of CD28 to T cell activation. Microarray analysis has revealed TCR stimulation induces the expression of thousands of genes that are impacted by CD28 engagement but that no new gene was expressed upon CD28 costimulation compared with TCR signalling [146]. Interestingly, global phosphoproteomic studies on Jurkat cells stimulated with anti-CD3 and anti-CD28 antibodies reported both quantitative and qualitative impacts on T cell signalling through CD28 costimulation [147, 140]. Taken together this data suggests that CD28 may exert it's effect primarily by altering phosphorylation states of signalling mediators. Overall CD28 signalling is thought to synergise with TCR signalling at several levels including proximally to the TCR [148] through the association with PI3K as well as exerting more distal effects on downstream effectors and stabilisation of IL-2 mRNA [84, 143].

Biological Consequences of CD28 Costimulation

It is clear from a multitude of *in vivo* studies that CD28 plays an important biological role. CD28-deficient mice and CD86/80 deficient mice display markedly reduced immune responses [149, 150] across a range of infectious and auto-immune models [151–154]. Furthermore studies have revealed that even though $CD4^+$ responses were diminished cytotoxic immune function was unaltered in CD28 knock out mice [151, 155]. The cytotoxic function of $CD8^+$ T cells is aimed towards any infected cell in the body, not just professional APCs. Therefore it makes sense that this function does not rely on CD28 signalling, overall suggesting a discrepancy in the role of CD28 between T cell subsets.

Indeed, the importance of CD28 costimulation in $CD4^+$ T cell responses has been well-established across both *in vitro* and *in vivo* studies that have shown T cells

becoming anergic without CD28 [40, 156] and that CD28 engagement enhances T cell activation by improving survival, proliferation and IL-2 production [157–159].

The role of CD28 costimulation in $CD8^+$ T cell activation is less clear with some studies showing $CD8^+$ T cell activation does not depend upon CD28 costimulation *in vitro* [44, 160, 161], and others demonstrating that CD28 costimulation is needed for optimal $CD8^+$ T cell activation [162–165], and that it is essential for the *in vivo* establishment of peripheral tolerance [166]. Furthermore reduced expression of CD80 and CD86 ligands has been implicated in immune evasion by both viruses [167–169] and tumour cells [170]. Furthermore naïve T cells have been suggested to be more reliant on CD28 compared to antigen-experienced effector and memory T cell subsets.

However, immune responses are not completely abolished in CD28 knock-out mice and a large subset of human $CD8^+$ T cells lack CD28 expression, in contrast to mouse T cells that display homogenous expression of CD28 [171, 172], suggesting that CD28 is not critical for human $CD8^+$ T cell activation. Our understanding of CD28 costimulation is further complicated by CTLA-4, that also binds CD80/CD86, and is known to be a negative regulator of T cell activation. Consequently effects observed in the absence of CD28 (such as the induction of anergy), have been proposed to be a result of preferential coinhibition by CTLA-4, rather than a lack of CD28 costimulation.

Table 1.1: Comparison of the CD28, CD2 & LFA-1 Costimulatory Receptors Across Structural, Biochemical and Functional Features

	CD2	LFA-1	CD28
Primary Human Ligand	CD58	ICAM-1	CD86 / CD80
Protein family	Immunoglobulin Superfamily (CD2 Subfamily)	Integrin	Immunoglobulin Superfamily (CD28 Subfamily)
Receptor Expression	All mature lymphocytes	All mature lymphocytes	~80% $CD4^+$ T cells, ~50% $CD8^+$ T cells
Affinity for Ligand	K_D: 9-22μM	K_D: 0.2μM (high affinity state)	K_D: 4μM (CD80) K_D: 20μM (CD86)
Ligand Expression	Broadly expressed on hematopoietic and non-hematopoietic cells	In most tissues: endothelial cells & immune cells	All APCs. CD86 constitutively expressed. CD80 expression induced upon activation
Receptor Stoichiometry	Monomeric	Monomeric	Dimeric
Adhesive Properties	Yes	Yes	No
Downstream Signalling Pathways	PKC, Ras/MAPK [76]	JNK/AP-1, STAT3, PI3K & p38 MAPK [119]	PI3K, Ras/MAPK [173]

1.6 Therapeutic Importance of Costimulation

Given their central role in modulating T cell responses, costimulatory receptors have attracted mounting therapeutic interest. For example, within the context of autoimmune conditions therapeutics aim to reduce the activity of costimulatory receptors in order to dampen T cell responses. The drug Abatacept is used to treat rheumatoid arthritis, whose pathogensis arises from the erroneous production of IL-6 by T cells. Abatacept binds CD80/CD86 preventing CD28 costimulation and ultimately reducing IL-6 production from T cells. Additionally, another drug, Alefacept, targets CD2 costimulation by blocking interactions with it's endogenous ligand, CD58 on APCs and is used to treat patients with moderate to severe chronic plaque psoriasis [174]. Although costimulation is dampened for the treatment of autoimmune conditions, it is desirable to promote the ability of costimulation to enhance T cell activation in other pathological contexts such as cancer.

1.7 Chimeric Antigen Receptors

Our understanding of T cell biology has paved the way for the development of adoptive cell therapies that harness directed TCR signalling against cancer. Cytotoxic T cells have long been recognised as capable in eradicating cancer cells, however tumors can evolve to escape this immune recognition. Consequently, adoptive cell therapies have been developed that focus on re-directing T cells to target cancer. The basis of these therapies involve isolating autologuous T cells from patients, expanding them *ex vivo*, before re-introducing them back into the same patient. Chimeric antigen receptors (CARs) are synthetic receptors that have been designed to target

specific antigens of choice. CAR-T cell immunotherapy is a specific type of adoptive cell therapy that uses the transfer of autologous T cells that are genetically modified to express CARs. Crucially, these CAR-T cells, are not MHC-restricted because their extracellular antigen recognition domains are often taken from antibodies that can potentially recognise any surface protein on cancer cells [175]. This is particularly important when targeting tumours that downregulate their surface MHC molecules [176].

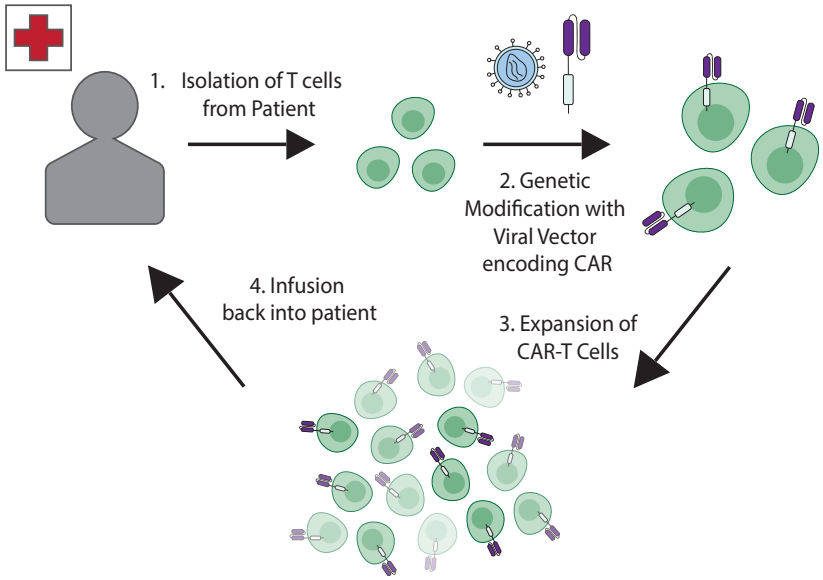


Figure 1.4: Overview of Adoptive Cell Therapy with CARs Adoptive Cell Therapy is a specific type of immunotherapy that harnesses the cytotoxic potential of T cells to treat cancer. T cells are first isolated from a patient and genetically engineered to express chimeric antigen receptors. These modified T cells are then expanded *ex vivo*, before reintroduction back into the same patient.

The Structure of CARs

CARs typically encode an extracellular region that directs antigen binding fused to an intracellular domain(s) that modulates T cell activation [176] via a small hinge region. The extracellular antigen binding domain is derived from the variable region of monoclonal antibodies and consists of a variable heavy and light chain joined by a short linker peptide in a single chain. Therefore, CARs can be theoretically produced to target any surface antigen for which an antibody can be raised against. A small hinge region links the extracellular domain to a transmembrane domain, which is often taken from the CD8α chain or CD28, and confers stable CAR expression. This is fused to an intracellular domain that initially included the CD3ζ chain of the TCR alone. However these first (1^{st}) generation CARs failed to elicit effective immune responses (evaluated via IL-2 production and T cell expansion) and tumor control with *in vivo* mice models [177, 178], hampering further clinical progress. Subsequently, the signalling domain of costimulatory receptors were incorporated into the intracellular CAR domain to recapitulate endogenous costimulation and elicit optimal T cell activation [179]. Indeed, second (2^{nd}) generation CARs with CD28 or 4-1BB costimulation, elicit improved CAR-T cell effector function compared to 1^{st} generation CARs [180–184], and form the basis of the only currently FDA approved CAR-T cell treatments in the clinic.

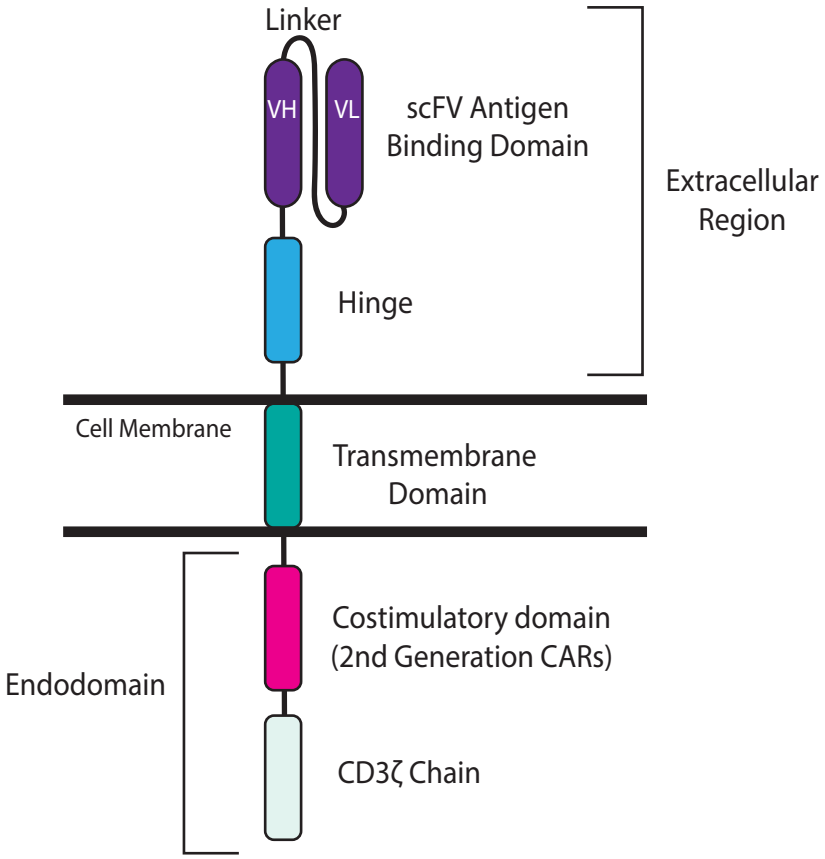


Figure 1.5: Typical CAR Structure Chimeric Antigen Receptors (CARs) are synthetic antigen receptors engineered by fusing an antigen binding domain derived from antibodies (scFV) against a target of choice to T cell signalling machinery. Specifically, the extracellular region consists of a variable heavy and light chain joined by a short linker peptide, and connected to a small hinge domain. The hinge region is also linked to a transmembrane domain. The CAR intracellular region consists of CD3ζ chain, and in the case of 2nd generation CARs, a costimulatory domain.

Clinical CAR-T Cells

CAR-T cell immunotherapy has achieved significant success for hematological malignancies. The first FDA-approved CAR-T cell immunotherapy, tisagenlecleucel, (Kymriah®) is used to treat acute lymphoblastic leukemia in children. These CARs specifically target the CD19 antigen expressed upon B cells and contain a CD28 costimulatory domain. Soon after, another CAR-T treatment for Diffuse B Cell Lymphoma and Non-Hodgkin's Lymphoma, axicabtagene ciloleucel (also known as Yescarta ®) was approved, incorporating the 4-1BB costimulatory receptor shown to have an overall 82% response rate for Large B-Cell Lymphoma [185]. To date, six 2nd generation CAR-T cell immunotherapies have been approved for treatment of B cell malignancies that target the CD19 or CD20 antigens and contain signalling domains from either CD28 or 4-1BB. Many more CAR-T cell therapies are undergoing clinical trials for treatment of a range of cancers, including solid tumors [186].

Costimulation for CAR-T cells

Following the clinical success of 2nd generation CAR-T cells incorporating costimulatory domains, there has been growing interest around how best to harness costimulatory receptors that are key modulators of T cell activation. Given that current limitations of CAR-T cell therapy include limited T cell expansion and *in vivo* persistence, an immunosuppresive tumor microenvironment, T cell exhaustion and adverse side effects (such as cytokine release syndrome (CRS) and neurotoxicity resulting from cytokine production and off-target toxicities), there is specific interest in understanding the contribution of costimulation in CAR-T cell activation and utilising this information to deliver improved and safer therapies.

Importantly, our understanding of the behaviour of endogenously expressed and full length costimulatory receptors cannot be extrapolated to costimulatory domains incorporated within CARs. Notably, costimulation within CARs does not rely on engagement with costimulatory ligand and is linked together with CD3ζ signalling. In contrast, endogenous costimulatory receptors exhibit differential expression kinetics. For example CD2 and CD28 are expressed constituively alongside the TCR, whereas 4-1BB is expressed after T cell activation. In addition, the stoichiometry of CAR costimulatory domains may differ from their physiological counterparts. Indeed, 4-1BB can form trimers upon ligand binding that forms the basis of a signalosome structure that provides optimal cosignalling [187].

Moreover, individual costimulatory domains exert different effects on CAR function. For example, anti-CD19 CARs with CD28 domains induce a faster, more potent effector response compared to anti-CD19 CARs with 4-1BB domains that exhibit better *in vivo* persistence [188]. The distinct effects of individual costimulatory domains may be beneficial in different clinical contexts. For example, enhanced persistence may be beneficial for ensuring long-term remission, whereas early and potent antitumor activity may be more effective for fast-growing lymphomas [189].

Costimulation incorporated within CAR-T cells is known to enhance the production of pro-inflammatory cytokines such as IL-2, IFN-γ and TNF-α, that are considered important components of anti-tumor responses coordinated by CAR-T cells [188]. However reports of fatal incidences of inflammatory syndromes such as CRS and ICANS (Immune effector cell-Associated Neurotoxicity Syndrome) following CAR-T cell immunotherapy has focused efforts to understand how cytokine production is controlled by CARs. Furthermore, CD28 CARs result in more severe CRS and ICANS in patients treated for B-Cell Acute Lymphoblastic Leukemia compared to

4-1BB CARs, and it has been suggested that differential activation intensities and signalling pathways induced by each costimulatory domain has an important impact on the safety profile of CAR-T cells [190].

There is also evidence to suggest that costimulation affects T cell differentiation pathways. Indeed, the 4-1BB costimulatory domain in CARs induced growth of $CD8^+$ T cells with a central memory phenotype, whereas CARs with the CD28 domain stimulated development of effector memory T cells [191]. In addition, like their endogenous counterparts, individual costimulatory domains may function differently between T cell subsets. There is mounting evidence showing differential behaviour between $CD4^+$ and $CD8^+$ CAR-T cells [192] but further clarification of the role of costimulatory receptors within different T cells subsets (effector, memory, $CD4^+$ and $CD8^+$) is still needed [193].

Future Approaches for CAR-T Cell Costimulation

Given that 2nd generation CAR-T cells exhibit enhanced anti-tumor responses, proliferation and *in vivo* persistence and that different improvements were associated with CD28 and 4-1BB CARs, 3rd generation CAR-T cells incorporating domains from both CD28 and 4-1BB have been developed. These 3rd generation CARs exhibit further enhancements in cytotoxicity, IFN-γ production and persistence [194–196]. An additional consideration with 3rd generation CARs is the relative positioning of each costimulatory domain within the receptor, especially as it has been proposed that the more membrane-proximal domain in 3rd generation CARs has a greater impact on cytokine production [197].

So far, the costimulatory domains discussed in CAR-T cells are incorporated within the CAR construct. However, CAR-T cells also express endogenous costimulatory

receptors that will interact with their corresponding ligands on the opposing cell. As the expression of costimulatory ligands can be sparse within the tumour microenvironment, 4th generation CARs have been designed to express costimulatory ligands alongside the CAR. For example, delivering 4-1BBL with a 2nd generation CAR containing CD28 signalling improved anti-tumor function [198]. However there is still a lack of understanding on how extrinsic costimulatory receptors function in CAR-T cells, and specifically the interplay between intrinsic costimulatory domains within CARs and extrinsic costimulation from the ligation of costimulatory receptors with their ligands.

1.8 Quantitative Phenotypes

Whilst the specific functional characteristics of T cells (e.g. proliferation, cytokine production and cytotoxicity) can influence the quality of the overall immune response, it is widely recognised that the magnitude of T cell responses plays a significant role in determining the outcome of immune responses.

For example, stronger T cell responses with higher efficacy and antigen sensitivity can enhance the clearance of pathogens or cancer cells. Additionally, the adaptation of T cells to antigen over time may limit sustained immune function leading to exhaustion or tolerance. Therefore, understanding and harnessing the quantitative features of T cell responses is important. This thesis considers three quantitative phenotypes of T cell responses (Fig. 1.6):

1. **Antigen sensitivity** can be defined as the concentration of antigen required to elicit T cell activation. Specifically the EC_{50}, defined as the concentration of antigen required to elicit half of the maximum response, can be used to quantify antigen sensitivity (Fig. 1.6A). T cells are incredibly sensitive, recognising as few as ~1-10 cognate antigens with studies revealing that even a single pMHC can elicit a response from $CD4^+$ T cells *in vitro* [22, 199], whilst 1-3 peptide antigens can induce $CD8^+$ T cells to become functionally responsive [200].

2. **Maximal efficacy, $\mathbf{E}_{Max}$**, can be defined as the maximum T cell response (e.g. maximum cytokine output) across antigen concentrations, corresponding to amplification of responses (Fig. 1.6B).

3. **Antigen adaptation** can be defined as the ability of T cells to initially respond to antigen by, for example, producing cytokine for a period of time be-

fore secretion stops despite the persistence of the antigen (Fig. 1.6C). This inability of T cells to produce cytokine in the presence of constant antigen has been termed adaptation, exhaustion and dysfunction depending on the context that it has been observed.

Although T cell accessory receptors can regulate cytokine production, their specific impact on these quantitative T cell responses has been under-explored.

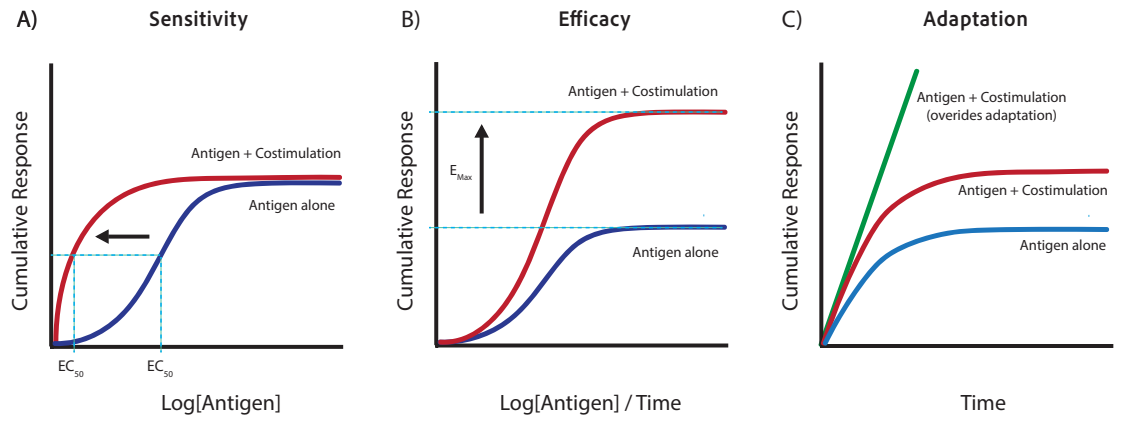


Figure 1.6: Quantitative Phenotypes of T Cell Responses Three ways in which T cell responses can differ quantitatively are through their sensitivity to antigen, maximal response achieved and adaptation of responses over time. **A)** Assessing response over antigen dose provides the dose at which half the maximal response is achieved, called the EC_{50}. A decrease in EC_{50} under costimulation, means an increase in T cell antigen sensitivity. **B)** The maximal response (E_{Max}) of T cells over varying antigen dose or time can be measured to provide a quantification of efficacy under costimulation compared with antigen alone. **C)** Measuring response over time allows the impact of costimulation on the adaptation of T cells to constant antigen exposure to be assessed. Costimulation may be able to increase the maximal response achieved but have no effect on the rate of response over time (red line), or costimulation may be able to increase the rate of response over time compared to antigen alone (green line).

1.9 This Thesis

Using three well-established costimulatory receptors, CD2, LFA-1 and CD28, this study tests the hypothesis that different costimulatory receptors have different impacts on quantitative T cell phenotypes, including antigen efficacy, sensitivity and adaptation.

In Chapter 2, the impact of the costimulatory receptors CD2, LFA-1 and CD28 on antigen adaptation by T cells is systematically investigated. Although all receptors increased cytokine production, consistent with costimulation, only CD2 and LFA-1 were able to prolong the duration over which cytokine was produced. Interestingly, when T cells recognise antigen through a 2nd generation CAR adaptation is not observed and instead the rate of cytokine production increased over time.

In Chapter 3, the impact of costimulatory receptors CD2, LFA-1 and CD28 on antigen sensitivity is systematically studied. Although CD2 and LFA-1 increase antigen sensitivity, we find no impact of CD28 on antigen sensitivity in this experimental system.

In Chapter 4, a novel ligand presentation system is developed whereby purified ligands can be covalently coupled directly onto the surface of cells. We show that different combinations and concentrations of purified ligands can be titrated onto cells, and that T cells can recognise these ligands and use the platform to study the quantitative impact of CD2, LFA-1 and CD28 on T cell activation by the TCR and CARs.

Chapter 2

The Impact of Costimulation on Antigen Adaptation by TCRs & CARs

2.1 Introduction

2.1.1 The Duration of T Cell Responses has Important Biological Consequences

The duration of T cell responses is an important feature governing T cell function. In the context of peripheral tolerance, T cell responses are constrained to limit autoreactivity with self-peptides. Indeed, the "Tuneable Activation Threshold" [201] and subsequent "Discontinuity of Immunity" [202] theories of immune responses postulate that T cells become tolerant to the continuous exposure of antigen to prevent self-reactivity outside the thymus. Additionally, during chronic infection and cancer, continuous antigenic stimulation leads to dysfunctional T cell state (e.g. exhaustion) [203]. A diverse set of immunotherapies, such as checkpoint blockades and adoptive cell therapy, aim to reverse T cell dysfunction by addressing the recovery and maintenance of T cell responses over time [204].

2.1.2 Adaptation of T cell Responses to Constant Antigen Exposure is Associated with *in vivo* Dysfunction

Biological adaptation at the cellular level is defined by an input stimulus initiating a cellular response that is attenuated over time, despite the persistence of the stimulus [205]. This definition applies to several *in vivo* and *in vitro* observations showing that T cells exhibit a limited period of response upon exposure to persistent or chronic antigen [36, 206–208]. The T cell state following this transient response has been variously defined as T cell dysfunction, T cell exhaustion, T cell adaptive

tolerance and T cell anergy [209–211]. It is currently unclear whether these states, produced in different experimental systems, have a shared molecular mechanism. In many *in vivo* systems the mechanism is often associated with stable epigenetic modifications [203]. In an *in vitro* system where T cells experience purified antigen in isolation, it has been suggested that the downregulation of the TCR is sufficient to explain adaptation [36, 208]. In the case of other surface receptors that have been shown to induce cellular adaptation the molecular mechanism has also been traced to surface receptor downregulation.

The *in vitro* defined adaptation phenotype most closely resembles adaptive tolerance observed *in vivo*, in that $CD8^+$ T cells across a range of antigen doses become unresponsiveness over hours of constant stimulation. Indeed, clonal anergy is associated with impaired IL-2 secretion whilst exhaustion is associated with upregulation of inhibitory receptors such as PD-1 that is observed days after stimulation. In contrast, adaptation occurs within hours of antigen exposure which is before upregulation of PD-1 is observed [212].

2.1.3 The Importance of Costimulation in Adaptation

Costimulatory receptors are important regulators of T cell activation. Given that individual costimulatory receptors display differential expression kinetics it has been proposed that distinct receptors are important at different stages over the duration of T cell activation [35]. However, the specific impact of costimulatory receptors on adaptation has received limited attention. Previous work has shown that costimulatory receptors of the TNF superfamily of receptors (TNFSFR), can differentially affect the duration of T cell responses over time [36], and that PD-1 is partly responsible for *in vivo* adaptation of IFN-γ production after several hours of antigen

stimulation [213]. In a similar context, PD-1 blockade has been shown to reverse T cell exhaustion, with this effect dependent on CD28 [214]. However, although CD28 together with CD2 and LFA-1 are well established costimulatory receptors that can increase cytokine production, a systematic study to examine their relative quantitative impact on cytokine production and in particular on adaptation, has yet to be performed.

Adaptation to antigen can be investigated by measuring the rate of T cell responses such as cytokine production over time (Fig. 2.1). With antigen alone the rate of cytokine production drops over time, eventually returning to baseline levels meaning the cumulative amount of cytokine produced stabilises over time (Fig. 2.1, blue line). Costimulation can impact this adaptation phenotype by either overriding adaptation, meaning the rate of cytokine production continues to rise (Fig. 2.1, green line), or by initially increasing the rate of production before it eventually drops back to baseline levels (Fig. 2.1, red line). By focusing on whether the rate of cytokine production with costimulation increases, stabilises or decreases over the time period where adaptation to antigen is observed without costimulation, the impact of individual costimulatory receptors on the duration of the T cell response can be studied.

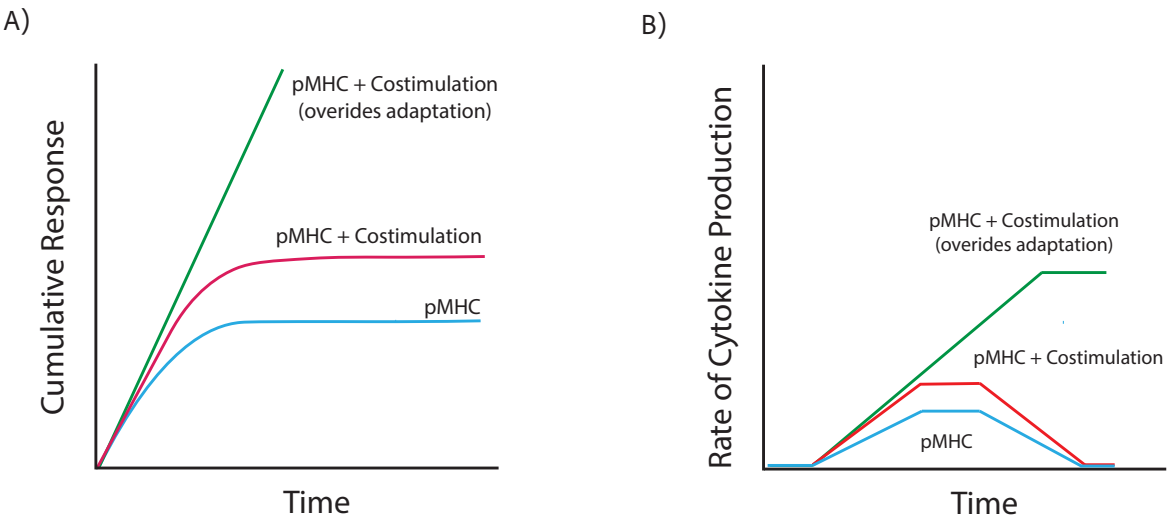


Figure 2.1: Adaptation of T Cells to Antigen with and Wihout Costimulation
A) Schematic illustrating the adaptation phenotype measured as cumulative response across time, and **B)** rate of cytokine production over time. Antigen (pMHC) alone causes the response to plateau over time, corresponding to a decrease in the rate of response production.

2.1.4 Adaptation in CAR-T Cells

CAR-T cell immunotherapy, where T cells engineered to express CAR constructs are adoptively transferred into patients, has been used for several years to treat haematological malignancies. A major challenge still facing CAR-T immunotherapy is the long-term remission of patients, with less than 50% of patients with B cell malignancies achieving a durable response 6 months following CAR-T therapy [185, 215–221]. Long-term persistence of CAR-T cells *in vivo* has been increasingly linked to sustained remission and improved clinical outcomes [222, 223], and CAR-T cell persistence has also been noted to be important in the treatment of solid tumors [224–226]. Given that CAR-T cells are exposed to chronic cancer antigens, and that the duration of CAR-T cell responses has critical implications for therapeutic efficacy, it is important to better understand the adaptation of CAR-T cells to constant antigen stimulation. Previous work has utilised an *in vitro* plate system to present different concentrations of purified antigen to CAR-T cells and observed that first

(1st) generation CAR-T cells adapt to antigen over time. However, 2nd generation CARs containing an intrinsic costimulatory domain were able to prevent adaptation [208]. Interestingly, costimulatory domains within 2nd generation CAR-T cells have also been linked to their enhanced *in vivo* persistence [197, 198]. However, the impact of engaging different costimulatory receptors alongside CARs on the duration of responses is still unclear. Given the important therapeutic applications of CAR-T cell responses, improving our understanding of the roles of individual costimulatory receptors on CAR-T cell function will allow us to harness costimulation more effectively for better therapeutic outcomes.

2.1.5 Aim of the Study

Using a reductionist *in vitro* system in which specific concentrations of biotinylated antigen and costimulatory ligand for the costimulatory receptors CD2, LFA-1 and CD28 are stably presented to primary human $CD8^+$ T cells expressing TCRs or CARs, we measure the rate of cytokine production. By precisely controlling the concentration and combination of ligands, we can quantitatively compare antigen recognition by different receptors over time. This enables the impact of different costimulatory receptors on the adaptation of T cells and CAR-T cells to constant antigen exposure to be assessed.

2.2 Results

2.2.1 All Costimulatory Receptors tested Increased Maximum Efficacy of Cytokine Production Compared with Antigen Alone

To study the contributions of individual costimulatory receptors to antigen adaptation, a reductionist system is needed where their ligands can be precisely controlled. To this end, we utilised purified biotinylated ligands immobilised on streptavidin-coated plates, as used in previous work [36, 208, 227]. To validate the system, we activated primary human $CD8^+$ T cells transduced with the 1G4 TCR and subsequently expanded them *in vitro*. The 1G4 TCR recognises the NY-ESO-1 antigen, with this study harnessing the 9V peptide variant (SLLMWITQ**V**), that confers improved MHC stability, presented on HLA-A*02:01 [228].

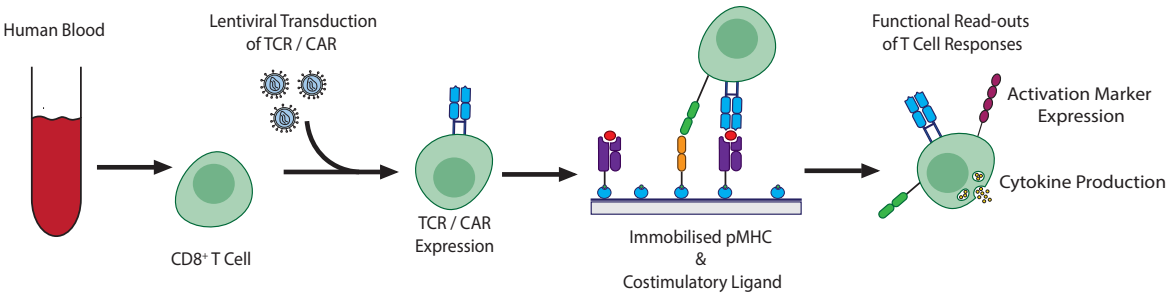


Figure 2.2: T Cell Stimulation Assay Primary Human $CD8^+$ T cells are isolated from human blood cones (see Material & Methods 6.2.3) and transduced with a viral vector encoding either the 1G4 TCR or CAR with D52N ScFV (that recognises the 9V peptide) depending on specific assay requirement. Purified extracellular domains of biotinylated 9V peptide-MHC and costimulatory ligand are bound to 96-well streptavidin-coated plates. Transduced T cells are then added to the ligand-coated plates for the required length of time. T cell responses are measured by flow cytomertry analysis of cell-surface activation markers (CD69 or 4-1BB) and/or ELISA measurement of cytokine levels in the supernatant.

When T cells were added to immobilised 9V-pMHC and the immobilised extracellular domain of CD58, ICAM-1, CD28, CD70 or 4-1BBL for 20 hours, the total concentration of IL-2, IFN-γ and TNF-α measured in the supernatant significantly increased, compared to when T cells were exposed to pMHC alone (Fig. 2.3). This confirmed that in this experimental system, engagement of these surface receptors induced T cell costimulation as assessed by cytokine production. This has been observed previously with immoblised ligands on plates, confirming that all ligands were functional [212, 229].

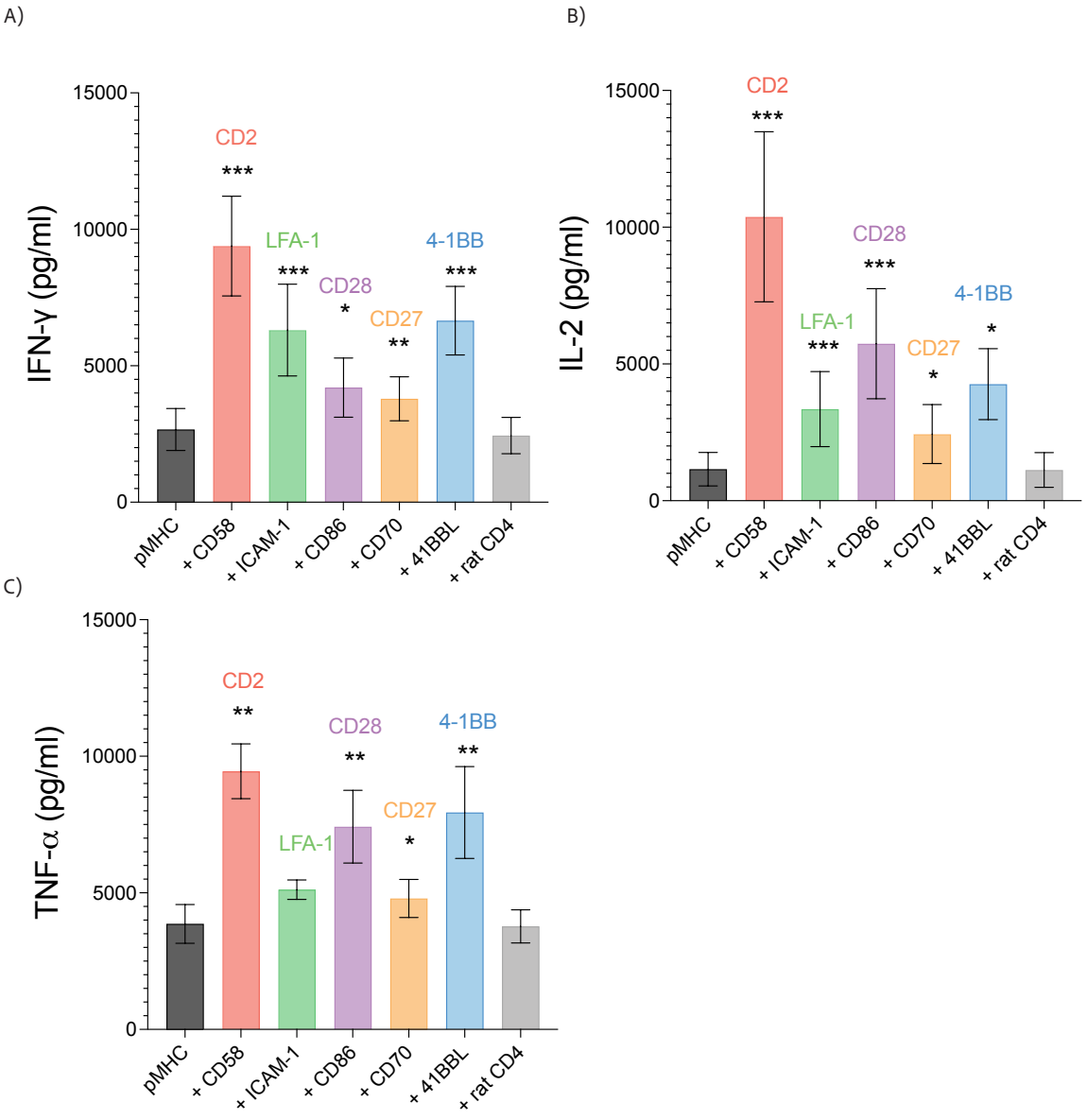


Figure 2.3: Ligation of CD2, LFA-1, CD28, 4-1BB & CD27 costimulatory receptors by their plate-bound ligands amplifies total cytokine production over 20 hours. Biotinylated 9V pMHC alone (black, 250 ng/well) or in combination with the indicated ligand (colours, 250 ng/well) were immobilised on streptavidin-coated plates. Primary Human T cells transduced with the 1G4 TCR were then added, and incubated for 20 hours. The final concentration of **A)** IFN-γ **B)** IL-2 & **C)** TNF-α was measured via ELISAs. Rat CD4 was included as a negative control for biotinylated proteins in our system. The costimulatory receptor engaged under each condition is labelled above each bar. Data is shown as a mean +/- SEM of at least 6 independent experiments (i.e. 6 independent human donors). Statistical significance was determined by 2-way ANOVA on log-transformed data. Abbreviations: * = p-value$\leqslant$0.05, ** = p-value$\leqslant$0.01, *** = p-value$\leqslant$0.001, **** = p-value$\leqslant$0.0001, ns = not significant.

2.2.2 Adaptation of T cells to Antigen under TCR-pMHC Engagement

Having validated the ability of each costimulatory receptor to increase the total amount of cytokine produced at 20 hours, we next tested the impact of each receptor on T cell activation. We hypothesised that the receptors could affect the kinetics of cytokine production in different ways: by either increasing the initial rate of cytokine production but not at later time points (i.e. no effect on adaptation, Fig. 2.1 red line) or allowing for continued cytokine production (i.e. overriding adaptation, Fig. 2.1 green line).

To measure the rate of cytokine production, the amount of cytokine produced in the first 12 hours ('Early Collection') and the following 8 hours ('Late Collection') was measured when T cells were presented with surfaces consisting of antigen alone or together with ligands to costimulatory receptors. To do this, the supernatant at 12 hours was removed and replaced with fresh media. As a control, a condition where the medium was not replaced was included to assess the total cytokine produced at 20 hours. The experiment was limited to 20 hours to avoid confounding the results with T cell proliferation and because previous work has shown that T cell cytokine production adapts on this timescale [36].

When T cells were presented with surfaces containing pMHC alone, without any costimulation, the rate of IL-2, IFN-γ and TNF-α production decreased between the first 12 hours of stimulation and the last 8 hours (Fig. 2.4), consistent with previous observations of T cell adaptation in this experimental system [36, 208].

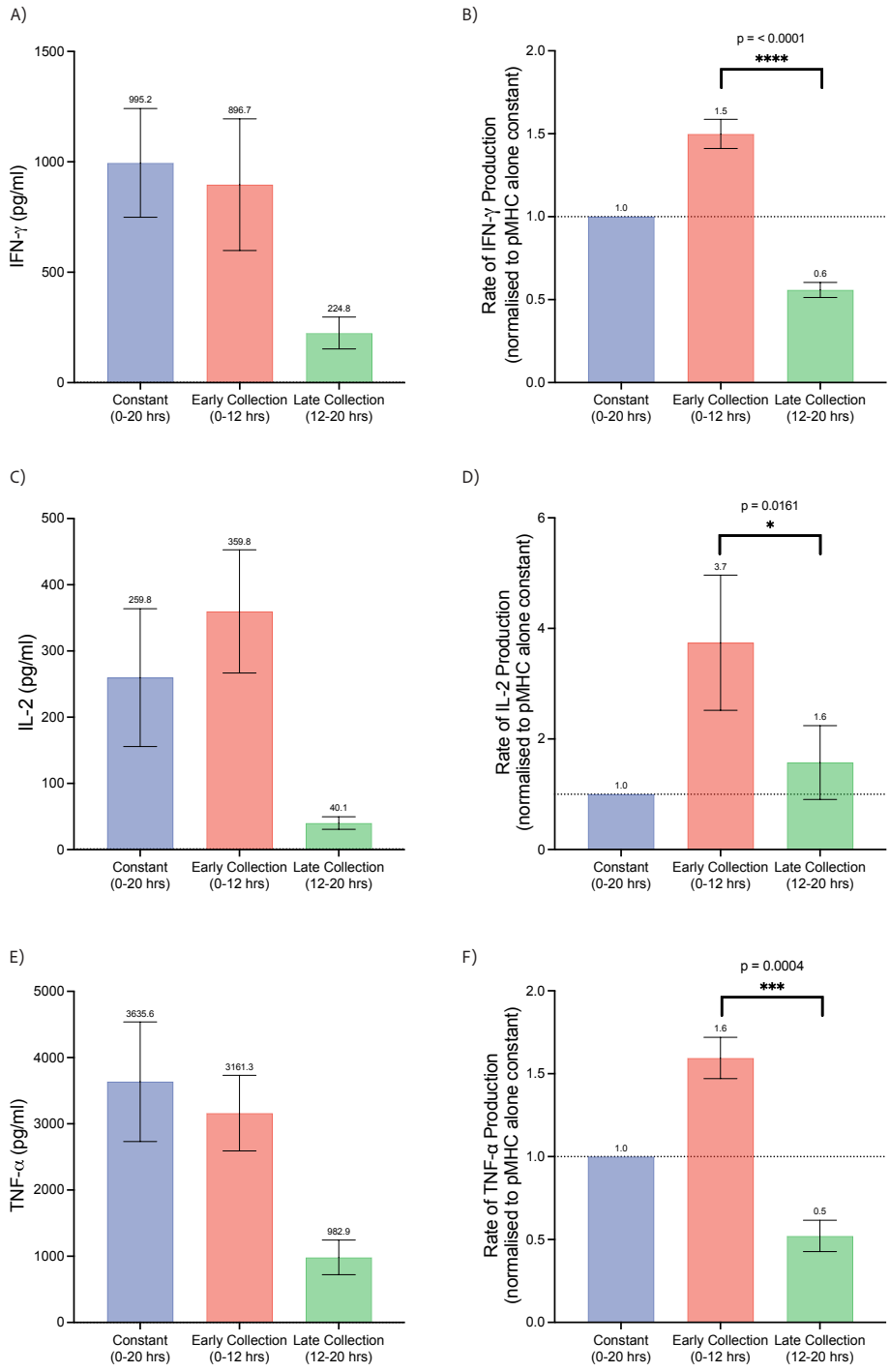


Figure 2.4: T cells adapt to constant antigen stimulation. T cells were either incubated constantly with antigen for 20 hours ("Constant") or incubated initially for 12 hours with the supernatant harvested ("Early Collection") and replaced with fresh media for a further 8 hour incubation ("Late Collection"). **A) ,C), E)** The final concentration of IFN-γ (A), IL-2 (C) and TNF-α (E), in the supernatant was measured by ELISA. **B), D), F)** The rate of production across each timepoint was calculated by dividing the level of supernatant cytokine by time period (Constant: 20 hours, Early Collection: 12 hours, Late Collection: 8 hours). Statistical significance was determined by paired t-test on log-transformed data. Abbreviations: * = p-value$\leqslant$0.05, ** = p-value$\leqslant$0.01, *** = p-value$\leqslant$0.001, **** = p-value$\leqslant$0.0001, ns = not significant. Data is shown as a mean +/- SEM of 6 independent experiments (i.e. 6 independent human donors).

To test the impact of CD2, LFA-1 and CD28 on this adaptation phenotype observed with antigen alone, T cells were activated with a combination of pMHC and biotinylated ligand specific to each costimulatory receptor. 4-1BBL (for 4-1BB costimulation), and CD70 (for CD27 costimulation), were included as their impact on adaptation has been established previously in this experimental system. CD27 engagement increased early production of cytokine, whereas 4-1BB engagement increased later production of cytokine [230]. Therefore 4-1BB acted as a positive control, whereas CD27 was a negative control. In addition rat CD4 was included as a further negative control to ensure that the addition of biotinylated protein did not sterically interfere with T cells recognising the antigen. Due to variation between T cell donors, the cytokine production rates calculated across 20 hours, 12 hours and the final 8 hours (Fig. 2.5 A, C & E) were normalised to the rate observed under pMHC alone (Fig. 2.5 B, D & F).

With IFN-γ production, the addition of CD58, ICAM-1 and 4-1BBL prevented a significant drop in cytokine production rate between the first 12 hours and later 8 hours. Therefore, engaging the CD2, LFA-1 and 4-1BB costimulatory receptors prevented adaptation over time. Interestingly when the rate of IL-2, and TNF-α was measured over time, CD58 and ICAM-1 no longer prevented adaptation, exhibiting a cytokine-specific phenotype. $CD8^+$ T cells consume IL-2 themselves, and upon activation upregulate the high-affinity α chain of the IL-2 receptor, CD25 [231, 232]. Consequently, the expression of CD25 on the T cells in this assay was checked, as an indicator of IL-2 uptake. After 20 hours, T cells that had been stimulated by pMHC exhibited significant CD25 upregulation compared to unstimulated cells, over the course of the assay (Fig. 2.6).

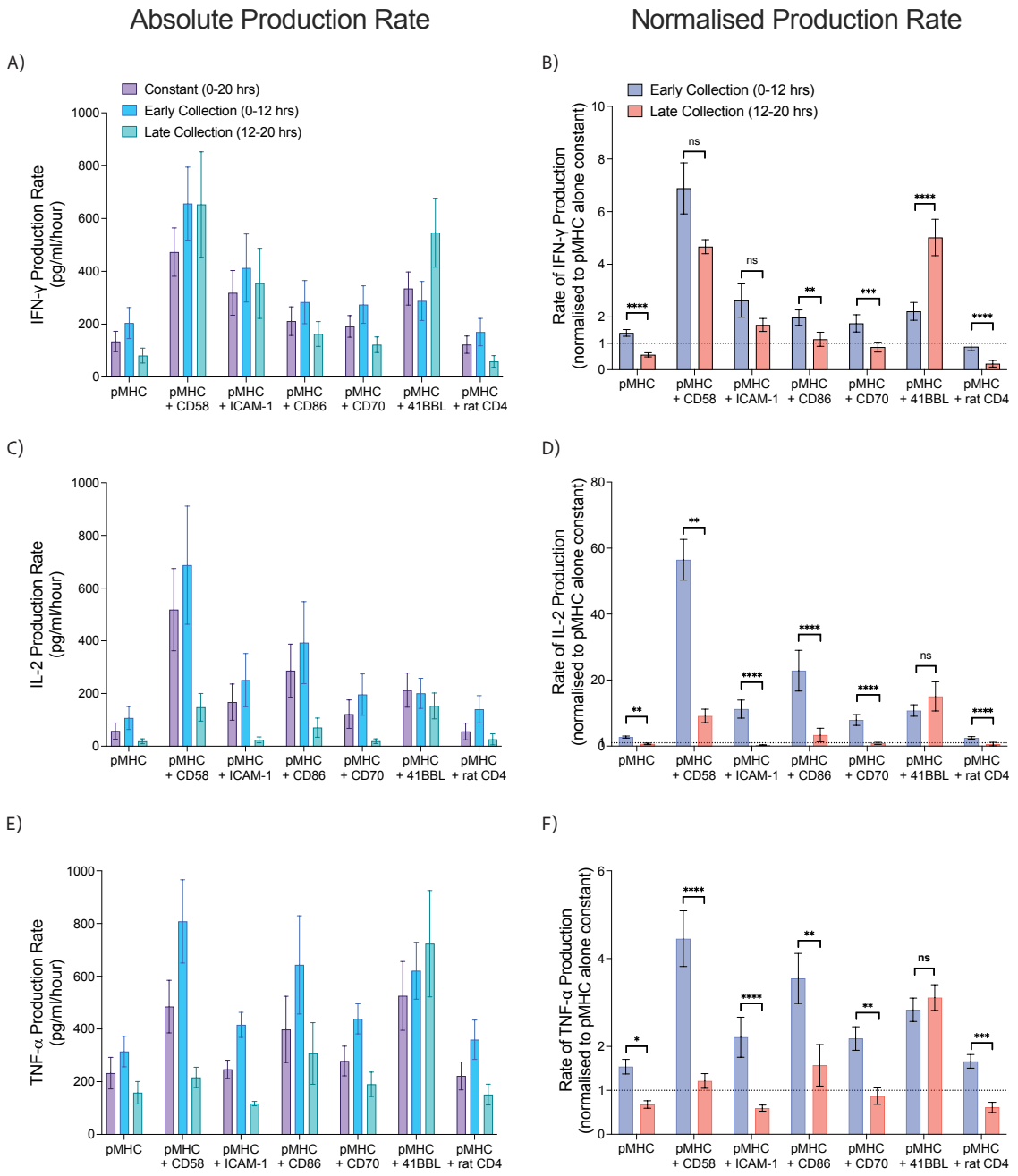


Figure 2.5: CD2, LFA-1, and 4-1BB but not CD28 or CD27 costimulation prevents adaptation to antigen. Biotinylated 9V pMHC and biotinylated costimulatory ligand were immobilised on plates at a concentration of 250ng/well. Primary Human T Cells transduced with the 1G4WT TCR were then added, and incubated for 20 hours. The final concentration of **A)** IFN-γ **C)** IL-2 & **E)** TNF-α was measured via ELISAs. These rates were then normalised to the pMHC "constant" condition across independent donors (**B, D, & F)**Rat CD4 was included as a negative control for biotinylated proteins in our system. Statistical significance was determined by 2-way ANOVA on log-transformed data. Abbreviations: * = p-value$\leqslant$0.05, ** = p-value$\leqslant$0.01, *** = p-value$\leqslant$0.001, **** = p-value$\leqslant$0.0001, ns = not significant. Data is shown as a mean +/- SEM of 6 independent experiments (i.e. 6 independent human donors).

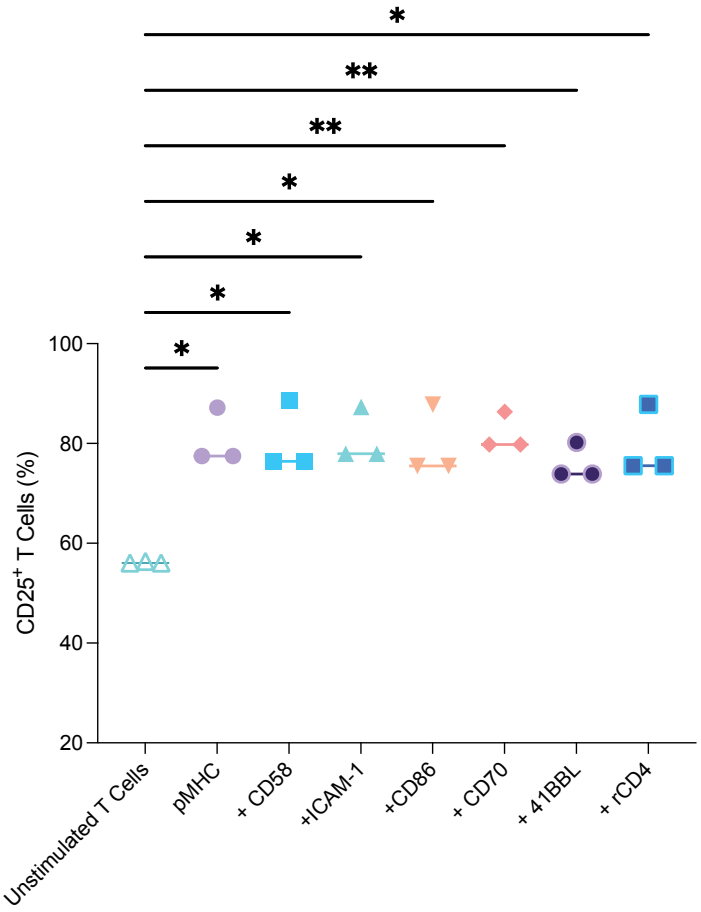


Figure 2.6: CD25 Expression on T Cells is upregulated after Antigen Stimulation. After 20 hours of stimulation with pMHC T Cells were stained for CD25 expression and analysed with Flow Cytometry. Statistical significance was determined by 2-way ANOVA on log-transformed data. Abbreviations: * = p-value⩽0.05, ** = p-value⩽0.01, *** = p-value⩽0.001, **** = p-value⩽0.0001, ns = not significant. Data is shown as a mean +/- SEM of 3 independent experiments (i.e. 3 independent human donors).

2.2.3 Adaptation of T cells to antigen under CAR-pMHC engagement

The ability of CAR-T cells to continue cytokine production over time, and how this compares to T cells, is not fully understood. Furthermore, 2nd generation CARs containing intrinsic costimulatory domains are able to out-perform 1st generation CARs *in vivo*, however when compared *in vitro* perform similarly to 1st generation CARs. Therefore we wanted to test the ability of first and 2nd generation CARs to capitalise on extrinsic costimulation for cytokine production over time.

2nd Generation CAR-T cells Produce More Cytokine Over Time

Firstly T cells transduced with the 1G4 TCR, D52N-CD28α-ζ CAR (1st generation) (Fig. 2.9, A) or D52N-CD28α-28ζ CAR (2nd generation) (Fig. 2.9, B), all recognising the same 9V-pMHC, were incubated with antigen for 20 hours and the total level of IL-2, IFN-γ and TNF-α secreted into the supernatant measured. As expected, 2nd generation CAR-T cells produced significantly higher levels of all cytokines compared to the TCR and 1st generation CAR T cells (Fig. 2.3), supporting previous findings that intrinsic costimulation incorporated within 2nd generation CARs amplifies cytokine production compared to first-generation CARs [181, 233].

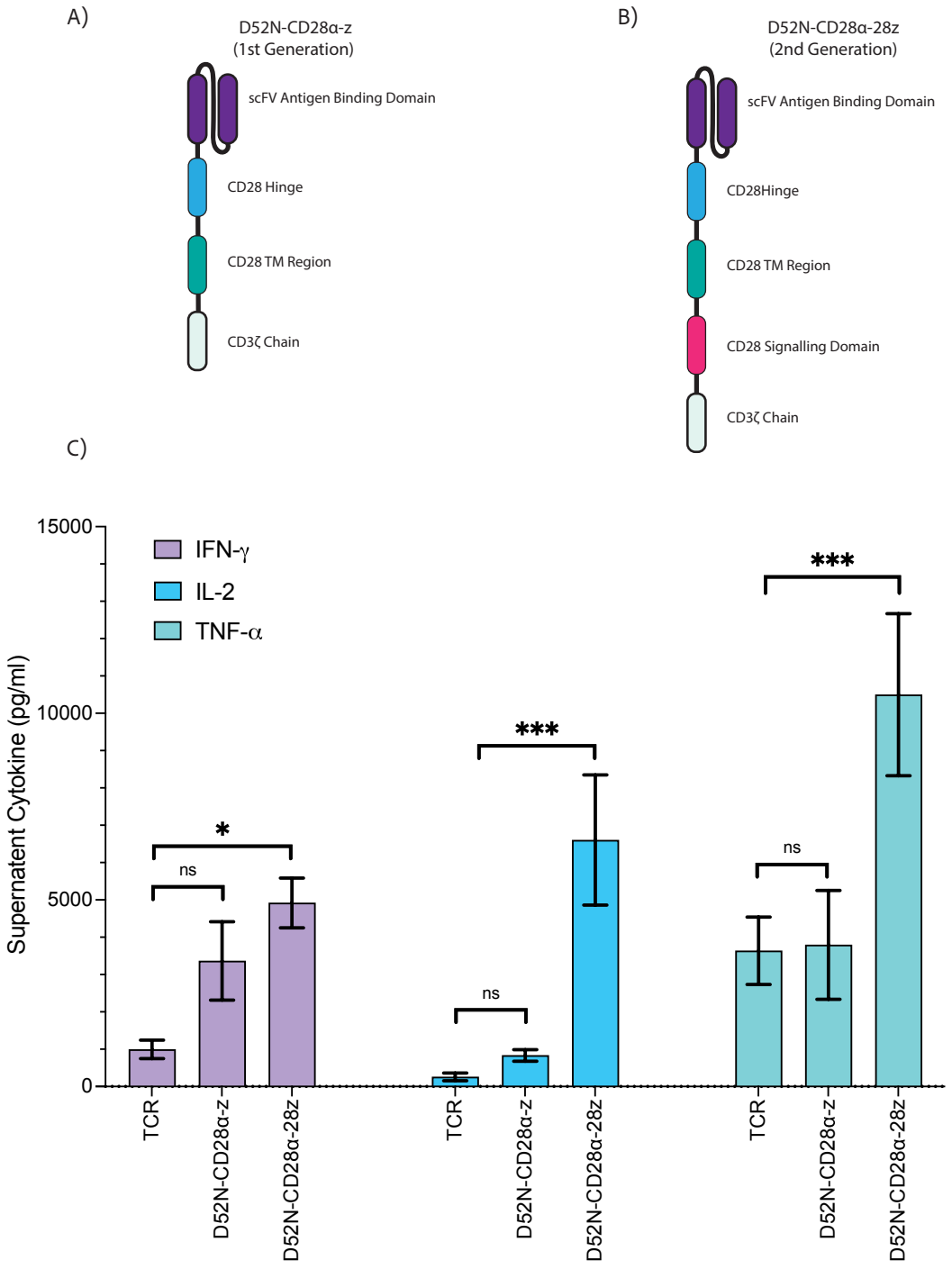


Figure 2.7: 2nd Generation CAR-T cells produce significantly more cytokine compared to TCR-T cells. Primary Human T cells were transduced with either a 1st generation **(A)** CAR containing the D52N scFv that recognises the 9V NYES0-1 pMHC or a 2nd generation **(B)** with the same D52N scFV but also contains the cosignalling domain of CD28. The T Cells were then incubated with 9V pMHC for 20 hours. **(C)** The total concentration of IFN-γ, IL-2 & TNF-α was measured via ELISA. Statistical significance was determined by 2-way ANOVA. Abbreviations: * = p-value$\leqslant$0.05, ** = p-value$\leqslant$0.01, *** = p-value$\leqslant$0.001, **** = p-value$\leqslant$0.0001, ns = not significant. Data is shown as a mean +/- SEM of 5 independent experiments (i.e. 5 independent human donors).

CARs were Expressed to Similar Levels to the TCR

To check whether differences in cytokine production was due to differences in antigen receptor expression, the expression of 1st and 2nd generation CARs was assessed (Fig. 2.8). No significant difference in the percentage of cells expressing each construct (TCR, 1st generation CAR, or 2nd generation CAR), or the level of each receptor per cell (as measured by gMFI) was found.

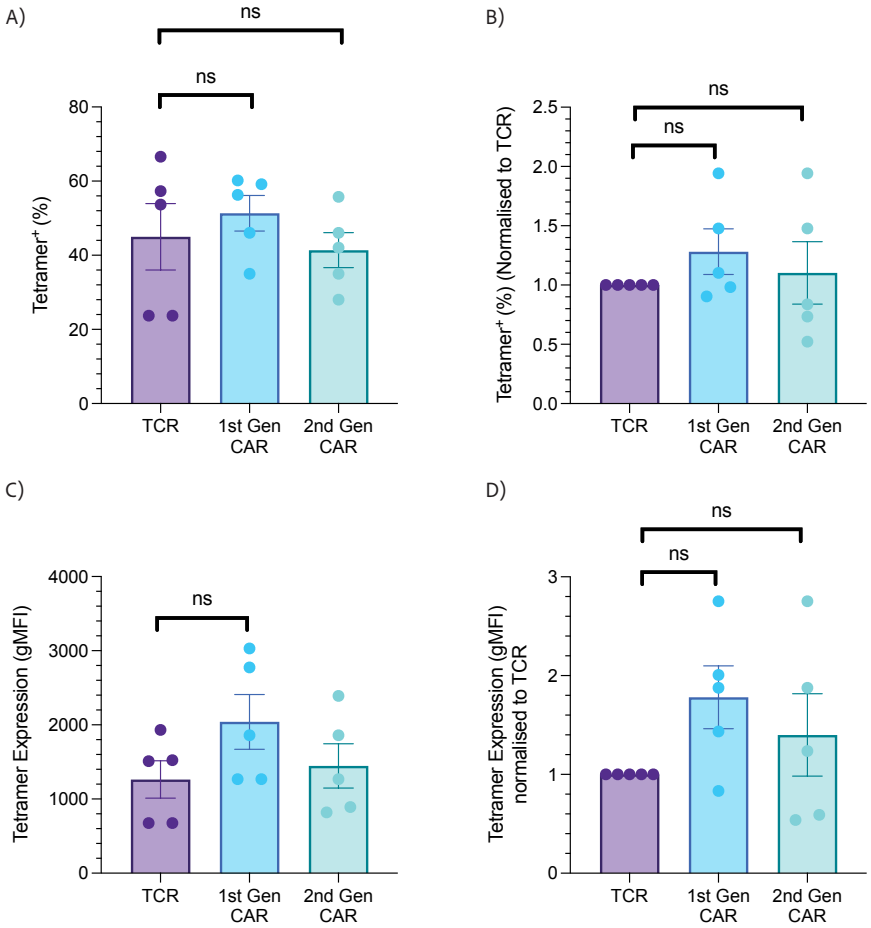


Figure 2.8: The Expression of TCR, 1st generation CAR or 2nd generation CAR on Primary Human CD8+ T cells dœs not Differ Significantly Primary Human CD8+ T cells were isolated from healthy blood donors, and transduced with lentivirus encoding either the 1G4 TCR, D52N-CD28α-ζ (1st generation) CAR or D52N-CD28α-28ζ (2nd generation) CAR. To detect TCR/CAR expression fluorescently-conjugated peptide-MHC tetramers were added the cells, followed by flow cytometry analysis.

Adaptation of 1st and 2nd Generation CAR-T cells to Constant Antigen Exposure

To investigate the rate of CAR-T cell cytokine production, the adaptation assay was performed as before by measuring cytokine production at early (first 8 hours) and late (subsequent 12 hours) times following constant antigen stimulation. Cytokine production under the 1st generation CAR was comparable to what we observe with the TCR - namely that the rate of production decreases over time. Interestingly, with the 2nd generation CAR, the rate of IFN-γ production increased over time, and the rate of production did not drop over time with IL-2 and TNF-α (Fig. 2.9), showing that the incorporation of intrinsic CD28 costimulation prevented adaptation to antigen.

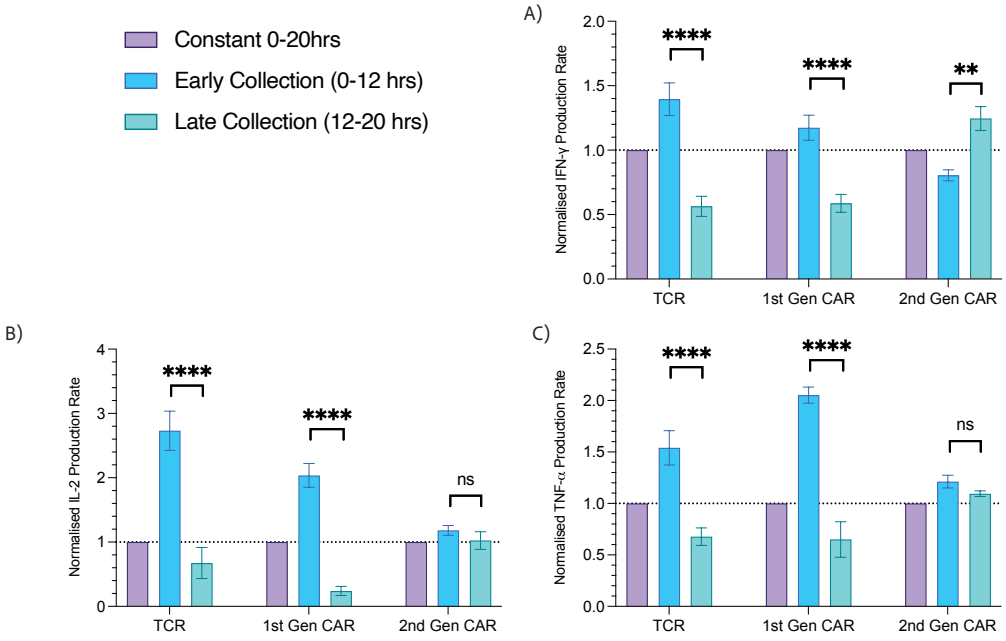


Figure 2.9: 1st but not 2nd generation CAR-T cells undergo adaptation to constant antigen stimulation. Primary Human T cells were transduced with either a first or 2nd generation CAR containing the D52N scFv that recognises the 9V pMHC. The rate of cytokine production (IFN-γ **(A)**, IL-2 **(B)** & TNF-α **(C)**) was calculated over time (see **Fig. 2.4** for details). The rate of production is normalised to the constant condition with T cells expressing the TCR. Statistical significance was determined by 2-way ANOVA on log-transformed data. Abbreviations: * = p-value$\leqslant$0.05, ** = p-value$\leqslant$0.01, *** = p-value$\leqslant$0.001, **** = p-value$\leqslant$0.0001, ns = not significant. Data is shown as a mean +/- SEM of 5 independent experiments (i.e. 5 independent human donors).

Next, extrinsic costimulation was assessed, by presenting costimulatory ligands and the rate of cytokine production measured over time (Fig. 2.10). With the 1st generation CAR, the addition of CD58 and 4-1BBL prevented the adaptation of IFN-γ production, as we observe with the TCR (Fig. 2.5). With the 2nd generation CAR, extrinsic costimulation had little additional impact on cytokine production over time. In particular, the rate of IFN-γ production increased over time, without the need for costimulation.

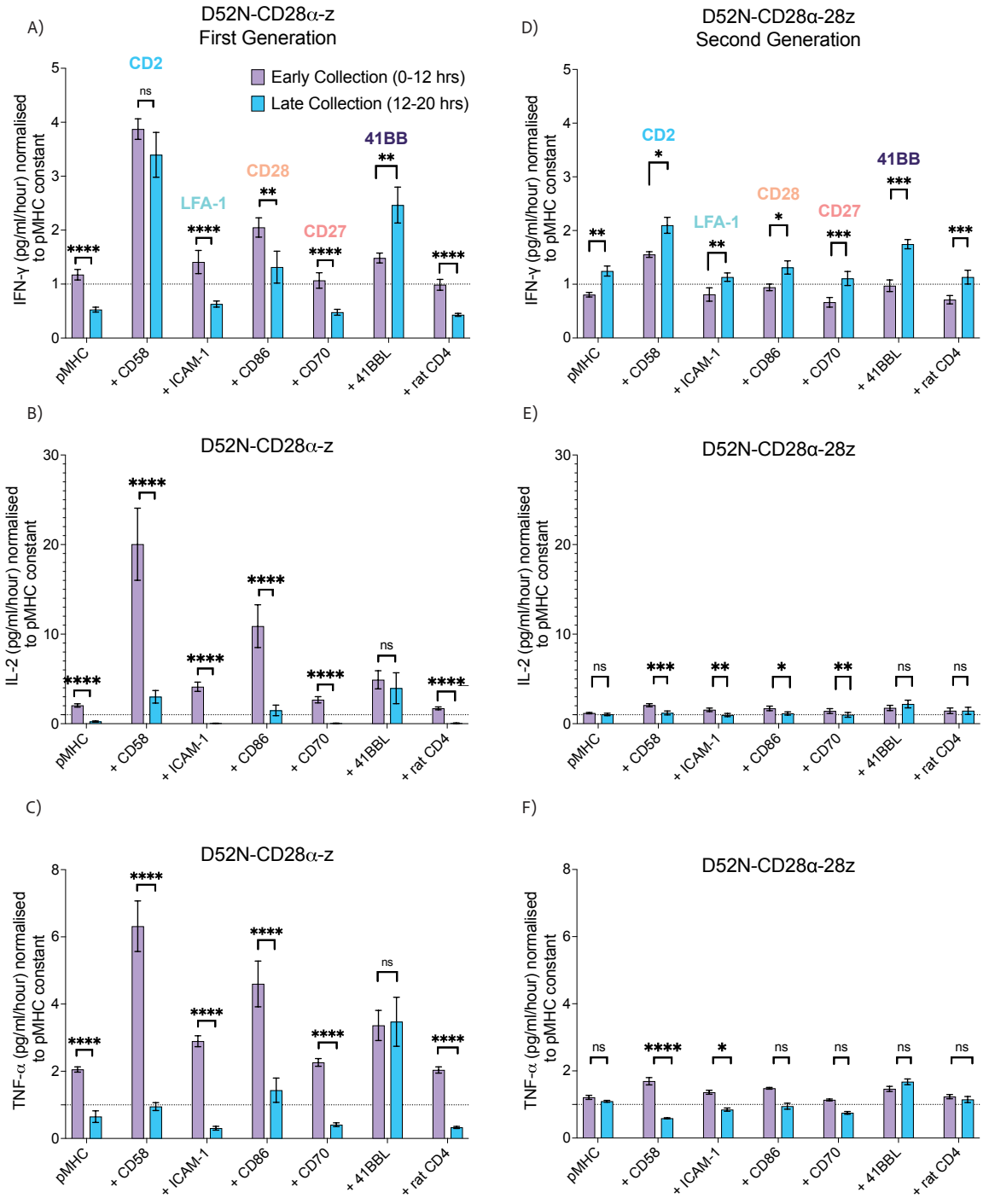


Figure 2.10: Extrinsic costimulation has a larger impact on 1st compared to 2nd generation CAR-T cells. Primary Human T cells were transduced with either a 1st generation (**A-C**) or 2nd generation (**D-F**) CAR targeting the 9V NYES0-1 pMHC. The cells were added to immobilised 9V pMHC and the rate of cytokine production (IFN-γ **(A,D)**, IL-2 **(B,E)** & TNF-α **(C,F)**) was calculated over the first collection (0-12 hours) and later collection (12-20 hours) (see **Fig. 2.4** for details). Statistical significance was determined by 2-way ANOVA on log-transformed data. Abbreviations: * = p-value$\leqslant$0.05, ** = p-value$\leqslant$0.01, *** = p-value$\leqslant$0.001, **** = p-value$\leqslant$0.0001, ns = not significant. Data is shown as a mean +/- SEM of 5 independent experiments (i.e. 5 independent human donors).

To investigate how the difference in cytokine production rate was affected under each costimulatory receptor, the rate across the late collection was divided by the rate across the early time-point to obtain a ratio that represents the extent of adaptation. A value greater than 1 corresponds to a higher rate of cytokine production over the late collection relative to the early collection, meaning that adaptation was not occurring, whereas a value below 1 meant that cytokine production was decreasing over time (Fig. 2.11). By comparing the value of this ratio under each costimulatory ligand with the ratio of antigen alone, the impact on adaptation could be quantitatively assessed. From this analysis, it is clear that 4-1BB is able to prevent adaptation of all three cytokines, with T cells expressing the TCR, 1st generation CAR, and 2nd generation CAR. Furthermore, although ICAM-1 was able to prevent a drop in IFN-γ with the TCR, the ligand could not prevent adaptation of IL-2 and TNF-α production with the TCR or 1st generation CAR. Interestingly, CD86 was able to prevent IFN-γ adaptation with the 1st generation CAR.

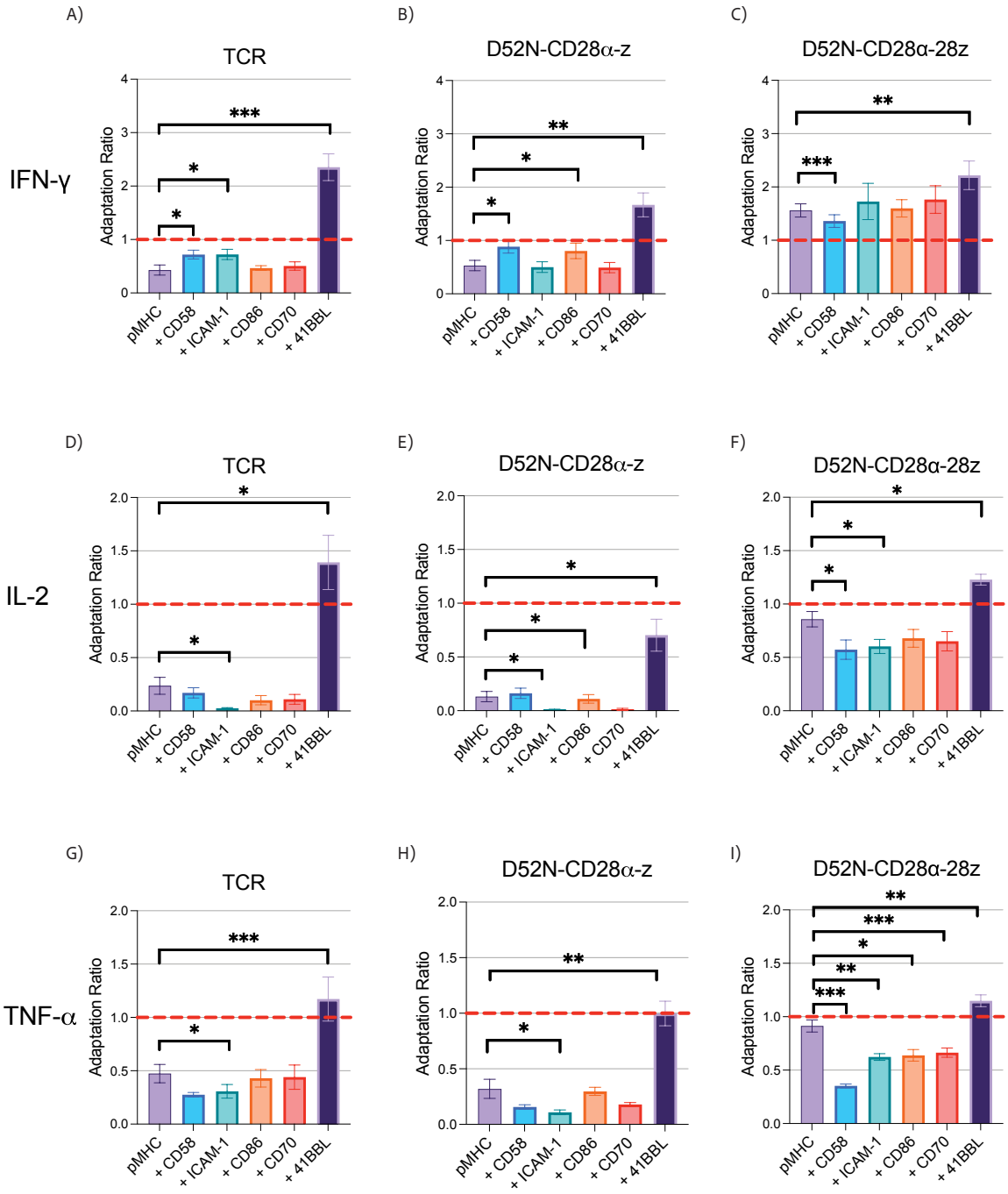


Figure 2.11: Extrinsic costimulation has a larger impact on the rate of cytokine production for the TCR and 1st generation CARs compared to 2nd generation CARs The difference in production rate between the early collection and late collection timepoints from Fig. 2.10 is represented as an adaptation ratio, whereby the late collection rate is divided by the early collection rate. A ratio of 1 means there is no difference in the rate of cyotkine production between the 2 timepoints. A ratio below 1 means cytokine production is higher over the first 12 hours of the assay. A ratio above 1 means that cytokine production is higher during the last 8 hours. Statistical significance compared to the pMHC condition was determined by 2-way ANOVA on log-transformed data. Abbreviations: * = p-value⩽0.05, ** = p-value⩽0.01, *** = p-value⩽0.001, **** = p-value⩽0.0001, ns = not significant. Data is shown as a mean +/- SEM of 5 independent experiments (i.e. 5 independent human donors).

The Supernatant Cytokine Level Scales with the Number of T Cells

As T cells sense and respond to environmental cues, we also wanted to check if harvesting the supernatant (containing the secreted cytokines) and replacing it with fresh media would impact cytokine production. By plotting the amount of cytokine produced when the T cells were incubated for 20 hours constantly over the amount produced during the early and late collection, any differences originating from the media replacement process could be observed.

Previous work has suggested that T cells can change their rate of cytokine production based on the amount of supernatant cytokine. This feedback has been suggested for IL-2 [31], indicating that replacing the supernatant at 8 hours with fresh media may have impacted the rate of cytokine production in our experimental setup. To assess this, the total amount of cytokine produced at 20 hours (without media replacement) was plotted over the sum of cytokine measured at the early and late collection (with media replacement at 8 hours) (Fig. 2.12). A slope with gradient 1 represents equal amounts of cytokine produced between the 2 conditions. For all cytokines the slope did not differ significantly from 1, meaning that replacing the media had no impact on overall cytokine production.

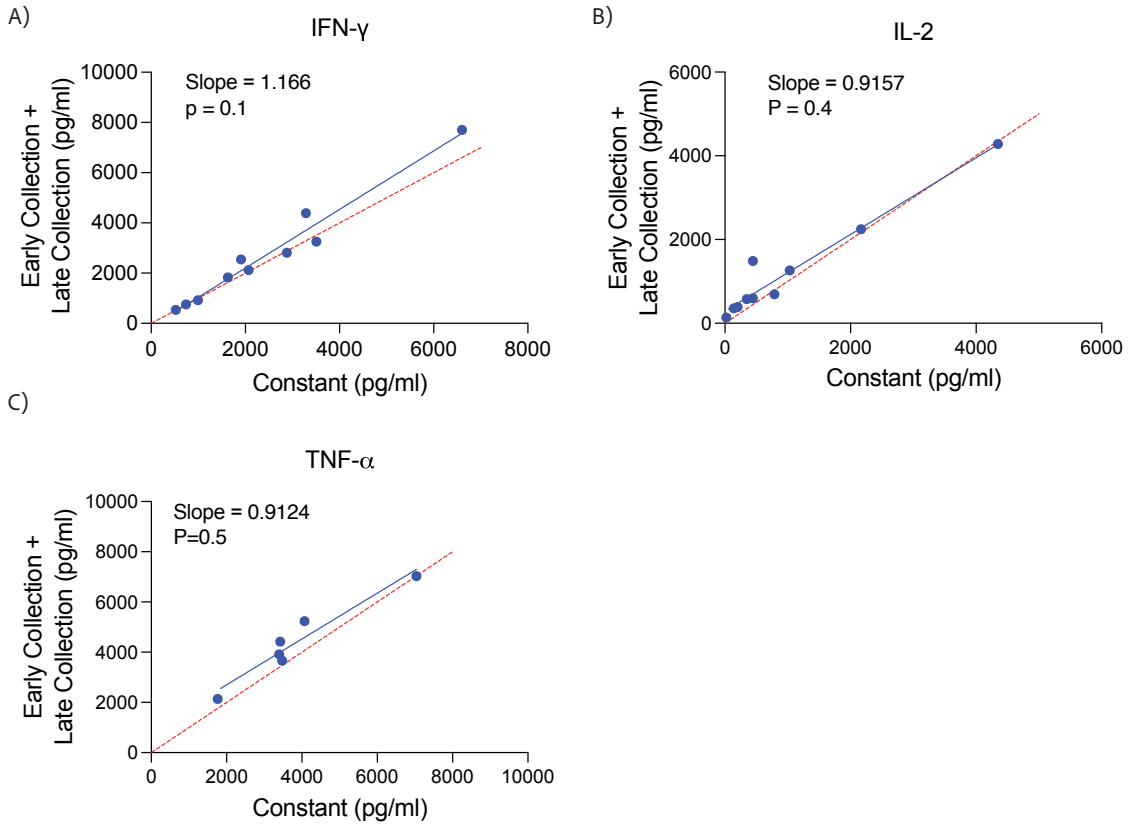


Figure 2.12: Total Cytokine produced over Collection 1 & 2 is not significantly different from total cytokine produced over 20 hours constantly. T Cells were stimulated with a fixed concentration of 9V peptide-MHC under 3 different time conditions (see **Fig. 2.4**). The sum of the cytokine concentration IFN-γ **(A)**, IL-2 **(B)** & TNF-α **(C)** over the "Early Collection" and "Late Collection" was plotted against the total concentration over the "Constant" condition. The gradient of the slopes was analysed and compared to a slope of 1 (shown in red), that represents an equal concentration of cytokine produced over the constant condition, and combining the cytokine produced over the early and late collection. Each measurement is from an independent human T cell donor.

The possibility that cytokine production by individual T cells depends on the supernatant cytokine levels raises the possibility that the number of T cells producing cytokine may impact the rate of cytokine production. To further test whether this T cell cooperativity was taking place in this experimental system, we tested whether the number of T cells had a non-linear relationship with cytokine production. To investigate whether these rates are proportional to the number of T cells, we next tested whether varying the number of T cells affects cytokine production rates (Fig. 2.13 A & B). Interestingly, the rate of cytokine production was not affected by varying the number of T cells. To test whether costimulation affects single cell behaviour, we repeated the assay with CD58, and found that the rate of IL-2 and IFN-γ, was unaltered (Fig. 2.13 C & D). The number of cells used in the adaptation assays above is indicated in red (75,000). Together with the data showing that replacing media part-way through the assay does not affect cytokine production, these results suggest that adaptation is a cell-intrinsic mechanism that is not affected by changes in the cytokine environment surrounding the T cells in this setup.

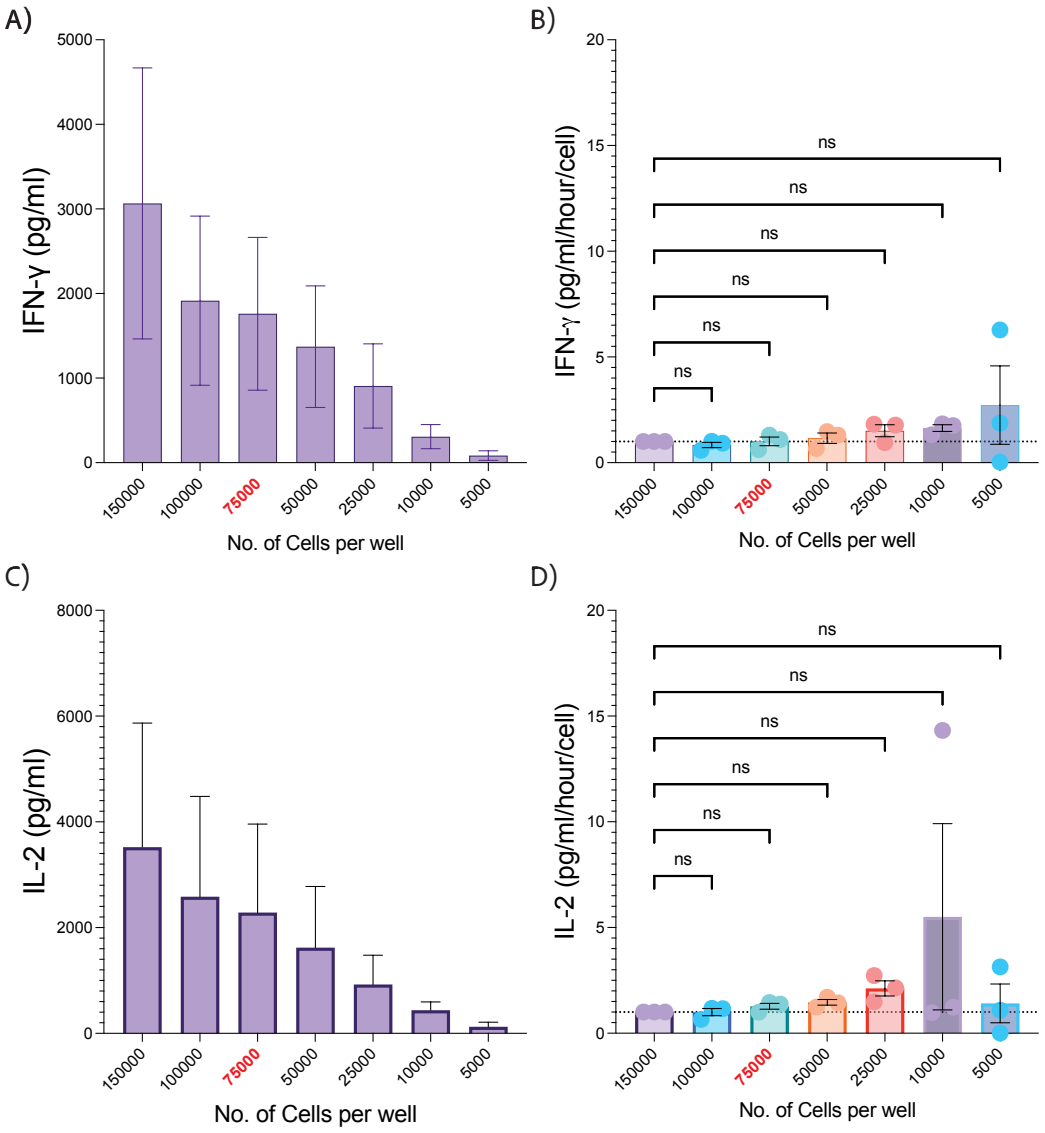


Figure 2.13: See below

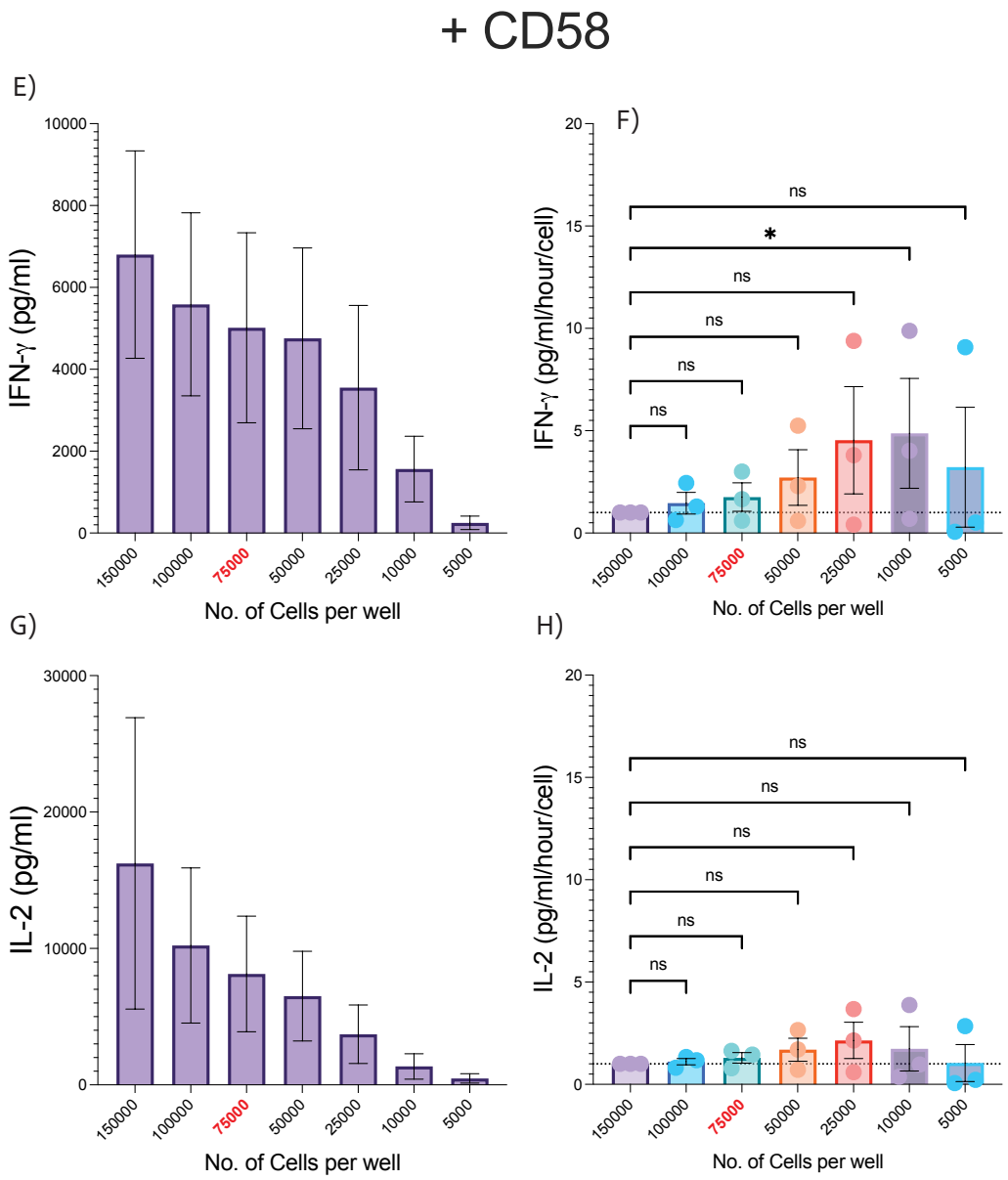


Figure 2.13: The number of T Cells does not impact the rate of cytokine production. Decreasing numbers of T cells (from 150,000 per well to 5000 per well), were added to wells coated with biotinylated 9V pMHC and biotinylated CD58 (as indicated). The cells were stimulated for 20 hours with the concentration of IFN-γ **(A & E** & IL-2 **(C & G)** under each condition analysed by ELISAs. The rate of cytokine production per hour per cell was then calculated by dividing final IFN-γ **(B & F** & IL-2 **(D & H)** concentration after stimulation by 20, then by the number of cells added to each well. Indicated in red is the number of cells (75,000), used in the adaptation assays above.

2.3 Discussion

T cells express a diverse range of costimulatory receptors that shape T cell activation [35]. Although the expression pattern and signalling mechanisms of these receptors have been extensively studied, there has been relatively few studies on their quantitative impact on T cell adaptation to antigen. Consequently, in this chapter we sought to understand the role of individual costimulatory receptors through a temporal lens, with the aim of elucidating how they function over time. It is important to clarify the dynamic role of receptors, to better understand the underlying T cell biology, and to harness these molecules more effectively in T cell therapies.

To this end we investigated the cytokine production (a key functional T cell response) over time, and the subsequent impact of the engagement of individual costimulatory receptors. With antigen alone T cells are known to become adapted over time meaning their response decreases back to a baseline level, despite persistent antigen exposure in both *in vivo* and *in vitro* studies [206–208, 234]. We were able to validate these findings, by measuring a drop in the rate of cytokine production over 20 hours, with primary human $CD8^+$ T cells. This adaptation to antigen has been suggested to play an important physiological role in regulating T cell effector function and limiting excess inflammation [235].

CD2, LFA-1 and 4-1BB costimulation prevented a drop in IFN-γ production over time. Indeed, the addition of CD58 induced a high rate of production over the earlier timepoint, whereas 4-1BBL triggered an increase in production rate over the last timepoint. Previously, differences in receptor expression have been sufficient to explain the effects of 4-1BB and CD27 on T cell adaptation [36]. Whether, the expression pattern of CD2 and LFA-1 is able to explain their ability to prevent IFN-γ

adaptation is currently unclear. However, both are constitutively expressed on resting $CD8^+$ T cells (see Chaper 3 Fig. 3.3), meaning they are well-suited to exert early effects on T cell activation (both increase cytokine production rate over the first 12 hours compared to antigen alone). Analysis of CD2 expression levels of $CD8^+$ memory T cells has revealed that the costimulatory receptor is also upregulated upon T cell activation [236].

Interestingly, CD2 and LFA-1 were unable to prevent a drop in the rate of IL-2 and TNF-α over time. As the level of cytokines in the supernatant are subject to decay via biochemical degradation and/or consumption by the T cells themselves [237], and T cells express receptors for IL-2 and TNF-α upon activation and down-regulate the R2 subunit of the IFN-γ receptor [238–240], these specific cytokine receptor kinetics suggest that IL-2 and TNF-α are consumed as the assay progresses, whereas IFN-γ consumption is reduced over time.

As cytokine consumption involves T cell sensing to their environment and responding accordingly, it would be expected that harvesting cytokine-containing media mid-way through the assay would impact their uptake by T cells. However, when the impact of media replacement on cytokine production was calculated, no effect was observed. Another factor contributing to cytokine production rates is the individual production kinetics of the cytokines themselves. For example, previous work using this experimental system has has shown that in $CD8^+$ T cells stimulated by plate-bound antigen, TNF-α production peaks at 2 hours, whilst the production of IL-2 and TNF-α returns to baseline levels by 4-6 hours [208]. In contrast, IFN-γ levels continue to rise at 8 hours. Therefore, our assay setup is better suited to capture the increase in IFN-γ production, compared to the rise in TNF-α and IL-2 that most likely occurs within the first time point. Taken together, our results suggest that

supernatant IFN-γ most faithfully represents cumulative cytokine produced by T cells with little impact of degradation or uptake. Based on IFN-γ, we can therefore conclude that CD2 and LFA-1 can prevent adaptation of T cells to antigen for the TCR.

To resolve whether levels of IL-2 and TNF-α are subject to consumption/degradation, a more direct measurement of cytokine production such as mRNA level analysis, or cytokine capture on individual T cells would be useful. Intracellular staining is also an established method for cytokine detection, however we chose not to use this as our main measurement of cytokine production as the method requires blocking secretion, that may have varying impacts on different cytokines that are secreted via different mechanisms [237].

It is still unclear whether adaptation is a cell intrinsic phenomenon, or is reliant on cell-cell communication. Our analysis focused on population level read-outs of the T cell response, however analysis of the impact of cell number and surrounding cytokine levels on cytokine production revealed little impact on cytokine production, suggesting that adaptation is not reliant on changes in the surrounding environment. A more direct measurement of single-cell cytokine production would help clarify the mechanism behind adaptation. Interestingly, a previous study using single cell cytokine measurements, revealed that $CD4^+$ T cells exhibited digital cytokine production at low pMHC densities [22]. Consequently, population level changes in cytokine levels would result from a higher proportion of responding T cells (as opposed to individual T cells producing more cytokine). Therefore measuring single cell cytokine production would provide further information of how adaptation is overridden by certain costimulatory receptors.

T cells also express co-inhibitory receptors, that are known to play a role in T cell dysfunction [210, 241]. Therefore, it would be interesting to test the interplay of costimulatory and coinhibitory receptors in overriding T cell responses. Our reductionist experimental platform allows individual ligands against receptors of interest to be varied independently. This would provide a valuable insight into how costimulatory molecules behave *in vivo*, and how costimulation affects adaptation in the overall context of T cell biology.

CAR-T Cells & Adaptation

Adaptation to antigen is particularly important in chronic conditions where T cells undergo persistent stimulation, such as in cancer. Indeed, maintaining T cell responses within the tumor microenvironment is a key area of current CAR-T cell research [242]. As a challenge of current CAR-T immunotherapy is the limited persistence of CAR-T cells *in vivo*, and CAR-T cell function has been shown to dampen with constant antigen exposure over time [243], we were especially interested to investigate the adaptation phenotype of CARs in our system, with and without costimulation. This is important given that the persistence of infused CAR-T cells is linked with long-term remission, and patient survival [222, 223, 244–246].

Harnessing a system in which the TCR and 1st and 2nd generation CARs could target the same antigen (NY-ESO1 9V), 1st generation CARs containing CD3-ζ signalling domains exhibited adaptation phenotypes that were largely comparable to the TCR. With antigen alone, 1st generation CAR-T cells adapted to antigen over time, which was prevented by the engagement of CD58 and 4-1BBL. In contrast, 2nd generation CAR-T cells, that generate intrinsic CD28 cosignalling, were able to prevent adaptation over time independent of extrinsic costimulation. In addition, the rate of IFN-γ

production actively increased during the later timepoint, resembling what we observe with 4-1BB costimulation of the TCR. Consequently, the effect observed with the 2nd generation CAR could be due to increased CAR expression relative to the TCR at later stages of activation. This is supported by observations that lower CAR expression is associated with lowered T cell responsiveness [247–249], implicating receptor expression in CAR-T cell effector function.

In addition, as 1st and 2nd generation CARs have displayed similar killing capacities *in vitro*, the ability of 2nd generation CARs to be more effective *in vivo* has been noted to be likely due to their enhanced persistence and cytokine production [180, 194, 195, 198, 250]. Our observations that 2nd generation CARs display more persistent cytokine production than 1st generation CARs, and prevent adaptation support these *in vivo* findings.

Interestingly, the engagement of extrinsic 4-1BB on 2nd generation CAR-T cells was able to further enhance the rate of cytokine production compared to antigen alone, highlighting the ability of the CAR-T cells to capitalise on 4-1BB costimulation to further accelerate cytokine production. Indeed, a CD28-containing CAR co-expressing 4-1BBL displayed improved T cell persistence and anti-tumour activity [198], highlighting the added impact of extrinsic costimulation on 2nd generation CARs. This is particularly relevant as costimulatory molecules display varying behaviour, depending on whether they are incorporated within the CAR structure, or engaged separately. In our study, CD28 within a CAR was able to override adaptation, however when CD28 was engaged by CD86 alongside the CAR, no impact on adaptation was observed. Further studies testing the incorporation of different costimulatory molecules within CARs and the impact on adaptation to antigen would be useful. For example, although 4-1BB has the strongest ability to prevent adaptation, CARs

incorporating 4-1BB have been shown to drive mouse CAR-T cells to dysfunction ([243]. CD2 is able to prevent adaptation but the rate of cytokine production is lower compared to 4-1BB at later timepoints, therefore CD2 may be able to provide a more measured and sustained T cell response. Our findings, together with *in vivo* work on T cell persistence, highlights the importance of careful consideration of costimulation in CAR-T cell design. To address challenges in achieving long-term remission of cancer patients treated with CAR-T cell therapy, incorporation of particular costimulation within the CAR could help sustain cytokine production over time, leading to improved therapeutic outcomes.

Chapter 3

The Effect of Costimulatory Receptors on T Cell Sensitivity to Antigen

3.1 Introduction

3.1.1 T Cell Sensitivity to Antigen

T cells are remarkably sensitive: they can recognise and respond to as few as ~1-10 cognate antigens. Studies have revealed that $CD4^+$ T cells respond to a single pMHC *in vitro* [22, 199], whilst 1-3 peptide antigens are sufficient to induce $CD8^+$ T cells to become functionally responsive [200].

This high sensitivity is thought to be important in the context of infection and cancer, where mounting effective immune responses relies on the recognition of a few viral or tumour pMHC molecules. Indeed, infected cells [251], and cancer cells [252] have been found to reduce antigen present at the cell surface to evade immune detection. An *in vitro* study of human cytomegalovirus (HCMV) infection found HCMV able to lower pMHC levels from 10,000 to fewer than 100 [253]. Furthermore, in both murine and human infection models, $CD8^+$ T cells that can detect extremely low levels of antigen are more effective at eliminating viruses [254–257]. High sensitivity to antigen is therefore an important feature governing an effective immune response.

3.1.2 Mechanisms of T cell Sensitivity to Antigen

A number of mechanisms have been suggested to contribute to a T cell's sensitivity to antigen [258]. They can be classified as either promoting TCR/pMHC binding (increasing the k_{on} rate and/or decreasing the k_{off} rate), amplifying proximal TCR signalling (via phosphorylation of TCR-associated ITAMS or ZAP-70) or amplify-

ing downstream (distal) TCR signalling. Given that the TCR interacts with pMHC in the context of many other costimulatory receptors *in vivo*, the impact of these costimulatory receptors on the antigen sensitivity of T cells has been of increasing interest. CD2 and LFA-1, have both been found to increase antigen sensitivity in early functional studies involving CD2-deficient and LFA-1-deficient murine T cells [114, 87]. This was subsequently supported by studies showing that engagement of CD2 and LFA-1 with their human ligands (CD58 and ICAM-1), lowered the amount of antigen required for human T cell activation [229]. In addition, both costimulatory receptors have been found to increase TCR downregulation [87, 259, 260]. Given that TCR downregulation is partly induced by binding to pMHC, this observation is consistent with these adhesion receptors promoting TCR/pMHC binding.

The role of CD28 on antigen sensitivity, however, is less clear. Early murine studies showed that CD28 allows T cells to respond to low concentrations of antigen by reducing the signalling threshold for T cell activation [114, 261–263]. However, a more recent comparison of the impact of CD2 and CD28 on antigen sensitivity with human $CD8^+$ T cells, revealed that CD28 had only a modest impact on antigen sensitivity [227]. Moreover, a large number of studies have claimed that CD28 improves antigen sensitivity but often with an imprecise definition of sensitivity that confused changes in efficacy (E_{Max}) with changes in sensitivity (EC_{50}) [130, 139, 264–267].

3.1.3 Quantitatively Defining Sensitivity

The sensitivity of T cells to antigen can be assessed by measuring T cell activation (e.g. the expression of a surface protein by flow cytometry or the secretion of a cytokine protein by ELISA) for different antigen concentrations [268]. Antigen sensitivity can be quantified by generating dose-response curves and calculating the antigen dose that elicits half of the maximal response, termed the EC_{50}.

So far there is no study to date that directly compares the quantitative impact of CD2, LFA-1 and CD28 on the sensitivity of primary human $CD8^+$ T Cells to antigen. Here, we employed a reductionist system to titrate purified pMHC alone or in combination with different concentrations of ligands to CD2, LFA-1, and CD28 to quantitatively compare the antigen sensitivity of primary human $CD8^+$ T cells. Whereas engagement of CD2 and LFA-1 are able to increase the antigen sensitivity of the TCR, no evidence is found that CD28 can impact antigen sensitivity. The implications and limitations of these results are discussed.

3.2 Results

3.2.1 Ligands to CD2 and LFA-1, but not CD28, can Increase the Antigen Sensitivity of Primary Human CD8$^+$ T cells

To systematically quantify the relative abilities of CD2, LFA-1, and CD28 to increase T cell antigen sensitivity, an experimental system is required where these ligands can be independently controlled. Therefore, we used the system described in Chapter 2 where purified biotinylated pMHC antigen was titrated alone or in combination with different concentrations of purified biotinylated ligands to CD2, LFA-1, and CD28.

Titrating concentrations of biotinylated CD58, ICAM-1 and CD86, together with different concentrations of pMHC were presented to blasted human CD8$^+$ T cells, transduced with the 1G4 TCR, that recognises the short 9V peptide from NY-ESO-1 protein presented on HLA-A*02:01 (9V pMHC). After 6 hours, the expression of T cell surface activation markers, CD69 and 4-1BB, were analysed by flow cytometry, and the level of IL-2, IFN-γ and TNF-α in the supernatant measured by ELISAs (Fig. 3.1).

Stimulating T cells with pMHC alone (without costimulatory ligand), resulted in the expected dose-dependent increase in the up-regulation of 4-1BB and CD69. Addition of ligands to CD2 (CD58) and LFA-1 (ICAM-1), but not CD28 (CD86) induced T cell activation at lower concentrations of pMHC (i.e. increased antigen sensitivity) (Fig. 3.1 A, B). The impact of each costimulatory ligand presented at the highest concentration was quantified across multiple independent experiments (using T cells from different leukocyte cones), by extracting the EC_{50} from fitting a Hill model to individual dose-response curves (Fig. 3.1 D, F).

The ligation of CD2 and LFA-1 with CD58 and ICAM-1 resulted in a significant decrease in EC_{50}, with both receptors inducing a ~250-fold decrease in EC50 (increase in antigen sensitivity) as measured by surface 41BB upregulation after 6 hours (Fig. 3.1 D). Interestingly, the engagement of CD28 with CD86 had little impact on sensitivity, even at the highest concentration of costimulatory ligand, with no significant difference in EC_{50} observed, compared to antigen alone.

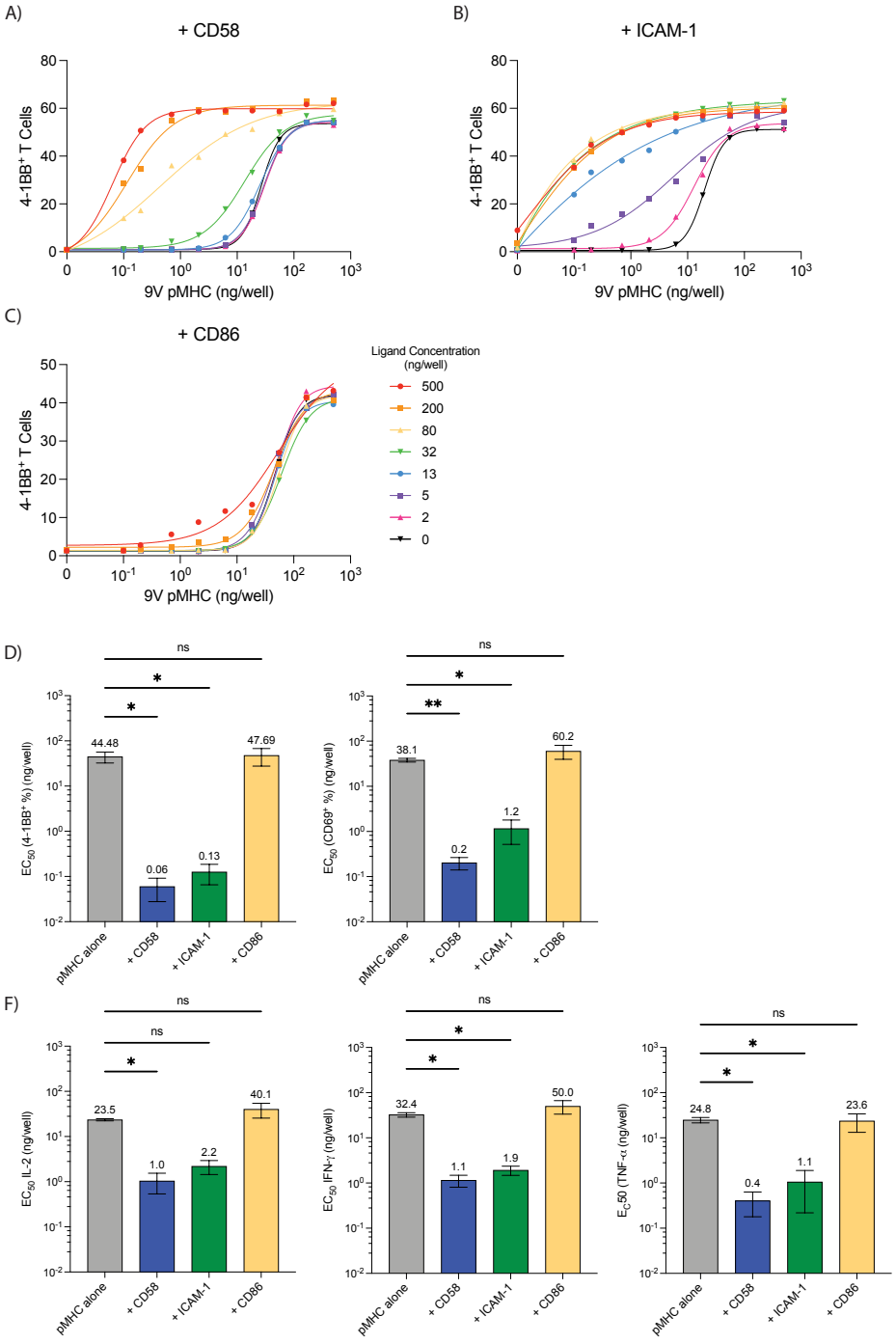


Figure 3.1: Plate-Bound CD58 and ICAM-1 enhances T Cell Sensitivity to Antigen over 6 Hours Biotinylated 9V pMHC (250 ng/well) and a titrating concentration of costimulatory ligand were immobilised on streptavidin-coated plates. Primary Human $CD8^+$ T cells transduced with the 1G4 TCR were added to ligands for 6 hours. At the end of the assay the expression of 4-1BB and CD69 was analysed by flow cyotmetry, and the concentration of cytokines (IL-2, IFN-γ, and TNF-α) in the supernatant analysed by ELISAs. **D) & F)**The resulting dose-response curves were fitted using a sigmoidal fit in PRISM, with the EC_{50} values from the highest concentration of ligand (500ng/well) and pMHC alone condition extracted. Statistical significance was determined by paired t-test on log-transformed data. Abbreviations: * = p-value$\leqslant$0.05, ** = p-value$\leqslant$0.01, *** = p-value$\leqslant$0.001, **** = p-value$\leqslant$0.0001, ns = not significant. Data is shown as a mean +/- SEM of 3 independent experiments (i.e. 3 independent human donors).

The kinetics of each functional read-out is different raising the possibility that CD28 can enhance antigen sensitivity but on a different timescale compared to CD2 and LFA-1. For example, the surface expression of 4-1BB is induced on primary human $CD8^+$ T cells following antigen recognition on a timescale of 8-16 hours, whilst IFN-γ production has been observed to continue to increase past 16 hours [36, 269]. Therefore we repeated the assay over 20 hours, to investigate whether the phenotype of CD28 observed was time-dependent.

After 24 hours, CD2 and LFA-1 significantly enhanced antigen sensitivity across both activation markers and cytokines (Fig. 3.2 D, F), whereas CD28 engagement did not impact antigen sensitivity, consistent with our findings at 6 hours.

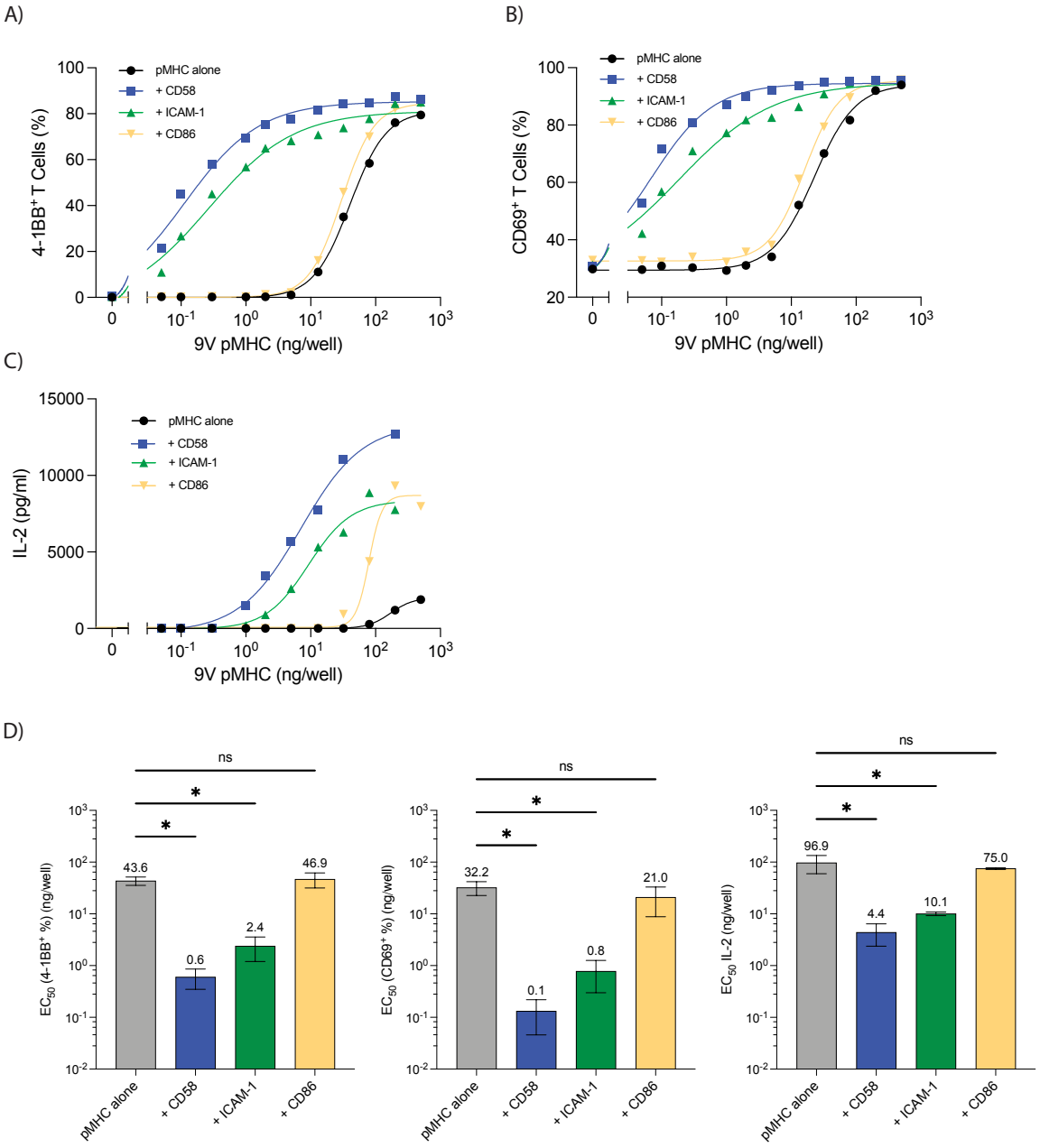


Figure 3.2: Plate-Bound CD58 and ICAM-1 enhances T Cell Sensitivity to Antigen over 24 Hours T cells were added to increasing concentrations of immobilised 9V pMHC and costimulatory ligand (250ng /well) for 24 hours before 4-1BB and CD69 expression was analysed by flow cytometry and IL-2 levels in the supernatant measured by ELISAs. Data was fit using sigmoidal curves in PRISM. Statistical significance was determined by paired t-test on log-transformed data. Abbreviations: * = p-value⩽0.05, ** = p-value⩽0.01, *** = p-value⩽0.001, **** = p-value⩽0.0001, ns = not significant. Data is shown as a mean +/- SEM of 3 independent experiments (i.e. 3 independent human donors).

Previous work has highlighted that CD28 expression decreases with age on $CD8^+$ T cells [131]. Therefore, we analysed CD28 expression across multiple donors, (Fig. 3.3), and found that in contrast to the uniform expression of CD2 and LFA-1, the expression of CD28 varied between 40-80%, which is in agreement with previous findings [131, 270–272]. Moreover, when the expression of CD69 and 4-1BB was analysed specifically on $CD28^+$ T cells no differences in antigen sensitivity were found between this subset and the overall population of T cells used (Fig. 3.4).

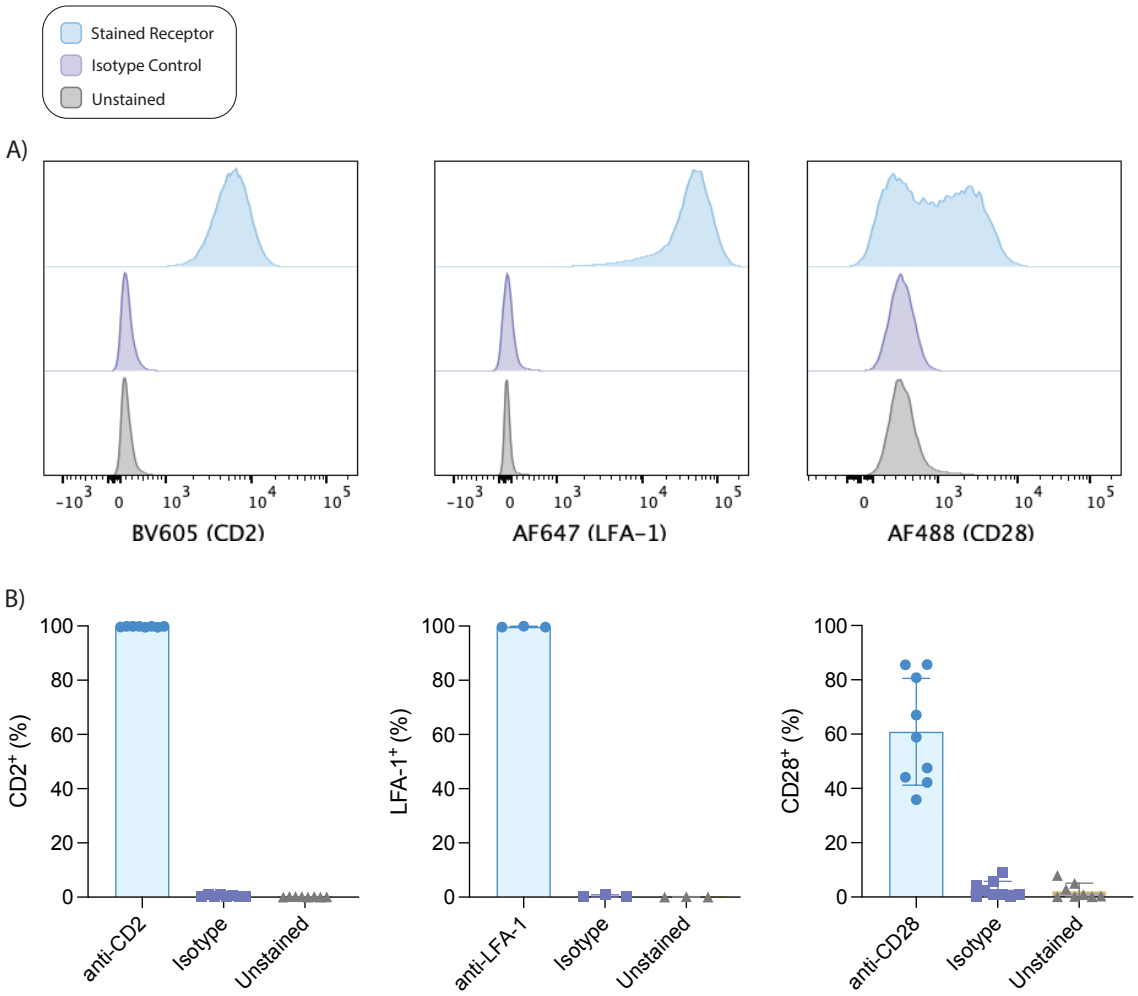


Figure 3.3: The Expression of CD28 on Resting CD8$^+$ T Cells Varies Between Human Donors, whilst the expression of CD2 and LFA-1 remains constant. Resting CD8$^+$ T cells were stained with fluorescently-conjugated antibodies against the CD2, LFA-1 and CD28 costimulatory receptors. **(A)** Flow cytometry histograms comparing the expression of each costimulatory receptor with unstained samples and and isotype control for each antibody used. **B)** Expression of CD2, LFA-1 and CD28 was quantified across multiple donors. Data is shown as a mean +/- SEM of at least 3 independent experiments (i.e. 3 independent human donors).

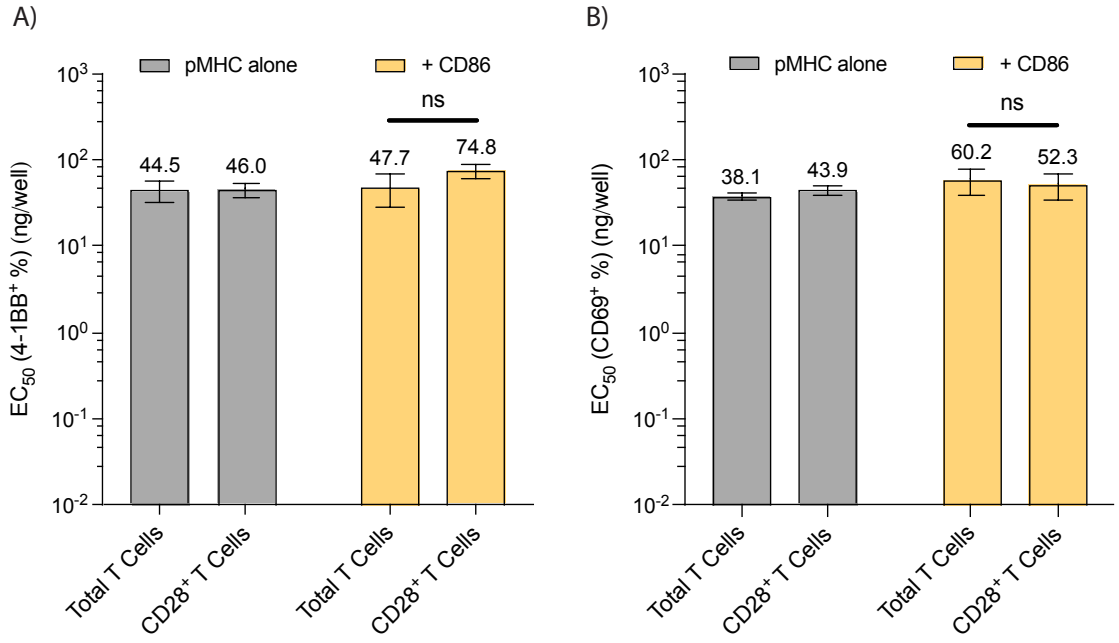


Figure 3.4: The Expression of CD28 on T cells has no Impact on Antigen Sensitivity. T cells were stimulated with 9V pMHC or a combination of 9V pMHC and CD86 (500ng/well) for 6 hours before 4-1BB and CD69 expression was analysed by flow cytometry. T cells were gated on $CD28^+$ expression and analysed for 4-1BB and CD69 expression. The data was fitted in PRISM. Statistical significance was determined by paired t-test on log-transformed data. Abbreviations: * = p-value$\leqslant$0.05, ** = p-value$\leqslant$0.01, *** = p-value$\leqslant$0.001, **** = p-value$\leqslant$0.0001, ns = not significant. Data is shown as a mean +/- SEM of 3 independent experiments (i.e. 3 independent human donors).

3.2.2 Engagement of CD2, LFA-1 & CD28 Amplify Total Cytokine Produced

Although engagement of CD28 by CD86 did not impact antigen sensitivity, we observed that it increased antigen efficacy which is defined as the maximum amount of cytokine produced (i.e. E_{Max}). Antigen efficacy was calculated for both the 6 hour (Fig. 3.5) and 20 hour experiment Fig. 3.6).

After 6 hours, ligation of CD2 resulted in significant increases in IL-2, IFN-γ and TNF-α in the supernatant [227]. Although ligation of LFA-1 did not produce a significant increase in cytokine production, ligation of CD28 significantly increased IL-2 production. After 20 hours, CD2, LFA-1 and CD28 significantly increased IL-2 production, whilst CD2 and LFA-1 also enhanced the total concentration of IFN-γ. Taken together, all costimulatory receptors elevated levels of cytokines compared to antigen alone. Furthermore, this confirms that the purified CD86 is a functional protein that can increase antigen efficacy but not antigen sensitivity when binding to CD28 in this experimental system.

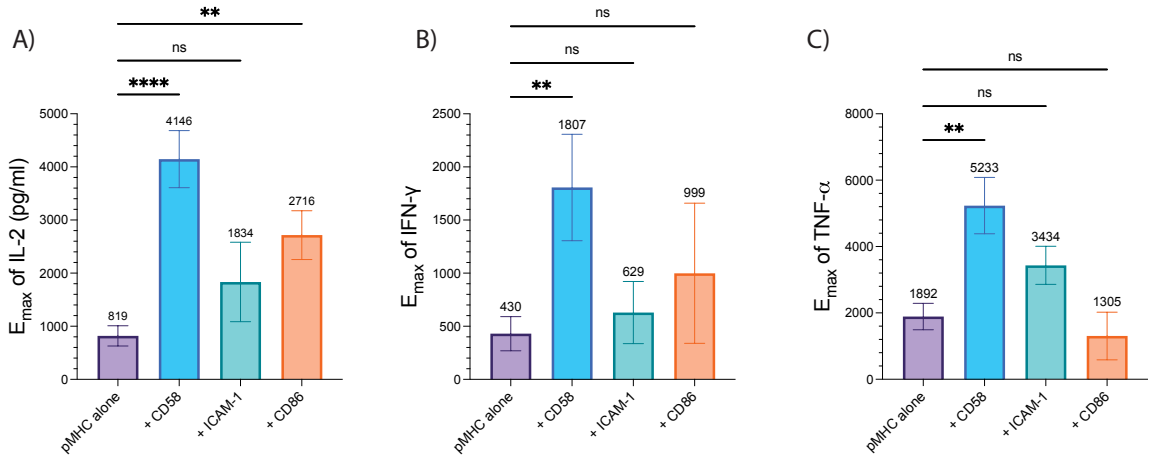


Figure 3.5: Ligation of CD2 amplifies Cytokine Production after 6 hours T cells were stimulated with an increasing titration of 9V pMHC and 500ng/well costimulatory ligand (CD58, ICAM-1 or CD86), as indicated for 6 hours.The supernatant was harvested and concentration of IL-2, IFN-γ and TNF-α analsyed via ELISAs. The data was fit in PRISM, with the maximum amount of cytokine under each condition extracted. Statistical significance was determined by paired t-test on log-transformed data. Abbreviations: * = p-value$\leqslant$0.05, ** = p-value$\leqslant$0.01, *** = p-value$\leqslant$0.001, **** = p-value$\leqslant$0.0001, ns = not significant. Data is shown as a mean +/- SEM of 3 independent experiments (i.e. 3 independent human donors).

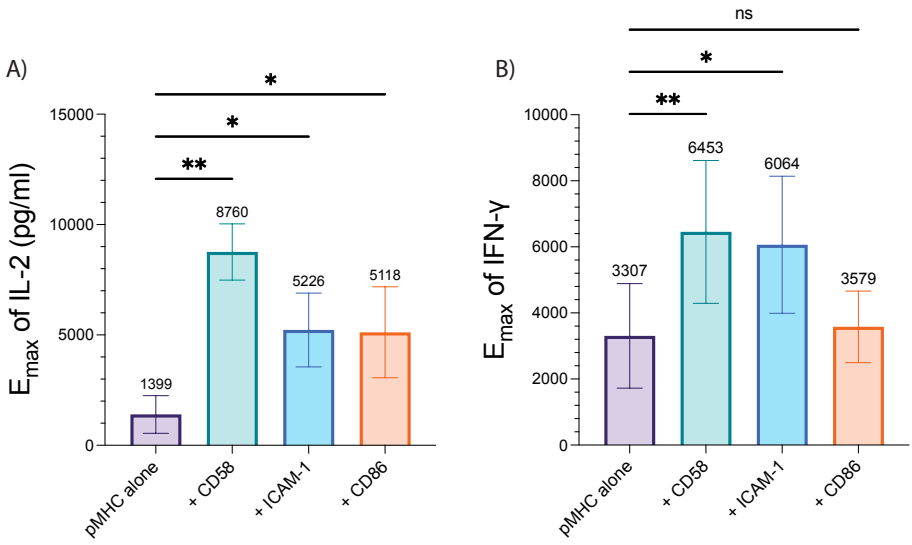


Figure 3.6: Ligation of CD2, LFA-1, CD28 amplifies IL-2 Production over 20 hours. T cells were stimulated with an increasing titration of 9V pMHC and 200ng/well costimulatory ligand (CD58, ICAM-1 or CD86), as indicated for 20 hours.The supernatant was harvested and concentration of IL-2, IFN-γ and TNF-α analsyed via ELISAs. The data was fit in PRISM, with the maximum amount of cytokine under each condition extracted. Statistical significance was determined by paired t-test on log-transformed data. Abbreviations: * = p-value$\leqslant$0.05, ** = p-value$\leqslant$0.01, *** = p-value$\leqslant$0.001, **** = p-value$\leqslant$0.0001, ns = not significant. Data is shown as a mean +/- SEM of 3 independent experiments (i.e. 3 independent human donors).

3.3 Discussion

Using a reductionist plate-based system, that allows careful control of purified antigen and ligands to different accessory receptors, we was able to directly compare the impact of CD2, LFA-1 and CD28 costimulation on the antigen sensitivity using primary human $CD8^+$ T cells. We were able to confirm previous findings that CD2 and LFA-1, strongly enhanced T cell sensitivity to antigen [87, 229, 273]. Indeed, ligation of CD58 and ICAM-1 induced a decrease in EC_{50} after 6 hours, quantitatively consistent with previous work [274]. Murine studies, conducted on the antigen sensitivity of CD2 and LFA-1, are also qualitatively in line with our observations that CD2 and LFA-1 enhance T cell antigen sensitivity but found the impact to be lower. Indeed, ligation of CD2, resulted in a $3 - 100$ fold reduction in antigen dose required to elicit proliferative and cytokine secretion responses from murine T cells [87, 275, 276], and LFA-1 knock-out T cells required $10 - 100$ fold higher doses of antigen to elicit the same level of expression of activation markers and TCR down-regulation [260, 114, 121]. However, the murine counterpart of CD58 (CD48) binds CD2 with a lower affinity, which may explain its smaller quantitative impact [277]. Indeed, murine studies have found a more subtle role for CD2 [278] which would also explain the more restricted tissue expression of murine CD48 [279] compared to the ubiquitously expressed human CD58 [280]. In addition, the murine experiments were performed using APCs and therefore, additional costimulatory ligands could be present, that compensate for the lack of CD2/CD48 in the context of antigen sensitivity.

Although ligation of CD28 with CD86 increased antigen efficacy (the maximum amount of cytokine produced), it did not impact antigen sensitivity. In contrast, previous work has reported that ligation of CD28 increases antigen sensitivity [263, 281, 114].

A key difference between these studies and the present work is the use of naïve T cells in the former studies and previously activated T cells in our work. Indeed, a study directly comparing naïve and effector T cells with agonistic anti-CD28 antibodies, showed a more modest impact of CD28 on the antigen sensitivity of effector cells [282]. Mechanistically, ligation of CD28 does not impact TCR downregulation [260, 114, 282], which is a proxy for TCR/pMHC binding and therefore, any impact that CD28 may have on antigen sensitivity is likely a result of intracellular signal integration.

Further work on investigating the role of CD28 on antigen sensitivity in naïve T cells would be interesting in order to clarify how CD28 could impact antigen sensitivity in one T cell subset but not another. In addition, as T cells interact with multiple costimulatory ligands simultaneously, it would be useful to investigate the impact of CD28 on antigen sensitivity in the context of engaging additional costimulatory receptors. In particular, T cells showed a reduced ability to adhere to planar bilayers containing CD80 compared to CD58 [283], therefore CD28 may require the aid of adhesion molecules such as CD2 and LFA-1 to exert an impact on antigen sensitivity.

CD2 and LFA-1's positive impact on sensitivity is consistent with their role as adhesion molecules in promoting T cell activation via stabilisation of TCR and pMHC interactions (by increasing the number of engaged TCRs through binding kinetics). Indeed, both CD2 and LFA-1, when engaged with their ligands, have been found to enhance TCR downregulation [87, 259, 260], further supporting their enhancement of TCR-pMHC interactions. The intermembrane distance between receptor/ligand pairs has been proposed to play a key role in the kinetic segregation model of TCR triggering, via the formation of close contact zones [109]. The CD2-CD58 complex spans a length of approximately 14nm, resulting in a distance that matches the

height of TCR-pMHC interactions [18]. Consequently, CD2 has been suggested to promote TCR-pMHC binding through the formation of close contact zones [51, 278]. In contrast LFA-1-ICAM-1, that spans a distance of ~40nm [54, 284, 285], and has found to be segregated away from the TCR [286, 273], allowing the formation of the close contact zones [51, 287]. Therefore, although both CD2 and LFA-1 enhance the sensitivity of T cells to antigen, it is likely they contribute to the stabilisation of TCR-pMHC binding in different ways due to large structural differences between the receptor-ligand interactions.

CD2, LFA-1 and CD28 were found to increase antigen efficacy when measuring IL-2 production (i.e. the maximum amount of IL-2 produced). The ability of CD28 to increase antigen efficacy without impacting antigen sensitivity is likely a result of a more distal signal integration with the TCR signalling pathway. Specifically, CD28 has been demonstrated to amplify PI3K which is downstream of the TCR complex and therefore, is unlikely to participate in the response decision.

Although CD2 [62, 61, 288], and LFA-1 [289, 290, 119, 291, 292] have both been found to induce intracellular signalling through their cytoplasmic tails, which is independent to their adhesive functions, it is currently unclear whether the amplification of downstream cytokine production is due to the signalling capabilities of the receptors. In particular, the avidity of CD2-CD58 interactions has been proposed to increase upon TCR signalling [59, 74, 293, 288], meaning that a positive feedback loop could exist involving increased TCR signalling from increased avidity, ultimately leading to elevated cytokine production. To further dissect the role of adhesion and intracellular signalling on total cytokine production, mutations of their cytoplasmic tail could be carried out to see to what extent they affect cytokine production.

3.3.1 Limitations of a Plate Based System for Studying T Cell Activation

Although our *in vitro* system permits careful control over the surface T cells interact with, in a high-throughput manner, it has several limitations. This system relies upon immobilising costimulatory ligand and pMHC onto a solid surface. However, these ligands are typically presented on the cell surface where they undergo diffusion. This mobility likely facilitates the formation of close-contacts and the large-scale immunological synapse that follows [43, 294]. Consequently, we cannot exclude the possibility that the inability of CD28 to increase antigen sensitivity is a result of its ligand, CD86, being immobile in our plate-based system. The other primary human ligand for CD28 is CD80, that exists physiologically as a dimer and requires dimerization for optimal costimulation of T cell proliferation [132]. Therefore, ligand mobility is important to fully understand the impact of CD28 on T cell activation. In addition, given that naïve T cells have been shown to be more reliant on costimulation compared to effector and memory subsets [295], with subsequent studies confirming that memory and effector T cells exhibit a lower activation threshold requiring less antigen to be activated than naïve T cells [296–300], it would be interesting to study the effect of the CD2, LFA-1 and CD28 costimulatory receptors on naïve T cells.

Overall we have shown that by harnessing a reductionist plate system, the individual impact of CD2, LFA-1 and CD28 on antigen sensitivity of primary human $CD8^+$ T cells was established, with differences observed between CD2 and LFA-1 that exhibit adhesion functions that may facilitate their ability to enhance antigen sensitivity, and CD28 that is unable to exert an effect on T cell sensitivity to antigen.

Chapter 4

A Cellular System to study T Cell-APC Interactions using SpyCatcher / SpyTag

4.1 Introduction

4.1.1 Studying Individual Cell-Cell Interactions

T cells recognise peptide antigens (pMHC) in the context of many additional accessory receptors that bind their ligands on the opposing cell. It is widely known that the surface composition and density of ligands for T cell accessory receptors can vary significantly across different cells. For example, tumour cells have been found to downregulate CD58, which has been suggested to be a potential mechanism for immune evasion [301–304]. Similarly, cells infected with human cytomegalovirus (HCMV) exhibit suppressed CD58 expression. Despite these differences in ligand composition, studying how different combinations and concentrations of ligands impact T cell activation has been challenging due to the difficulty of titrating them onto the surface of cells. In contrast, surface receptors such as GPCRs, RTKs, and cytokine receptors, which recognize soluble ligands, have been relatively easier to study, as the concentration and combination of these ligands are easier to control. Consequently, these experimental limitations have impeded our progress in understanding how receptor/ligand interactions at the cell surface impact T cell responses.

4.1.2 Limitations of Current Approaches to Present Ligands to T cells

Established systems used to currently study T cell interactions are limited in their ability to present physiological, surface-bound ligands, in a dose-specific manner to T cells. In previous chapters, we have highlighted the importance of studying dose-dependent phenotypes of T cell responses, to understand the distinct roles of costimulatory receptors in T cell activation. However, it is challenging to manipulate the concentration of antigen along with costimulatory ligand on the surface of cells with current experimental systems.

One approach involves surface-bound assays (as utilised in Chapters 2 and 3), which use recombinant ligand or antibody immobilized to a solid-phase surface, enabling precise dose control. However, these assays do not allow for lateral receptor/ligand mobility, a crucial feature for the coordinated clustering of membrane and signalling proteins and subsequent T cell responses [294]. Supported lipid bilayers offer ligand mobility and are routinely used to study T cell activation [305], but it is challenging to produce planar bilayers in a high throughput 96-well format and indeed, most studies focus on producing a handful of conditions [306–308].

Artificial APCs have been developed to mimic physiological membrane dynamics, however, they are limited in their ability to precisely control ligand dosage, requiring the additional use of cell sorting by expression level, inducible expression systems, or neutralizing antibodies to manipulate ligand levels [309]. For example, murine stimulator cells expressing human costimulatory ligands have been successfully employed to study the effect of costimulatory receptors. Nevertheless, these cells rely on an anti-CD3 antibody to stimulate antigenic signalling in primary human T cells

[310]. Human cells expressing pMHC complexes against major viral epitopes and costimulatory ligands have also been developed to provide antigen-specific T cell responses, but they lack control over the level of ligand presented [311]. The current gold standard involves the individual removal of unwanted ligands from target cells (e.g. via CRISPR). However, the interplay of multiple ligands quickly becomes challenging because removing, for example, 10 ligands in all combinations requires the generation of over a thousand cell lines. Moreover, this system does not allow precise titration of ligand levels on the cell surface.

Taken together, there is a lack of experimental platforms that can enable the direct titration of different combinations of ligands on the cell surface. This has hindered progress towards a comprehensive understanding of how receptor/ligand interactions at cellular interfaces impact cellular responses

4.1.3 SpyCatcher/SpyTag Protein Coupling Pair

In this study we first demonstrate that SpyCatcher protein (SpyCatcher003), that forms a covalent bond with a short peptide tag known as SpyTag (SpyTag003) [312], can be engineered to be expressed on the surface of mammalian cells. This coupling enables the attachment of purified protein ligands engineered to contain SpyTag to the cell membrane. We then show that these purified ligands are functional and assess their ability to control T cell activation through their native TCRs or through chimeric antigen receptors (CARs).

4.2 Results

4.2.1 Expressing SpyCatcher in Mammalian Cells

Here, we developed a novel system allowing the covalent coupling of purified ligands with SpyTag, to cells displaying surface SpyCatcher. The SpyTag and SpyCatcher coupling proteins are fragments (13 amino acids and 138 amino acids, respectively) isolated from the Fibronectin Binding Protein (FbaP) of *Streptococcus pyogenes*. Together they spontaneously form an isopeptide bond [312], that has been optimised to bind together specifically, rapidly, and irreversibly under a range of pHs and temperatures. The third generation SpyTag/SpyCatcher pair used in our study, SpyTag003/SpyCatcher003, reacts within minutes, with a rate constant of $5.5\times10^5 M^{-1}s^{-1}$ [313]. SpyTag003 and SpyCatcher003 can be genetically fused to proteins, allowing for versatile applications within protein biology. Here we exploit the above features and stability to develop a cellular system of presenting ligands to T cells.

In order to express SpyCatcher in mammalian cells, three different constructs were designed - each fusing SpyCatcher to distinct ligand anchors at the peptide's C-terminus (Fig. 4.1A). We have chosen to use SpyCatcher003 with SpyTag003 as this version has been engineered to have the fastest binding kinetics compared to previous iterations of the protein couple [313]. SpyCatcher003-mCD80 is fused to the hinge, transmembrane and cytoplasmic domains of mouse CD80. Mouse CD80 was selected as it has been shown to express well in mammalian cells previously when fused to SpyTag [309]. To reduce the distance of SpyCatcher from the cell surface, a more compact version of SpyCatcher003-mCD80 using a truncated mouse-CD80 hinge was also designed (SpyCatcher003-mCD80 (short)). Addition-

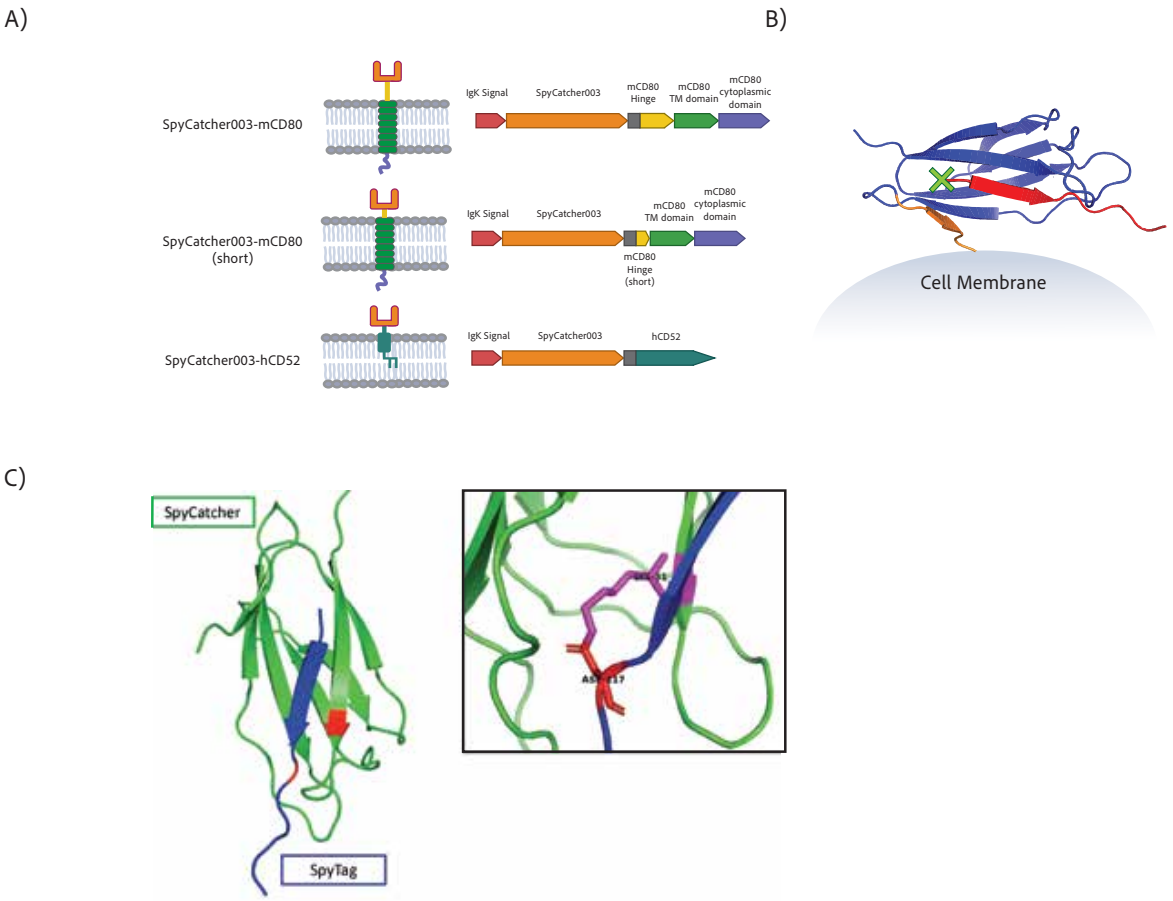


Figure 4.1: SpyCatcher constructs with different hinges for expression on the surface of mammalian cells. A) Annotated Constructs of SpyCatcher fused to mouse CD80, mouse CD80 (short hinge) and human CD52. **B)** Cartoon depiction of SpyTag003 (red) bound to surface-displayed SpyCatcher (blue). SpyCatcher C Terminus (orange) is membrane-anchored by fusion to a hinge (see panel A). SpyTag N terminus (green cross) is fused to the extracellular domain of a ligand of choice. Figure created with Pymol. **C)** Interacting residues between SpyCatcher (Lysine-31) and SpyTag (Aspartate-117).

ally, a SpyCatcher construct fused to human CD52 was designed to obtain a GPI-anchored form of the protein. The constructs were designed so that the C-terminus of SpyCatcher is membrane-anchored (Fig. 4.1B, in orange), and SpyTag003 binds to the N-terminus of SpyCatcher. An isopetide bond forms between Lysine-31 on SpyCatcher and Aspartate-117 in SpyTag (Fig. 4.1C).

Each SpyCatcher construct was transduced into Chinese hamster ovary (CHO) cells, and expression was verified by incubating the cells with a purified fluorescent protein fused to SpyTag (SpyTag-mCLOVER3) (Fig. 4.2A). A titration of SpyTag-mCLOVER3 with each SpyCatcher-CHO cell line revealed that SpyCatcher003-hCD52 was the most highly expressed construct (Fig. 4.2B).

To confirm that the surface SpyCatcher molecules were mobile on the cell surface, their diffusion coefficients were determined using fluorescence correlation spectroscopy (FCS) (Fig. 4.3A). We found that SpyTag-mClover3 coupled to surface SpyCatcher exhibited similar diffusion coefficients independent of the ligand anchor (Fig. 4.2B) with the absolute diffusion coefficient of $0.2\mu m^2/s$, similar to that found for other membrane proteins [314–318]. We consequently chose to use SpyCatcher-hCD52 for future experiments as it displayed the highest surface expression.

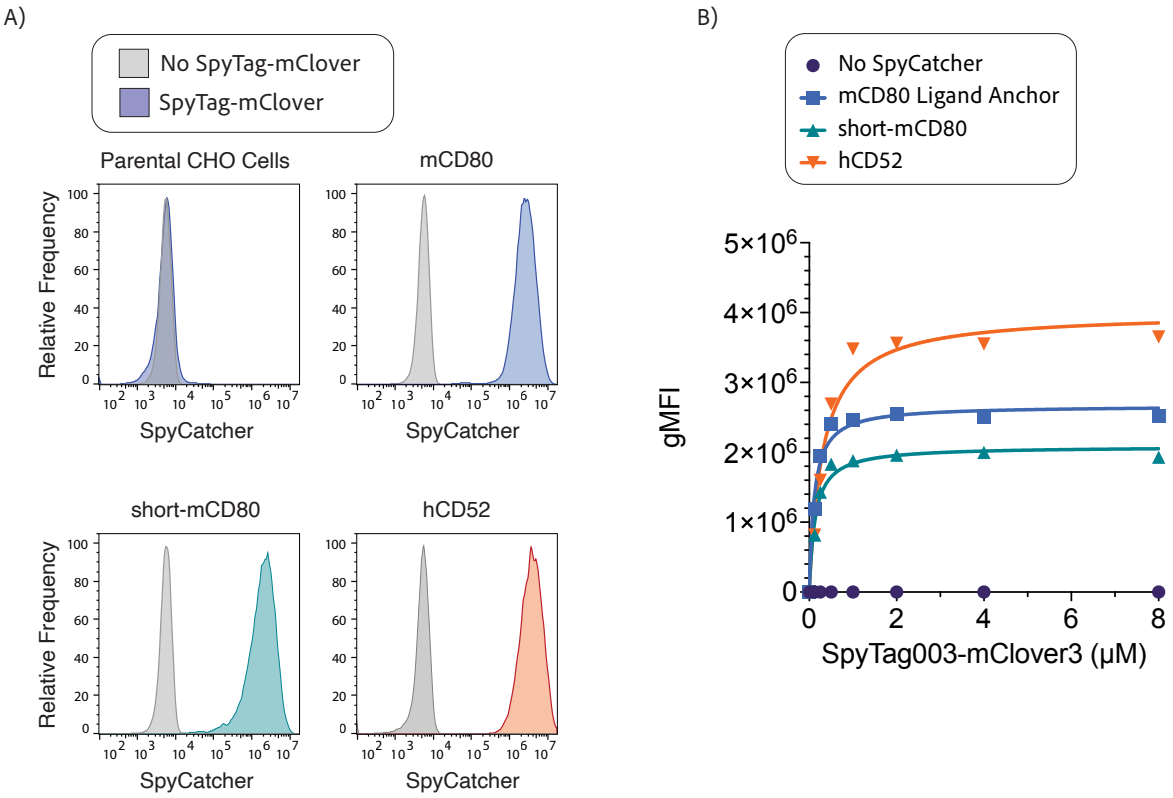


Figure 4.2: The human-CD52 membrane anchor produces the largest surface expression of SpyCatcher on CHO cells. A) Purified SpyTag003-mClover was added to 200,000 CHO cells transduced with indicated SpyCatcher constructs (mouse CD80 (mCD80), short-mouse-CD80 (short-mCD80), or human CD52 (hCD52) for 40 minutes at 4°C. **B)** SpyCatcher Expression as measured by gMFI values across a titrating concentration of 8μM SpyTag-mClover. Data generated by Eleanor Denham.

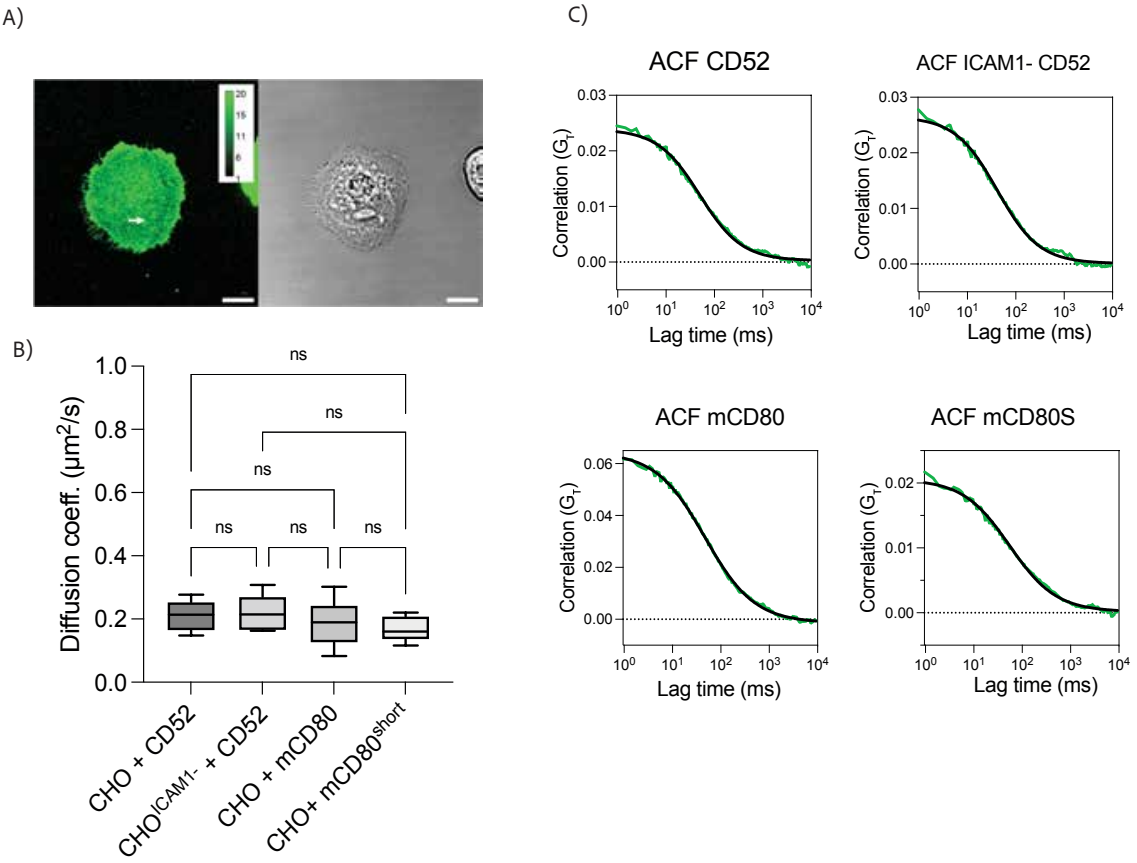


Figure 4.3: SpyCatcher with different hinges have similar membrane diffusion cœfficients. **A)** Confocal image of a CHO cell expressing CD52-SpyCatcher labelled with SpyTag-mClover3 acquired in photon-counting mode. Calibration bar indicates the number of photons detected per pixel. The white arrow indicates the approximate position of the sFCS line. Scale bars = 10μm. **B)** Diffusion Cœfficient Analysis of SpyCatcher Constructs Expressed on CHO Cells. Diffusion Cœfficients extracted from Auto Correlation Functions shown in C). **C)** Representative auto-correlation functions (ACFs) for raw data (green) and fits (black). Each curve represents the spatially averaged ACF for measurements from a single cell. Data generated by Alexander Morch.

4.2.2 T Cell Ligands Can be Stably Presented on CHO Cells in A Dose-Dependent Way

T cell activation is regulated by accessory receptors such as CD2, LFA-1, and CD28 binding their ligands (CD58, ICAM-1, and CD86 (or CD80), respectively). To study the individual contributions of these receptor-ligand interactions, it is necessary to use a target cell that lacks the expression of the corresponding ligands to limit cross-reactivity. Given that the CHO-K1 cell line is derived from hamster ovary cells, and is unlikely to express these ligands with the exception of ICAM-1, which has been shown to be functional [319], it is a suitable target cell candidate. Therefore, we harnessed CRISPR Cas9 to selectively knockout hamster ICAM-1 expressed by the CHO cells (Fig. 4.8), and generated a cell line that stably expresses SpyCatcher003 from these ICAM-1 deficient cells, named CombiCell.

Constructs containing the extracellular domain of CD58, ICAM-1, CD86 and CD80 costimulatory ligands fused to C-terminal SpyTag (to couple SpyCatcher), and a His-Tag (for purification) were designed. Furthermore, we coupled SpyTag to the C-terminus of HLA-A2, and refolded it with β2M, and 9V peptide (Fig. 4.4A). These ligands were produced, purified, and then added to CHO cells expressing SpyCatcher, across a range of concentrations (Fig. 4.5A). Using fluorescently labeled antibodies against each specific protein of interest, we confirmed that all ligands could be loaded on the surface of the CHO cells in a dose-dependent manner, allowing us to achieve a titration of each ligand. This approach enables the quantification of T cell response phenotypes.

To understand the approximate number of SpyTag/SpyCatcher complexes presented by CHO cells, quantification beads (Bangs Laboratories), containing a predefined

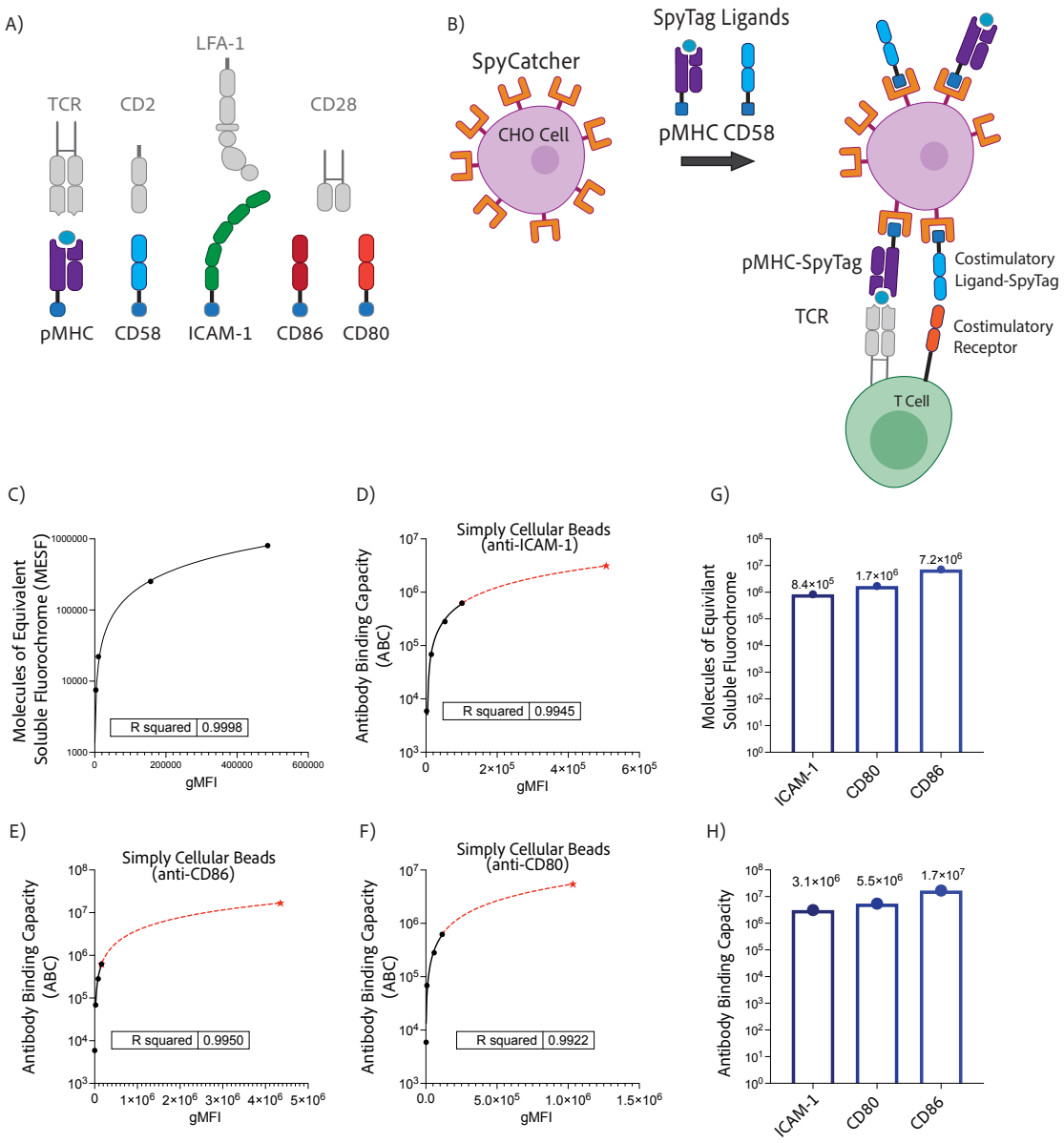


Figure 4.4: Purified T Cell Ligands Fused to SpyTag can be coupled to Surface-Displayed SpyCatcher and results in high absolute surface expression A) Schematic of Human T Cell ligands generated with SpyTag added to their C-Terminus. Corresponding T cell receptors shown above in grey. **B)** Loading of combinations of SpyTag ligands to surface-displayed SpyCatcher expressed by CHO cells, with subsequent interaction with their receptors expressed by T Cells. **C)** Simply Cellular Quantification beads (Bangs Laboratories) were incubated across a titration of ligand-specific antibodies and the gMFI measured. A standard curve was fitted from known MESF (Molecules of Equivalent Soluble Fluorophores) values and used to calculate the absolute number of 0.5μM indicated ligand loaded onto the CombiCell platform from gMFI values (**G**). **D-F)** Simply-Cellular Beads (Bangs Laboratories) were stained with antibodies against ICAM-1 **(D)**, CD86 **(F)**, or CD80 **(G)**, followed by flow cytometry to obtain gMFI values. gMFI was then plotted against the Antibody Binding Capacity (ABC) of each set of beads to obtain a standard curve. **H)** The absolute number of ligands was measured through ligand-specific ABC values, extrapolated from standard curves.

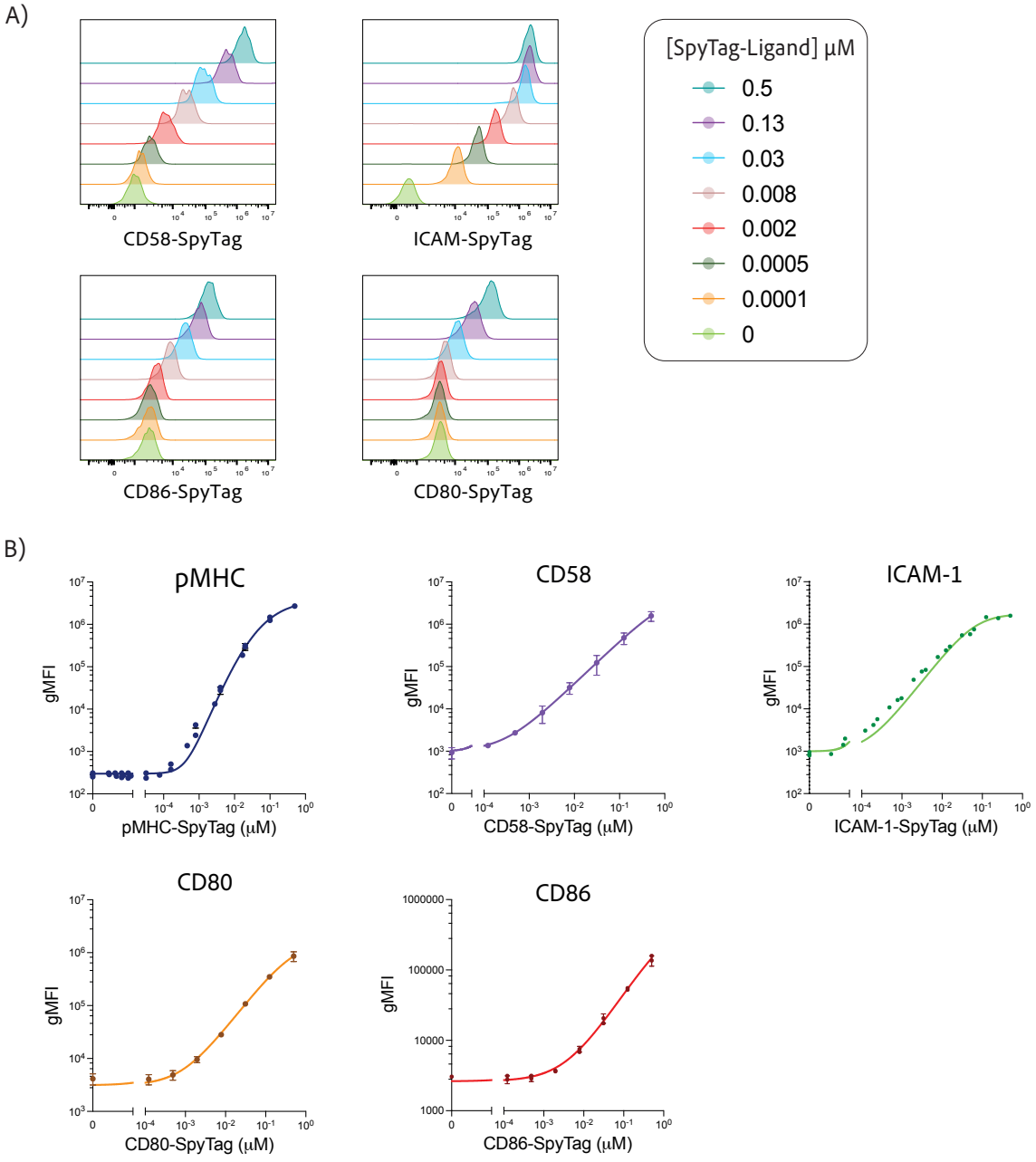


Figure 4.5: Ligands with a SpyTag Can be Readily be Titrated on Surface SpyCatcher. Purified, SpyTag forms of pMHC, CD58, ICAM-1, CD86 and CD80 were incubated with SpyCatcher-CHO cells across a range of concentrations, starting at 0.5 μM for 40 minutes at 37°C. The cells were then stained with the corresponding antibody against each specific T Cell ligand, followed by flow cytometry analysis. **A)** Representative Histograms of SpyTag ligand Titrations. **B)** gMFI values extracted across repeats. n = 2.

number of Ig domains (MESF beads) or fluorescent molecules (ABC beads), were harnessed to generate a standard curve from which MFI values of SpyTag ligands can be be interpolated/extrapolated (Fig. 4.4 D-I). Three different SpyTag ligands (ICAM-1, CD86 and CD80) were coupled to CHO cells expressing SpyCatcher at a high concentration (3μM), to ensure saturation of all binding sites. The expression (as MFI values) were extracted through flow cytometry. Using the MFI values representing expression of each SpyTag protein, the number of molecules per CHO cell was calculated, using two different standard curves (one generated with MESF beads, the other with ABC beads). All three proteins produced similar results across both quantification methods, with the number of SpyCatcher/SpyTag molecules found to be between ~1-10 million (Fig. 4.4 H&I).

To study the stability of the loaded proteins on the surface of CHO cells the expression of each SpyTag protein was measured over 26 hours (Fig. 4.6). First, antibodies against each specific protein (HLA-A2, CD58, ICAM-1, CD86 and CD80) were used (Fig. 4.6A-B). The gMFI values at 2 hour intervals was calculated to plot a curve (Fig. 4.6A) that was fitted with a one-phase decay model to extract the mean lifetime of each ligand (Fig. 4.6B). Mean lifetime of the ligands was found to be between 6-9 hours, possibly due to membrane protein cellular turnover. SpyCatcher levels expressed by the CHO cells was also checked at each time-point and remained constant throughout the assay, as expected. Additionally, harnessing the His-Tag incorporated within the recombinant SpyTag proteins for protein purification, loaded SpyTag-CD58, ICAM-1 and CD86 were detected with anti-HisTag antibodies, to enable a more direct comparison of gMFI values across the different ligands. The mean lifetime of ligands was found to be approximately 7 hours with His-Tag labelling.

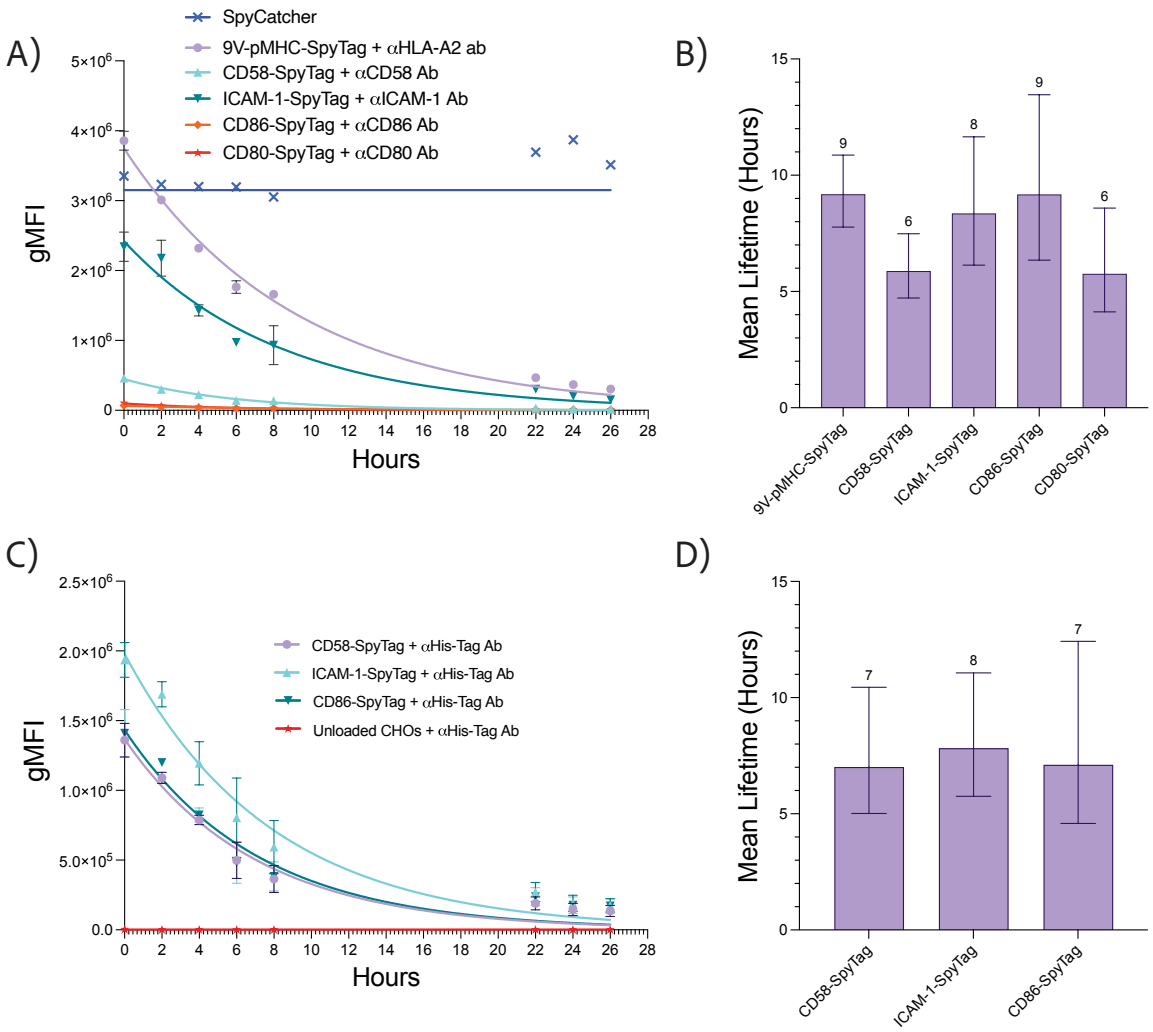


Figure 4.6: Ligands Coupled to SpyCatcher Have a Mean Surface Lifetime of more than 7 Hours. The expression of SpyTag ligands was measured over 26 hours, at 2 hour intervals, by staining each ligand with either a ligand specific antibody **A-B)** or anti-His-Tag **C-D)** antibody. SpyCatcher was stained with SpyTag-mCLOVER. Data was fit using a one-phase decay model in Prism. To extract mean lifetime (tau) values **B & D)**, the gMFI values were normalised to baseline expression at 0 hours for each condition. A one-phase decay was then fit to the normalised data and the mean lifetime values extracted. n=3.

4.2.3 T Cell Ligands presented on Surface-Displayed SpyCatcher are Functional

We next determined whether SpyTag ligands coupled to SpyCatcher on CHO cells were functional. At first, we incubated primary human $CD8^+$ T cells transduced with the 1G4 TCR with parental CHO cells loaded with a titration of SpyTag-pMHC and SpyTag-ICAM-1. Following 6 hours of co-culture, T cell activation was measured by the surface expression of 4-1BB (Fig. 4.7A). With antigen alone (Fig. 4.7A, grey line), as the concentration of pMHC-SpyTag was increased, the higher the proportion of T cells were activated, as expected. Surprisingly, as the concentration of SpyTag-ICAM-1 was increased, there was no significant impact on the EC_{50} (Fig. 4.7C). This is in contrast to what is observed on the plate system - where ICAM-1 has been shown to significantly enhance the sensitivity of T cells to antigen. We confirmed that the density of SpyTag-ICAM-1 on the surface of the CHO cells was dependent on the concentration of ICAM-1 added in solution and independent of the pMHC concentration.

Given the previous implication of hamster ICAM-1 expressed by CHO cells to be able to costimulate murine mice T cells [319] we were concerned by the cross-reactivity of human LFA-1 on T cells with hamster ICAM-1 expressed by CHO cells in our assay. Consequently, we used CRISPR Cas 9 to knock out endogenous hamster ICAM-1 on the CHO cells (Fig. 4.9). Indeed, knocking out hamster ICAM-1 reduced the sensitivity of human T cells to antigen, resulting in a 25-fold reduction in sensitivity as measured by CD69 upregulation (Fig. 4.9 B), and a 7.5-fold reduction as measured by 4-1BB upregulation (Fig. 4.9 D).

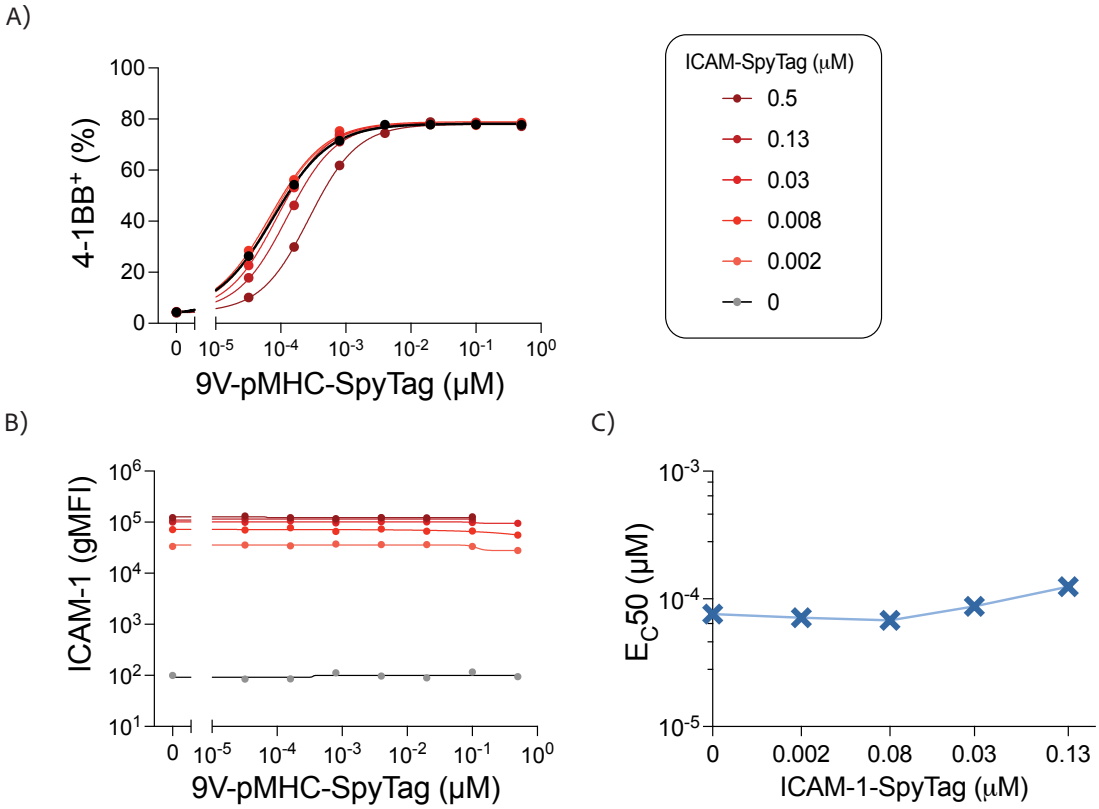


Figure 4.7: ICAM-1-SpyTag Added to CHO cells expressing Endogenous Hamster ICAM-1 has Modest Impact on Antigen Sensitivity Dose-Response Curves of **A)** T Cell Activation (as measured by 4-1BB up-regulation), and **B)** ICAM-1-SpyTag Loading (gMFI), across increasing concentrations of pMHC-SpyTag and ICAM-1 SpyTag.**C)** EC_{50} values were extracted from fitting data in **A)** in PRISM, and plotted over ICAM-1-SpyTag concentration.

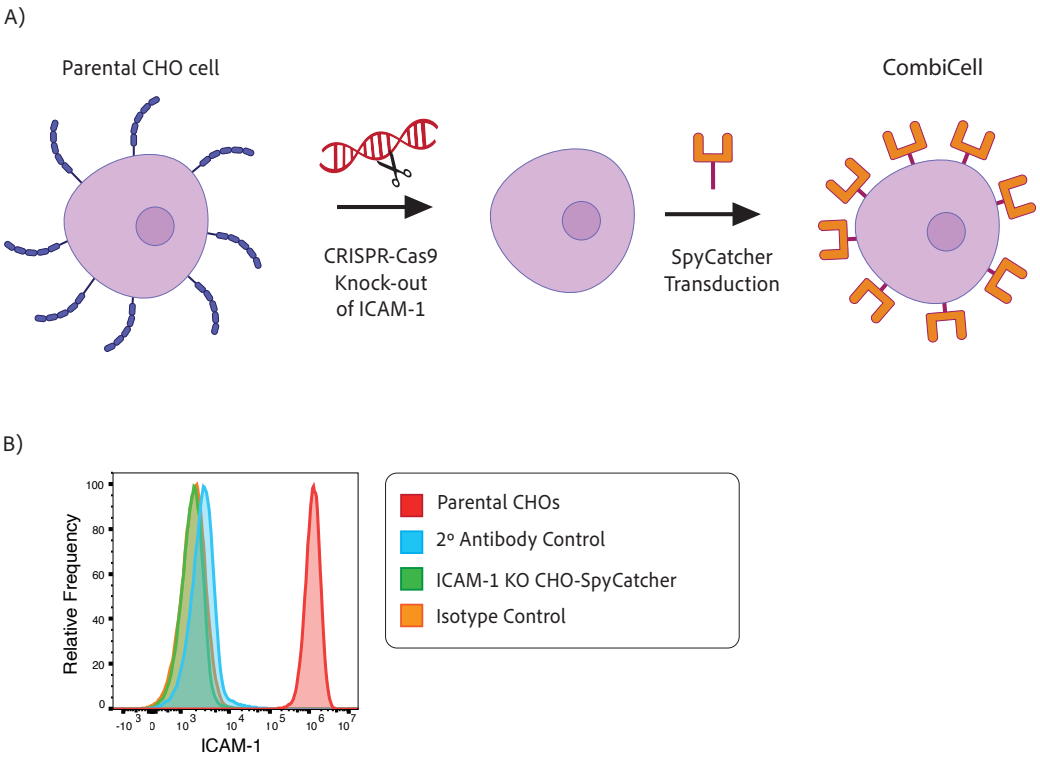


Figure 4.8: Generation of CombiCell

A) CRISPR-Cas9 knock-out of Hamster ICAM-1 was performed on Parental CHO-K1 cells, followed by transduction of SpyCatcher-hCD52. The resulting ICAM-1 deficient, SpyCatcher003 expressing CHO cells are named CombiCell.

B) Validation of CRISPR Knock out of Hamster ICAM-1 on CHO cells. Cells were stained with anti-hamster ICAM-1 antibody derived from J5-3F9 hybridoma (gifted by Vijay Kuchroo, Harvard Medical School) followed by AF488 anti-mouse secondary antibody. Cell Line was generated by Johannes Pettmann.

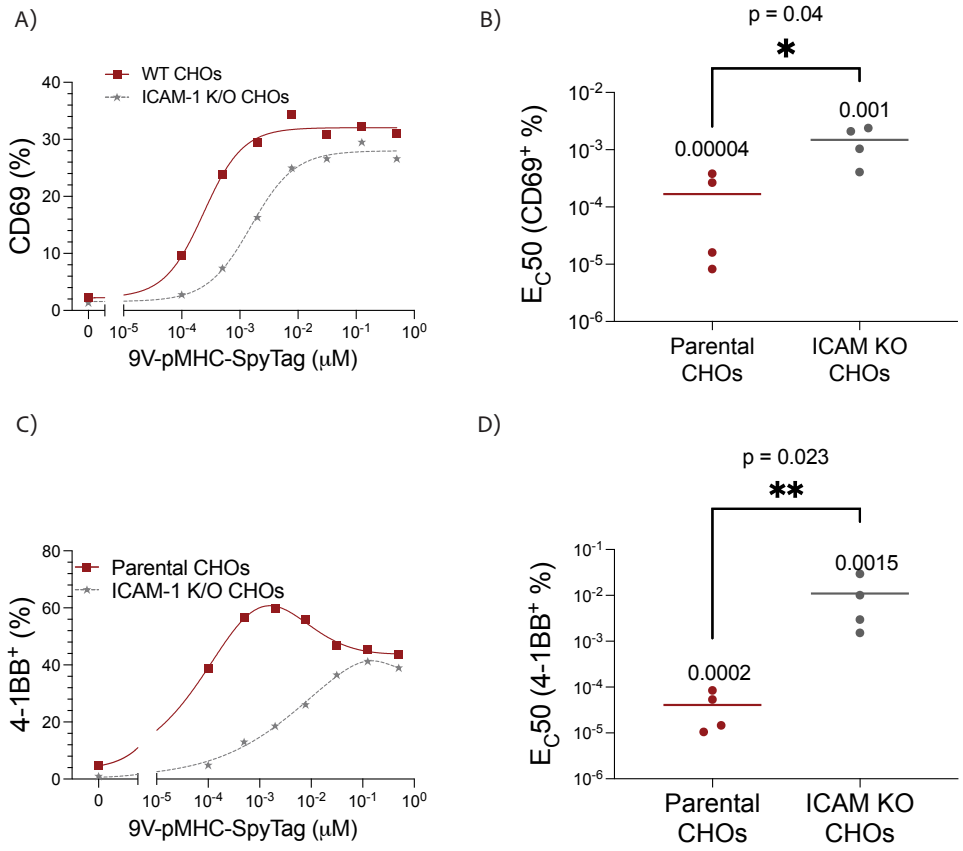


Figure 4.9: Exogenous SpyTag ICAM-1 Increases Antigen Sensitivity when Loaded on Hamster ICAM-1 Knockout CHO Cells. A) Representative dose-response curve of T Cell activation by CHO cells expressing Hamster ICAM-1 and ICAM-1 Knock Out CHO cells, as measured by CD69 **(A)** and 4-1BB **(C)** up-regulation over increasing concentrations of pMHC-SpyTag. **B)** EC_{50} values extracted from curves represented in **A)**. **D)** EC_{50} values extracted from curves represented in **C)**. Statistical significance is determined by a paired t-test performed on log-transformed data. Data is shown as a mean +/- SEM of 4 independent experiments (i.e. 4 independent human donors). Abbreviations: * = p-value$\leqslant$0.05, ** = p-value$\leqslant$0.01, *** = p-value$\leqslant$0.001, **** = p-value$\leqslant$0.0001, ns = not significant.

Furthermore, human ICAM-1-SpyTag was able to rescue this reduction in sensitivity in the hamster ICAM-1 deficient CHO cells (Fig. 4.10 A-D), further implicating ICAM-1 in T cell sensitivity to antigen. Moreover, coupling SpyTag-CD58 to wild-type CHO cells caused a smaller shift in EC_{50} than in the ICAM Knock-out CHO cells (Fig. 4.10 E-H). Taken together, these results indicate that hamster ICAM-1 on CHO cells cross-reacts with human LFA-1 masking the antigen sensitivity phenotypes of SpyTag coupled ICAM-1 and CD58. Therefore, in subsequent experiments we used the hamster ICAM-1 knockout CHO cell, termed CombiCell, to study the impact of these costimulation ligands on T cell responses.

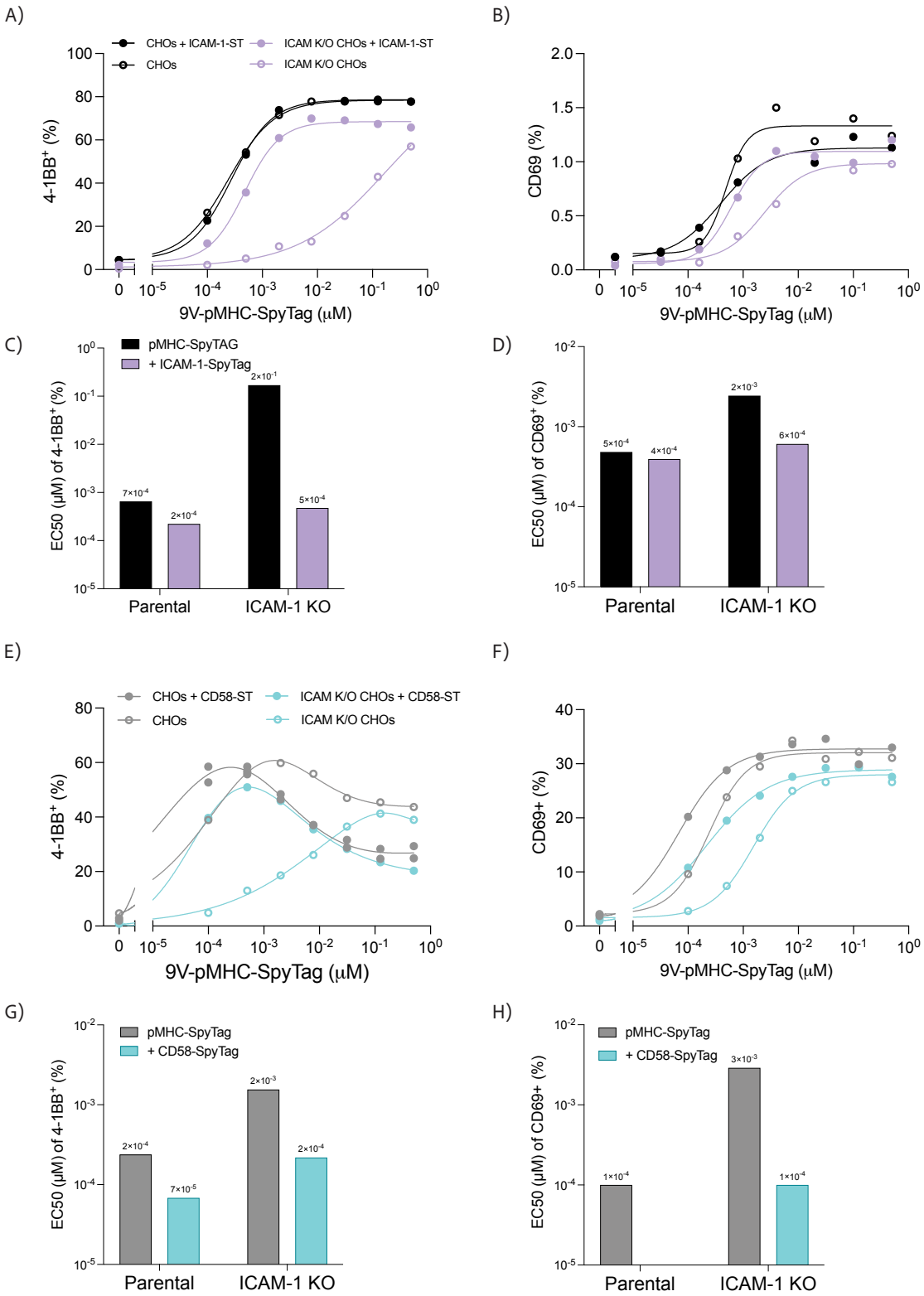


Figure 4.10: ICAM-1-ST and CD58-ST Can Rescue T Cell Antigen Sensitivity from ICAM-1 Knock Out CHO cells. 0.03μM ICAM-1-SpyTag **(A-B)** and 0.5μM CD58-SpyTag **(E-F)** was added to CHO cells expressing SpyCatcher (in red) and Hamster ICAM-1 Knockout CHO cells (in blue), for 40 minutes at 37°C. T cell activation was measured by 4-1BB **(A& E)** and CD69 **(B & F)** upregulation. **(C-D, G-H)** EC_{50} values were extracted for parental and ICAM-1 knockout CHO cells under ICAM-1 or CD58 costimulation.

4.2.4 Comparison of Loaded SpyTag Ligands with the Endogenous Expression of Costimulatory Ligands on Antigen-Presenting Cells.

Having confirmed the loading of SpyTag ligands onto surface-displayed SpyCatcher expressed by CHO cells, and their ability to activate primary human T cells, we sought to compare the level of SpyTag ligands presented by the CombiCell system with the levels expressed endogenously by different cell types.

Firstly, SpyCatcher-CHO cells were loaded with a titration of CD58-SpyTag, ICAM-1-SpyTag, CD86-SpyTag and CD80-SpyTag, and measured before being compared to the corresponding expression of each ligand on T2 cells, a hybrid B/T-lymphoblast cell line, that expresses each ligand endogenously. The gMFI values of each ligand concentration was then normalised to the gMFI of each ligand on T2 cells (Fig. 4.11), allowing for direct comparison of ligand expression on the CombiCell system with endogenously expressed versions. The results showed that the maximum coupling of each ligand on the surface of CombiCells exceeded the endogenous expression on T2 cells by approximately 10-fold.

The endogenous expression of each ligand was then measured on several different human cell types, including both cell lines and primary cells, and normalized to the expression on T2 cells (Figure 4.12). This allowed for comparison of the relative expression of individual costimulatory ligands across different cells. As expected, professional antigen-presenting cells (*in vitro* differentiated monocytes) displayed the highest expression of all ligands.

To ensure that the range of loaded SpyTag ligand could represent a physiological level presented to T cells *in vivo*, the maximum concentration of SpyTag ligand

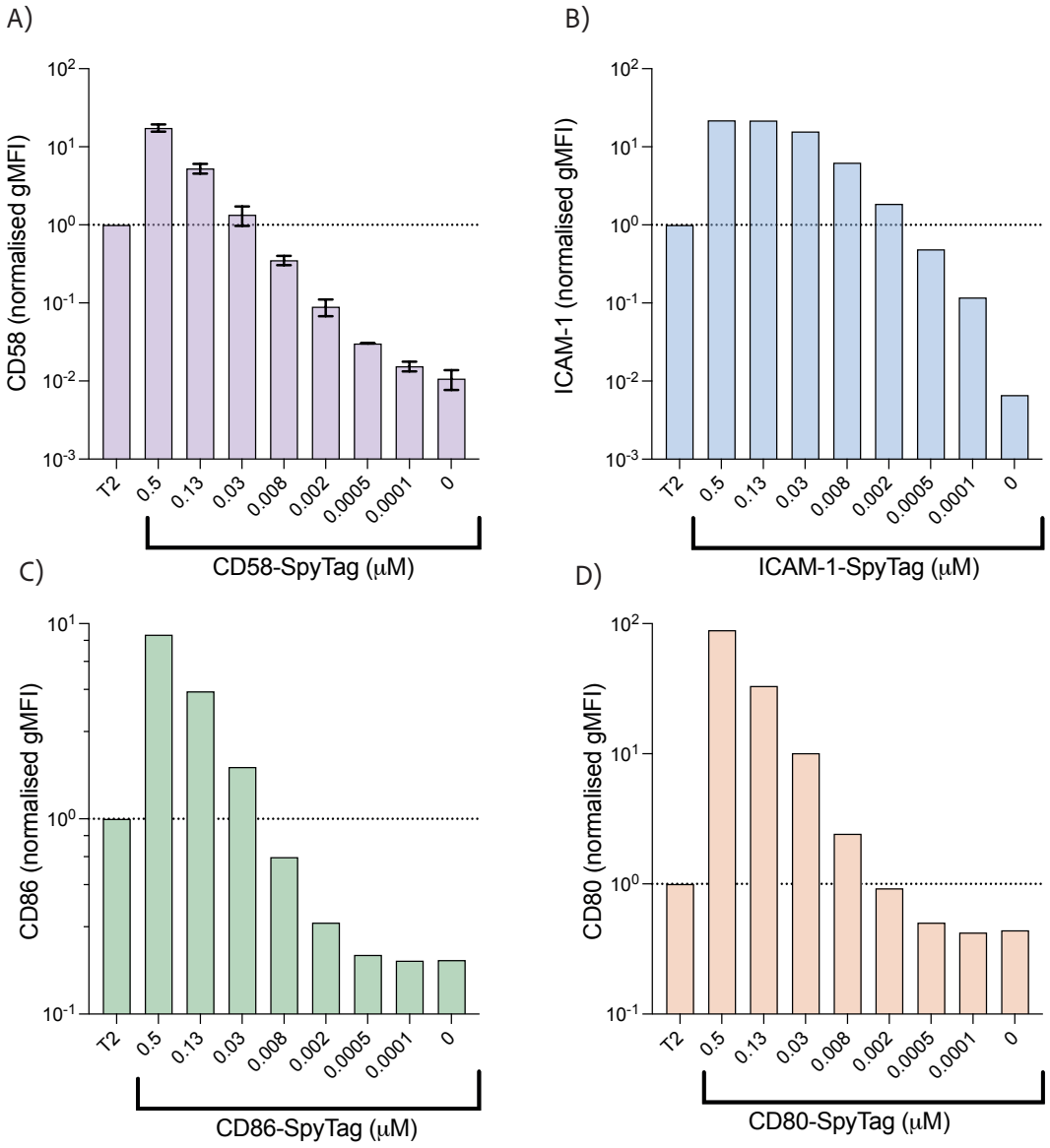


Figure 4.11: Expression of SpyTag Ligands Presented on CHO cells relative to T2 cells. CombiCells were incubated with the indicated SpyTag ligands for 40 minutes at 37°C followed by analysis of CD58 **(A)**, ICAM-1 **(B)**, CD86 **(C)** and CD80 **(D)** expression by flow cytometry. Using the same antibodies, endogenous costimulatory ligand expression was analysed on T2 cells (hybrid B/T-lymphoblast cell line). gMFI values of the SpyTag versions of costimulatory ligands were normalised to the gMFI of the corresponding ligands expressed by T2 cells.

loaded onto SpyCatcher-CHO cells (0.5μM), normalised to T2 expression, was compared to each cell type analysed. For U87 cells (a human glioblastoma cell line), THP1 cells (a human leukemia monocytic cell line), primary human blasted $CD8^+$ T cells and $CD11c^+$ macrophages, the highest concentration of SpyTag ligand (indicated by the dotted line in Fig. 4.12) exceeded the endogenous expression level of CD58, ICAM-1, CD86 and CD80. Consequently by titrating the ligands, our system can be used to display a physiological level of costimulatory ligands found on different cell types.

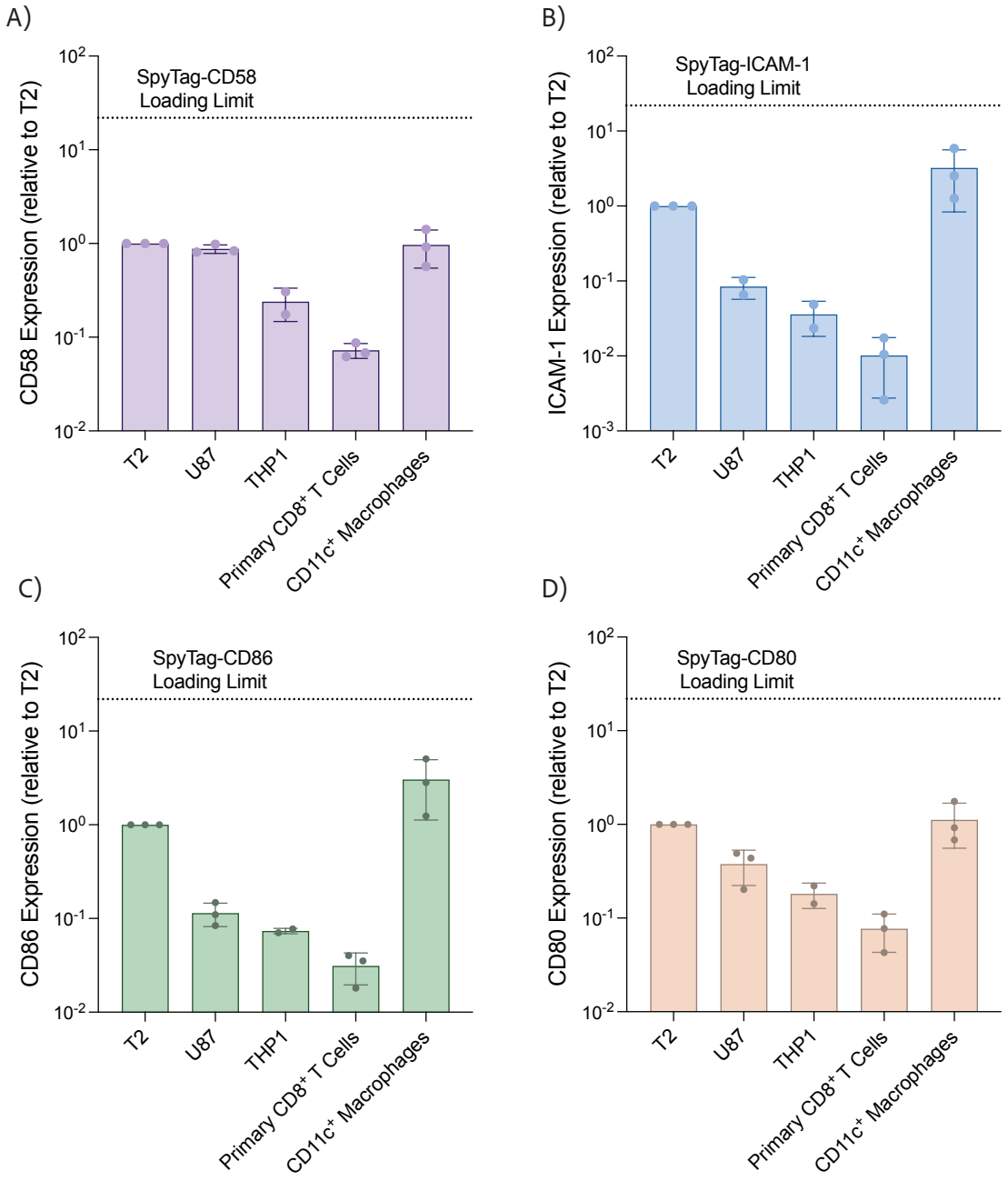


Figure 4.12: The Ligand Loading Limit of CombiCells is Higher than the Endogenous Surface Expression of Different Ligands on Different Primary Cells and Cell Lines T2 (hybrid B/T-lymphoblast cell line), U87 (Glioblastoma derived cell line), THP1 (monocyte derived cell line), Primary $CD8^+$ T cells, and $CD11c^+$ Macrophages (*in vitro* differentiated from primary human monocytes), were analysed for CD58 **(A)**, ICAM-1 **(B)**, CD86 **(C)** and CD80 **(D)** expression. gMFI values are normalised to the expression of each ligand on T2 cells. The highest gMFI detected by the SpyTag version of each ligand loaded onto CombiCells (see **Fig. 4.11**) is also indicated. n = 3.

4.2.5 A Combination of Different Ligands can be Loaded onto CombiCell

The interaction between T cells and APCs involves multiple receptor/ligand interactions. To test the loading of multiple ligands onto the SpyCatcher system, a titration of 9V peptide-MHC SpyTag was loaded with varying concentrations of CD58-SpyTag, ICAM-1-SpyTag, CD86-SpyTag, or CD80-SpyTag as shown in Fig. 4.13. Loading pMHC with each ligand had minimal effect on pMHC expression, except for ICAM-1 where pMHC presentation was reduced only at the two highest ICAM-1 concentrations (0.125μM and 0.5μM) when loaded with the two highest pMHC concentrations (0.5μM and 0.1μM).

Additionally, from Fig. 4.13 C and D the gMFI of CD86 and ICAM-1 reaches a plateau at 1μM. Therefore, 1μM was established as the maximum loading concentration of the CombiCell system, beyond which competition between SpyTag ligands may occur.

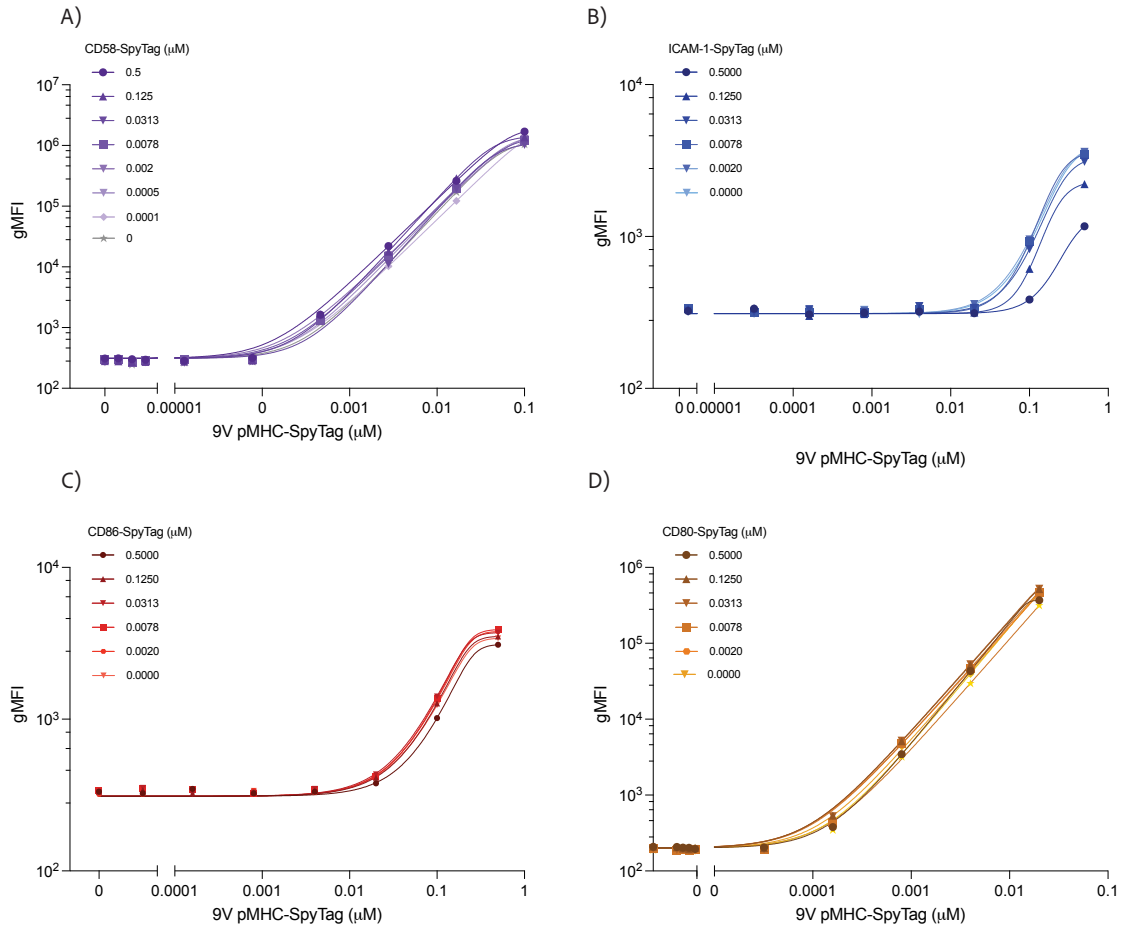


Figure 4.13: Combinations of Ligands Can Be Loaded onto CombiCells without Compromising pMHC Loading Titrating concentrations of 9V-pMHC-SpyTag together with titrating concentrations of **A)** CD58-SpyTag, **B)** ICAM-1-SpyTag, **C)** CD86-SpyTag and **D)** CD80-SpyTag, were added to CombiCells for 40 minutes at 37°C. Expression of SpyTag-pMHC was analysed by staining with an anti-HLA-A2 antibody followed by extraction of gMFI values from flow cytometry analysis.

4.2.6 The Effects of CD2, LFA-1 & CD28 on T Cells using CombiCell

The Impact of CD2, LFA-1 & CD28 on T Cell Activation over 6 Hours

Having validated the CombiCell system to stably present physiological levels of ligands, we next sought to harness this platform to investigate the role of individual costimulatory ligands on T cell sensitivity to antigen. To do this 9V-pMHC-SpyTag was co-loaded with each SpyTag ligand onto CombiCells, which were then presented to T cells for 6 hours. T cell activation was measured through surface expression of 4-1BB (Fig. 4.14), and CD69 (Fig. 4.15). Firstly, T cell activation increased dependent on surface level of presented pMHC (along the x axis). This has been previously observed with natural APCs pulsed with different concentrations of peptide antigen [320].

Upon the addition of an increasing levels of CD58 and ICAM-1, the concentration of pMHC required for T cell activation decreased, as measured by 4-1BB (Fig. 4.14) and CD69 (Fig. 4.15) upregulation. Consequently the ligation of CD2 and LFA-1 resulted in T cells responding at a lower antigen concentration, indicating an increase in T cell sensitivity to antigen. In contrast, engaging CD28 with CD86 or CD80 had little impact on antigen sensitivity. We observe qualitatively similar phenotypes when T cells are engaged with CD58, ICAM-1 and CD86 immobilised on plates (see Chapter 2).

We next measured, the concentration of cytokines in the supernatant after 6 hours of T cell stimulation by CombiCell presented ligands. All costimulatory ligands resulted in a dose-dependent increase in IL-2 (Fig. 4.16 A-D), IFN-γ (Fig. 4.16 E-H) and TNF-α (Fig. 4.16 I-L), showing that the engagement of CD2, LFA-1 and CD28 all enhanced cytokine production.

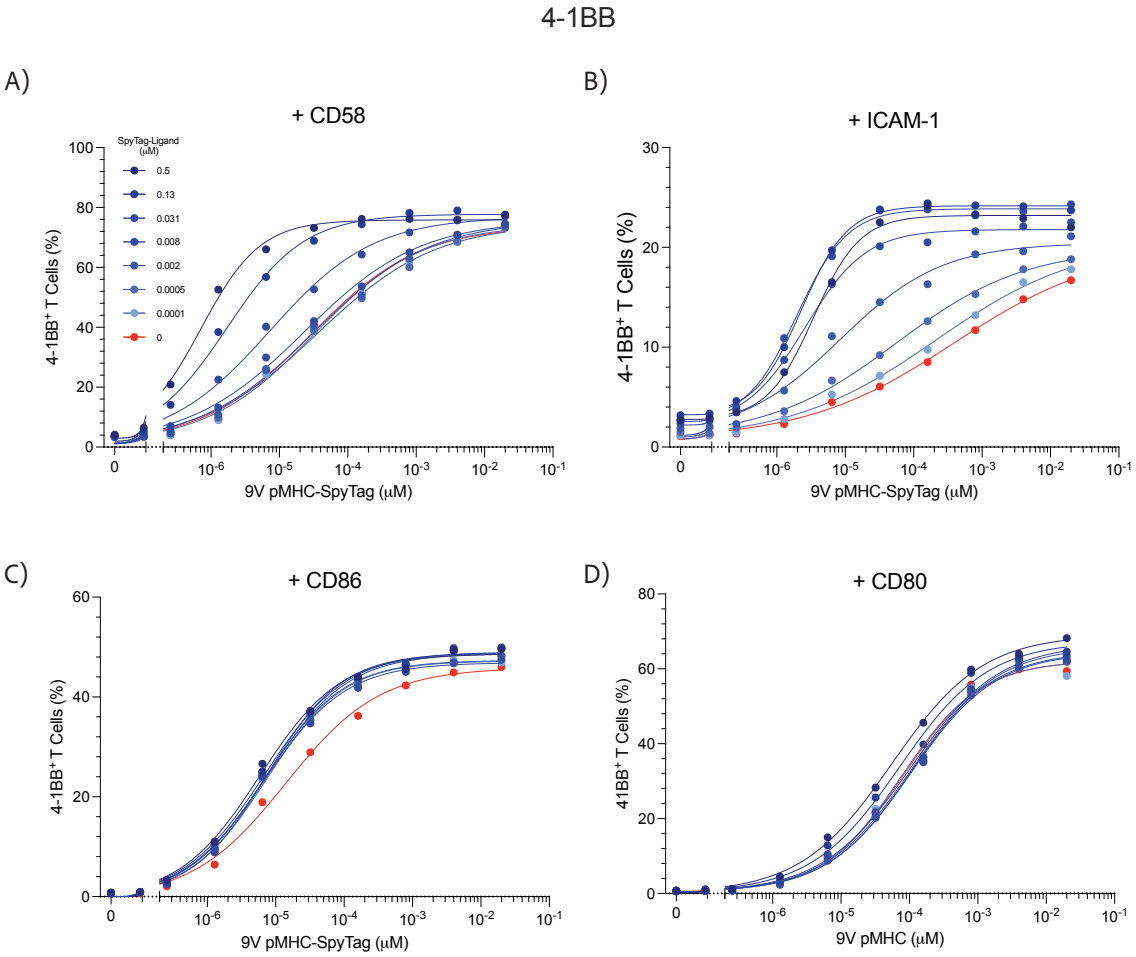


Figure 4.14: Ligation of CD2 and LFA-1, but not CD28, Enhances Antigen Sensitivity at 6 hours as measured by 4-1BB Surface Expression CombiCells were incubated with titrating concentrations of 9V pMHC-SpyTag and costimulatory ligand **(A-D)**. Primary human T Cells were added for 6 hours, after which T Cell activation was measured by 41BB up-regulation.

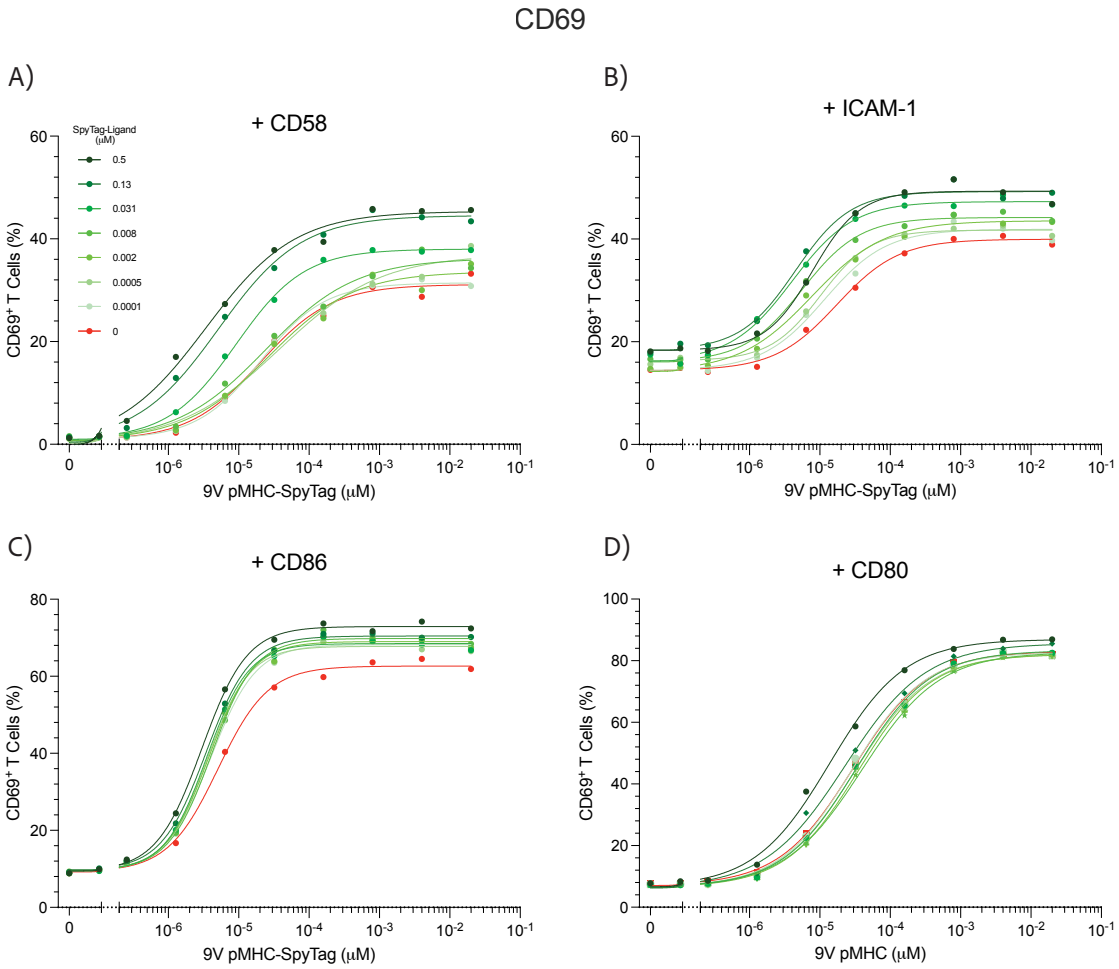


Figure 4.15: Ligation of CD2 and LFA-1, but not CD28, Enhances Antigen Sensitivity at 6 hours as measured by CD69 Surface Expression CombiCells were incubated with titrating concentrations of 9V pMHC-SpyTag and costimulatory ligand **(A-D)**. Primary human T Cells were added for 6 hours, after which T Cell activation was measured by CD69 up-regulation.

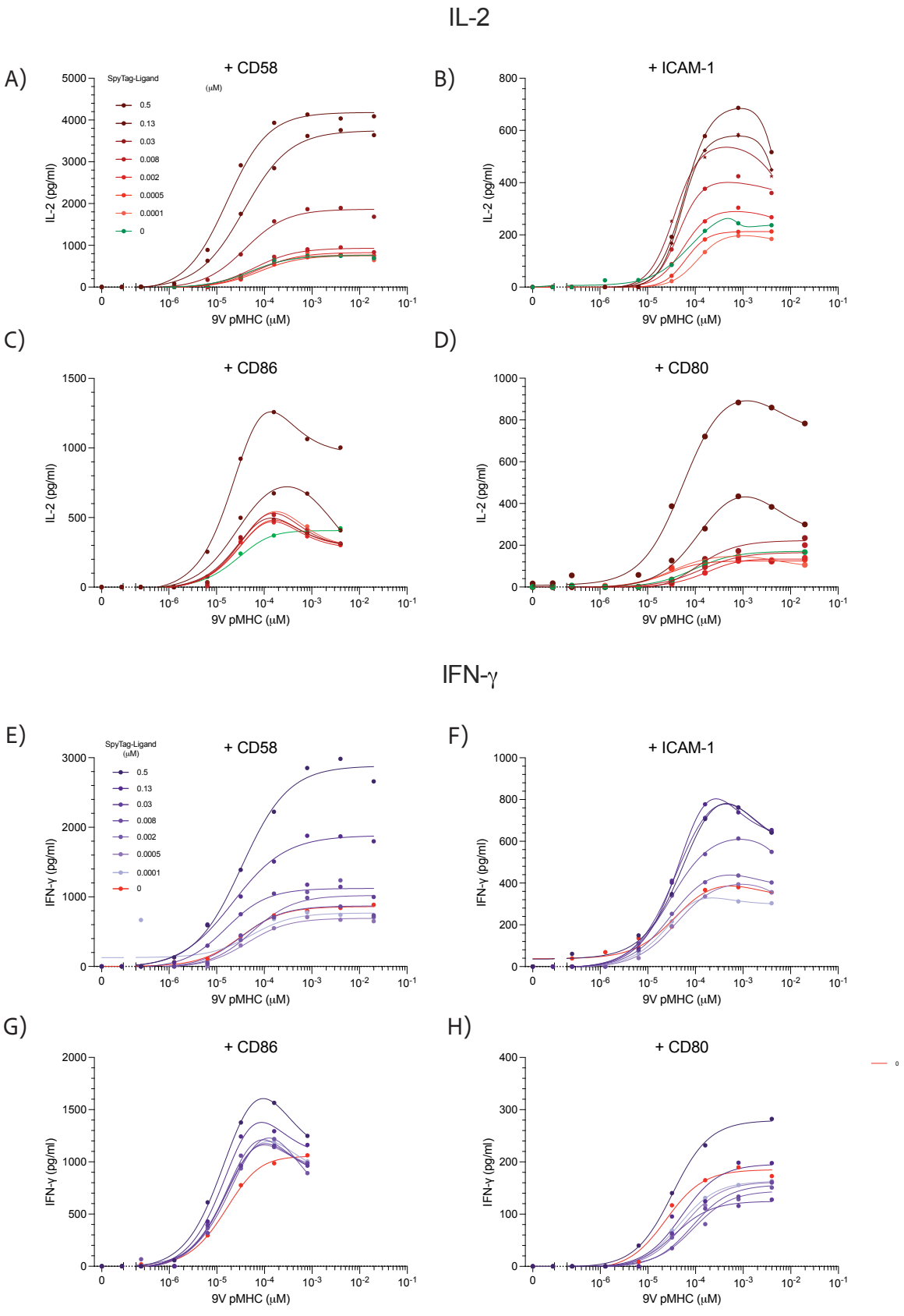

IL-2
A)
+ CD58
SpyTag-Ligand (μM)
0.5
0.13
0.03
0.008
0.002
0.0005
0.0001
0
IL-2 (pg/ml)
9V pMHC (μM)
B)
+ ICAM-1
C)
+ CD86
D)
+ CD80
IFN-γ
E)
+ CD58
IFN-γ (pg/ml)
F)
+ ICAM-1
G)
+ CD86
H)
+ CD80

Figure 4.16

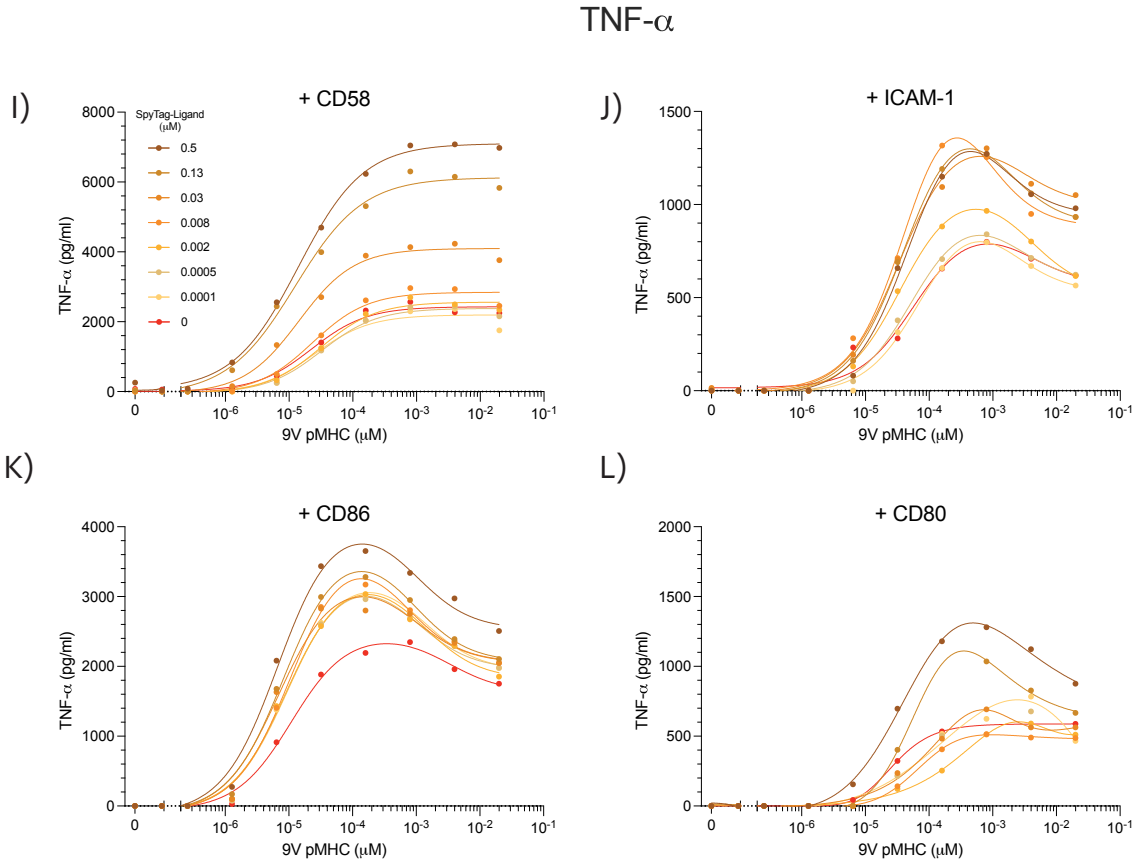


Figure 4.16: Ligation of CD2, LFA-1 and CD28 Increases Cytokine Production over 6 Hours CombiCells were incubated with pMHC-SpyTag and costimulatory ligand for 6 Hours as described in Fig. 4.14 & Fig. 4.15. IL-2 **(A-D)**, IFN-γ **(E-H)**, and TNF-α (IL-2) concentration in the supernatant was measured through ELISA. Independent T Cell donors were used per costimulatory ligand.

The Impact of CD2, LFA-1 & CD28 on T Cell Activation over 20 Hours

We next examined the functional outcomes of engaging each costimulatory ligand over an extended stimulation period of 20 hours to determine whether the impact of each individual costimulatory receptor varies at a later stage of T cell activation. Current understanding suggests that the adhesion receptors CD2 and LFA-1 affect the early stages of T cell activation, during which T cells establish initial contact with APCs, while other costimulatory receptors, such as 4-1BB, are upregulated at later timepoints and therefore have a more delayed effect on T cell activation [36]. Thus, examining the effects of these ligands at a later time point would enable us to observe any effects exerted by ligands that act later in T cell activation. Analysis of 4-1BB (Fig. 4.17) and CD69 (Fig. 4.18) expression after 20 hours showed that CD58-SpyTag still increased T cell sensitivity to antigen in a dose-dependent way (similar to the effect observed after 6 hours), whereas CD28 engagement with CD86-SpyTag or CD80-SpyTag did not affect antigen sensitivity, as observed over 6 hours of antigen stimulation (Fig. 4.14) (Fig. 4.15). However, unlike at 6 hours, ICAM-1-SpyTag did not impact antigen sensitivity after 20 hours (Fig. 4.17 B and E) (Fig. 4.18 B and E).

The concentration of cytokines in the supernatant after 20 hours was also analysed (Fig. 4.24). For IL-2 and IFN-γ, supernatant cytokine levels dramatically increased as the concentration of each costimulatory ligand increased. CD58, CD86 and CD80 were also able to amplify TNF-α levels, however ICAM-1 costimulation was unable to impact TNF-α production over 20 hours (Fig. 4.18 J).

Taken together, these initial screens have confirmed that SpyTag ligands coupled to CombiCells are functional and have a concentration-dependent phenotypes. We have found that whilst CD58 increases antigen sensitivity at both 6 and 20 hours,

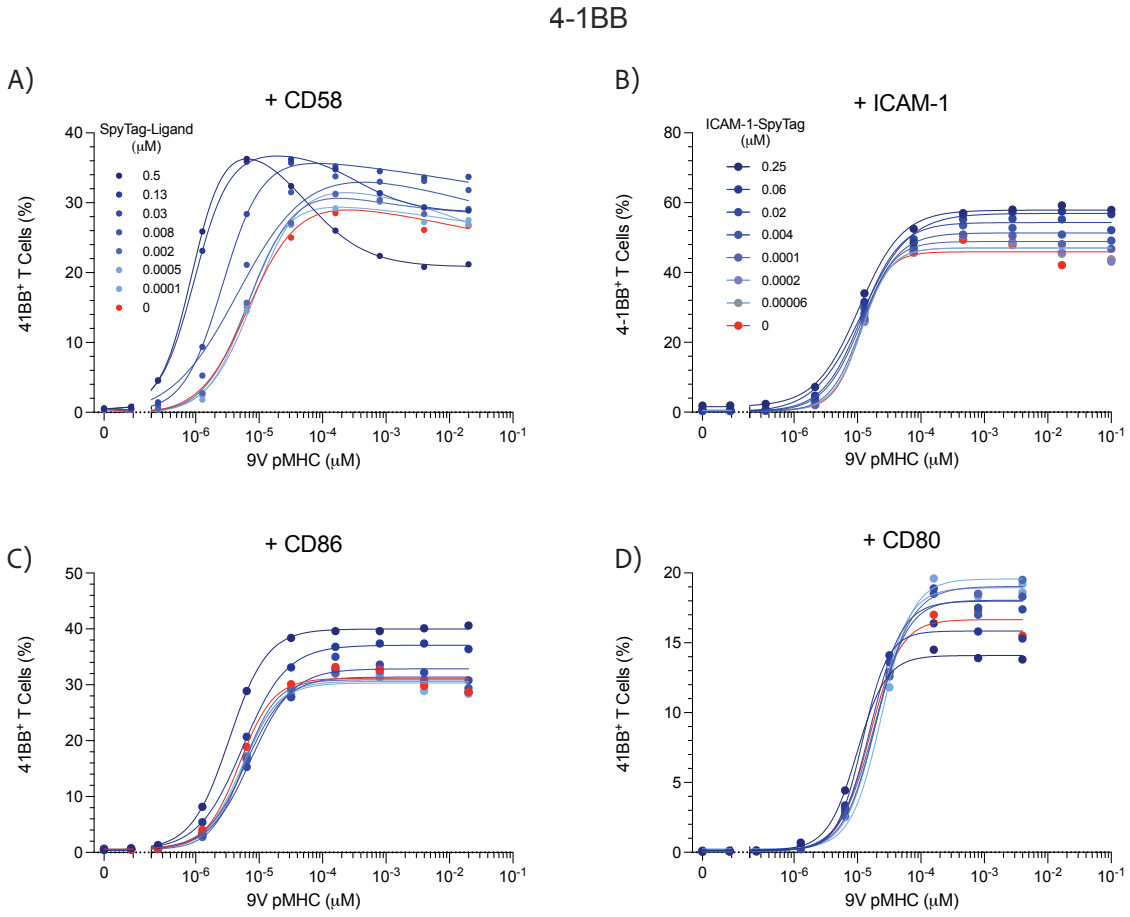


Figure 4.17: Ligation of CD2 and LFA-1, but not CD28, Enhances Antigen Sensitivity at 20 hours as measured by 4-1BB Surface Expression CombiCells cells were incubated with titrating concentrations of 9V pMHC-SpyTag and costimulatory ligand **(A-D)**. Primary human T Cells were added for 20 hours, after which T Cell activation was measured by 41BB up-regulation. The EC_{50} of each costimulatory ligand concentration was extracted by fitting the data with sigmoidal curves in Prism **(E)**.

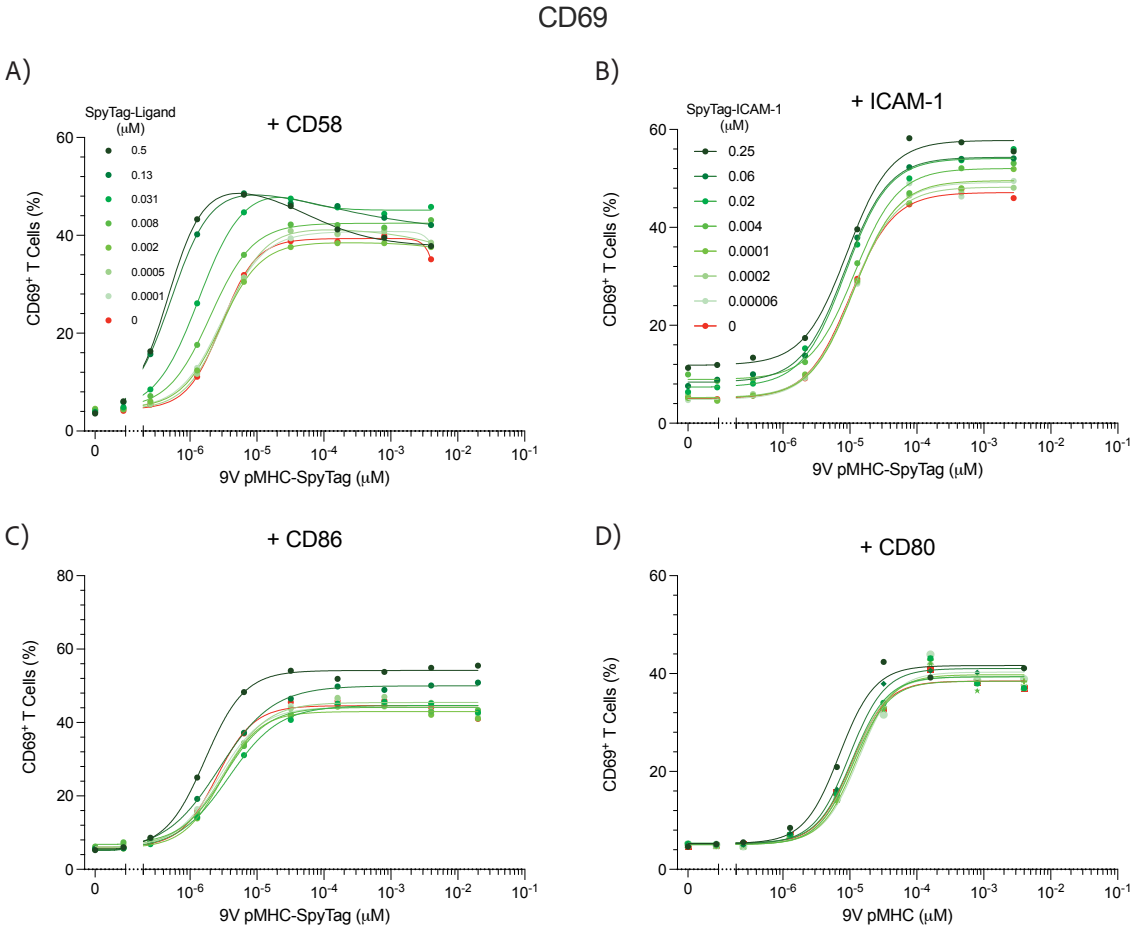
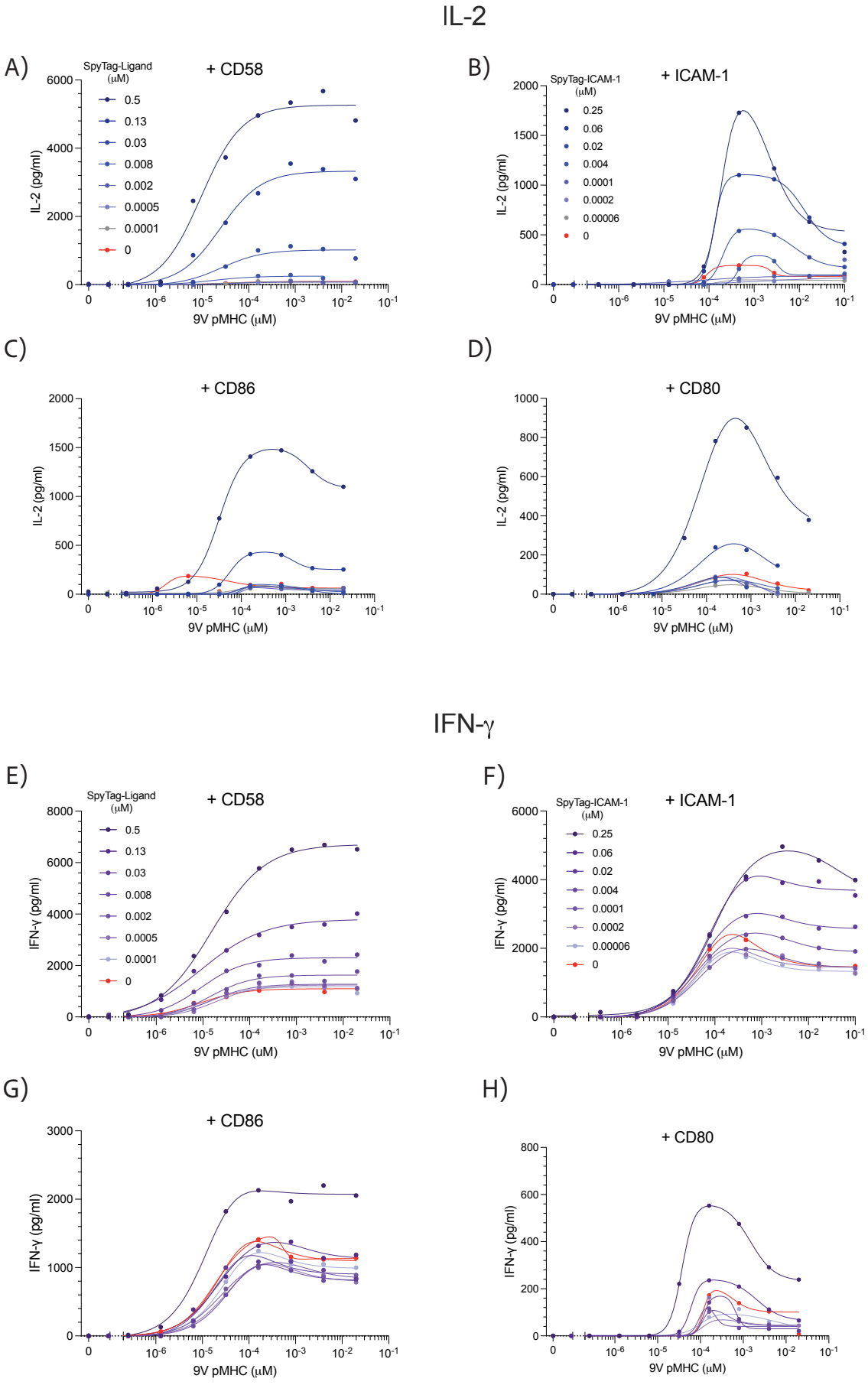


Figure 4.18: Ligation of CD2 and LFA-1, but not CD28, Enhances Antigen Sensitivity at 20 hours as measured by CD69 Surface Expression. CHO-SpyCatcher were incubated with titrating concentrations of 9V pMHC-SpyTag and costimulatory ligand **(A-D)**. Primary human T Cells were added for 20 hours, after which T Cell activation was measured by CD69 up-regulation. The EC_{50} of each costimulatory ligand concentration was extracted by fitting the data with sigmoidal curves in Prism **(E)**.


IL-2
A)
SpyTag-Ligand (μM)
0.5
0.13
0.03
0.008
0.002
0.0005
0.0001
0
+ CD58
IL-2 (pg/ml)
9V pMHC (μM)
B)
SpyTag-ICAM-1 (μM)
0.25
0.06
0.02
0.004
0.0001
0.0002
0.00006
0
+ ICAM-1
IL-2 (pg/ml)
9V pMHC (μM)
C)
+ CD86
IL-2 (pg/ml)
9V pMHC (μM)
D)
+ CD80
IL-2 (pg/ml)
9V pMHC (μM)
IFN-γ
E)
SpyTag-Ligand (μM)
0.5
0.13
0.03
0.008
0.002
0.0005
0.0001
0
+ CD58
IFN-γ (pg/ml)
9V pMHC (uM)
F)
SpyTag-ICAM-1 (μM)
0.25
0.06
0.02
0.004
0.0001
0.0002
0.00006
0
+ ICAM-1
IFN-γ (pg/ml)
9V pMHC (μM)
G)
+ CD86
IFN-γ (pg/ml)
9V pMHC (μM)
H)
+ CD80
IFN-γ (pg/ml)
9V pMHC (μM)

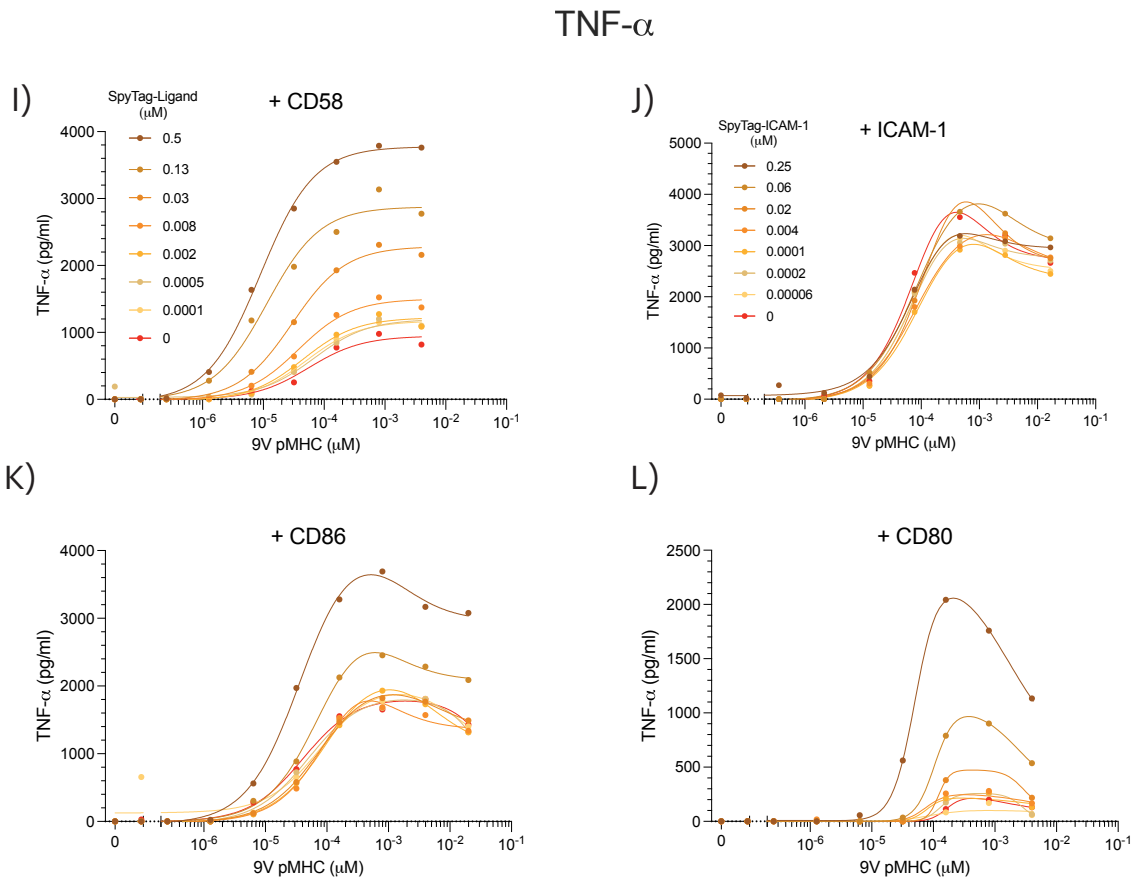


Figure 4.18: Ligation of CD2, LFA-1 and CD28 Increases Cytokine Production over 20 Hours. CHO-SpyCatcher were incubated with pMHC-SpyTag and costimulatory ligand for 20 Hours as described in Fig. 4.17 & Fig. 4.18. IL-2 **(A-D)**, IFN-γ **(E-H)**, and TNF-α (IL-2) concentration in the supernatant was measured through ELISA.

ICAM-1 only enhances sensitivity at 6 hours, whereas CD28 does not impact antigen sensitivity. However, all ligands increased antigen efficacy (the maximum amount of cytokine produced), which is consistent with their costimulation classification.

Investigating the Combined Effect of Costimulatory Ligands on T Cell Activation

Given that many cells simultaneously express ICAM-1 with other ligands to T cell accessory receptors (including ligands to CD2 and CD28), we next investigated the impact of presenting ICAM-1 alongside ligands to CD2 and CD28 together with pMHC. Given that ICAM-1 did not impact antigen sensitivity at 20 hours and that the lifetime of ligands on CombiCells was shorter than 20 hours, we decided to investigate ligand synergy at 6 hours.

Harnessing the ability of the CombiCell system to load combinations of multiple different ligands on the same platform, we added ICAM-1-SpyTag across a titrating concentration of pMHC, together with either CD58-SpyTag, CD86-SpyTag or CD80-SpyTag. The loading of ICAM-1, CD86 and CD80 was unaffected across all pMHC concentrations and the loading of ICAM-1 together with CD80 and CD86 did not affect the loading of either ligand (Fig. 4.19). A subsaturating concentration of ICAM-1 and CD58/CD86/CD80 was chosen (0.03μM).

T cells were then stimulated with these ligand-loaded CombiCells for 6 hours, and T cell activation measured by 4-1BB and CD69 upregulation as well as total IL-2 production (Fig. 4.20). The addition of ICAM-1 and CD58-SpyTag alone caused a reduction in the EC_{50} of 4-1BB$^+$ and CD69$^+$ T cells. Combining ICAM-1 and CD58 resulted in an even smaller decrease in EC_{50} than each ligand individually. In contrast adding ICAM-1 to CD86 or CD80 had no further impact on T cell sensitivity to antigen than with ICAM-1 alone (dotted horizontal line).

In addition, the concentration of IL-2 in the supernatant under combined CD58 and ICAM-1, and CD80 and ICAM-1 costimulation exceeded the individual concentration of CD58, CD80 or ICAM-1 suggesting cooperativity between ligands for cytokine

production / amplification of the T cell response. Combining CD80 with ICAM-1 costimulation resulted in an additive effect upon IL-2 production, in which the total concentration under both ligands equated that of each ligand individually, suggesting subcooperavity between CD80 and ICAM-1 at 0.03μM (Fig. 4.20 E and F).

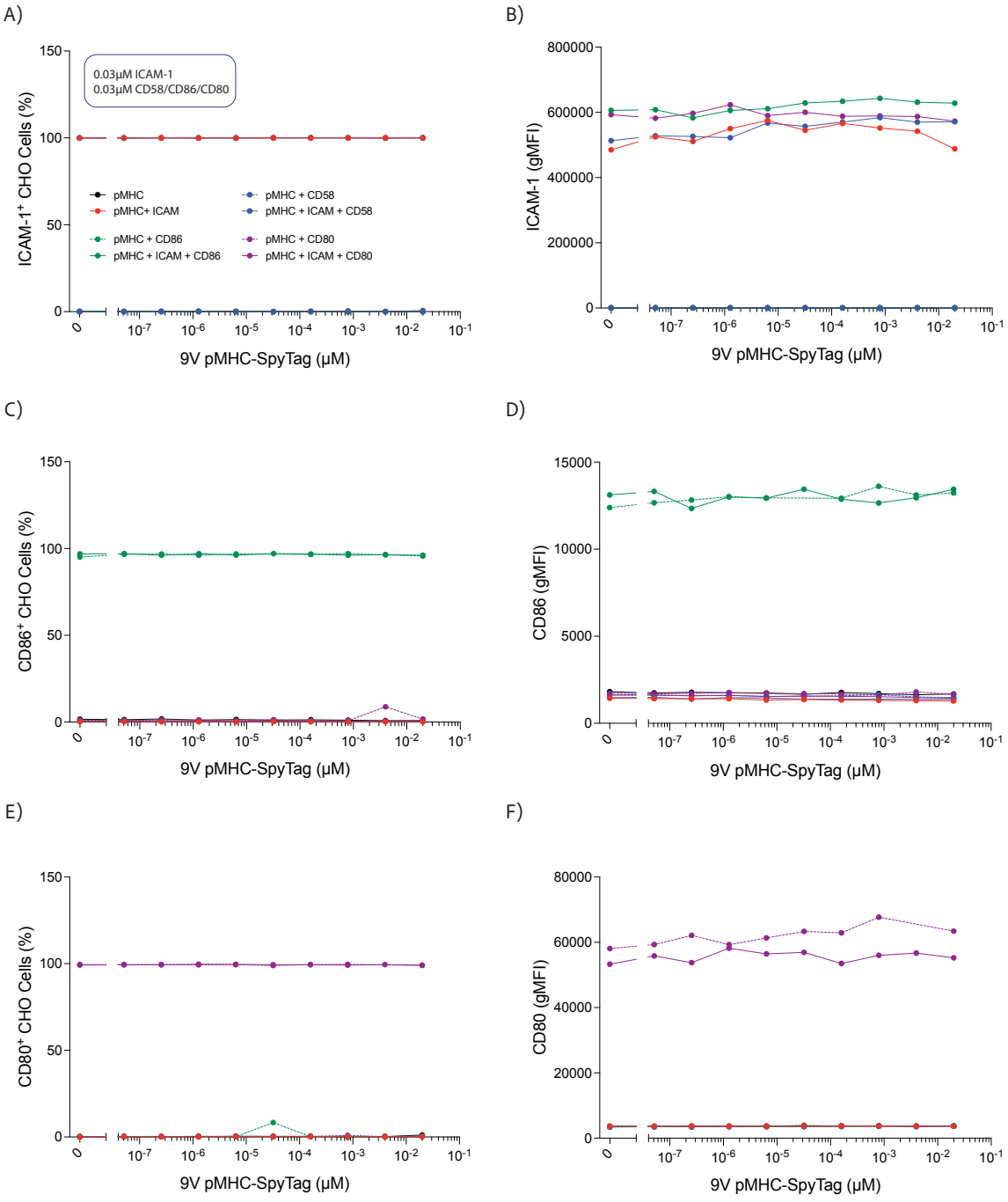


Figure 4.19: Combinations of Three SpyTag-Ligands can be loaded onto SpyCatcher-CHO cells. ICAM-1-SpyTag (0.03 μM) and CD58-SpyTag, CD86-SpyTag or CD80-SpyTag (0.03 μM) was added to SpyCatcher-CHO cells, together with titration of 0.03 μM pMHC-SpyTag. The cells were then stained for ICAM-1 **(A)** & **(B)**, CD86 **(C)** & **(D)** and CD80 **(E)** & **(F)**. Expression was analysed by flow cytometry analysis.

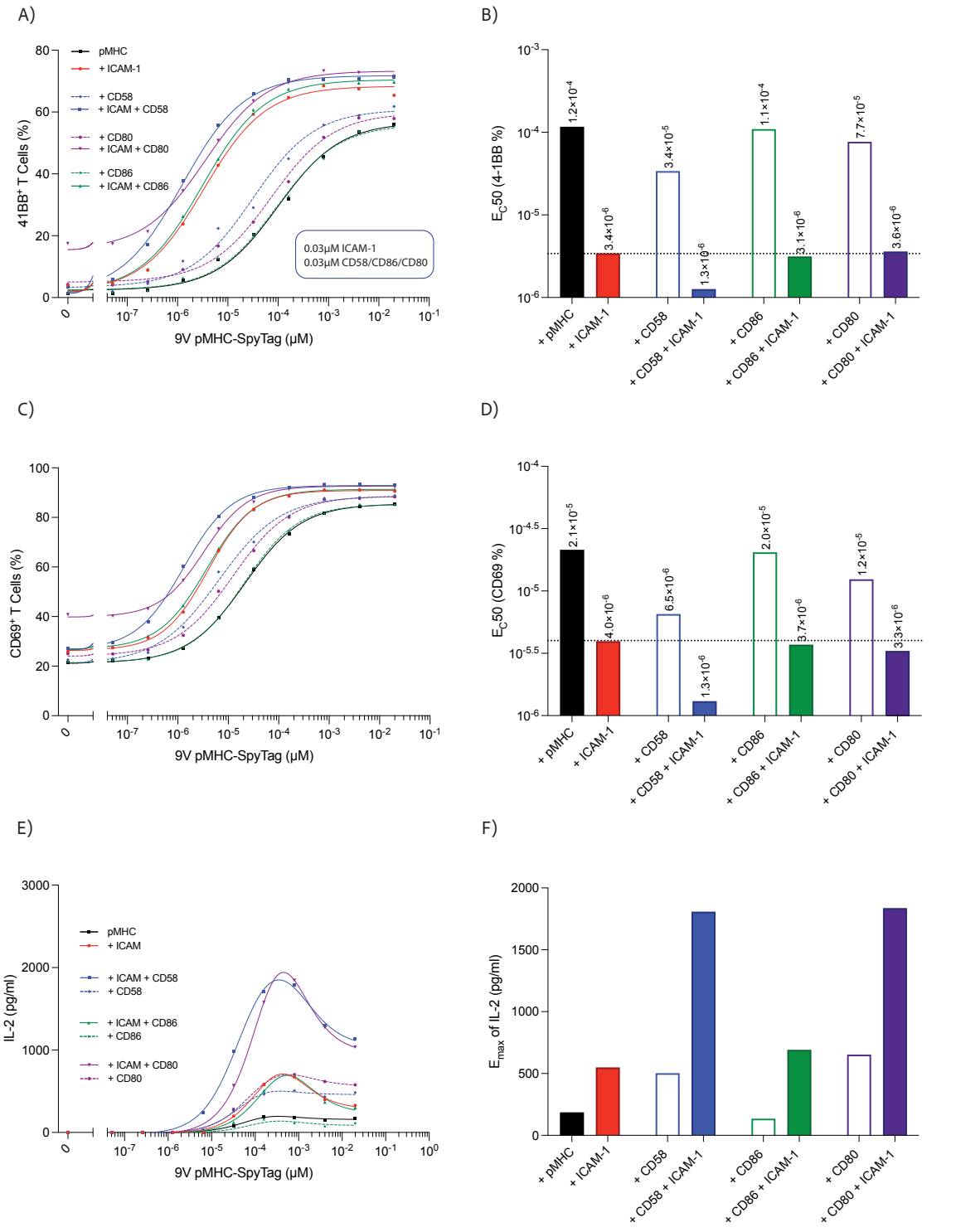


Figure 4.20: ICAM-1 has a Additive effect on IL-2 production with CD28 and CD2, and CD58-induced T Cell sensitivity to antigen. T Cell were stimulated with different combinations of costimulatory ligands for 6 hours. T Cell activation was measured through flow cytometry analysis of 4-1BB and CD69 expression, and IL-2 production through ELISA. The EC_{50} and E_{Max} values were extracted by fitting the data in Prism. n = 1.

4.2.7 Impact of Costimulatory Receptors on CAR-T Cell Activation

Having established the impact of CD2, LFA-1 and CD28 on $CD8^+$ T cell activation through their T cell receptor, we next sought to establish the role of these receptors in T cell activation through a chimeric antigen receptor. As previously introduced in Chapter 2, CARs are synthetic receptors that redirect T cells to target specific antigens (HLA or non-HLA). In Chapter 2, we investigated the ability of T cells to continue to produce cytokines when recognising antigens through CARs.

In addition to continued cytokine production, the antigen sensitivity of CARs is also critical to their function [321]. Recent research has demonstrated that CAR-T cells have an antigen sensitivity defect compared to TCRs, requiring more than 100 times more antigen for T cell activation [229, 322, 307]. This contrasts with the TCR which can respond to even a single antigen [200]. The mechanism underlying the defect in antigen sensitivity has recently been traced to the inability of CARs to exploit the accessory receptors CD2 and LFA-1 [229]. However, these conclusions were based on plate-immobilized ligands, and it is possible that a different conclusion may apply when ligands are mobile.

Therefore, we aimed to investigate the influence of CD2, LFA-1, and CD28 on antigen sensitivity for CAR-T cells relative to that observed in T cells expressing TCRs against the same antigen. This has been previously challenging since it is difficult to modulate the concentration of target antigen alone, let alone together with costimulatory ligands on the surface of cells. However, as our new system allows the presentation of a combination of ligands together with antigen, we harnessed it to investigate the impact of costimulatory receptors on CAR-T cell activation.

Primary human $CD8^+$ T cells from the same donor were transduced with either the 1G4 TCR or D52N-CD28α-28z 2^{nd} generation CAR (with intrinsic CD28 cosignalling, Fig. 4.21 G). These were then added to CombiCells loaded with pMHC-SpyTag alone or with 0.1μM CD58, ICAM-1, CD86 or CD80. After 6 hours T cell activation was measured through 4-1BB (Fig. 4.21 A) and CD69 upregulation (Fig. 4.21 B), and IL-2, IFN-γ, and TNF-α production (Fig. 4.22).

The sensitivity of CAR-T cell to antigen, without costimulation, was impaired compared to the TCR alone (Fig. 4.21 A-B, black line). We observed a ~22-fold decrease in sensitivity between the TCR and CAR under stimulation with antigen alone (Fig. 4.21 H).

As observed previously, we found that ligands to CD2 and LFA-1 but not CD28 significant increased the antigen sensitivity of the TCR. This conclusion was also reproduced for the CAR (Fig. 4.21). However, the effect size (fold-change in EC_{50}) for the CAR was substantially lower than the TCR. Whilst CD2 and LFA-1 increased the antigen sensitivity of the TCR by 230 and 21-fold, respectively, they only increased the antigen sensitivity of the CAR by 11 and 5.4 fold, respectively. As a result, the fold-change in antigen sensitivity between the TCR and CAR increased from 4.7-fold when antigen was presented alone to 76.4 and 18.5 fold when antigen was presented with CD58 or ICAM-1, respectively. These findings suggest that CARs fail to efficiently exploit CD2 and LFA-1 to increase their antigen sensitivity relative to the TCR.

Cytokine levels in the supernatant over increasing antigen concentration was also measured. After 6 hours, as with the cell surface activation markers, the EC_{50} of IL-2, IFN-γ and TNF-α was significantly reduced under CD2 costimulation for both the

TCR and CAR, and this reduction in costimulation was the most impaired between the 2 receptors (Fig. 4.22).

Over 20 hours, CD2 engagement resulted in a lowered EC_{50} with the CAR, but to a much lesser extent than the TCR (Fig. 4.23 G-H), as seen after 6 hours. However ICAM-1 had no effect on antigen sensitivity with both the TCR and CAR after 20 hours, unlike what is observed on the plate system after 24 hours with ICAM-1. However, unlike with 4-1BB and CD69 expression, ICAM-1 increased the EC_{50} of cytokine production with both the TCR and CAR, meaning that antigen sensitivity worsened with the engagement of LFA-1 over a longer time-point (Fig. 4.24).

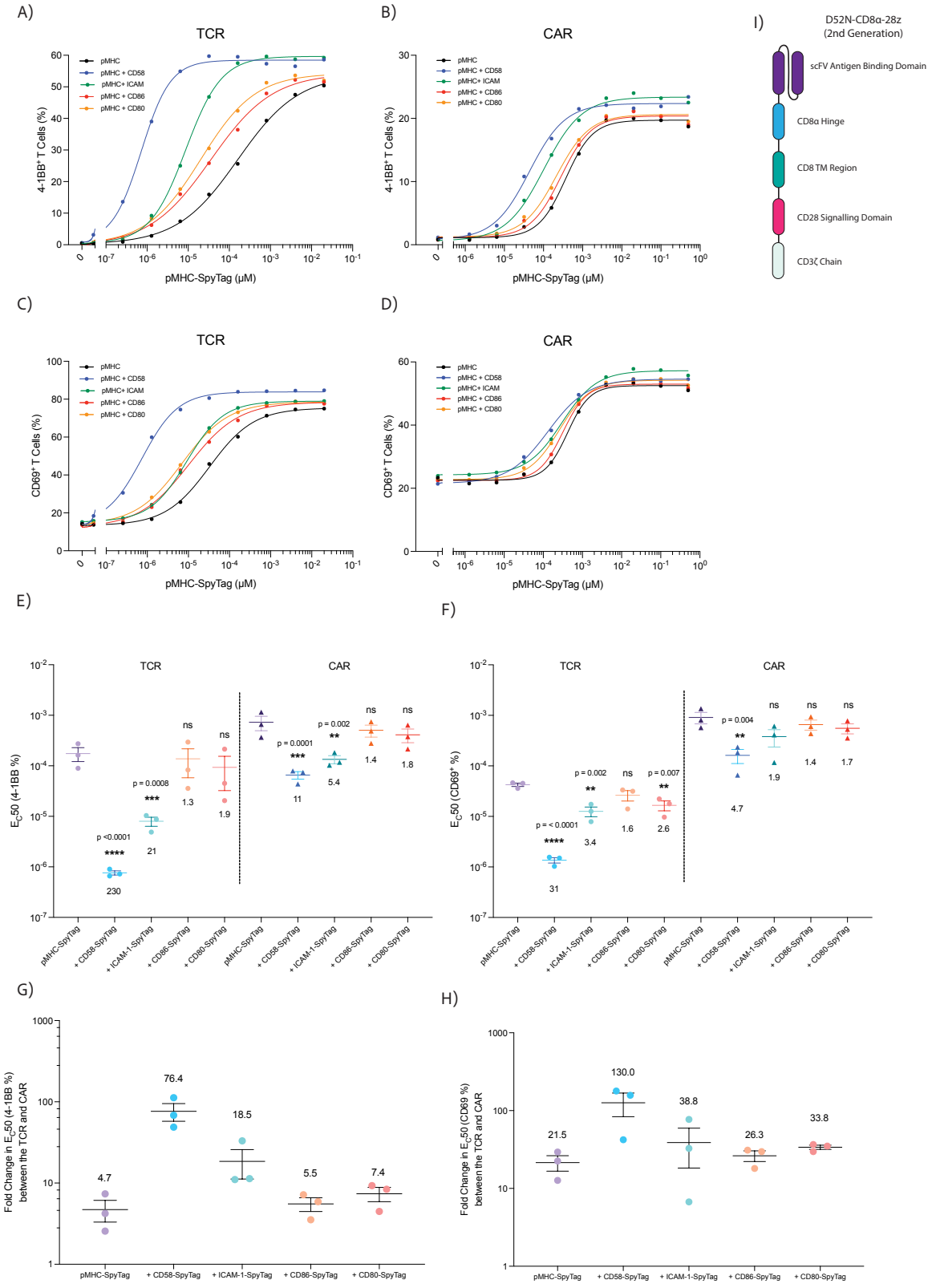


Figure 4.21: See below

Figure 4.21: The antigen sensitivity of CARs is impaired after 6 hours, relative to the TCR in the presence of ligands to CD2 and LFA-1 (measured by T Cell Surface Activation Markers). CombiCells were loaded with a titration of pMHC-SpyTag and 0.5μM of the indicated costimulatory ligand. T cells transduced with a TCR, or CAR **(I)** were added to the cells for 6 hours. **A-D)**. Representative dose-response data of T Cell activation measured by 4-1BB and CD69 up-regulation, fit using sigmoidal curves in PRISM. **E-F)** EC_{50} values were extracted from represented curves. The values below each point indicate the fold-change in EC_{50} induced by the costimulatory ligand relative to the pMHC alone condition ("pMHC-SpyTag"). **(G-H)** Data from **E-F)** was used to calculate the fold difference in antigen sensitivity between the TCR and CAR under each condition. Statistical significance relative to pMHC alone is determined by paired t-tests on log-transformed data. Data is shown as a mean +/- SEM of 3 independent experiments (i.e. 3 independent human donors) . Abbreviations: * = p-value$\leqslant$0.05, ** = p-value$\leqslant$0.01, *** = p-value$\leqslant$0.001, **** = p-value$\leqslant$0.0001, ns = not significant.

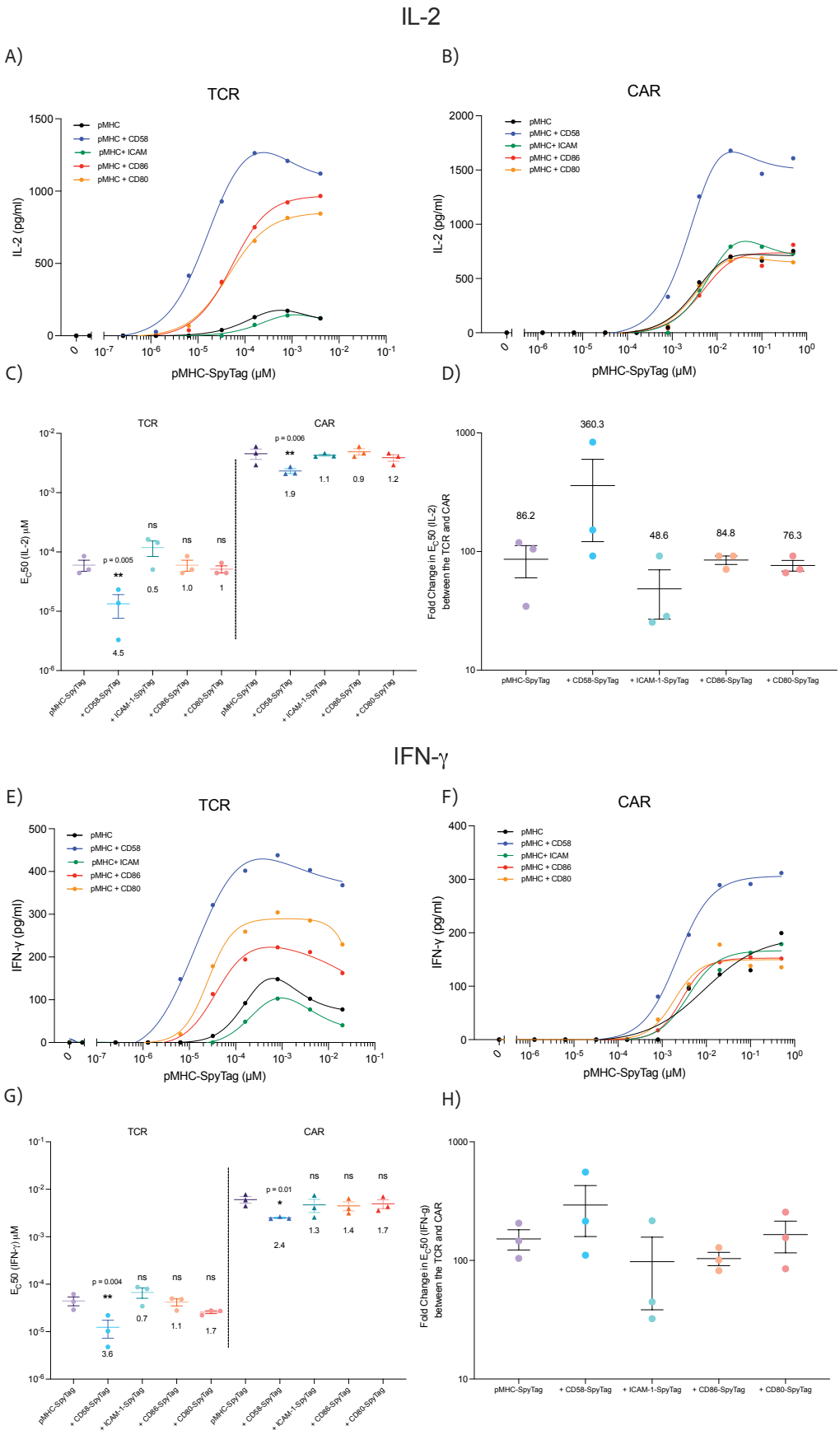


Figure 4.22: See below

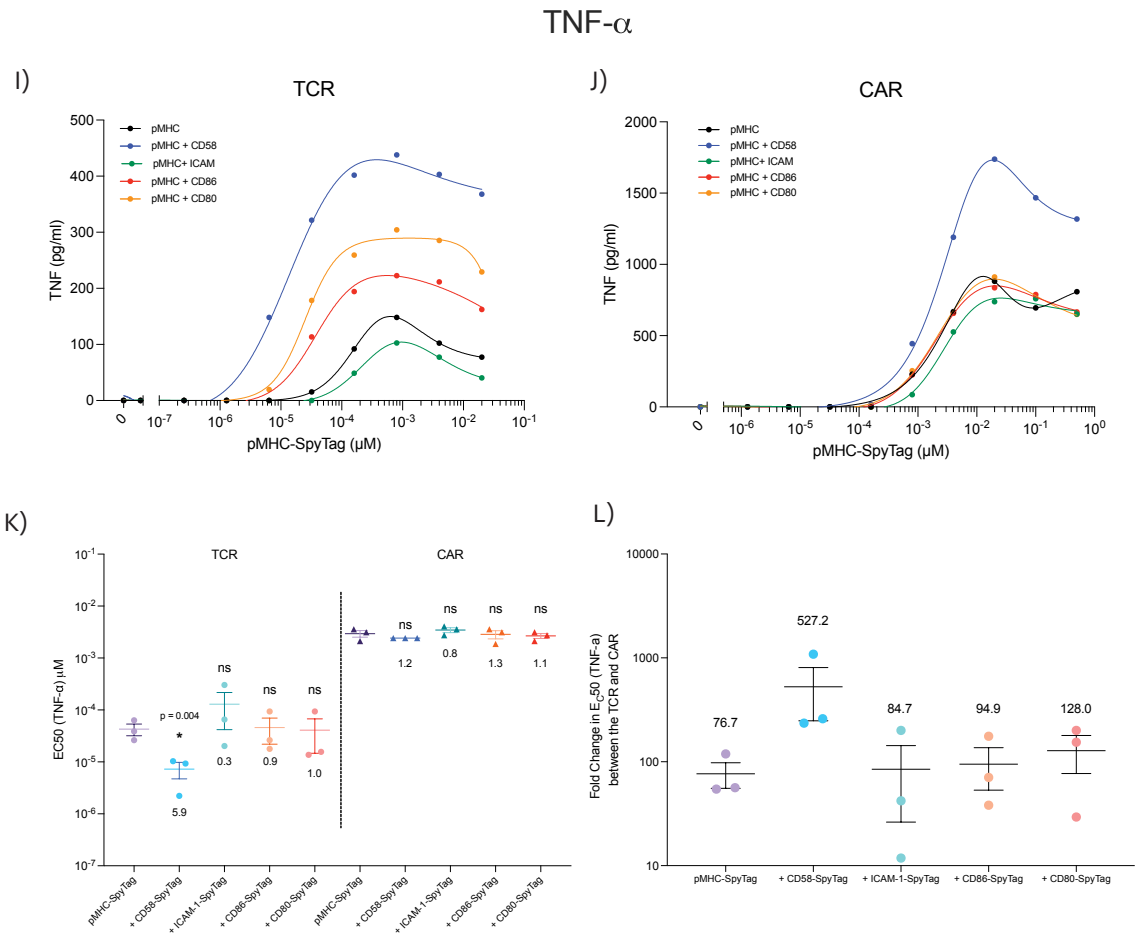


Figure 4.22: The antigen sensitivity of CARs is impaired after 6 hours, relative to the TCR in the presence of ligands to CD2 and LFA-1, as measured by Cytokine Production.. CombiCells were loaded with pMHC-SpyTag and 0.5μM of the indicated costimulatory ligand. T cells transduced with a wild-type TCR, or CAR recognising the same 9V NYESO-1 pMHC were then added to CHO cells for 6 hours. The concentration of IL-2 **(A, B)**, IFN-γ **(D,E)** and TNF-α **(G,H)** secreted into the supernatant measured by ELISA. **C)** EC_{50} values from IL-2 dose-response curves. **F)** EC_{50} values from IFN-γ dose-response curves. **I)** EC_{50} values from TNF-α dose-repsone curves. Bellshaped data was fit in MATLAB and sigmoidal data was fit in PRISM. The numbers indicate the fold-change in EC_{50} induced by the costimulatory ligand relative to the pMHC alone condition ("pMHC-SpyTag"). Statistical significance relative to pMHC alone is determined by paired t-tests on log-transformed data. Data is shown as a mean +/- SEM of 3 independent experiments (i.e. 3 independent human donors). Abbreviations: * = p-value$\leqslant$0.05, ** = p-value$\leqslant$0.01, *** = p-value$\leqslant$0.001, **** = p-value$\leqslant$0.0001, ns = not significant.

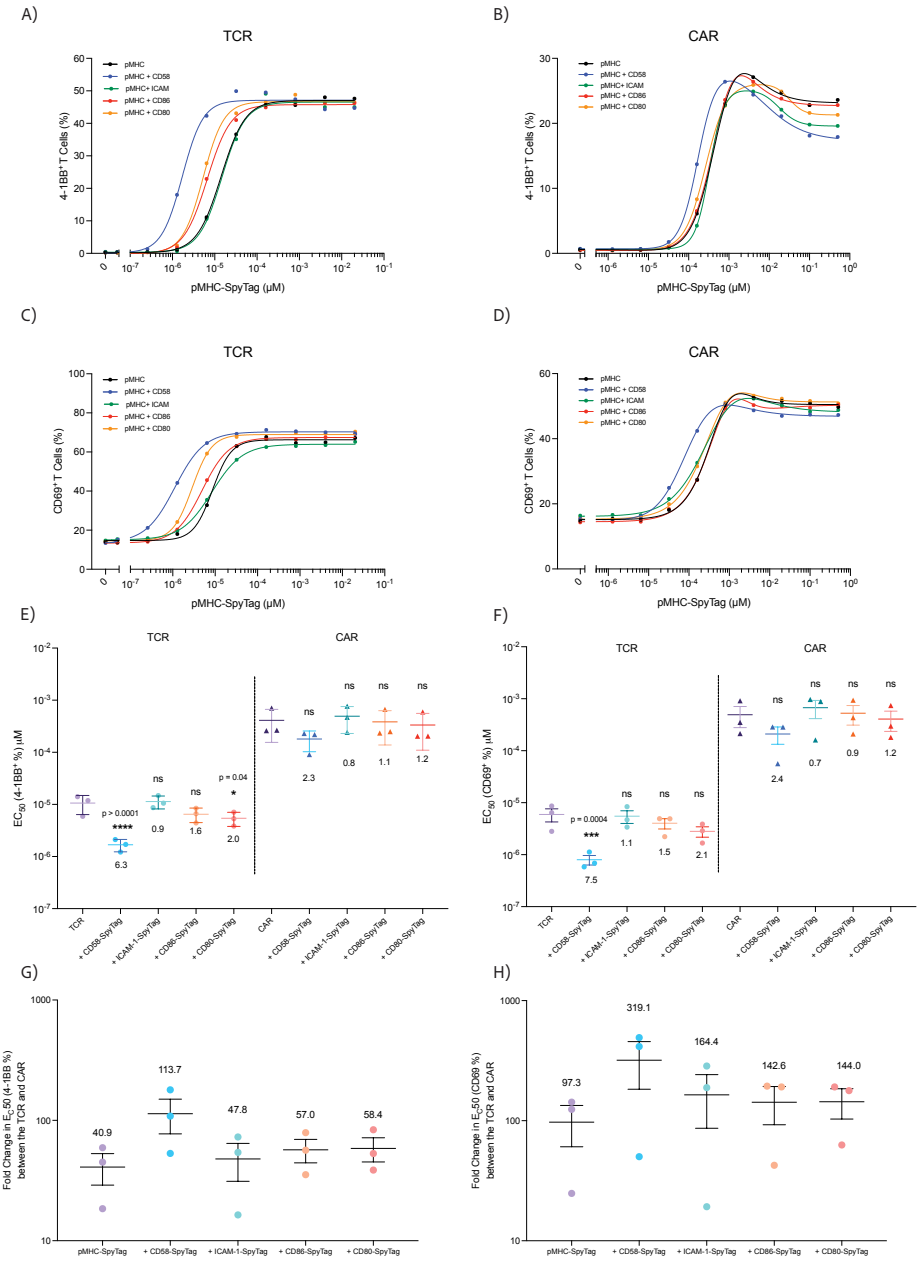


Figure 4.23: The antigen sensitivity of CARs is impaired after 20 hours, relative to the TCR in the presence of ligands to CD2 and LFA-1, as measured by T Cell Surface Activation Markers.. CombiCells were loaded with pMHC-SpyTag and 0.5μM of the indicated costimulatory ligand. T cells transduced with a wild-type TCR, or CAR recognising the same 9V NYESO-1 pMHC were then added to CHO cells for 20 hours. **A-B)**. Representative dose-response data of T Cell activation measured by 4-1BB up-regulation, fit using sigmoidal curves in PRISM. **C-D)** Representative data of T Cell activation measured by CD69 up-regulation, fit using sigmoidal curves in PRISM. **E-F)** EC_{50} values were extracted from curves illustrated in **A-D)**, and compared to the numbers indicate the fold-change in EC_{50} induced by the costimulatory ligand relative to the pMHC alone condition ("pMHC-SpyTag"). Statistical significance relative to pMHC alone is determined by paired t-tests on log-transformed data. Data is shown as a mean +/- SEM of 3 independent experiments (i.e. 3 independent human donors). Abbreviations: * = p-value$\leqslant$0.05, ** = p-value$\leqslant$0.01, *** = p-value$\leqslant$0.001, **** = p-value$\leqslant$0.0001, ns = not significant.

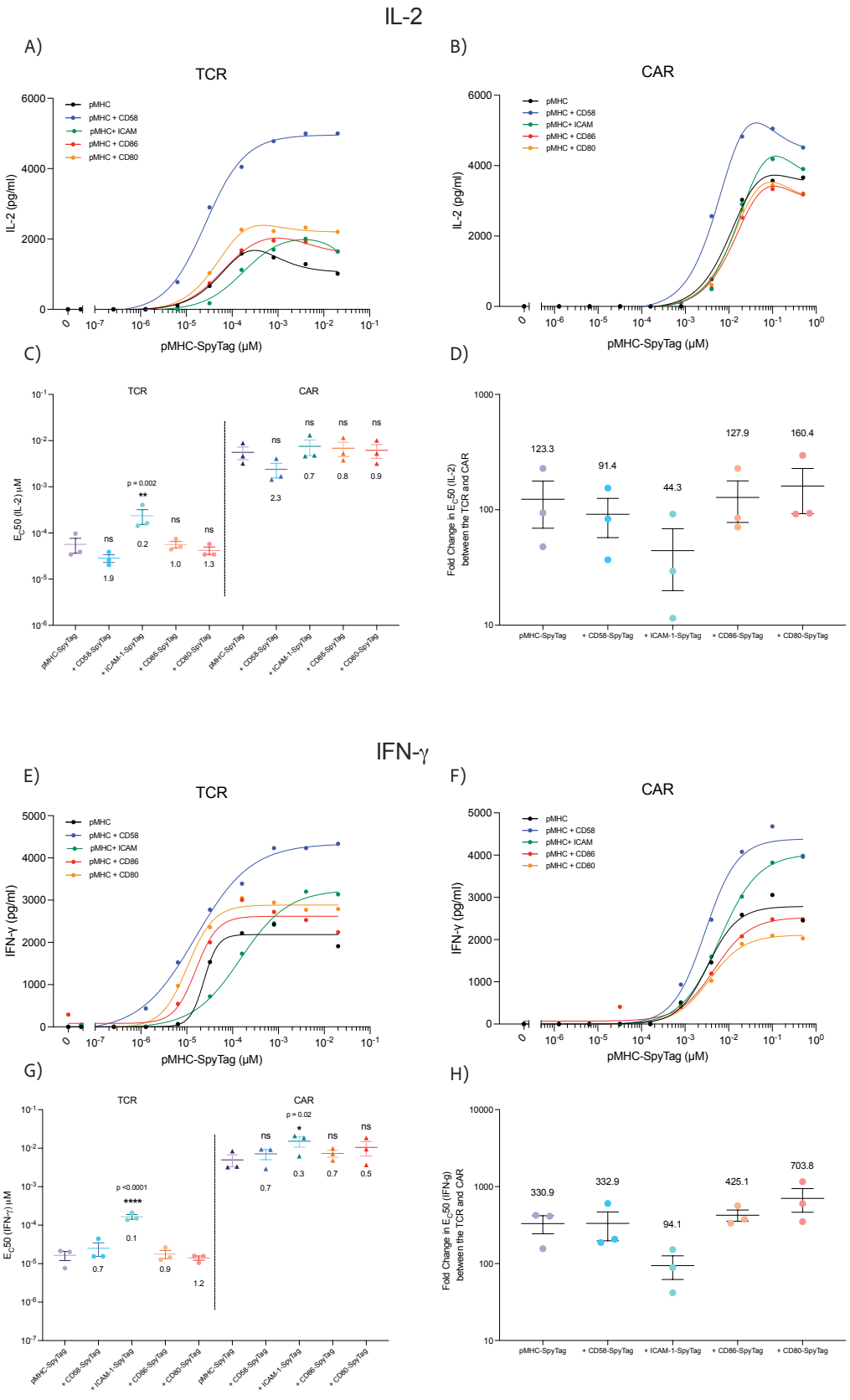


Figure 4.24: See below

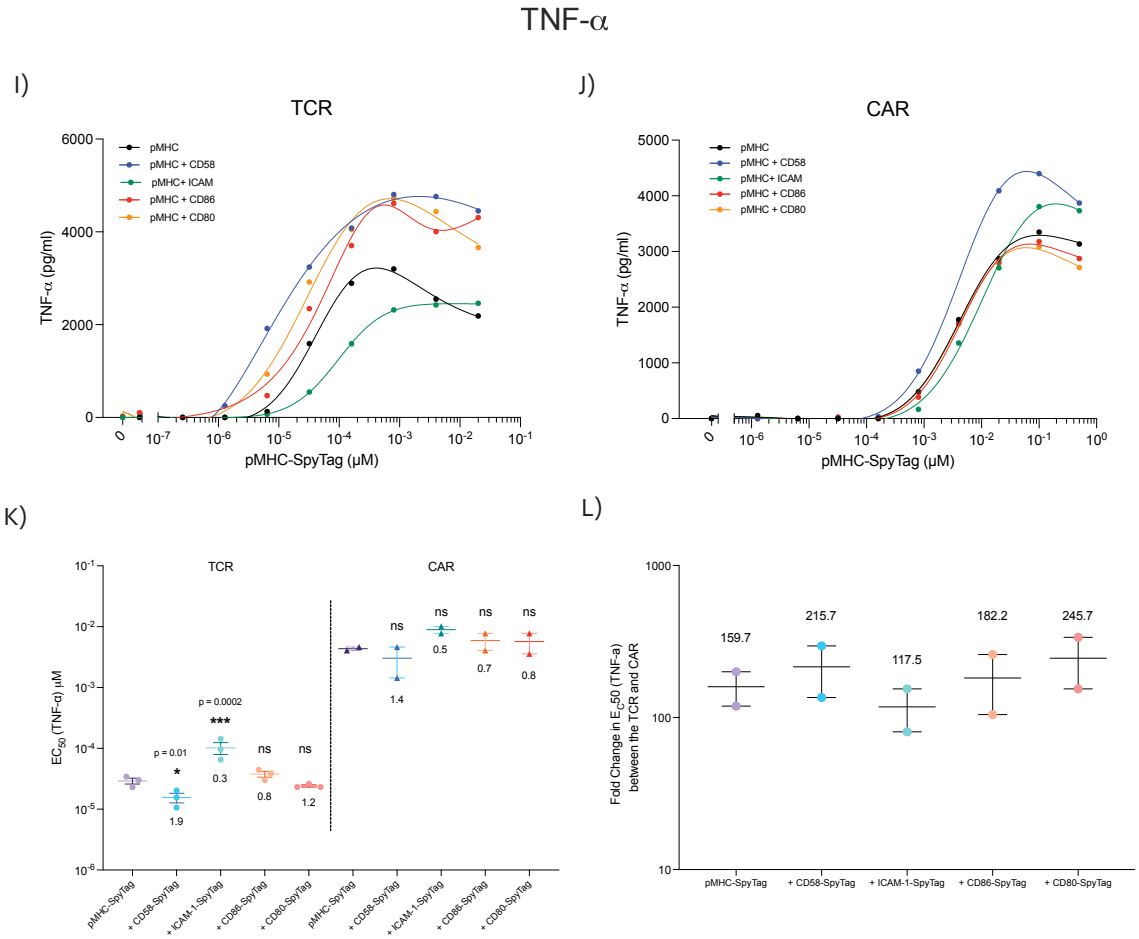


Figure 4.24: The antigen sensitivity of CARs is impaired after 20 hours, relative to the TCR in the presence of ligands to CD2 and LFA-1, as measured by Cytokine Production. CombiCells were loaded with pMHC-SpyTag and 0.5μM of the indicated costimulatory ligand. T cells transduced with a wild-type TCR, or CAR recognising the same 9V NYESO-1 pMHC were then added to CHO cells for 20 hours. The concentration of IL-2 **(A, B)**, IFN-γ **(D,E)** and TNF-α **(G,H)** secreted into the supernatant measured by ELISA. **C)** EC_{50} values from IL-2 dose-response curves. **F)** EC_{50} values from IFN-γ dose-response curves. **I)** EC_{50} values from TNF-α dose-repsone curves. Bellshaped data was fit in MATLAB and sigmoidal data was fit in PRISM. The numbers indicate the fold-change in EC_{50} induced by the costimulatory ligand relative to the pMHC alone condition ("pMHC-SpyTag"). Statistical significance relative to pMHC alone is determined by paired t-tests on log-transformed data. Data is shown as a mean +/- SEM of 3 independent experiments (i.e. 3 independent human donors). Abbreviations: * = p-value$\leqslant$0.05, ** = p-value$\leqslant$0.01, *** = p-value$\leqslant$0.001, **** = p-value$\leqslant$0.0001, ns = not significant.

The Impact of CD2, LFA-1 & CD28 on TCR and CAR Downregulation

CD2 and LFA-1 are adhesion molecules, known to promote T cell receptor (TCR) binding to peptide-MHC (pMHC) complexes, which suggests that they can increase antigen sensitivity by enhancing TCR-pMHC engagement. Using TCR / CAR downregulation as a measure of receptor engagement, we therefore tested whether CD2 and LFA-1 are able to induce a comparable level of downregulation of the CAR compared to the TCR, particularly as the CAR exhibits a defect in harnessing the ability of CD2 and LFA-1 to enhance antigen sensitivity (Fig. 4.25). We found that CD2 and LFA-1 were able to strongly downregulate the TCR, with CD2 inducing a 5-fold decrease in Ic50 (Fig. 4.25 C), and LFA-1 inducing a 2-fold decrease. In contrast, CD2 was only able to downregulate the CAR 2-fold, whilst LFA-1 was unable to induce any meaningful change in receptor downregulation (Fig. 4.25 D).

Additionally, we measured the expression of TCR and CAR before stimulation and found that CAR expression was overall higher than that of the TCR across 6 independent donors (Fig. 4.25 E), indicating that the reduced antigen sensitivity observed with the CAR was not due to lower surface receptor expression. These findings suggest that CD2 and LFA-1 may not efficiently increase antigen sensitivity with CARs, despite their ability to promote TCR-pMHC engagement.

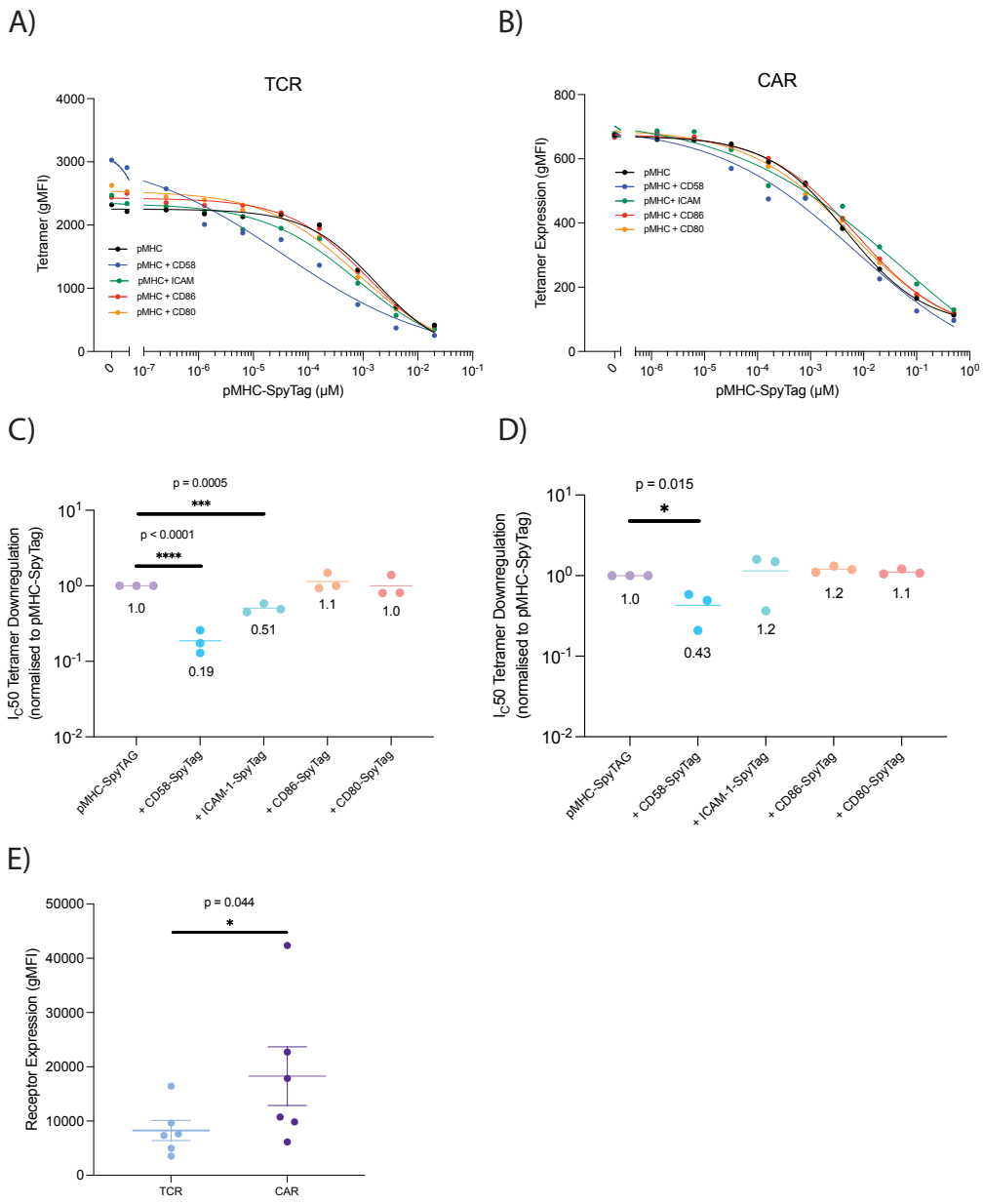


Figure 4.25: CARs Downregulate less efficiently than the TCR under CD2 & LFA-1 Costimulation. T cells were transduced with a wild-type TCR, or CAR recognising the same pMHC. CHO cells were loaded with a titrating concentration of pMHC, and 0.5μM costimulatory ligand, then incubated with T cells for 6 hours. CAR and TCR expression was measured by staining with fluorescently labelled tetramer of pMHC. Representative curves of **A)** TCR and **B)** CAR expression over increasing antigen dose under CD58, ICAM-1, CD86 and CD80 costimulation. **C)** Fold change in IC50 values of TCR downregulation, extracted from 3 donors represented in A). **D)** Fold change in IC50 CAR downregulation values extracted from 3 donors represented in A). **E)** TCR and CAR expression on resting $CD8^+$ T cells, across different donors prior to stimulation assay. Statistical significance relative to pMHC alone is determined by paired t-tests on log-transformed data. Data is shown as a mean +/- SEM of at least 3 independent experiments (i.e. 3 independent human donors). Abbreviations: * = p-value$\leqslant$0.05, ** = p-value$\leqslant$0.01, *** = p-value$\leqslant$0.001, **** = p-value$\leqslant$0.0001, ns = not significant.

The Impact of CD2, LFA-1 & CD28 on the Amplification of CAR-T Cell Activation

From the dose-response curves generated for IL-2, IFN-γ and TNF-α production over an increasing concentration of pMHC-SpyTag (Fig. 4.22 and Fig. 4.24), the maximum of each curve (E_{Max}) was extracted, to compare the final concentration of cytokine produced with the TCR and CAR under each costimulatory condition (Fig. 4.26 A, C, E and Fig. 4.27 A, C, E).

We observed high variability in the absolute amount of cytokine produced across independent experiments where the TCR or CAR are transduced into T cells from different leukocyte cones (i.e. different donors) (Fig. 4.26 & 4.27). The variability cannot be explained by the transduction efficiency (the percent of T cells expressing the TCR or CAR) and this has been discussed previously [229]. Therefore, the amount of cytokine was normalised within each experiment to the amount generated to antigen alone to calculate a fold-change in E_{Max} at 6 or 20 hours (Fig. 4.26 B, D, E and Fig. 4.27 B, D, E).

After both 6 and 20 hours, CD58 significantly enhanced the fold change in E_{Max} of IL-2, IFN-γ and TNF-α with both the TCR and CAR, although the impact of CD58 was consistently stronger with the TCR.

Additionally, LFA-1 was able to significantly increase IL-2 production with the CAR after 6 hours, but not 20 hours. (Fig. 4.26 B). Interestingly, the engagement of CD28 with the CAR had little effect on IL-2 and TNF-α production after 20 hours, but did increase production of these cytokines with the TCR.

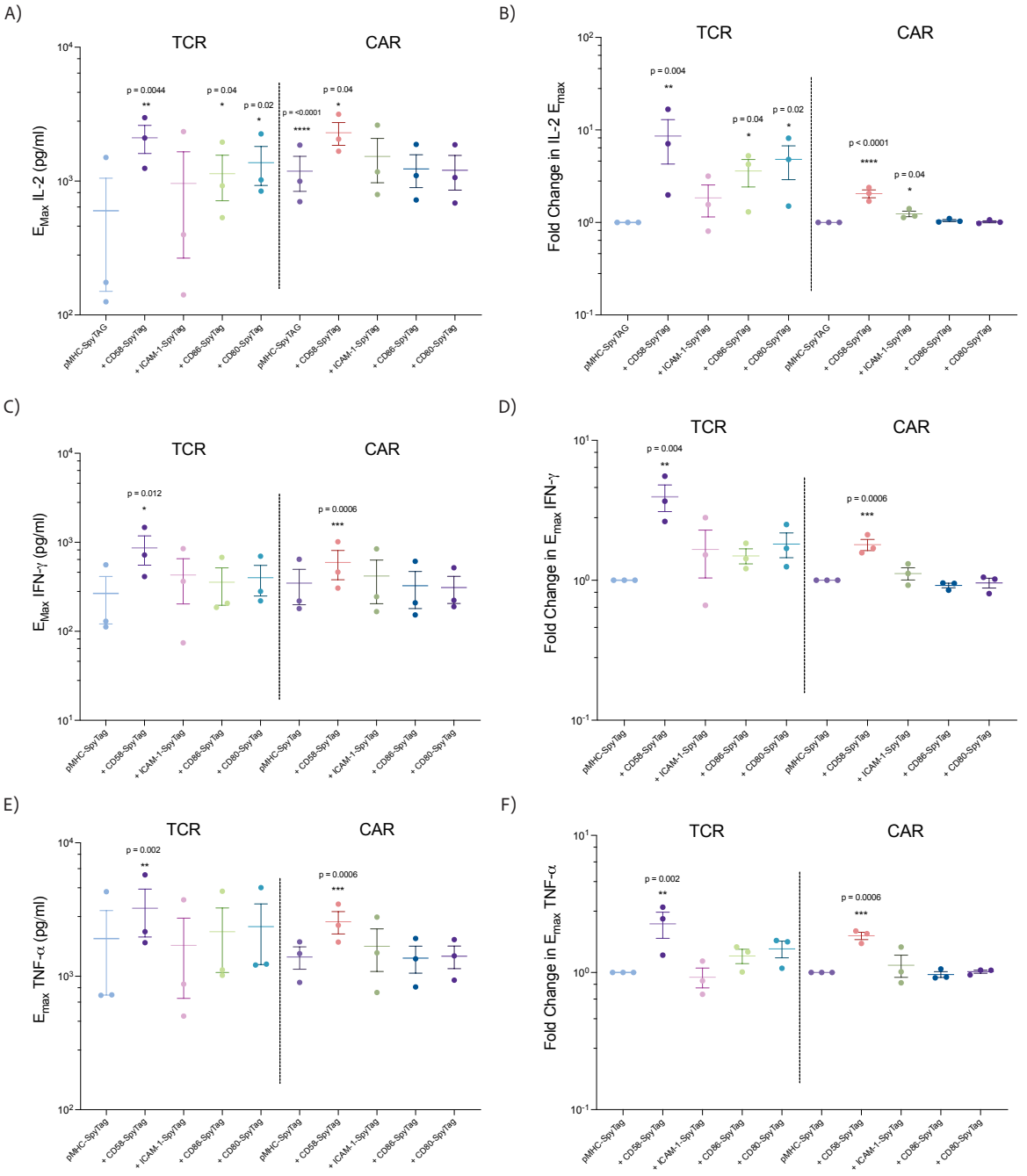


Figure 4.26: CD58-SpyTag amplifies Cytokine Production in both TCR-T Cells and CAR-T Cells over 6 Hours. Dose-Response represented in 4.22 were fitted with Bell-Shaped curves in MATLAB and E_{Max} values extracted (**A, C, E**). (**B, D, F**) The fold-change in E_{Max} induced by each costimulatory ligand relative to the pMHC alone condition ("pMHC-SpyTag"). Statistical significance relative to pMHC alone is determined by paired t-tests on log-transformed data. Data is shown as a mean +/- SEM of 3 independent experiments (i.e. 3 independent human donors). Abbreviations: * = p-value⩽0.05, ** = p-value⩽0.01, *** = p-value⩽0.001, **** = p-value⩽0.0001, ns = not significant.

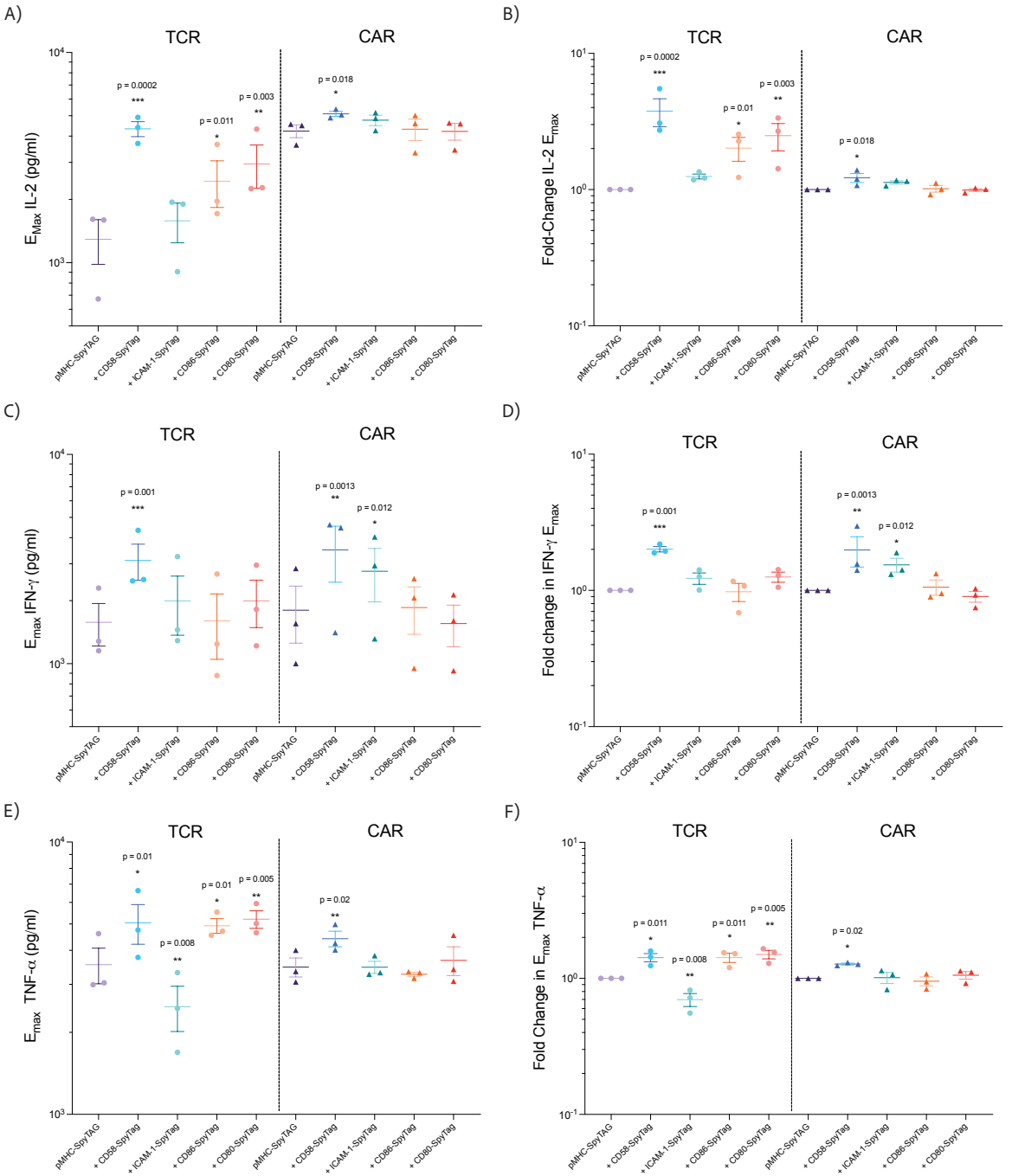


Figure 4.27: CD58-SpyTag amplifies Cytokine Production in both TCR-T Cells and CAR-T Cells over 20 Hours. Dose-Response represented in 4.24 were fitted with Bell-Shaped curves in MATLAB and E_{Max} values extracted **A,C,E. B,D,F)** The fold-change in E_{Max} induced by each costimulatory ligand relative to the pMHC alone condition ("pMHC-SpyTag"). Statistical significance relative to pMHC alone is determined by paired t-tests on log-transformed data. Data is shown as a mean +/- SEM of 3 independent experiments (i.e. 3 independent human donors). Abbreviations: * = p-value⩽0.05, ** = p-value⩽0.01, *** = p-value⩽0.001, **** = p-value⩽0.0001, ns = not significant.

Antigen Sensitivity of Therapeutic CAR-T Cells with the CombiCell System

CD19 CAR-T cell therapy has shown promising results for the treatment of B cell malignancies. However, one of the main challenges in this therapy is the emergence of tumours with low levels of antigen, leading to over 20% of patients experiencing relapse after anti-CD19 CAR-T therapy [223, 221, 323, 307].

Therefore, we exploited CombiCell to study the antigen sensitivity of two FDA/EMA/MHRA approved CARs for the treatment of B cell malignancies, Yescarta®, (manufactured by Gilead) and Kymriah®, (manufactured by Novartis). Both 2^{nd} generation CARs recognise CD19 on B cells, but contain different hinge, transmembrane and cosignalling domains. Yescarta® contains intrinsic CD28 signalling (Fig. 4.28 A), whilst Kymriah® has 4-1BB signalling (Fig. 4.28 B).

To assess their antigen sensitivity, we transduced primary human $CD8^+$ T cells with Yescarta® or Kymriah® and co-cultured them for 6 hours with CombiCells loaded with varying concentrations of SpyTag-CD19.

Yescarta® out-performed Kymriah® when CAR-T cell activation was measured over CD19 concentration via 4-1BB and CD69 upregulation. Specifically, Yescarta® exhibited a higher sensitivity to antigen (lower EC_{50}) (Fig. 4.28 E), and a higher proportion of activated T Cells (E_{Max}) (Fig. 4.28 F), at the highest concentration of CD19 (0.5μM). Our findings suggest that Yescarta® may be more effective in treating B cell malignancies with low levels of CD19 antigen compared to Kymriah®.

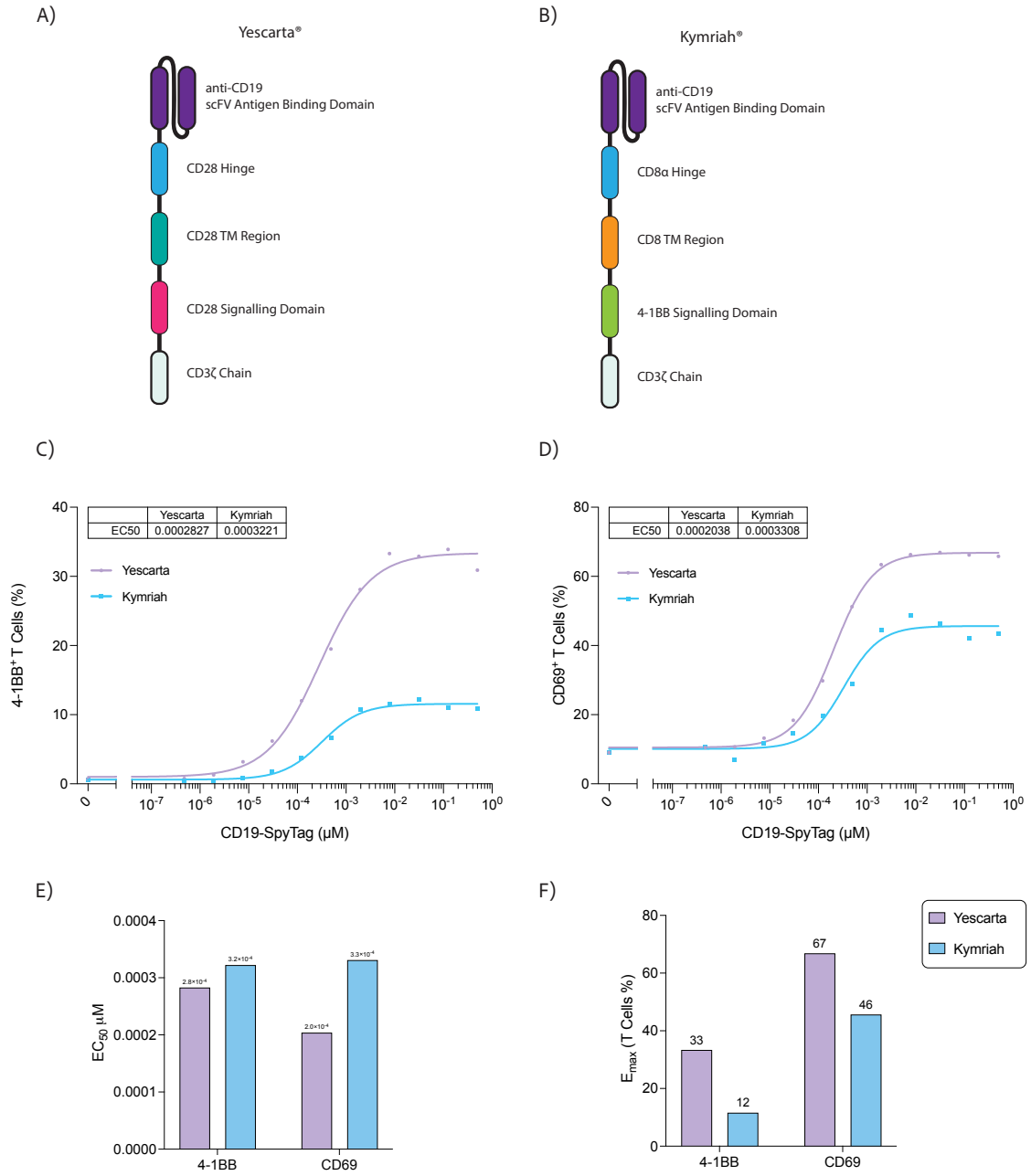


Figure 4.28: The CombiCell System can be used to assess the Sensitivity of anti-CD19 CAR-T Cells. Primary Human T Cells were transduced with two clinical anti-CD19 constructs, each containing different intrinsic costimulatory signalling domains - **A)** Yescarta® (CD28 domain), (Gilead) and **B)** Kymriah® (4-1BB domain) (Novartis). A titrating concentration of CD19-SpyTag was loaded onto CombiCells, and CAR-T Cell activation after 6 hours was measured by **C)** 4-1BB and **D)** CD69 up-regulation. **E)** EC_{50} and **F)** E_{50} values extracted from data fitting to sigmoidal curves in PRISM.

4.3 Discussion

4.3.1 A Novel System for studying Receptor-Ligand Interactions at the Cell-Cell Interface

Here, we present a new approach to present purified, folded, physiological ligands onto the surface of mammalian cells in a dose-controlled way. Our novel method utilizes SpyTag/SpyCatcher technology to couple purified ligands to cells displaying surface SpyCatcher. This enables the generation of antigen-presenting cells with desired ligand combinations and concentrations within minutes. This approach offers several advantages over established methods for studying T cell interactions, such as solid-phase supports and supported lipid bilayers, as it allows receptor/ligand interactions to be studied quantitatively in a physiological context.

Previously, Denham et al [309] demonstrated the potential of SpyTag/SpyCatcher technology for studying immune receptor signalling. By fusing SpyTag to a ligand anchor derived from mouse CD80, they were able to express SpyTag on the surface of CHO cells, allowing subsequent binding of SpyCatcher conjugated to Strep-Tactin. The resulting SpyCatcher-Strep-Tactin complexes were able to interact with twin Strep-tags linked to cell surface receptors of interest, thereby enabling control over receptor signalling. The study demonstrated that pMHC bound to the SpyTag-SpyCatcher-Strep-Tactin complex could load and activate T cells in a comparable way to peptide loaded onto the single-chain dimer of HLA-A*02, providing a titratable, cellular system for studying T cell interactions. This motivated the development of our new system for surface ligand presentation.

Our results showed that surface SpyCatcher expressed using three different hinges was mobile on the surface of CHO-K1 cells, with a diffusion coefficient of approximately $0.2\mu m^2 \cdot s^{-1}$. This value is characteristic of surface proteins that are not bound by ligands, as previously reported [314–318, 324].

The ligands fused to SpyTag that were coupled to surface SpyCatcher on CHO-K1 cells remained stable for 7 hours. As SpyCatcher003 and SpyTag003 have been designed to bind together with an irreversible covalent bond within minutes [313], and we observe consistent levels of SpyCatcher expression (Fig. 4.6), the reduction in ligand levels on the surface of CHO cells is likely due to membrane protein turnover or internalization of SpyTag/SpyCatcher complexes. Therefore, functional data collected after this time, including the 20 hour assays, cannot ensure consistent levels of ligand presented to the T cell throughout the assay.

4.3.2 Role of CD2, LFA-1 & CD28 in T cell Activation

Utilising this cellular platform, called CombiCell, we conducted titrations of purified antigen with various combinations of ligands for three prominent accessory receptors expressed by T cells: CD2, LFA-1, and CD28.

It is important to note that previous chapters (Chapters 2 & 3) using immobilised costimulatory ligands presented to T cells, did not investigate CD80 as it is a dimeric protein at the cell surface [325–327], requiring lateral mobility to be functional. Specifically, CD80 dimerisation is mediated through it's extracellular domain [328], therefore dimerisation would be expected to take place in our system that harnesses the ECDs of ligands. As SpyTag fused to SpyCatcher is mobile within the plasma

membrane, we produced CD80-SpyTag to incorporate in functional assays with this cellular platform to test it's functionality alongside monomeric CD86.

Our findings indicate that ligands to CD2 and LFA-1 can enhance antigen sensitivity by up to 100-fold when antigen is recognized by the TCR, but only about 5-fold when antigen is recognized through a chimeric antigen receptor (CAR), while ligands to CD28 had little impact on T cell antigen sensitivity. These results are consistent with existing data demonstrating the ability of CD2 and LFA-1 to enhance antigen sensitivity in murine models [87, 114, 121] and with immobilized ligands on plates [229] (Chapter 2) using a system that allows for ligand mobility. Interestingly, this suggests that CD2 & LFA-1 do not require ligand mobility to improve antigen sensitivity or increase cytokine production. This is consistent with the role of CD2 and LFA-1 as T cell adhesion molecules, facilitating close contacts between the TCR and APC, either by matching the intermembrane distance between the pMHC and TCR (CD2), or by segregating from the TCR and stabilising close contact zones peripherally (LFA-1) [258, 287, 286].

Furthermore, we found that CD2 consistently showed the largest impact on E_{Max} and EC_{50} compared to CD28 and LFA-1, which is consistent with previous work comparing the costimulation induced by CD58, CD86, and CD70 on plates [227]. We can now confirm that compared to another critical T cell adhesion molecule, ICAM-1, CD58 has the most potent impact on T cell activation.

Given the modest effect of CD28 engagement on T cell antigen sensitivity with immobilised CD86 on a solid-phase surface, we were interested to test this phenotype in a system that permits ligand mobility. Our experiments with SpyTag-CD86 and SpyTag-CD80 loaded onto CombiCells revealed little impact on antigen sensitivity, despite both ligands resulting in increased total cytokine production. These findings

are consistent with previous studies indicating that CD28 has only a minor effect on antigen sensitivity when engaged with immobilized CD86 on plates [229], and HEK cells expressing CD86 or CD80 had only a minor effect on primary T cell sensitivity to antigen [121].

In addition to observing the distinct impact of CD58, ICAM-1 and CD86 on T cell activation, we found time-dependent differences on the EC_{50} with ICAM-1. Engagement of LFA-1 improved antigen sensitivity after 6 hours, but after 20 hours, ICAM-1 exhibited minimal effects on antigen sensitivity or total cytokine production, which contrasts with the observations made in the plate system. Unlike the fixed ligand concentration observed on plates, ligand mobility on cells enables fluctuations in ligand density. As has been demonstrated for natural T cell/APC conjugates and T cell/bilayer interfaces, T cells can cluster ligands at the interface [329]. Ligand clustering can increase the local concentration of ligand (e.g. pMHC) at the receptor's surface, increasing the avidity of receptor-ligand interactions, and lowering the EC_{50}. We speculate that over an extended time period (such as 20 hours), the effective concentration of pMHC surrounding T cells reaches a point that cannot be enhanced further through ICAM-1 engagement. Interestingly, CD2 is able to lower the EC_{50} at this longer time point, highlighting a possible differential role between both adhesion receptors.

4.3.3 Role of CD2, LFA-1 & CD28 in CAR-T cell Activation

It has become increasingly clear that tumors can evade CAR-T cell therapy by down-regulating or losing the target antigen, leading to disease relapse [330]. Therefore, understanding the mechanisms behind antigen sensitivity in CAR-T cells is crucial for the development of effective clinical therapies. Until now, it has been difficult to titrate folded antigen onto the surface of target cells to study the efficacy of CAR-T cells over a range of antigen densities. Consequently a defect in the antigen sensitivity of CARs compared to the TCR is a relatively recent finding [307, 331, 322, 332]. In light of these findings, we investigated CAR-T cell function with the engagement of different costimulatory receptors to better understand the role of costimulation in CARs compared to the TCR.

Interestingly, over both 6 and 20 hours, we found that 2nd generation CAR-T cells exhibited impaired antigen sensitivity under both CD2 and ICAM-1 costimulation, compared to the TCR. This was accompanied with an impaired ability to downregulate the CAR, suggesting that this defect in antigen sensitivity arises at least partly from the impairment of antigen engagement between CARs and pMHC, as has been suggested previously [229].

It is important to note that the D52N CAR used in this study has a higher affinity for 9V pMHC than the 1G4 TCR. However, when a lower affinity variant of the same pMHC was used with the CAR, the discrepancy in antigen sensitivity between the TCR and CAR was enhanced, not reduced [229]. Therefore, it is unlikely that the defect displayed by the CAR is due to enhanced affinity for pMHC. Taken together, the CombiCell platform has shown that CARs are inefficient at exploiting the adhesion receptors CD2 and LFA-1 compared to the TCR, in agreement with our previous findings [229].

Through this experimental setup we could also assess the total production of cytokines by CAR-T cells. After 6 hours of stimulation, the maxmimum amount of cytokine produced was similar between the TCR and CAR. However after 20 hours, the CAR produced much more IL-2. This is interesting as extrinsic CD28 engagement had little impact on IL-2 production with the CAR-T cells. This suggests that intrinsic CD28 signalling within the cytoplasmic tail of the CAR may be more efficient than extrinsic CD28 signalling in primary human $CD8^+$ T cells. A possible explanation for this is that CD28 surface expression can be variable on human $CD8^+$ T cells [333, 334] (Fig. 3.3) so that providing CD28 signalling within the CAR ensures that all T cells are able to respond.

Finally, we have demonstrated the use of a system to compare the phenotype of therapeutic anti-CD19 CAR-T cells. Yescarta® CAR-T cells, incorporating CD28 signalling, were activated at a lower antigen density compared with Kymriah® CAR-T cells that contain 4-1BB signalling. This is consistent with previous work directly comparing the cytotoxic ability of these CARs, with Yescarta® showing enhanced IL-2 production and cytotoxicity at lower levels of CD19 antigen [321], and enhanced signal strength through phosphoproteomic analysis [335].

Interestingly, as discussed above, CD28 has little impact on the antigen sensitivity of CAR-T cells when engaged with CD86 or CD80 extrinsic to the CAR. However when a CD28 domain is incorporated within the CAR itself, as in Yescarta®, the CAR is able to respond to lower concentrations of antigen. Replacing the extracellular $CD8\alpha$ hinge region of Kymriah with a CD28 hinge, recovered antigen sensitivity to a level comparable to Yescarta® [330], implicating the CD28 hinge region of the CAR in the sensitivity to antigen. However although the extracellular hinge region of CARs is influential in altering antigen sensitivity [336], it is still unclear how this is achieved.

4.3.4 System Limitations

Endogenous ligands presented on APCs, can maintain more stable expression over extended lengths of time. However, when SpyTag-ligands are coupled to the surface of CombiCells, their lifetime is determined by the turnover rate of surface SpyCatcher, which we have measured to be approximately 7 hours. Therefore, to ensure continuous ligand presentation, additional ligand would need to be added at regular intervals. However, this also provides a unique opportunity to add ligands at any time point to specifically investigate their impact in different temporal contexts. This is particularly important in studying costimulatory receptors, which undergo temporal changes in expression in response to changes in the local environment, as described by the tide model of co-signalling [42].

Additionally, CombiCell is currently based on CHO cells derived from hamsters, and therefore express ligands that are less likely to cross-react with human receptors, facilitating the study of individual human receptor function. However, a more clinically relevant system to study CAR-T cell function would involve expressing SpyCatcher on a cancer cell line, such as Nalm6 cells, that would also enable the cytotoxic function of CAR-T cells under different cell-cell interactions to be investigated.

4.3.5 Future Work: Expanding CombiCell

T cells can interact will nearly all cells *in vivo*, recognising peptide antigens on normal, infected or cancerous cells. These target cells have a diverse combination of ligands, expressed in varying amounts, that interact with surface receptors on T cells that ultimately shape T cell function. Therefore a system that allows us to systematically study different cell-cell interactions is valuable in helping us understand T

cell biology. However other immune cells, such as B cells and phagocytes also interact with a wide range of targets, meaning our platform can be used to further understand key receptors (e.g. the BCR) that contribute to the specialised function of these cells types.

4.3.6 Conclusion

In summary, we have introduced a novel experimental system, CombiCell, which allows for systematic investigation of cell-cell interactions on a platform that enables lateral mobility of dose-controlled physiological ligand, distinguishing it from previous systems. Harnessing these features, we explored the contribution of various costimulatory receptors in T cell activation. Our results confirm prior findings regarding the role of CD2 and LFA-1 in modulating antigen sensitivity, and also indicate that CAR-T cells are not as effective as TCR-expressing T cells in exploiting adhesion molecules to enhance sensitivity. Furthermore, we demonstrated the ability of CombiCell to assess the antigen sensitivity of clinically-approved anti-CD19 CARs, paving the way for future use of this system in evaluating various CAR constructs. Ultimately, Combicell has broad applicability and could be used to study receptor-ligand interactions on a range of cell types, yielding new insights into receptor function.

Chapter 5

Discussion

5.1 Summary

A vast number of costimulatory receptors have now been identified. As it is evolutionarily unlikely they all have overlapping functions we sought to understand how they may differ in their quantitative contributions to $CD8^+$ T cell activation.

To this end, the quantitative impact of CD2, LFA-1 and CD28 on T cell activation was systematically assessed using at first a reductionist plate stimulation system, followed by the development of our novel cellular system, enabling the combinatorial presentation of physiological ligands on mammalian cells. The quantitative impact of each costimulatory receptor on T cell activation was assessed using phenotypes that have important biological consequences for effective immunity: the sensitivity of T cells to antigen dose, the duration of T cell responses over time and the antigen efficacy (maximum T cell response). Furthermore, as these responses are particularly relevant to CAR-T cell immunotherapy that relies upon sufficient activation of T cell effector responses, we studied the impact of costimulation on CARs, to ultimately help address their *in vivo* limitations.

First, we assessed the contribution of CD2, LFA-1 and CD28 to T cell responses over time using a plate system that enabled precise control over the specific costimulatory ligand presented to T cells allowing individual costimulatory receptors to be engaged independently and in a high-throughput manner. CD2 and LFA-1 were able to prolong T cell responses to constant antigen exposure. Interestingly, 1st generation CAR-T cells were also able to capitalise on CD2 to prevent a drop in cytokine production over time. On the other hand, 2nd generation CAR-T cells, containing an intrinsic CD28 signalling domain, were able to accelerate cytokine production over time without the aid of external costimulation. Notably CD28 exhibited different

effects on adaptation depending on whether the molecule was incorporated within a CAR or engaged extrinsically (no impact on adaptation).

Next, we utilised the same plate-stimulation system to investigate the impact of each costimulatory receptor over a range of pMHC doses to assess their individual contribution to the antigen sensitivity of T cells (through EC_{50} measurements), and the efficacy of response (through E_{max} measurements). Whilst the engagement of all receptors enhanced the efficacy of the T cell cytokine response, CD2 and LFA-1 were able to enhance antigen sensitivity in line with previous *in vivo* [87, 114, 121, 275, 276, 260] and *in vitro* [87, 229, 273] observations whereas we found CD28 to have no impact on antigen sensitivity.

Given that we did not observe a shift in antigen sensitivity by engaging CD28 with immobilised CD86, and that *in vivo* costimulatory ligands can freely diffuse within the plasma membrane, we were motivated to develop a system that would enable us to study these quantitative phenotypes with mobile ligands titrated directly on the surface of cells. Harnessing the SpyCatcher/SpyTag fusion proteins, we developed CombiCell that enabled us to present purified pMHC together with purified costimulatory ligand to primary T cells. Using this system, we recapitulated our findings that CD2 and LFA-1 enhance T cell sensitivity to antigen, and previous findings that CARs exhibit an impaired ability to capitalise on these adhesion receptors to improve antigen sensitivity compared to the TCR [229].

5.2 Implications of Findings

5.2.1 Costimulation with the TCR

Although it is known that CD2, LFA-1 and CD28 exert impacts on specific T cell responses (such as cytokine production, proliferation, and cytotoxicity), their relative quantitative contribution to T cell function is understudied. Furthermore, many studies have used non-physiological stimulation conditions; either through anti-CD3 activation beads, PMA, ionomycin and/or agonist antibodies against costimulatory receptors to decipher the role of receptors on T cell activation. Here we have shown that by engaging CD2, LFA-1 and CD28 with their physiological ligand, alongside pMHC, they exhibit different quantitative impacts on T cell responses.

CD2 and LFA-1 are both adhesion molecules and are both able to enhance T cell sensitivity to antigen on a plate and cellular system, consistent with previous findings. Together with CD28's inability to impact antigen sensitivity as a receptor that also has limited adhesion capabilities, our work supports suggestions that CD2 and LFA-1 improves antigen sensitivity by influencing pMHC-TCR binding kinetics [320], and stabilising interactions between T cells and APCs. CD2 and LFA-1 have also been shown to enhance TCR proximal signalling [112, 236] by promoting the recruitment of effector molecules to their intracellular tails. It remains unclear to what extent signalling by CD2 and LFA-1 impact their ability to improve antigen sensitivity. Mutating specific residues responsible for coordinating intracellular signalling within the cytoplasmic tails of CD2 and LFA-1 could reveal further insight into how the receptors achieve improved T cell antigen sensitivity.

CD28 is often regarded as the strongest costimulatory receptor within the context of naïve T cell activation. Compounded by the use of imprecise definitions of costimulation, and non-physiological experimental conditions (e.g. agonist anti-CD28 antibodies), it has been difficult to establish whether CD28 exerts such an influential role in other contexts of T cell activation. Our work illustrates that across different quantitative measurements of blasted $CD8^+$ T cell activation, CD28 is unable to improve antigen sensitivity and unable to prolong the duration of T cell responses when engaged with physiological ligand.

In contrast CD2 is both able to dramatically enhance antigen sensitivity and prolong T cell responses. As a result the data presented on antigen experienced human $CD8^+$ T cells suggests that CD28 does not exert the strongest effect on effector T cell responses. It is important to note that throughout our study we have used similar concentrations of each costimulatory ligand. However, we cannot rule out that at higher ligand concentrations, CD28 may improve sensitivity. Furthermore, given that different T cell subsets exhibit differential costimulatory requirements [337, 338], it is important to establish the role of these costimulatory receptors across both $CD4^+$ and $CD8^+$ T cells and naïve, effector and memory subsets. In particular it would be interesting to see whether CD28 exerts a strong effect on naïve $CD4^+$ T cells, using our cellular system, as has been described previously [130].

In addition, our work focuses on engaging costimulatory receptors with the extracellular domains (ECDs) of their respective ligands. However, CD58 (transmembrane isoform), ICAM-1, CD86 and CD80 all have cytoplasmic tails that are involved in intracellular signalling themselves. Indeed, the cytoplasmic tail of CD86 has been implicated in polarising the ligand to the immunological synapse for effective IL-2 production in T cells [339]. Therefore, further work on understanding the contribu-

tion of the cytoplasmic tail of costimulatory ligands to T cell costimulation, would provide a better understanding of the full capacity of these receptors.

5.2.2 Costimulation with CARs

As important modulators of T cell responses, our study has also focused on the impact of costimulatory receptors on CAR-T cell activation. In the context of CAR-T cell immunotherapy the phenotypes we investigated hold specific biological relevance. For example, sensitivity to antigen is important to consider for target antigens that are downregulated by tumour cells as an immune escape mechanism. In addition, antigen sensitivity needs to be tightly regulated when the target antigen is expressed at high levels on tumours but also at low levels on healthy cells, to prevent unwanted autoimmune responses ('on-target off-tumour' toxicity). The duration of T cell responses is important in providing anti-tumour activity over sufficient lengths of time, to ensure clearance of chronic disease and confer long-lasting disease remission. Therefore, understanding the specific impact of individual costimulatory receptors on CAR-T cell responses, empowers us to regulate their behaviour in a more controlled way for optimal therapeutic outcomes.

Importantly, our work supports previous findings [340] illustrating differences between costimulatory receptors engaged external to the CAR, compared with incorporating costimulatory domains inside the construct itself. Here we show that CD28 had no impact on prolonging T cell or CAR-T responses when engaged with CD86, however 2nd generation CARs containing a CD28 intracellular domain were able to accelerate cytokine production over time. This highlights the need to specifically understand the impact of costimulatory domains when they are incorporated within CAR constructs, and to avoid extrapolating our understanding of how these costim-

ulatory behave when engaged externally, when designing CARs. As well as testing the incorporation of different costimulatory domains within CARs on quantitative T cell response phenotypes, the interplay between internal and external forms of costimulation would allow us to better harness the costimulatory context *in vivo*, particularly for fourth generation CAR-T cells that incorporate intracellular costimulation whilst also targeting external costimulation through the surface expression of costimulatory ligands. Overall, several aspects of CAR-T cell behaviour such as *in vivo* persistence, killing capacity, target antigen loss, CAR-T cell survival and safety dictate the efficacy of clinical CAR-T cell treatments. Consequently, the most appropriate costimulatory conditions will need to balance all these requirements and it is unlikely that one single costimulatory receptor will be able to aid all aspects of CAR-T cell behaviour.

5.2.3 A Novel Experimental System for Studying Receptor-Ligand Interactions

Our understanding of membrane bound receptor/ligand interactions at the cell-cell interface has been hampered by the lack of experimental systems enabling the presentation of physiological ligand on the surface of cells in a high-throughput manner. Furthermore, the composition and density of these ligands varies dramatically across different cells. Unlike soluble ligands, it is difficult to control the combination and concentration of surface ligands and this has hampered progress on understanding how receptor/ligand interactions impact T cell responses. Currently, studying the impact of different surface ligands depends on genetic manipulation but this requires a large number of different cell lines and it cannot easily be used to control surface density. Consequently, we developed CombiCell, a novel system

for the presentation of combinations of purified, folded, physiological ligands on the surface of cells. Here we illustrate how it can be used to study the function of individual T cell costimulatory receptors expressed by T cells. Furthermore, Combi-Cell can also be extended to explore the behaviour of many other immune receptors (such as the BCR), and as a result this platform has significant implications for the field of immune receptor signalling, allowing the distinct effect of receptors to be systematically explored in a novel cellular system.

5.3 Future Directions

We have illustrated the different quantitative impact of CD2, LFA-1 and CD28 in $CD8^+$ T cells that have experienced antigen before. Our study uses blasted T cells generated with a protocol closely resembling that used for adoptive cell therapy. However, it has been recognised that different T cell subsets have differential costimulatory requirements [341], although the exact nature of these requirements is still under debate. For example, naïve T cells primarily rely on dendritic cells for activation, and have been observed to be more dependent on CD28 costimulation compared to memory T cells [296, 342–344]. However, more recent genomic analysis using a bacterial toxin, TSST (Toxic Shock Syndrome Toxin-1), as a TCR ligand has revealed that memory T cells are in fact more sensitivity to CD28 costimulation compared to naïve T cells [338]. However TSST is a superantigen that induces non-specific T cell activation and therefore has limited physiological relevance. In addition, most clinical trials on adoptive cell therapies, harness bulk T cell populations, containing undefined ratios of $CD4^+$ and $CD8^+$ T cells [345]. However, $CD4^+$ CAR-T cells exhibit different behaviours compared to $CD8^+$ T cells such as slower tumour killing and increased resilience against exhaustion *in vivo*, and the ratio of

$CD4^+$: $CD8^+$ T cells is important in conferring optimal anti-tumor activity in CAR-T cells [346]. Consequently understanding the differential impacts of costimulatory requirements in different T cell subsets would allow better therapeutic ratios of these subsets to be administered.

Additionally, this study has focused on the individual contribution of costimulatory receptors to T cell activation, but *in vivo* these receptors behave in concert with a whole array of additional accessory receptor-ligand pairs expressed on T cells and APCs. Therefore, to better understand their biological impact on T cell function, testing the contribution of combinations of costimulatory engagement would be helpful to understand the interplay that occurs *in vivo*. It would be particularly interesting to understand which receptors are able to synergise with one another for the design of third generation CAR-T cells, which contain more than one cosignalling domain. In addition, understanding costimulation in the context of coinhibition would provide greater insights into the biological role of these receptors. Our novel system, CombiCell easily allows combinations of physiological ligand to be titrated onto the surface of cells and the dose and species of these ligands to be systematically varied, providing a suitable platform for investigating different combinations of costimulation on T cell responses.

Having observed that CD2, LFA-1 and CD28 exert differential impacts on T cell activation, future work could help decipher the mechanisms behind these distinct phenotypes. One approach could harness phenotypic modelling (as described previously [347, 212]) that fits the simplest model possible to the experimental data. For example stimulating T cells with defined inputs (pMHC concentration and costimulatory ligand concentration), and measuring the resultant phenotypes, allows us to test the minimal set of processes required to reproduce the experimental data.

From this we can extract coarse-grain information on how individual costimulatory receptors exert their distinct effects (e.g. if they act proximal or more distal to TCR signalling to produce the phenotype observed), and use this to help direct experiments to test important players for each costimulation phenotype. For example, as adhesion molecular CD2 and LFA-1 may exert effects proximal to TCR signalling to impact antigen sensitivity, whereas CD28 signalling may integrate further downstream to increase overall efficacy of response.

5.4 Conclusions

Here, we have shown that three well-established costimulatory receptors, CD2, LFA-1 and CD28, exhibit different impacts across quantitatively defined phenotypes of T cell responses. Notably, we have also introduced a new cellular system that enables the investigation of quantitative phenotypes of T cell responses with physiological ligands presented on the surface of cells.

CD2 and LFA-1 are able to dramatically enhance T cell sensitivity to antigen, however are unable to exert a comparable effect in CAR-T cells, with CD2 exhibiting the strongest increase in sensitivity. CD28 is unable to impact antigen sensitivity of T cells or CAR-T cells, but when incorporated within 2nd generation CAR-T cells, is able to accelerate T cell responses over time. These results have important implications for the role of these receptors in T cell biology, and also for the use of the receptors in therapeutic applications such as CAR-T cell immunotherapy.

Overall, we highlight the differences of costimulatory receptors across multiple phenotypes and the importance of using different metrics to quantify costimulation. In the future this approach can be extended to many more accessory receptors to re-

frame how we assess costimulation in the context of T cell function to further our understanding of T cell biology.

Chapter 6

Materials & Methods

6.1 Reagents

Table 6.1: Antibodies for flow cytometry.
For flow cytometry, all antibodies were used at a dilution of 1:200 unless indicated otherwise.

Target	Clone	Conjugation	Supplier
CD69	FN50	AF488	Biolegend
		BV421	
		AF647	
41BB	4B4-1	AF647	Biolegend
CD45	HI30	BV421	Biolegend
		BV510	
HLA-A2	BB7.2	BV421	Biolegend
		PE	
CD2	TS1/8	BV421	Biolegend
ICAM1	HCD54	AF647	Biolegend
CD80	2D10	BV421	Biolegend
CD86	BU63	FITC	Biolegend
Isotype Ctrl	MOPC-21	BV421	Biolegend
		PE	
CD58	TS2/9	APC	Biolegend
LFA-1	m24	AF647	Biolegend
(CD11a/CD18)			
CD28	CD28.2	AF488	Biolegend
His-Tag	J095G46	AF647	Biolegend
anti-mouse IgG1	RMG1-1	AF488	Biolegend

Table 6.2: Cell lines.

Name	Source	Notes
HEK293T	Previously obtained	Identity was not verified.
Lenti-X 293T	Takara Bio	For production of lentivirus.
Freestyle 293F	Nicole Zitzmann University of Oxford	For protein production.
CHO-K1	Michael Barton	Identity was no verified
CHO-K1 A11/6	Johannes Pettmann University of Oxford	Hamster ICAM-1 knock out + SpyCatcher003 (Combi-Cell).
T2	Jesús Siller Farfán	Identity was not verified.
THP-1	Eleanor Denham	Identity was not verified.

Table 6.3: General reagents.

Name	Supplier	Catalog number
Streptavidin-PE	Biolegend	405245
Biotinylated BSA	Thermo Fisher Scientific	29130
Streptavidin	Thermo Fisher Scientific	434301
IL-2	PeproTech	200-02
RosetteSep Human T Cell Enrichment Cocktail	Stemcell Technologies	15063
Zombie Fixable UV viability kit	Biolegend	423107
Zombie Fixable NIR viability kit	Biolegend	423105
96 well streptavidin Coated High Capacity Plates	Thermo Fisher Scientific	15500
Amine coupling kit	GE Healthcare Life Sciences	BR100050
CD3/CD28 Human T-activator dynabeads	Thermo Fisher Scientific	11132D
X-tremeGENE 9	Sigma-Aldrich	6365809001
X-tremeGENE HP	Sigma-Aldrich	6366546001
IL-2 Human Uncoated ELISA Kit	Thermo Fisher Scientific	88-7025-77
TNF Human Uncoated ELISA Kit	Thermo Fisher Scientific	88-7346-77
IFN-γ Human Uncoated ELISA Kit	Thermo Fisher Scientific	88-7316-77
Lipofectamine CRISPRMAX Cas9 Transfection Reagent	Thermo Fisher Scientific	CMAX00001
TrueCut Cas9 Protein v2	Thermo Fisher Scientific	A36497
tracrRNA	Thermo Fisher Scientific	A35506
BirA biotin-protein ligase bulk reaction kit	Avidity	N/A
Nunc MaxiSorp 96-well plates	Thermo Fisher Scientific	442404

Table 6.4: Cell culture media & buffers

Name	Content
Complete RPMI	RPMI
	10% FCS
	1% Penicillin/Streptomycin
Complete DMEM	DMEM
	10% FCS
	1% Penicillin/Streptomycin
Complete OptiMEM	OptiMEM
	5% FCS
	1% Penicillin/Streptomycin
HBS-EP	pH 7.4
	0.01 M HEPES
	0.15 M NaCl
	3 mM EDTA
	0.005% v/v Tween20
CHO selection medium	DMEM
	10% dialysed FCS
	1X GSEM supplement
	20-50μM MSX
	1% Penicillin/Streptomycin
CHO production medium	DMEM
	2-5% FCS
	1X GSEM supplement
	20μM MSX
	2 mM sodium butyrate
	1% Penicillin/Streptomycin

Table 6.5: Instruments and equipment

Name	Company
Superdex 75 column	GE Healthcare
Superdex 200 column	GE Healthcare
X-20 flow cytometer	BD Biosciences
CytoFlex flow cytometer	Beckman Coulter

Table 6.6: Software and packages.

Name	Version	Company
FlowJo	v10	BD Biosciences
GraphPad Prism	v7–9	GraphPad Software
MATLAB	v2021a	Mathworks

6.2 Experimental Methods

6.2.1 Protein Production

Peptides

The 9V variant (SLLMWITQ**V**) derived from the wild-type NY-ESO-$1_{157-165}$ 9C peptide was synthesised at a purity of > 95% (Peptide Protein Research, UK).

Peptide-MHC

Class 1 pMHCs were produced by expressing Human HLA-A*0201 heavy chain and human β-2microglobulin with a C-terminal BirA tag in *E.coli* as inclusion bodies and refolded with the 9V peptide *in vitro* as described previously [348]. Protein was biotinylated using the BirA enzyme (Avidity, USA) and purified via size-exclusion chromatography (Superdex S75 column, GE Healthcare, USA), in HBS-EP buffer (10 mM M HEPES pH 7.4, 150 mM NaCl, 3 mM EDTA, 0.005% v/v Tween-20). Purified protein was aliquoted and stored at -80°C until use.

To produce SpyTag-pMHC, Spytag003 was appended to the C-terminus of HLA-A*0201 heavy chain and produced as described above.

Biotinylated Costimulatory Ligand

The soluble extracellular domain (ECD), with added C-Terminus His-tag and AviTag of human CD58 (Uniprot residues 29–204), ICAM-1 (Uniprot Q5NKV8, residues 28-480), CD86 (Uniprot P42081, residues 18-232), 4-1BBL (Uniprot P41273, residues 84-246) and CD70 (Uniprot P32970, residues 52-193) were produced in Freestyle 293 suspension HEKs (Thermo Fisher), or adherent HEK 293T cells. Freestyle suspension cells were transfected using Freestyle Max transfection reagent. Adherent HEK 293T cells were transfected with Xtremegene HP reagent (Roche) according to manufacturer's protocol. Supernatants were filtered using a 0.45μM filter and proteins purified on a Ni-NTA agarose column. Biotinylation of proteins was performed either *in vitro* as described above, or *in situ* through co-transfection of BirA encoding plasmid (10%) with 100μM D-biotin added [349]. Additional purification with removal of excess biotin was performed through size-exlcusion chromatography in HBS-EP. Purified proteins were aliquoted and stored at -80°C until use.

SpyTag Costimulatory Ligand

The soluble ECD of CD58, ICAM-1, CD86 and CD80 (Uniprot P33681, residues 1-242) with added C-terminus SpyTag003 and HisTag were produced in Freestyle suspension HEKs (Thermo Fisher). Transfection was performed using Freestyle Max transfection reagent according to manufacturer's protocol. supernatants were filtered using a 0.45μM filter and proteins purified on a Ni-NTA agarose column. Additional purification with removal of excess biotin was performed through size-exclusion chromatography in HBS-EP. Purified proteins were aliquoted and stored at -80°C until use.

pMHC Tetramers

Fluorescently conjugated pMHC tetramers were produced to enable detection of antigen receptors (TCR/ CAR). Streptavidin-PE was gradually added to biotinylated 9V pMHC at a 4:1 Molar ratio, whilst shaking. Tetramers were stored for up to 3 months at 4°C.

Production of mCLOVER-Spytag003

SpyTag003 followed by monomeric mCLOVER3 (mCLOVER) and a C-terminus His-Tag were expressed in *E.coli*. Bacteria were pelleted at 6000g for 15 minutes at 4°C, then washed in BugBuster (Merck Millipore 70921) with added lysozyme, protease inhibitors, DNase I, and magnesium sulphate as per the manufacturers' instructions. 10 mM imidazole was added to the lysates, which was then mixed with Nickel-NTA agarose, and loaded onto gravity flow columns. Columns were washed with His-Tag wash bugger (50 mM NaH_2PO_4, 300 mM NaCl, 20 mM imidazole (pH 8)), and SpyTag-mCLOVER was eluted with elution buffer (50 mM NaH_2PO_4, 300 mM NaCl, 250 mM imidazole (pH 8)). Following purification, protein was concentrated in vivaspin columns and and buffer exchanged into PBS, and stored in the dark at -80°C until use.

6.2.2 Lentiviral Production

HEK 293T cells were seeded in complete DMEM (with added 10% FBS and 1% penicllin-streptamycin) in 6-well plates to reach 60–80% confluency on the next day. Cells were transfected with 0.25μg pRSV-Rev (Addgene, 12253), 0.53μg pMDLg /pRRE (Addgene, 12251), 0.35μg pMD2.G (Addgene, 12259), and 0.8μg of transfer plasmid using 5.8μL X-tremeGENE HP (Roche). After 16 hours media was replaced and supernatant harvested after a further 24 hours by filtering through a 0.45 μm cellulose acetate filter. Supernatant from one well of a 6-well plate was used to transduce 1 million T cells / CHO cells.

6.2.3 T Cell Blasts Production

$CD8^+$ T Cell Isolation

Human $CD8^+$ T cells were isolated from leukocyte cones purchased from the National Health Service's (UK) Blood and Transplantation service. Rosette-Sep Human CD8+ enrichment cocktail (Stemcell) was added to blood at 150μL/mL for 20 minutes, following by a 3.1 fold dilution with PBS before layering on Ficoll Paque Plus (GE) at a 0.8:1.0 ficoll to sample ratio. Ficoll- sample preparation was centrifuged at 1200g for 20 minutes at room temperature. Buffy coats were collected and washed twice. Cells were counted and resuspended in complete RMPI (supplemented with 10% FBS, 1% penicillin-streptamycin) and 50 Units/mL of IL-2 (PeproTech). CD3/CD28 Human T-activator Dynabeads (Thermo Fisher) were then added at a 1:1 bead to cell ratio. Isolated human $CD8^+$ T cells were cultured at 37 °C and 5% CO_2.

T Cell Blasts

1 million cells in 1mL of complete RPMI were grown overnight in TC-treated 12 well plates. On the following day T Cells were transduced using lentivirus encoding for 1G4 TCR or CAR contructs. On days 2 and 4 post-transduction, 1 mL of media was exchanged and IL-2 was added to a final concentration of 50 Units/mL. Dynabeads were magnetically removed on day 5 post-transduction. T cells were then cultured at a density of 1 million cells/mL and supplemented with 50 Units/mL IL-2 every other day. T cells were used between 10 and 16 days after transduction.

6.2.4 CRISPR Knock-out of ICAM-1 on CHO cells

CRISPR Cas9 RNP (ribonucleoprotein complexes) transfection was used to knock out Hamster ICAM-1 expressed on CHO cells (gifted by Mike Barton). First tracrRNA:crRNA complexes (gRNA) were produced according to the manufacturer's instructions. Two custom guides for Hamster ICAM-1 were used. 200,000 CHO cells were seeded in 0.5mL DMEM (with 10% FCS) in a 6-well plate and incubated overnight. The following day, 25μL OptiMEM and 1.5μL Lipofectamine CRISPRMAX per reaction was incubated for 1 minute before being added to a mixture of 25μL OptiMEM (Thermo Fisher, 31985070), 1.25μL TrueCut Cas9 Protein v2 (Thermo Fisher, A36496), 1.5μL annealed crRNA:tracrRNA, and 2.5μL Lipofectamine Cas9 Plus (Thermo Fisher), according to manufacturer's instructions. After 15 minutes the 50μL of the mixture was added to each well of seeded CHO cells. After 4 days the cells were screened and sorted via flow cytometry, and a single clone selected for transduction with SpyCatcher. Hamster ICAM-1 Knockout was verified using

Y5-3F9 hybridoma supernatant (gifted by Ed Greenfield) with anti-mouse AF488 antibody.

6.2.5 Generation CHO Cells expressing SpyCatcher

500,000 CHO cells were seeded in complete DMEM and incubated overnight at 37°C and 10% CO_2. HEK cells were transfected with DNA encoding SpyCatcher003 fused to a human-CD52 GPI anchor to produce lentiviral particles (see section 6.2.2, above). 500,000 CHO cells were then seeded in 12 well plate and the following day they were transduced. On days 2 and 4 post-transduction, 1 mL of media was exchanged. CHOs were maintained in complete DMEM and split every 2 days.

6.2.6 Plate Stimulation

Biotinylated pMHC and biotinylated costimulatory ligand (CD58, ICAM-1 or CD86) were diluted to the required concentration and added to Pierce Streptavidin Coated High Capacity 96 well plates (Thermo Fisher) in 50μL PBS and incubated for 45 minutes at room temperature or left overnight at 4 °C.

The 96-well plates were the washed twice in PBS to remove excess protein. $CD8^+$ T cell blasts T cells transduced with TCR or CAR, were counted and washed before being added to wells in the 96 well plate. 75,000 T cells were added in 200μL complete RPMI unless otherwise stated. Cells were spun briefly at 50g, 37 °C for 1 minute to allow them to settle at the bottom of each well and make contact with relevant protein, before incubation for the required time at 37 °C 5% CO_2.

At the end of the stimulation assay, the supernatant was carefully removed and saved for ELISA analysis. 10mM EDTA in PBS was then added to detach the T cells and CHOs. The cells were then aspirated and transferred to a v-bottom plate and washed once in 200μL PBS 1% BSA (500g, 4°C, 5 minutes). Antibodies against T cell activation markers were diluted in PBS 1% BSA at a 1:200 dilution. An anti-CD45 antibody was used to selectively stain T cells and distinguish them from CHO cells during flow cytometry analysis. To detect TCR-CAR expression fluorescently-conjugated peptide-MHC tetramers were added to the staining antibodies at a 1:1000 dilution. A viability dye was also added at a dilution if 1:2500 to distinguish live cells from dead cells. 50μL of this staining solution was to the cells, before incubating them for 20 minutes at 4°C in the dark. The cells were washed twice in PBS, and resuspended in 75μL PBS, before running on a flow cytometer.

6.2.7 CombiCell Stimulation

Coupling of ligands to CHO-K1 cells

50,000 CHO cells were seeded in a TC-coated 96-well flat-bottom plate and incubated overnight at 37°C, 10% CO_2 in complete DMEM. Spytag ligands were diluted to required concentration in complete DMEM (10% FCS, 1% Penicillin-Streptomycin). Existing media was removed from CHOs and the diluted ligands added in a volume of 50μL, and incubated for 40 minutes at 37°C, 10% CO_2. CHOs were then washed twice with complete DMEM. An extra plate of ligand-loaded CHO cells was produced for analysis of ligand loading levels (see below) at the start of each CombiCell assay.

Ligand Loading Analysis

Straight after ligand coupling and subsequent washing, 10mM EDTA was added to the CHO cells to detach them. The cells were transferred to a v-bottom plate and spun for 5 minutes at 500g, 4°C. The cells were washed once with PBS-BSA 1% for 5 minutes at 500g, 4°C. The cells were then stained and analysed using flow cytometry to check ligand loading levels at the start of the assay

Co-culture assays with TCR or CAR transduced T cells

For stimulation experiments, T cells transduced with TCR or CAR were counted, and washed once in complete RMPI. 50,000 T cells in 200μl complete RPMI were added to CHO cells coupled with ligand in a 96-well flat-bottomed plate. The cells were spun at 50g for 1 minute to ensure the T cells settle to the bottom of the plate and make contact with adherent CHO cells. The cells were then incubated at 37°C, 5% CO_2 for 6 or 20 hours.

At the end of the stimulation assay, the supernatant was carefully removed and saved for ELISA analysis. 10mM EDTA in PBS was then added to detach the T cells and CHOs. The cells were then aspirated and transferred to a v-bottom plate and washed once in 200μL PBS 1% BSA (500g, 4°C, 5 minutes). Antibodies against T cell activation markers were diluted in PBS 1% BSA at a 1:200 dilution. An anti-CD45 antibody was used to selectively stain T cells and distinguish them from CHO cells during flow cytometry analysis. To detect TCR-CAR expression fluorescently-conjugated peptide-MHC tetramers were added to the staining antibodies at a 1:1000 dilution. A viability dye was also added at a dilution if 1:2500 to distinguish live cells from dead cells. 50μL of this staining solution was to the cells, before incubating them for

20 minutes at 4°C in the dark. The cells were washed twice in PBS, and resuspended in 75μL PBS, before running on a flow cytometer.

6.2.8 Flow Cytometry

After staining and washing, cells from the stimulation assays were run on either BD LSR Fortessa X-20 (BD Biosciences) or CytoFLEX LX (Beckman Coulter) flow cytometer. Data was then analysed using FlowJo v10 (BD Bio- sciences).

6.2.9 ELISAs

IL-2 Human uncoated ELISA kit, TNF-α Human uncoated ELISA kit, or IFN-γ Human uncoated ELISA kit and Nunc MaxiSorp 96-well plates were used according to the manufacturer's instructions. The supernatant from stimulation assays was diluted 1 in 15 for ELISAs. The absorbance at 450 nm and 570nm were measured using a SpectraMax M5 plate reader (Molecular Devices).

6.2.10 Quantification of Surface SpyCatcher Molecules

To quantify the number of Surface SpyCatcher Molecules, Quantum™ MESF and Quantum™ Simply Cellular® beads (Bangs Laboratories), were used according to the manufacturer's instructions. Quantum Simply Cellular anti-Mouse IgG beads (Bangs Laboratories, 815), or Combicells were incubated with 50μL anti-ICAM-1, anti-CD80 and anti-CD86 mouse antibodies conjugated to AF647 at a dilution of 1:200 in PBS, in the dark for 30 minutes at 4 °C. Beads/cells were washed twice

(bead: at 2500g, cells at 500g) for 5 mins, and re-suspended in PBS. Quantum™ Alexa Fluor® 647 MESF beads (Bangs Laboratories, 647) were added to a 96-well plate. All samples were analysed by flow cytometry and gMFI values extracted. Standard curve from bead MFI values were created as per the manufacturer's instructions, and used to interpolate the number of ligands per cell using.

6.2.11 Fluoresence Correlation Spectroscopy of Surface SpyCatcher

10^5 CHO cells were seeded in 8-well chambered coverslips (μ-Slide #1.5H, ibidi) overnight followed by labeling with 50 nM SpyTag-mClover3 for 30 minutes at 37°C. Cells were washed 2x in PBS and imaged in complete medium. Imaging was performed on a Zeiss LSM 780 inverted confocal microscope (Carl Zeiss) equipped with a 40x C-Apochromat NA 1.2 W FCS objective. mClover3 fluorescence was excited with a 488 nm Argon laser and collected onto hybrid GaAsP detectors (Channel S) using a 488 MBS with the pinhole set to 1 AU. The size of the observation area was calibrated using point-FCS measurements of a dye solution (Alexa Fluor 488, 20 nM) with a known diffusion coefficient [350], yielding an average ω of 214 nm. Diffusion coefficients (D) were then calculated using the equation $\omega^2 = D \times 4 \times t_{xy}$ where t_{xy} is the transit time. Line-scan FCS was performed by switching the ChS to photon-counting mode and data were collected at the basal cell membrane by acquiring a 52-pixel line (digital zoom 40x) at maximum scanning speed for 10^5 cycles. Files were saved as lsm5 files and correlated externally using open-source FoCuS software [351].

6.3 Sequences

Sequence 1: Soluble HLA-A2 heavy chain with AviTag for expression in *E. coli*.
Sequence of heavy chain: GenBank: AAA98727.1 (amino acids 25–298).

```
MGSHSMRYFF TSVSRPGRGE PRFIAVGYVD DTQFVRFDSD AASQRMEPRA PWIEQEGPEY
WDGETRKVKA HSQTHRVDLG TLRGYYNQSE AGSHTVQRMY GCDVGSDWRF LRGYHQYAYD
GKDYIALKED LRSWTAADMA AQTTKHKWEA AHVAEQLRAY LEGTCVEWLR RYLENGKETL
QRTDAPKTHM THHAVSDHEA TLRCWALSFY PAEITLTWQR DGEDQTQDTE LVETRPAGDG
TFQKWAAVVV PSGQEQRYTC HVQHEGLPKP LTLRWEPGSG GGLNDIFEAQ KIEWHE*
```

Sequence 2: β2M for expression in *E. coli*.

```
>sp|P61769|21--119
MIQRTPKIQV YSRHPAENGK SNFLNCYVSG FHPSDIEVDL LKNGERIEKV EHSDLSFSKD
WSFYLLYYTE FTPTEKDEYA CRVNHVTLSQ PKIVKWDRDM*
```

Sequence 3: Insert of pHR-1G4 lentiviral transfer plasmid.
Contains 1G4 α-linker-P2A

```
METLLGLLIL WLQLQWVSSK QEVTQIPAAL SVPEGENLVL NCSFTDSAIY NLQWFRQDPG
KGLTSLLLIQ SSQREQTSGR LNASLDKSSG RSTLYIAASQ PGDSATYLCA VRPTSGGSYI
PTFGRGTSLI VHPYIQNPDP AVYQLRDSKS SDKSVCLFTD FDSQTNVSQS KDSDVYITDK
TVLDMRSMDF KSNSAVAWSN KSDFACANAF NNSIIPEDTF FPSPESSCDV KLVEKSFETD
TNLNFQNLSV IGFRILLLKV AGFNLLMTLR LWSSGSRAKR SGSGATNFSL LKQAGDVEEN
PGPRMSIGLL CCAALSLLWA GPVNAGVTQT PKFQVLKTGQ SMTLQCAQDM NHEYMSWYRQ
DPGMGLRLIH YSVGAGITDQ GEVPNGYNVS RSTTEDFPLR LLSAAPSQTS VYFCASSYVG
NTGELFFGEG SRLTVLEDLK NVFPPEVAVF EPSEAEISHT QKATLVCLAT GFYPDHVELS
WWVNGKEVHS GVSTDPQPLK EQPALNDSRY CLSSRLRVSA TFWQNPRNHF RCQVQFYGLS
ENDEWTQDRA KPVTQIVSAE AWGRADCGFT SESYQQGVLS ATILYEILLG KATLYAVLVS
ALVLMAMVKR KDSRG*
```

Sequence 4: Insert of D52N-CD28.H.CD28TM-CD3ζ CAR lentiviral plasmid

```
MAEVQLLESG GGLVQPGGSLR LSCAASGFTFS TYQMSWVRQAP GKGLEWVSGIV SSGGSTAYADS
VKGRFTISRDN SKNTLYLQMNS LRAEDTAVYYC AGELLPYYGMD VWGQGTTVTVS SAKTTPKLEEG
EFSEARVQSEL TQPRSVSGSPG QSVTISCTGTE RDVGGYNYVSW YQQHPGKAPKL IIHNVIERSSG
VPDRFSGSKSG NTASLTISGLQ AEDEADYYCWS FAGGYYVFGTG TDVTVLGQPKA NPTVDPKIEVM
YPPPYLDNEKS NGTIIHVKGKH LCPSPLFPGPS KPFWVLVVVGG VLACYSLLVTV AFIIFWVRSKR
SRLLHSDYMNM TPRRPGPTRKH YQPYAPPRDFA AYRSLRVKFSR SADAPAYQQGQ NQLYNELNLGR
REEYDVLDKRR GRDPEMGGKPR RKNPQEGLYNE LQKDKMAEAYS EIGMKGERRRG KGHDGLYQGLS
TATKDTYDALH MQALPPR*
```

Sequence 5: Soluble CD58 for expression in mammalian cells.
Contains chicken RPTPσ signal peptide-CD58 ECD-AviTag-His.

```
MGILPSPGMP ALLSLVSLLS VLLMGCVAET GFSQQIYGVV YGNVTFHVPS NVPLKEVLWK
KQKDKVAELE NSEFRAFSSF KNRVYLDTVS GSLTIYNLTS SDEDEYEMES PNITDTMKFF
LYVLESLPSP TLTCALTNGS IEVQCMIPEH YNSHRGLIMY SWDCPMEQCK RNSTSIYFKM
ENDLPQKIQC TLSNPLFNTT SSIILTTGLN DIFEAQKIEW HEHHHHHH*
```

Sequence 6: Soluble CD86 for expression in mammalian cells.
Contains chicken RPTPσ signal peptide-CD86 isoform 2 ECD-AviTag-His.

```
MGILPSPGMP ALLSLVSLLS VLLMGCVAET GAPLKIQAYF NETADLPCQF ANSQNQSLSE
LVVFWQDQEN LVLNEVYLGK EKFDSVHSKY MGRTSFDSDS WTLRLHNLQI KDKGLYQCII
HHKKPTGMIR IHQMNSELSV LANFSQPEIV PISNITENVY INLTCSSIHG YPEPKKMSVL
LRTKNSTIEY DGIMQKSQDN VTELYDVSIS LSVSFPDVTS NMTIFCILET DKTRLLSSPF
SIELEDGLND IFEAQKIEWH EHHHHHH*
```

Sequence 7: Soluble ICAM1 for expression in mammalian cells.
Contains chicken RPTPσ signal peptide-ICAM1 ECD-AviTag-His.

```
MGILPSPGMP ALLSLVSLLS VLLMGCVAET GQTSVSPSKV ILPRGGSVLV TCSTSCDQPK
LLGIETPLPK KELLLPGNNR KVYELSNVQE DSQPMCYSNC PDGQSTAKTF LTVYWTPERV
ELAPLPSWQP VGKNLTLRCQ VEGGAPRANL TVVLLRGEKE LKREPAVGEP AEVTTTVLVR
RDHHGANFSC RTELDLRPQG LELFENTSAP YQLQTFVLPA TPPQLVSPRV LEVDTQGTVV
CSLDRLFPVS EAQVHLALGD QRLNPTVTYG NDSFSAKASV SVTAEDEGTQ RLTCAVILGN
QSQETLQTVT IYSFPAPNVI LTKPEVSEGT EVTVKCEAHP RAKVTLNGVP AQPLGPRAQL
LLKATPEDNG RSFSCSATLE VAGQLIHKNQ TRELRVLYGP RLDERDCPGN WTWPENSQQT
PMCQAWGNPL PELKCLKDGT FPLPIGESVT VTRDLEGTYL CRARSTQGEV TREVTVNVLS
PRYEGLNDIF EAQKIEWHEH HHHHH*
```

Sequence 8: SpyCatcher003-mouseCD80 for surface expression in mammalian cells.

```
METDTLLLWV LLLWVPGSTG DVTTLSGLSG EQGPSGDMTT EEDSATHIKF SKRDEDGREL
AGATMELRDS SGKTISTWIS DGHVKDFYLY PGKYTFVETA APDGYEVATP IEFTVNEDGQ
VTVDGEATEG DAHTGSSGSG GSHVSEDFTW EKPPEDPPDS KNTLVLFGAG FGAVITVVVI
VVIIKCFCKH RSCFRRNEAS RETNNSLTFG PEEALAEQTV FL*
```

Sequence 9: SpyCatcher003-shortmouseCD80 for surface expression in mammalian cells.

```
METDTLLLWV LLLWVPGSTG DVTTLSGLSG EQGPSGDMTT EEDSATHIKF SKRDEDGREL
AGATMELRDS SGKTISTWIS DGHVKDFYLY PGKYTFVETA APDGYEVATP IEFTVNEDGQ
VTVDGEATEG DAHTGSSGSG GSPPDSKNTL VLFGAGFGAV ITVVVIVVII KCFCKHRSCF
RRNEASRETN NSLTFGPEEA LAEQTVFL*
```

Sequence 10: SpyCatcher003-humanCD52 for surface expression in mammalian cells.

```
METDTLLLWV LLLWVPGSDT GVTTLSGLSG EQGPSGDMTT EEDSATHIKF SKRDEDGREL
AGATMELRDS SGKTISTWIS DGHVKDFYLY PGKYTFVETA APDGYEVATP IEFTVNEDGQ
VTVDGEATEG DAHTGSSGSG GSTSQTSSPS ASSNISGGIF LFFVANAIIH LFCFS*
```

Sequence 11: SpyTag003-CD58 for expression in mammalian cells.

```
MGILPSPGMP ALLSLVSLLS VLLMGCVAET GFSQQIYGVV YGNVTFHVPS NVPLKEVLWK
KQKDKVAELE NSEFRAFSSF KNRVYLDTVS GSLTIYNLTS SDEDEYEMES PNITDTMKFF
LYVLESLPSP TLTCALTNGS IEVQCMIPEH YNSHRGLIMY SWDCPMEQCK RNSTSIYFKM
ENDLPQKIQC TLSNPLFNTT SSIILTTRGV PHIVMVDAYK RYKHHHHHH*
```

Sequence 12: SpyTag003-CD86 for expression in mammalian cells.

```
MGILPSPGMP ALLSLVSLLS VLLMGCVAET GAPLKIQAYF NETADLPCQF ANSQNQSLSE
LVVFWQDQEN LVLNEVYLGK EKFDSVHSKY MGRTSFDSDS WTLRLHNLQI KDKGLYQCII
HHKKPTGMIR IHQMNSELSV LANFSQPEIV PISNITENVY INLTCSSIHG YPEPKKMSVL
LRTKNSTIEY DGIMQKSQDN VTELYDVSIS LSVSFPDVTS NMTIFCILET DKTRLLSSPF
SIELEDRGVP HIVMVDAYKR YKHHHHHH*
```

Sequence 13: SpyTag003-CD80 for expression in mammalian cells.

```
MGHTRRQGTS PSKCPYLNFF QLLVLAGLSH FCSGVIHVTK EVKEVATLSC GHNVSVEELA
QTRIYWQKEK KMVLTMMSGD MNIWPEYKNR TIFDITNNLS IVILALRPSD EGTYECVVLK
YEKDAFKREH LAEVTLSVKA DFPTPSISDF EIPTSNIRRI ICSTSGGFPE PHLSWLENGE
ELNAINTTVS QDPETELYAV SSKLDFNMTT NHSFMCLIKY GHLRVNQTFN WNTTKQEHFP
DNRGVPHIVM VDAYKRYKHH HHHH*
```

Sequence 14: SpyTag003-ICAM-1 for expression in mammalian cells.

```
QTSVSPSKVI LPRGGSVLVT CSTSCDQPKL LGIETPLPKK ELLLPGNNRK VYELSNVQED
SQPMCYSNCP DGQSTAKTFL TVYWTPERVE LAPLPSWQPV GKNLTLRCQV EGGAPRANLT
VVLLRGEKEL KREPAVGEPA EVTTTVLVRR DHHGANFSCR TELDLRPQGL ELFENTSAPY
QLQTFVLPAT PPQLVSPRVL EVDTQGTVVC SLDRLFPVSE AQVHLALGDQ RLNPTVTYGN
DSFSAKASVS VTAEDEGTQR LTCAVILGNQ SQETLQTVTI YSFPAPNVIL TKPEVSEGTE
VTVKCEAHPR AKVTLNGVPA QPLGPRAQLL LKATPEDNGR SFSCSATLEV AGQLIHKNQT
RELRVLYGPR LDERDCPGNW TWPENSQQTP MCQAWGNPLP ELKCLKDGTF PLPIGESVTV
TRDLEGTYLC RARSTQGEVT REVTVNVLSP RYERGVPHIV MVDAYKRYKH HHHHH*
```

Sequence 15: SpyTag003-mCLOVER003 for expression in *E.coli*.

```
RGVPHIVMVD AYKRYKSGGG SGVSKGEELF TGVVPILVEL DGDVNGHKFS VRGEGEGDAT
NGKLTLKFIC TTGKLPVPWP TLVTTFGYGV ACFSRYPDHM KQHDFFKSAM PEGYVQERTI
SFKDDGTYKT RAEVKFEGDT LVNRIELKGI DFKEDGNILG HKLEYNFNSH YVYITADKQK
NCIKANFKIR HNVEDGSVQL ADHYQQNTPI GDGPVLLPDN HYLSHQSKLS KDPNEKRDHM
VLLEFVTAAG ITHGMDELYK GSGSGSGSHH HHHH*
```

Sequence 16: RNA Guides for Knock Out of Hamster ICAM-1

```
>Guide 1|
CCACAGTTCTCAAAGCACAG

>Guide 2|
AAAGAAGCCTTCCTGCCTCG
```

6.4 Data Analysis

All statistical tests was performed in PRISM V.9 (GraphPad Software).

6.4.1 Dose-Response Curve Fitting

Sigmoidal curves were fit in PRISM, using the following four-parameter logistic regression:

$$Y = E_{Min} + \frac{E_{Max} - E_{Min}}{1 + 10^{(LogEC_{50} - X) * Hillslope}} \tag{6.1}$$

Where :

E_{Min} = Minimum Y value

E_{Max} = Maximal Y value

EC_{50} = X value at $\frac{E_{Max}}{2}$

Hillslope = Curve slope

Bell-Shaped curves were fit using MATLAB (Mathworks) using the following equation:

$$Y = p(1) + E_{Max} * Section1 - E_{Max} * p(2) * Section2 \tag{6.2}$$

Where:

$$Section1 = \frac{1}{\frac{1+EC_{50}}{x}^{p(3)}}$$

$$Section2 = \frac{1}{(\frac{1+EC_{50}*p(4)}{x})^{p(5)}}$$

p(1) = background response at y = 1

p(2) = maximum of inhibition (as a fraction of activation, <1)

p(3) = Hill number of activation - constrained as 3

p(4) = EC50 of inhibition (as a fold of activation, >1)

p(5) = Hill number of inhibition - constrained as 1.5

Bibliography

[1] C. Janeway et al. ***Immunobiology: The immune system in health and disease***. Garland Science, 5th edition, 2001.

[2] D. D. Chaplin. **Overview of the immune response**. *Journal of Allergy and Clinical Immunology*, 2010.

[3] H. Cantor et al. **Regulation of cellular and humoral immune responses by T cell subclasses Origins of Lymphocyte Diversity**. *Cold Spring Harbor Symposia on Quantitative Biology*, 1976.

[4] E. W. Hewitt. **The MHC class I antigen presentation pathway: strategies for viral immune evasion**. *Immunology*, 2003.

[5] R. Zinkernagel et al. **Restriction of in vitro T cell-mediated cytotoxicity in lymphocytic choriomeningitis within a syngeneic or semiallogeneic system**. *Nature*, 1974.

[6] W. Cui et al. **Generation of effector CD8+ T cells and their conversion to memory T cells**. *Immunological Reviews*, 2010.

[7] C. Stemberger et al. **A Single Naive CD8+ T Cell Precursor Can Develop into Diverse Effector and Memory Subsets**. *Immunity*, 2007.

[8] S. Kaech et al. **Heterogeneity and Cell-Fate Decisions in Effector and Memory CD8+ T Cell Differentiation during Viral Infection**. *Immunity*, 2007.

[9] T. Arstila et al. **A direct estimate of the human $\alpha\beta$ T cell receptor diversity**. *Science*, 1999.

[10] A. Mallabiabarrena et al. **An endoplasmic reticulum retention signal in the CD3ϵ chain of the T-cell receptor**. *Nature*, 1992.

[11] J. Smith-Garvin et al. **T cell activation.** *Annual Review of Immunology*, 2009.

[12] H. Wang et al. **ZAP-70: An Essential Kinase in T-cell Signaling**. *Cold Spring Harbor Perspectives in Biology*, 2010.

[13] A. Courtney et al. **TCR Signaling: Mechanisms of Initiation and Propagation**. *Trends in biochemical sciences*, 2018.

[14] P. Barton et al. **Super-killer CTLs are generated by single gene deletion of Bach2**. *European Journal of Immunology*, 2022.

[15] M. Harris et al. **Quantifying persistence in the T-cell signaling network using an optically controllable antigen receptor**. *Molecular Systems Biology*, 2021.

[16] D. Tischer et al. **Light-based tuning of ligand half-life supports kinetic proofreading model of T cell signaling**. *eLife*, 2019.

[17] D. Dong et al. **Structural basis of assembly of the human T cell receptor-CD3 complex**. *Nature*, 2019.

[18] L. Sušac et al. **Structure of a fully assembled tumor-specific T cell receptor ligated by pMHC**. *Cell*, 2022.

[19] J. Husson et al. **Force generation upon T cell receptor engagement**. *PLoS ONE*, 2011.

[20] J. Göhring et al. **Temporal analysis of T-cell receptor-imposed forces via quantitative single molecule FRET measurements**. *Nature Communications*, 2021.

[21] V. Chang et al. **Initiation of T cell signaling by CD45 segregation at 'close contacts'**. *Nature Immunology*, 2016.

[22] J. Huang et al. **A Single peptide-major histocompatibility complex ligand triggers digital cytokine secretion in CD4+ T Cells**. *Immunity*, 2013.

[23] S. Davis et al. **The kinetic-segregation model: TCR triggering and beyond**. *Nature Immunology*, 2006.

[24] K. Schroder et al. **Interferon-γ: an overview of signals, mechanisms and functions**. *Journal of Leukocyte Biology*, 2004.

[25] S. Kang et al. **Direct antiviral mechanisms of interferon-gamma**. *Immune Network*, 2018.

[26] D. Jorgovanovic et al. **Roles of IFN-γ in tumor progression and regression: a review**. *Biomarker Research*, 2020.

[27] A. Gocher et al. **Interferon-γ: teammate or opponent in the tumour microenvironment?** *Nature Reviews Immunology*, 2022.

[28] S. Seo et al. **Tumor Necrosis Factor Alpha Exerts Powerful Anti-Influenza Virus Effects in Lung Epithelial Cells**. *Journal of Virology*, 2002.

[29] P. Pandey et al. **Targeting tumour necrosis factor to ameliorate viral pneumonia**. *The FEBS Journal*, 2022.

[30] S. Josephs et al. **Unleashing endogenous TNF-alpha as a cancer immunotherapeutic**. *Journal of Translational Medicine*, 2018.

[31] V. Mayya et al. **What Scales the T Cell Response?** *Trends in Immunology*, 2016.

[32] K. Tkach et al. **T cells translate individual, quantal activation into collective, analog cytokine responses via time-integrated feedbacks**. *eLife*, 2014.

[33] S. Ross et al. **Signaling and Function of Interleukin-2 in T Lymphocytes**. *Annual review of immunology*, 2018.

[34] D. Cibrián et al. **CD69: from activation marker to metabolic gatekeeper**. *European Journal of Immunology*, 2017.

[35] L. Chen et al. **Molecular mechanisms of T cell co-stimulation and co-inhibition**. *Nature Reviews Immunology*, 2013.

[36] J. Nguyen et al. **Quantitative contributions of TNF receptor superfamily members to CD8 + T-cell responses** . *Molecular Systems Biology*, 2021.

[37] P. Bretscher et al. **A theory of self-nonself discrimination**. *Science*, 1970.

[38] K. Lafferty et al. **A new analysis of allogeneic interactions**. *Australian Journal of Experimental Biology and Medical Science*, 1975.

[39] M. Jenkins et al. **Antigen presentation by chemically modified splenocytes induces antigen-specific T cell unresponsiveness in vitro and in vivo**. *Journal of Experimental Medicine*, 1987.

[40] D. Mueller et al. **Clonal expansion versus functional clonal inactivation: A costimulatory signalling pathway determines the outcome of T cell antigen receptor occupancy**. *Annual Review of Immunology*, 1989.

[41] K. Frauwirth et al. **Activation and inhibition of lymphocytes by costimulation**. *Journal of Clinical Investigation*, 2002.

[42] Y. Zhu et al. **Cell Surface Signaling Molecules in the Control of Immune Responses: A Tide Model**. *Immunity*, 2011.

[43] M. L. Dustin. **The immunological synapse**. *Cancer immunology research*, 2014.

[44] B. Wang et al. **Naive CD8+ T Cells Do Not Require Costimulation for Proliferation and Differentiation into Cytotoxic Effector Cells**. *The Journal of Immunology*, 2000.

[45] P. Duttagupta et al. **Costimulation signals for memory CD8+ T cells during viral infections**. *Critical Reviews in Immunology*, 2009.

[46] D. Mascarelli et al. **Boosting Antitumor Response by Costimulatory Strategies Driven to 4-1BB and OX40 T-cell Receptors**. *Frontiers in Cell and Developmental Biology*, 2021.

[47] D. L. Mueller. **T cells: A proliferation of costimulatory molecules**. *Current Biology*, 2000.

[48] A. H. Sharpe. **Mechanisms of costimulation**. 2009.

[49] T. Mak et al. ***The immune response: Basic and clinical principles***. Elsevier, 2005.

[50] M. Sanders et al. **Human memory T lymphocytes express increased levels of three cell adhesion molecules (LFA-3, CD2, and LFA-1) and three other molecules (UCHL1, CDw29, and Pgp-1) and have enhanced IFN-gamma production.** *The Journal of Immunology*, 1988.

[51] M. Davis et al. **Ligand recognition by $\alpha\beta$ T cell receptors**. *Annual Review of Immunology*, 1998.

[52] S. Ikemizu et al. **Crystal structure of the CD2-binding domain of CD58 (lymphocyte function-associated antigen 3) at 1.8-Å resolution**. *PNAS*, 1999.

[53] T. Springer et al. **The lymphocyte function-associated LFA-1, CD2, and LFA-3 molecules: cell adhesion receptors of the immune system.** *Annual review of immunology*, 1987.

[54] T. A. Springer. **Adhesion receptors of the immune system**. *Nature*, 1990.

[55] O. Ariel et al. **Distinct membrane localization and kinase association of the two isoforms of CD58**. *Cellular Signalling*, 2004.

[56] P. van der Merwe et al. **Human Cell-Adhesion Molecule CD2 Binds CD58 (LFA-3) with a Very Low Affinity and an Extremely Fast Dissociation Rate but Does Not Bind CD48 or CD59**. *Biochemistry*, 1994.

[57] D. Zhu et al. **Analysis of two-dimensional dissociation constant of laterally mobile cell adhesion molecules**. *Biophysical Journal*, 2007.

[58] B. Bierer et al. **T cell adhesion, avidity regulation and signaling: A molecular analysis of cd2**. *Seminars in Immunology*, 1993.

[59] D. Zhu et al. **Mechanisms of Cellular Avidity Regulation in CD2-CD58-Mediated T Cell Adhesion.** *ACS chemical biology*, 2006.

[60] O. Ariel et al. **Signal transduction by CD58: The transmembrane isoform transmits signals outside lipid rafts independently of the GPI-anchored isoform**. *Cellular Signalling*, 2009.

[61] B. Bierer et al. **Synergistic T cell activation via the physiological ligands for CD2 and the T cell receptor**. *The Journal of Experimental Medicine*, 1988.

[62] P. Moingeon et al. **The Structural Biology of CD2**. *Immunological Reviews*, 1989.

[63] P. Anton van der Merwe et al. **Topology of the CD2-CD48 cell-adhesion molecule complex: implications for antigen recognition by T cells.** *Current Biology*, 1995.

[64] O. Leupin et al. **Exclusion of CD45 from the T-cell receptor signaling area in antigen-stimulated T lymphocytes**. *Current Biology*, 2000.

[65] A. Douglass et al. **Single-molecule microscopy reveals plasma membrane microdomains created by protein-protein networks that exclude or trap signaling molecules in T cells**. *Cell*, 2005.

[66] O. Milstein et al. **Nanoscale increases in CD2-CD48-mediated intermembrane spacing decrease adhesion and reorganize the immunological synapse**. *Journal of Biological Chemistry*, 2008.

[67] L. Bockenstedt et al. **The CD2 ligand LFA-3 activates T cells but depends on the expression and function of the antigen receptor.** *The Journal of Immunology*, 1988.

[68] S. Meuer et al. **An alternative pathway of T-cell activation: A functional role for the 50 kd T11 sheep erythrocyte receptor protein**. *Cell*, 1984.

[69] Q. He et al. **A role in transmembrane signaling for the cytoplasmic domain of the CD2 T lymphocyte surface antigen**. *Cell*, 1988.

[70] A. Carmo et al. **Physical association of the cytoplasmic domain of CD2 with the tyrosine kinases p56lck and p59fyn**. *European Journal of Immunology*, 1993.

[71] S. Kanner et al. **CD2/LFA-3 ligation induces phospholipase-C gamma 1 tyrosine phosphorylation and regulates CD3 signaling.** *The Journal of Immunology*, 1992.

[72] H. Chang et al. **Dissection of the human CD2 intracellular domain. Identification of a segment required for signal transduction and interleukin 2 production**. *Journal of Experimental Medicine*, 1989.

[73] Y. Kaizuka et al. **The coreceptor CD2 uses plasma membrane microdomains to transduce signals in T cells**. *Journal of Cell Biology*, 2009.

[74] M. Dustin et al. **A novel adaptor protein orchestrates receptor patterning and cytoskeletal polarity in T-cell contacts**. *Cell*, 1998.

[75] J. Li et al. **A cdc15-like adaptor protein (CD2BP1) interacts with the CD2 cytoplasmic domain and regulates CD2-triggered adhesion**. *EMBO Journal*, 1998.

[76] C. Binder et al. **CD2 Immunobiology**. *Frontiers in Immunology*, 2020.

[77] P. Moingeon et al. **CD3ζ dependence of the CD2 pathway of activation in T lymphocytes and natural killer cells**. *PNAS*, 1992.

[78] C. Steeg et al. **CD2-mediated signaling in T cells lacking the ζ-chain-specific immune receptor tyrosine-based activation (ITAM) motif**. *European Journal of Immunology*, 1997.

[79] A. Alcover et al. **Interdependence of CD3-Ti and CD2 activation pathways in human T lymphocytes.** *The EMBO journal*, 1988.

[80] F. Howard et al. **The CD3 zeta cytoplasmic domain mediates CD2-induced T cell activation.** *Journal of Experimental Medicine*, 1992.

[81] S. Danielian et al. **Both T cell receptor (TcR)-CD3 complex and CD2 increase the tyrosine kinase activity of p56lck. CD2 can mediate TcR-CD3-independent and CD45-dependent activation of p56lck**. *European Journal of Immunology*, 1992.

[82] I. Fukai et al. **A critical role for p59(fyn) in CD2-based signal transduction**. *European Journal of Immunology*, 2000.

[83] M. Martelli et al. **Signaling via LAT (linker for T-cell activation) and Syk/ZAP70 is required for ERK activation and NFAT transcriptional activation following CD2 stimulation**. *Blood*, 2000.

[84] S. Skånland et al. **T-cell co-stimulation through the CD2 and CD28 coreceptors induces distinct signalling responses**. *Biochemical Journal*, 2014.

[85] V. Zurli et al. **Phosphoproteomics of CD2 signaling reveals AMPK-dependent regulation of lytic granule polarization in cytotoxic T cells**. *Science Signaling*, 2020.

[86] E. Parra et al. **The role of B7-1 and LFA-3 in costimulation of CD8+ T cells.** *The Journal of Immunology*, 1997.

[87] M. Bachmann et al. **CD2 sets quantitative thresholds in T cell activation**. *Journal of Experimental Medicine*, 1999.

[88] N. Killeen et al. **Development and function of T cells in mice with a disrupted CD2 gene**. *EMBO Journal*, 1992.

[89] C. Evans et al. **CD2-deficient mice generate virus-specific cytotoxic T lymphocytes upon infection with lymphocytic choriomeningitis virus.** *The Journal of Immunology*, 1993.

[90] B. Kyewski et al. **The effects of anti-CD2 antibodies on the differentiation of mouse thymocytes**. *European journal of immunology*, 1989.

[91] A. Arulanandam et al. **A soluble multimeric recombinant cd2 protein identifies cd48 as a low affinity ligand for human cd2: Divergence of cd2 ligands during the evolution of humans and mice**. *Journal of Experimental Medicine*, 1993.

[92] S. Davis et al. **The structure and ligand interactions of CD2: Implications for T-cell function**. *Immunology Today*, 1996.

[93] E. Wang et al. **Suppression of costimulation by human cytomegalovirus promotes evasion of cellular immune defenses**. *PNAS*, 2018.

[94] E. Archimbaud et al. **Expression of surface adhesion molecules CD54 (ICAM-1) and CD58 (LFA-3) in adult acute leukemia: Relationship with initial characteristics and prognosis**. *Leukemia*, 1992.

[95] Y. Cao et al. **Mutations or copy number losses of CD58 and TP53 genes in diffuse large B cell lymphoma are independent unfavorable prognostic factors**. *Oncotarget*, 2016.

[96] C. Frangieh et al. **Multimodal pooled Perturb-CITE-seq screens in patient models define mechanisms of cancer immune evasion**. *Nature Genetics*, 2021.

[97] S. Patel et al. **Identification of essential genes for cancer immunotherapy**. *Nature*, 2017.

[98] M. Pech et al. **Systematic identification of cancer cell vulnerabilities to natural killer cell-mediated immune surveillance**. *eLife*, 2019.

[99] J. Leitner et al. **CD58/CD2 Is the Primary Costimulatory Pathway in Human CD28−CD8+ T Cells**. *The Journal of Immunology*, 2015.

[100] M. Dustin et al. **T-cell receptor cross-linking transiently stimulates adhesiveness through LFA-1**. *Nature*, 1989.

[101] J. Miller et al. **Intercellular adhesion molecule-1 dimerization and its consequences for adhesion mediated by lymphocyte function associated-1**. *Journal of Experimental Medicine*, 1995.

[102] F. Spring et al. **Intercellular adhesion molecule-4 binds α4β1 and αv-family integrins through novel integrin-binding mechanisms**. *Blood*, 2001.

[103] M. Shimaoka et al. **Reversibly locking a protein fold in an active conformation with a disulfide bond: Integrin αL I domains with high affinity and antagonist activity in vivo**. *PNAS*, 2001.

[104] Y. Tominaga et al. **Affinity and Kinetic Analysis of the Molecular Interaction of ICAM-1 and Leukocyte Function-Associated Antigen-1**. *The Journal of Immunology*, 1998.

[105] M. Kim et al. **The primacy of affinity over clustering in regulation of adhesiveness of the integrin αLβ2**. *Journal of Cell Biology*, 2004.

[106] T. Kinashi. **Intracellular signalling controlling integrin activation in lymphocytes**. *Nature Reviews Immunology*, 2005.

[107] B. Luo et al. **Integrin structures and conformational signaling**. *Current Opinion in Cell Biology*, 2006.

[108] C. Cairo et al. **Cytoskeletal Regulation Couples LFA-1 Conformational Changes to Receptor Lateral Mobility and Clustering**. *Immunity*, 2006.

[109] P. Van Der Merwe et al. **Cytoskeletal polarization and redistribution of cell-surface molecules during T cell antigen recognition**. *Seminars in Immunology*, 2000.

[110] B. Graf et al. **LFA-1-Mediated T Cell Costimulation through Increased Localization of TCR/Class II Complexes to the Central Supramolecular Activation Cluster and Exclusion of CD45 from the Immunological Synapse**. *The Journal of Immunology*, 2007.

[111] R. Evans et al. **The integrin LFA-1 signals through ZAP-70 to regulate expression of high-affinity LFA-1 on T lymphocytes**. *Blood*, 2011.

[112] N. Verma et al. **Adaptor regulation of LFA-1 signaling in T lymphocyte migration: Potential druggable targets for immunotherapies?** *European Journal of Immunology*, 2014.

[113] G. Van Seventer et al. **The LFA-1 ligand ICAM-1 provides an important costimulatory signal for T cell receptor-mediated activation of resting T cells.** *The Journal of Immunology*, 1990.

[114] M. Bachmann et al. **Distinct roles for LFA-1 and CD28 during activation of naive T cells: Adhesion versus costimulation**. *Immunity*, 1997.

[115] L. Zuckerman et al. **Functional Consequences of Costimulation by ICAM-1 on IL-2 Gene Expression and T Cell Activation**. *The Journal of Immunology*, 1998.

[116] G. Varga et al. **LFA-1 contributes to signal i of T-cell activation and to the production of T h 1 cytokines**. *Journal of Investigative Dermatology*, 2010.

[117] N. Anikeeva et al. **Distinct role of lymphocyte function-associated antigen-1 in mediating effective cytolytic activity by cytotoxic T lymphocytes**. *PNAS*, 2005.

[118] H. Ni et al. **LFA-1-Mediated Costimulation of CD8+ T Cell Proliferation Requires Phosphatidylinositol 3-Kinase Activity**. *The Journal of Immunology*, 2001.

[119] O. Perez et al. **Leukocyte functional antigen 1 lowers T cell activation thresholds and signaling through cytohesin-1 and Jun-activating binding protein 1**. *Nature Immunology*, 2003.

[120] A. Mor et al. **The lymphocyte function-associated antigen-1 receptor costimulates plasma membrane Ras via phospholipase D2**. *Nature Cell Biology*, 2007.

[121] Y. Wang et al. **LFA-1 decreases the antigen dose for T cell activation in vivo**. *International Immunology*, 2008.

[122] S. Kandula et al. **LFA-1 on CD4+ T Cells Is Required for Optimal Antigen-Dependent Activation In Vivo**. *The Journal of Immunology*, 2004.

[123] T. Kishimoto et al. **Heterogeneous mutations in the β subunit common to the LFA-1, Mac-1, and p150,95 glycoproteins cause leukocyte adhesion deficiency**. *Cell*, 1987.

[124] N. Schwab et al. **Fatal PML associated with efalizumab therapy Insights into integrin αLβ2 in JC virus control**. *Neurology*, 2012.

[125] R. Schmits et al. **LFA-1-deficient mice show normal CTL responses to virus but fail to reject immunogenic tumor**. *Journal of Experimental Medicine*, 1996.

[126] M. Perro et al. **Role of LFA-1 integrin in the control of a lymphocytic choriomeningitis virus (LCMV) infection**. *Virulence*, 2020.

[127] K. Franciszkiewicz et al. **CD103 or LFA-1 engagement at the immune synapse between cytotoxic T cells and tumor cells promotes maturation and regulates T-cell effector functions**. *Cancer Research*, 2013.

[128] H. Gmünder et al. **A 45-kDa human T-cell membrane glycoprotein functions in the regulation of cell proliferative responses**. *European Journal of Biochemistry*, 1984.

[129] C. June et al. **The B7 and CD28 receptor families**. *Immunology Today*, 1994.

[130] F. Harding et al. **CD28-mediated signalling co-stimulates murine T cells and prevents induction of anergy in T-cell clones**. *Nature*, 1992.

[131] N. Weng et al. **CD28- T cells: their role in the age-associated decline of immune function**. *Trends in Immunology*, 2009.

[132] S. Bhatia et al. **Different cell surface oligomeric states of B7-1 and B7-2: Implications for signaling**. *PNAS*, 2005.

[133] P. Riha et al. **CD28 co-signaling in the adaptive immune response**. *Self/Nonself - Immune Recognition and Signaling*, 2010.

[134] P. Van Der Merwe et al. **CD80 (B7-1) binds both CD28 and CTLA-4 with a low affinity and very fast kinetics**. *Journal of Experimental Medicine*, 1997.

[135] A. Kennedy et al. **Differences in CD80 and CD86 transendocytosis reveal CD86 as a key target for CTLA-4 immune regulation**. *Nature Immunology*, 2022.

[136] A. Sharpe et al. **The B7–CD28 superfamily**. *Nature Reviews Immunology*, 2002.

[137] B. Rowshanravan et al. **CTLA-4: A moving target in immunotherapy**. *Blood*, 2018.

[138] O. Qureshi et al. **Trans-endocytosis of CD80 and CD86: a molecular basis for the cell-extrinsic function of CTLA-4**. *Science*, 2011.

[139] S. Tseng et al. **CD80 Cytoplasmic Domain Controls Localization of CD28, CTLA-4, and Protein Kinase Cθ in the Immunological Synapse**. *The Journal of Immunology*, 2005.

[140] R. Tian et al. **Combinatorial proteomic analysis of intercellular signaling applied to the CD28 T-cell costimulatory receptor**. *PNAS*, 2015.

[141] F. Pagès et al. **Binding of phosphatidyl-inositol-3-OH kinase to CD28 is required for T-cell signalling**. *Nature*, 1994.

[142] A. August et al. **Activation of src family kinase lck following CD28 crosslinking in the jurkat leukemic cell line**. *Biochemical and Biophysical Research Communications*, 1994.

[143] M. Sanchez-Lockhart et al. **Cutting Edge: CD28-Mediated Transcriptional and Posttranscriptional Regulation of IL-2 Expression Are Controlled through Different Signaling Pathways**. *The Journal of Immunology*, 2004.

[144] A. McAdam et al. **The role of B7 co-stimulation in activation and differentiation of CD4+ and CD8+ T cells**. *Immunological Reviews*, 1998.

[145] O. Acuto et al. **CD28-mediated co-stimulation: A quantitative support for TCR signalling**. *Nature Reviews Immunology*, 2003.

[146] M. Diehn et al. **Genomic expression programs and the integration of the CD28 costimulatory signal in T cell activation**. *PNAS*, 2002.

[147] J. Kim et al. **Quantitative Analysis of Phosphotyrosine Signaling Networks Triggered by CD3 and CD28 Costimulation in Jurkat Cells**. *The Journal of Immunology*, 2006.

[148] L. Tuosto et al. **CD28 affects the earliest signaling events generated by TCR engagement**. *European Journal of Immunology*, 1998.

[149] A. H. Sharpe. **Analysis of lymphocyte costimulation in vivo using transgenic and 'knockout' mice**. *Current Opinion in Immunology*, 1995.

[150] A. Shahinian et al. **Differential T cell costimulatory requirements in CD28-deficient mice**. *Science*, 1993.

[151] H. Mittrücker et al. **Role of CD28 for the Generation and Expansion of Antigen-Specific CD8+ T Lymphocytes During Infection with Listeria monocytogenes** . *The Journal of Immunology*, 2001.

[152] C. King et al. **CD28-deficient mice generate an impaired Th2 response to Schistosoma mansoni infection**. *European Journal of Immunology*, 1996.

[153] S. Krinzman et al. **Inhibition of T cell costimulation abrogates airway hyperresponsiveness in a murine model**. *Journal of Clinical Investigation*, 1996.

[154] B. Salomon et al. **B7/CD28 costimulation is essential for the homeostasis of the CD4+CD25+ immunoregulatory T cells that control autoimmune diabetes**. *Immunity*, 2000.

[155] M. Suresh et al. **Role of CD28-B7 Interactions in Generation and Maintenance of CD8 T Cell Memory**. *The Journal of Immunology*, 2001.

[156] R. H. Schwartz. **A cell culture model for T lymphocyte clonal anergy**. *Science*, 1990.

[157] L. Boise et al. **CD28 costimulation can promote T cell survival by enhancing the expression of Bcl-xL**. *Immunity*, 1995.

[158] C. Thompson et al. **CD28 activation pathway regulates the production of multiple T-cell-derived lymphokines/cytokines**. *PNAS*, 1989.

[159] P. Linsley et al. **The role of the CD28 receptor during T cell responses to antigen**. *Annual Review of Immunology*, 1993.

[160] J. Goldstein et al. **Purified MHC Class I and Peptide Complexes Activate Naive CD8+ T Cells Independently of the CD28/B7 and LFA-1/ICAM-1 Costimulatory Interactions**. *The Journal of Immunology*, 1998.

[161] B. Wang et al. **Multiple Paths for Activation of Naive CD8+ T Cells: CD4-Independent Help**. *The Journal of Immunology*, 2001.

[162] J. Chai et al. **Critical Role of Costimulation in the Activation of Naive Antigen-Specific TCR Transgenic CD8+ T Cells In Vitro**. *The Journal of Immunology*, 1999.

[163] S. Guerder et al. **B7 costimulation is necessary for the activation of the lytic function in cytotoxic T lymphocyte precursors.** *The Journal of Immunology*, 1995.

[164] A. McAdam et al. **Either B7 Costimulation or IL-2 Can Elicit Generation of Primary Alloreactive CTL**. *The Journal of Immunology*, 2000.

[165] A. Borowski et al. **Memory CD8+ T Cells Require CD28 Costimulation**. *The Journal of Immunology*, 2007.

[166] M. Vacchio et al. **CD28 costimulation is required for in vivo induction of peripheral tolerance in CD8 T cells**. *Journal of Experimental Medicine*, 2003.

[167] A. Chaudhry et al. **The Nef protein of HIV-1 induces loss of cell surface costimulatory molecules CD80 and CD86 in APCs**. *Journal of immunology*, 2005.

[168] G. Morrow et al. **Varicella-zoster virus productively infects mature dendritic cells and alters their immune function**. *Journal of virology*, 2003.

[169] D. Dolfi et al. **Dendritic Cells and CD28 Costimulation Are Required To Sustain Virus-Specific CD8+ T Cell Responses during the Effector Phase In Vivo**. *The Journal of Immunology*, 2011.

[170] D. Gabrilovich et al. **Production of vascular endothelial growth factor by human tumors inhibits the functional maturation of dendritic cells**. *Nature Medicine*, 1996.

[171] J. Gross et al. **Identification and distribution of the costimulatory receptor CD28 in the mouse.** *The Journal of Immunology*, 1992.

[172] D. Mou et al. **CD28 negative T cells: Is their loss our gain?** *American Journal of Transplantation*, 2014.

[173] J. Boomer et al. **An enigmatic tail of CD28 signaling.** *Cold Spring Harbor perspectives in biology*, 2010.

[174] A. Gizinski et al. **Co-stimulation and T cells as therapeutic targets**. *Best Practice and Research: Clinical Rheumatology*, 2010.

[175] U. Ahmad et al. **Chimeric antigen receptor T cell structure, its manufacturing, and related toxicities; A comprehensive review**. *Advances in Cancer Biology - Metastasis*, 2022.

[176] S. Feins et al. **An introduction to chimeric antigen receptor (CAR) T-cell immunotherapy for human cancer**. *American Journal of Hematology*, 2019.

[177] T. Brocker. **Chimeric Fv-ζ or Fv-ϵ receptors are not sufficient to induce activation or cytokine production in peripheral T cells**. *Blood*, 2000.

[178] M. Sadelain et al. **The basic principles of chimeric antigen receptor (CAR) design**. *Cancer discovery*, 2013.

[179] J. Maher et al. **Human T-lymphocyte cytotoxicity and proliferation directed by a single chimeric TCRζ/CD28 receptor**. *Nature Biotechnology*, 2002.

[180] B. Savoldo et al. **CD28 costimulation improves expansion and persistence of chimeric antigen receptor-modified T cells in lymphoma patients**. *Journal of Clinical Investigation*, 2011.

[181] C. Kowolik et al. **CD28 costimulation provided through a CD19-specific chimeric antigen receptor enhances in vivo persistence and antitumor efficacy of adoptively transferred T cells**. *Cancer Research*, 2006.

[182] X. Zhong et al. **Chimeric antigen receptors combining 4-1BB and CD28 signaling domains augment PI 3 kinase/AKT/Bcl-X L activation and CD8 T cell-mediated tumor eradication**. *Molecular Therapy*, 2010.

[183] D. Song et al. **In vivo persistence, tumor localization, and antitumor activity of CAR-engineered T cells is enhanced by costimulatory signaling through CD137 (4-1BB)**. *Cancer Research*, 2011.

[184] S. Tammana et al. **4-1BB and CD28 signaling plays a synergistic role in redirecting umbilical cord blood t cells against b-cell malignancies**. *Human Gene Therapy*, 2010.

[185] S. Neelapu et al. **Axicabtagene Ciloleucel CAR T-Cell Therapy in Refractory Large B-Cell Lymphoma**. *New England Journal of Medicine*, 2017.

[186] R. Siddiqui et al. **A Systematic Review of the Role of Chimeric Antigen Receptor T (CAR-T) Cell Therapy in the Treatment of Solid Tumors**. *Cureus*, 2021.

[187] J. Zapata et al. **CD137 (4-1BB) signalosome: Complexity is a matter of TRAFs**. *Frontiers in Immunology*, 2018.

[188] S. Van Der Stegen et al. **The pharmacology of second-generation chimeric antigen receptors**. *Nature Reviews Drug Discovery*, 2015.

[189] R. Weinkove et al. **Selecting costimulatory domains for chimeric antigen receptors: functional and clinical considerations**. *Clinical and Translational Immunology*, 2019.

[190] X. Zhao et al. **Efficacy and Safety of CD28- or 4-1BB-Based CD19 CAR-T Cells in B Cell Acute Lymphoblastic Leukemia**. *Molecular Therapy - Oncolytics*, 2020.

[191] O. Kawalekar et al. **Distinct Signaling of Coreceptors Regulates Specific Metabolism Pathways and Impacts Memory Development in CAR T Cells**. *Immunity*, 2016.

[192] V. Golubovskaya et al. **Different subsets of T cells, memory, effector functions, and CAR-T immunotherapy**. *Cancers*, 2016.

[193] M. Milone et al. **Engineering-enhanced CAR T cells for improved cancer therapy**. *Nature Cancer*, 2021.

[194] R. Brentjens et al. **Genetically targeted T cells eradicate systemic acute lymphoblastic leukemia xenografts**. *Clinical Cancer Research*, 2007.

[195] C. Carpenito et al. **Control of large, established tumor xenografts with genetically retargeted human T cells containing CD28 and CD137 domains**. *PNAS*, 2009.

[196] C. Ramos et al. **In Vivo Fate and Activity of Second- versus Third-Generation CD19-Specific CAR-T Cells in B Cell Non-Hodgkin's Lymphomas**. *Molecular Therapy*, 2018.

[197] S. Guedan et al. **Enhancing CAR T cell persistence through ICOS and 4-1BB costimulation**. *JCI insight*, 2018.

[198] Z. Zhao et al. **Structural Design of Engineered Costimulation Determines Tumor Rejection Kinetics and Persistence of CAR T Cells**. *Cancer cell*, 2015.

[199] D. Irvine et al. **Direct observation of ligand recognition by T cells**. *Nature*, 2002.

[200] Y. Sykulev et al. **Evidence that a single peptide-MHC complex on a target cell can elicit a cytolytic T cell response**. *Immunity*, 1996.

[201] Z. Grossman et al. **Adaptive cellular interactions in the immune system: The tunable activation threshold and the significance of subthreshold responses**. *PNAS*, 1992.

[202] T. Pradeu et al. **The speed of change: Towards a discontinuity theory of immunity?** *Nature Reviews Immunology*, 2013.

[203] M. Hashimoto et al. **CD8 T Cell Exhaustion in Chronic Infection and Cancer: Opportunities for Interventions**. *Annual Review of Medicine*, 2018.

[204] H. Ghoneim et al. **Cell-Intrinsic Barriers of T Cell-Based Immunotherapy**. *Trends in Molecular Medicine*, 2016.

[205] W. Ma et al. **Defining Network Topologies that Can Achieve Biochemical Adaptation**. *Cell*, 2009.

[206] N. Singh et al. **The strength of persistent antigenic stimulation modulates adaptive tolerance in peripheral CD4+ T cells**. *Journal of Experimental Medicine*, 2003.

[207] P. Stamou et al. **Chronic Exposure to Low Levels of Antigen in the Periphery Causes Reversible Functional Impairment Correlating with Changes in CD5 Levels in Monoclonal CD8 T Cells**. *The Journal of Immunology*, 2003.

[208] N. Trendel et al. **Perfect adaptation of CD8+T cell responses to constant antigen input over a wide range of affinities is overcome by costimulation**. *Science Signaling*, 2021.

[209] A. Schietinger et al. **Tolerance and exhaustion: defining mechanisms of T cell dysfunction**. *Trends in immunology*, 2014.

[210] R. H. Schwartz. **T cell anergy**. *Annual Review of Immunology*, 2003.

[211] L. Chiodetti et al. **Adaptive Tolerance and Clonal Anergy Are Distinct Biochemical States**. *The Journal of Immunology*, 2006.

[212] N. Trendel. ***Phenotypic Modelling of the Polyfunctional T Cell Response***. PhD thesis, University of Oxford, 2018.

[213] T. Honda et al. **Tuning of Antigen Sensitivity by T Cell Receptor-Dependent Negative Feedback Controls T Cell Effector Function in Inflamed Tissues**. *Immunity*, 2014.

[214] A. Kamphorst et al. **Rescue of exhausted CD8 T cells by PD-1-targeted therapies is CD28-dependent**. *Science*, 2017.

[215] M. Boulch et al. **A cross-talk between CAR T cell subsets and the tumor microenvironment is essential for sustained cytotoxic activity**. *Science Immunology*, 2021.

[216] S. Schuster et al. **Chimeric Antigen Receptor T Cells in Refractory B-Cell Lymphomas**. *New England Journal of Medicine*, 2017.

[217] S. Schuster et al. **Tisagenlecleucel in Adult Relapsed or Refractory Diffuse Large B-Cell Lymphoma**. *The New England journal of medicine*, 2019.

[218] C. June et al. **Chimeric Antigen Receptor Therapy**. *The New England journal of medicine*, 2018.

[219] J. Abramson et al. **Lisocabtagene maraleucel for patients with relapsed or refractory large B-cell lymphomas (TRANSCEND NHL 001): a multicentre seamless design study**. *The Lancet*, 2020.

[220] L. Nastoupil et al. **Standard-of-Care Axicabtagene Ciloleucel for Relapsed or Refractory Large B-Cell Lymphoma: Results From the US Lymphoma CAR T Consortium**. *Journal of clinical oncology : official journal of the American Society of Clinical Oncology*, 2020.

[221] S. Maude et al. **Tisagenlecleucel in Children and Young Adults with B-Cell Lymphoblastic Leukemia**. *The New England journal of medicine*, 2018.

[222] D. Porter et al. **Chimeric antigen receptor T cells persist and induce sustained remissions in relapsed refractory chronic lymphocytic leukemia**. *Science Translational Medicine*, 2015.

[223] S. Maude et al. **Chimeric Antigen Receptor T Cells for Sustained Remissions in Leukemia**. *New England Journal of Medicine*, 2014.

[224] J. Fan et al. **Development of CAR-T Cell Persistence in Adoptive Immunotherapy of Solid Tumors**. *Frontiers in Oncology*, 2021.

[225] C. Louis et al. **Antitumor activity and long-term fate of chimeric antigen receptor-positive T cells in patients with neuroblastoma**. *Blood*, 2011.

[226] M. Mata et al. **Inducible activation of myD88 and CD40 in CAR T cells results in controllable and potent antitumor activity in preclinical solid tumor models**. *Cancer Discovery*, 2017.

[227] E. Abu-Shah et al. **Human CD8+ T Cells Exhibit a Shared Antigen Threshold for Different Effector Responses**. *The Journal of Immunology*, 2020.

[228] S. Bownds et al. **Induction of tumor-reactive cytotoxic T-lymphocytes using a peptide from NY-ESO-1 modified at the carboxy-terminus to enhance HLA-A2.1 binding affinity and stability in solution**. *Journal of Immunotherapy*, 2001.

[229] J. Burton et al. **Inefficient exploitation of accessory receptors reduces the sensitivity of chimeric antigen receptors**. *PNAS*, 2023.

[230] John Nguyen. ***Quantitative modelling of T cell activation and co-stimulation***. PhD thesis, University of Oxford, 2019.

[231] X. Wang et al. **Structure of the quaternary complex of interleukin-2 with its alpha, beta, and gamma receptors**. *Science*, 2005.

[232] D. Stauber et al. **Crystal structure of the IL-2 signaling complex: Paradigm for a heterotrimeric cytokine receptor**. *PNAS*, 2006.

[233] M. Sadelain et al. **The promise and potential pitfalls of chimeric antigen receptors**. *Current Opinion in Immunology*, 2009.

[234] C. Han et al. **Desensitized chimeric antigen receptor T cells selectively recognize target cells with enhanced antigen expression**. *Nature Communications*, 2018.

[235] A. Gallegos et al. **Control of T cell antigen reactivity via programmed TCR downregulation**. *Nature Immunology*, 2016.

[236] P. Demetriou et al. **CD2 expression acts as a quantitative checkpoint for immunological synapse structure and T-cell activation.** *bioRxiv*, 2019.

[237] M. Hoekstra et al. **Modulation of the tumor micro-environment by CD8+ T cell-derived cytokines**. *Current Opinion in Immunology*, 2021.

[238] J. Haring et al. **Dynamic Regulation of IFN-γ Signaling in Antigen-Specific CD8+ T Cells Responding to Infection**. *The Journal of Immunology*, 2005.

[239] E. Bach et al. **THE IFNγ Receptor:A Paradigm for Cytokine Receptor Signaling**. *The Annual review of Immunology*, 2003.

[240] J. Mazet et al. **IFNγ signaling in cytotoxic T cells restricts anti-tumor responses by inhibiting the maintenance and diversity of intra-tumoral stem-like T cells**. *Nature Communications*, 2023.

[241] A. D. Wells. **New Insights into the Molecular Basis of T Cell Anergy: Anergy Factors, Avoidance Sensors, and Epigenetic Imprinting**. *The Journal of Immunology*, 2009.

[242] N. Shah et al. **Mechanisms of resistance to CAR T cell therapy**. *Nature Reviews Clinical Oncology*, 2019.

[243] D. Wijewarnasuriya et al. **Excessive costimulation leads to dysfunction of adoptively transferred T cells A C**. *Cancer Immunology Research*, 2020.

[244] G. López-Cantillo et al. **CAR-T Cell Performance: How to Improve Their Persistence?** *Frontiers in Immunology*, 2022.

[245] M. Kershaw et al. **A phase I study on adoptive immunotherapy using gene-modified T cells for ovarian cancer**. *Clinical Cancer Research*, 2006.

[246] E. Hsieh et al. **Replacing CAR-T cell resistance with persistence by changing a single residue**. *Journal of Clinical Investigation*, 2020.

[247] H. Caruso et al. **Tuning Sensitivity of CAR to EGFR Density Limits Recognition of Normal Tissue While Maintaining Potent Antitumor Activity**. *Cancer research*, 2015.

[248] S. Han et al. **Role of antigen persistence and dose for CD4+ T-cell exhaustion and recovery**. *PNAS*, 2010.

[249] J. Eyquem et al. **Targeting a CAR to the TRAC locus with CRISPR/Cas9 enhances tumour rejection**. *Nature*, 2017.

[250] C. Kloss et al. **Combinatorial antigen recognition with balanced signaling promotes selective tumor eradication by engineered T cells**. *Nature Biotechnology*, 2013.

[251] D. Tortorella et al. **Viral Subversion of the Immune System**. *Annual review of immunology*, 2003.

[252] S. Spranger et al. **Mechanisms of Tumor Cell-Intrinsic Immune Evasion**. *Annual Review of Cancer Biology*, 2018.

[253] N. Lemmermann et al. **Immune Evasion Proteins of Murine Cytomegalovirus Preferentially Affect Cell Surface Display of Recently Generated Peptide Presentation Complexes**. *Journal of Virology*, 2010.

[254] M. Alexander-Miller et al. **Selective expansion of high-or low-avidity cytotoxic T lymphocytes and efficacy for adoptive immunotherapy**. *Immunology*, 1996.

[255] M. Derby et al. **High-Avidity CTL Exploit Two Complementary Mechanisms to Provide Better Protection Against Viral Infection Than Low-Avidity CTL**. *The Journal of Immunology*, 2001.

[256] J. Almeida et al. **Superior control of HIV-1 replication by CD8+ T cells is reflected by their avidity, polyfunctionality, and clonal turnover**. *The Journal of experimental medicine*, 2007.

[257] D. Yerly et al. **Increased Cytotoxic T-Lymphocyte Epitope Variant Cross-Recognition and Functional Avidity Are Associated with Hepatitis C Virus Clearance**. *Journal of Virology*, 2008.

[258] J. Siller-Farfán et al. **Molecular mechanisms of T cell sensitivity to antigen**. *Immunological Reviews*, 2018.

[259] M. Wild et al. **Dependence of T cell antigen recognition on the dimensions of an accessory receptor-ligand complex**. *Journal of Experimental Medicine*, 1999.

[260] Z. Cai et al. **Requirements for peptide-induced T cell receptor downregulation on naive CD8+ T cells**. *Journal of Experimental Medicine*, 1997.

[261] A. Murtaza et al. **Changes in the strength of co-stimulation through the B7/CD28 pathway alter functional T cell responses to altered peptide ligands**. *International Immunology*, 1999.

[262] M. Bachmann et al. **T cell responses are governed by avidity and co-stimulatory thresholds**. *European Journal of Immunology*, 1996.

[263] A. Viola et al. **T cell activation determined by T cell receptor number and tunable thresholds**. *Science*, 1996.

[264] J. Green et al. **Absence of B7-dependent responses in CD28-deficient mice**. *Immunity*, 1994.

[265] P. Lucas et al. **Naive CD28-deficient T cells can initiate but not sustain an in vitro antigen-specific immune response.** *The Journal of Immunology*, 1995.

[266] R. Abe et al. **Distinct signal transduction in mouse CD4+ and CD8+ splenic T cells after CD28 receptor ligation.** *The Journal of Immunology*, 1995.

[267] F. Harding et al. **CD28-B7 interactions allow the induction of CD8+ cytotoxic T lymphocytes in the absence of exogenous help**. *Journal of Experimental Medicine*, 1993.

[268] O. Dushek et al. **Antigen potency and maximal efficacy reveal a mechanism of efficient T cell activation**. *Science Signaling*, 2011.

[269] A. Abdalla et al. **Kinetics of Cytokine Gene Expression in Human CD4 + and CD8 + T-Lymphocyte Subsets Using Quantitative Real-Time PCR**. *Scandinavian Journal of Immunology*, 2003.

[270] F. Fagnoni et al. **Expansion of cytotoxic CD8+ CD28- T cells in healthy ageing people, including centenarians**. *Immunology*, 1996.

[271] M. Azuma et al. **CD28- T lymphocytes. Antigenic and functional properties.** *The Journal of Immunology*, 1993.

[272] N. Boucher et al. **CD28 expression in T cell aging and human longevity**. *Experimental Gerontology*, 1998.

[273] S. Bromley et al. **The Immunological Synapse**. *Annual Review of Immunology*, 2003.

[274] Johannes Pettmann. ***Antigen discrimination in primary human T cells***. PhD thesis, University of Oxford, 2021.

[275] T. Sasada et al. **A Critical Role for CD2 in Both Thymic Selection Events and Mature T Cell Function**. *The Journal of Immunology*, 2001.

[276] T. Sasada et al. **CD2 Facilitates Differentiation of CD4 Th Cells Without Affecting Th1/Th2 Polarization**. *The Journal of Immunology*, 2002.

[277] M. Dustin et al. **Low affinity interaction of human or rat T cell adhesion molecule CD2 with its ligand aligns adhering membranes to achieve high physiological affinity**. *Journal of Biological Chemistry*, 1997.

[278] P. A. Van der Merwe. **A subtle role for CD2 in T cell antigen recognition**. *Journal of Experimental Medicine*, 1999.

[279] K. Kato et al. **CD48 is a counter-receptor for mouse CD2 and is involved in T cell activation**. *Journal of Experimental Medicine*, 1992.

[280] P. Möller et al. **Frequency of abnormal expression of HLA-A,B,C and HLA-DR molecules, invariant chain, and LFA-3 (CD58) in colorectal carcinoma and its impact on tumor recurrence**. *International Journal of Cancer*, 1991.

[281] H. Lim et al. **Costimulation of IL-2 Production through CD28 Is Dependent on the Size of Its Ligand**. *The Journal of Immunology*, 2015.

[282] G. Iezzi et al. **The duration of antigenic stimulation determines the fate of naive and effector T cells**. *Immunity*, 1998.

[283] S. Bromley et al. **The immunological synapse and CD28-CD80 interactions**. *Nature Immunology*, 2001.

[284] D. Staunton et al. **The arrangement of the immunoglobulin-like domains of ICAM-1 and the binding sites for LFA-1 and rhinovirus**. *Cell*, 1990.

[285] M. Dustin et al. **The immunological synapse and the actin cytoskeleton: molecular hardware for T cell signaling**. *Nature Immunology 2000 1:1*, 2000.

[286] C. Monks et al. **Three-dimensional segregation of supramolecular activation clusters in T cells**. *Nature*, 1998.

[287] A. Grakoui et al. **The immunological synapse: A molecular machine controlling T cell activation**. *Science*, 1999.

[288] W. Hahn et al. **A distinct cytoplasmic domain of CD2 regulates ligand avidity and T-cell responsiveness to antigen**. *PNAS*, 1992.

[289] E. Bianchi et al. **Integrin LFA-1 interacts with the transcriptional coactivator JAB1 to modulate AP-1 activity**. *Nature*, 2000.

[290] J. Geginat et al. **CD28 and LFA-1 contribute to cyclosporin A-resistant T coil growth by stabilizing the IL-2 mRNA through distinct signaling pathways**. *European Journal of Immunology*, 2000.

[291] H. Ni et al. **Signaling Pathways Activated by Leukocyte Function-Associated Ag-1-Dependent Costimulation 1**. *The Journal of Immunology*, 1999.

[292] D. Li et al. **LFA-1 regulates CD8+ T cell activation via T cell receptor-mediated and LFA-1-mediated Erk1/2 signal pathways**. *Journal of Biological Chemistry*, 2009.

[293] B. William Hahn et al. **Separable portions of the CD2 cytoplasmic domain involved in signaling and ligand avidity regulation**. *The Journal of Experimental Medicine*, 1993.

[294] C. Hsu et al. **Ligand mobility modulates immunological synapse formation and T cell activation**. *PLoS ONE*, 2012.

[295] M. Croft. **Activation of naive, memory and effector T cells**. *Current Opinion in Immunology*, 1994.

[296] C. London et al. **Functional Responses and Costimulator Dependence of Memory CD4+ T Cells**. *The Journal of Immunology*, 2000.

[297] M. Pihlgren et al. **Resting memory CD8+ T cells are hyperreactive to antigenic challenge in vitro**. *Journal of Experimental Medicine*, 1996.

[298] P. Rogers et al. **Qualitative Changes Accompany Memory T Cell Generation: Faster, More Effective Responses at Lower Doses of Antigen**. *The Journal of Immunology*, 2000.

[299] K. Kimachi et al. **The minimal number of antigen-major histocompatibility complex class II complexes required for activation of naive and primed T cells**. *European journal of immunology*, 1997.

[300] K. Kimachi et al. **Effector T cells have a lower ligand affinity threshold for activation than naive T cells**. *International Immunology*, 2003.

[301] F. Abdul Razak et al. **CD58 mutations are common in Hodgkin lymphoma cell lines and loss of CD58 expression in tumor cells occurs in Hodgkin lymphoma patients who relapse**. *Genes and Immunity*, 2016.

[302] M. Quastel et al. **The CD58–CD2 axis in cancer immune evasion**. *Nature Reviews Immunology 2022 22:7*, 2022.

[303] X. Yan et al. **CD58 loss in tumor cells confers functional impairment of CAR-T cells**. *Blood Advances*, 2022.

[304] M. Challa-Malladi et al. **Combined Genetic Inactivation of β2-Microglobulin and CD58 Reveals Frequent Escape from Immune Recognition in Diffuse Large B Cell Lymphoma**. *Cancer Cell*, 2011.

[305] M. L. Dustin. **Supported bilayers at the vanguard of immune cell activation studies**. *Journal of structural biology*, 2009.

[306] S. Minguet et al. **Harnessing CD3 diversity to optimise CAR T cells**. *Nature Immunology*, 2023.

[307] V. Gudipati et al. **Inefficient CAR-proximal signaling blunts antigen sensitivity**. *Nature Immunology*, 2020.

[308] B. Manz et al. **T-cell triggering thresholds are modulated by the number of antigen within individual T-cell receptor clusters**. *PNAS*, 2011.

[309] E. Denham et al. **A generic cell surface ligand system for studying cell–cell recognition**. *PLoS Biology*, 2019.

[310] J. Leitner et al. **T cell stimulator cells, an efficient and versatile cellular system to assess the role of costimulatory ligands in the activation of human T cells**. *Journal of Immunological Methods*, 2010.

[311] M. Reithofer et al. **4-1BB costimulation promotes bystander activation of human CD8 T cells**. *European Journal of Immunology*, 2021.

[312] B. Zakeri et al. **Peptide tag forming a rapid covalent bond to a protein, through engineering a bacterial adhesin**. *PNAS*, 2012.

[313] A. Keeble et al. **Approaching infinite affinity through engineering of peptide-protein interaction**. *PNAS*, 2019.

[314] I. Urbančič et al. **Aggregation and mobility of membrane proteins interplay with local lipid order in the plasma membrane of T cells**. *FEBS Letters*, 2021.

[315] M. Tamkun et al. **A cytoskeletal-based perimeter fence selectively corrals a sub-population of cell surface Kv2.1 channels**. *Journal of Cell Science*, 2007.

[316] Y. Sako et al. **Barriers for lateral diffusion of transferrin receptor in the plasma membrane as characterized by receptor dragging by laser tweezers: Fence versus tether**. *Journal of Cell Biology*, 1995.

[317] J. Chojnacki et al. **Envelope glycoprotein mobility on HIV-1 particles depends on the virus maturation state**. *Nature Communications*, 2017.

[318] C. Nakada et al. **Accumulation of anchored proteins forms membrane diffusion barriers during neuronal polarization**. *Nature Cell Biology*, 2003.

[319] J. Gaglia et al. **Characterization of endogenous Chinese hamster ovary cell surface molecules that mediate T cell costimulation**. *Cellular Immunology*, 2001.

[320] J. Pettmann et al. **The discriminatory power of the t cell receptor**. *eLife*, 2021.

[321] R. Majzner et al. **Tumor antigen escape from CAR-T cell therapy**. *Cancer Discovery*, 2018.

[322] D. Harris et al. **Comparison of T Cell Activities Mediated by Human TCRs and CARs That Use the Same Recognition Domains**. *The Journal of Immunology*, 2018.

[323] C. Turtle et al. **CD19 CAR-T cells of defined CD4+:CD8+ composition in adult B cell ALL patients**. *Journal of Clinical Investigation*, 2016.

[324] P. Chan et al. **Influence of receptor lateral mobility on adhesion strengthening between membranes containing LFA-3 and CD2**. *Journal of Cell Biology*, 1991.

[325] S. Ikemizu et al. **Structure and dimerization of a soluble form of B7-1**. *Immunity*, 2000.

[326] A. Collins et al. **The Interaction Properties of Costimulatory Molecules Revisited**. *Immunity*, 2002.

[327] S. Bhatia et al. **Dynamic Equilibrium of B7-1 Dimers and Monomers Differentially Affects Immunological Synapse Formation and T Cell Activation in Response to TCR/CD28 Stimulation**. *The Journal of Immunology*, 2010.

[328] C. Stamper et al. **Crystal structure of the B7-1/CTLA-4 complex that inhibits human immune responses**. *Nature*, 2001.

[329] L. Balagopalan et al. **Microclusters as T Cell Signaling Hubs: Structure, Kinetics, and Regulation**. *Frontiers in Cell and Developmental Biology*, 2021.

[330] R. Majzner et al. **Tuning the Antigen Density Requirement for CAR T Cell Activity**. *Cancer discovery*, 2020.

[331] R. Oren et al. **Functional Comparison of Engineered T Cells Carrying a Native TCR versus TCR-like Antibody–Based Chimeric Antigen Receptors Indicates Affinity/Avidity Thresholds**. *The Journal of Immunology*, 2014.

[332] A. Salter et al. **Comparative analysis of TCR and CAR signaling informs CAR designs with superior antigen sensitivity and in vivo function**. *Science Signaling*, 2021.

[333] V. Appay et al. **Phenotype and function of human T lymphocyte subsets: Consensus and issues**. *Cytometry Part A*, 2008.

[334] V. Appay et al. **Memory CD8+ T cells vary in differentiation phenotype in different persistent virus infections**. *Nature Medicine*, 2002.

[335] A. Salter et al. **Phosphoproteomic analysis of chimeric antigen receptor signaling reveals kinetic and quantitative differences that affect cell function**. *Science Signaling*, 2018.

[336] M. Hudecek et al. **The non-signaling extracellular spacer domain of chimeric antigen receptors is decisive for in vivo antitumor activity**. *Cancer immunology research*, 2015.

[337] J. Whitmire et al. **Costimulation in antiviral immunity: Differential requirements for CD4+ and CD8+ T cell responses**. *Current Opinion in Immunology*, 2000.

[338] D. Glinos et al. **Genomic profiling of T-cell activation suggests increased sensitivity of memory T cells to CD28 costimulation**. *Genes and Immunity*, 2020.

[339] T. Girard et al. **A conserved polylysine motif in CD86 cytoplasmic tail is necessary for cytoskeletal association and effective co-stimulation**. *Biochemical and Biophysical Research Communications*, 2012.

[340] M. Chmielewski et al. **CD28 cosignalling does not affect the activation threshold in a chimeric antigen receptor-redirected T-cell attack**. *Gene Therapy*, 2011.

[341] B. Cho et al. **Functional differences between memory and naive CD8 T cells**. *PNAS*, 1999.

[342] M. Croft et al. **Naive versus memory CD4 T cell response to antigen. Memory cells are less dependent on accessory cell costimulation and can respond to many antigen-presenting cell types including resting B cells.** *The Journal of Immunology*, 1994.

[343] M. Luqman et al. **Activation requirements for CD4+ T cells differing in CD45R expression.** *The Journal of Immunology*, 1992.

[344] C. Dubey et al. **Costimulatory requirements of naive CD4+ T cells. ICAM-1 or B7-1 can costimulate naive CD4 T cell activation but both are required for optimum response.** *The Journal of Immunology*, 1995.

[345] H. Zhang et al. **Engineering better chimeric antigen receptor T cells**. *Experimental Hematology and Oncology*, 2020.

[346] D. Sommermeyer et al. **Chimeric antigen receptor-modified T cells derived from defined CD8+ and CD4+ subsets confer superior antitumor reactivity in vivo**. *Leukemia*, 2016.

[347] M. Lever et al. **Phenotypic models of T cell activation**. *Nature Reviews Immunology*, 2014.

[348] A. Achour et al. **Murine class I major histocompatibility complex H-2D(d): Expression, refolding and crystallization**. *Acta Crystallographica Section D: Biological Crystallography*, 1999.

[349] M. Parrott et al. **Metabolic biotinylation of secreted and cell surface proteins from mammalian cells**. *Biochemical and Biophysical Research Communications*, 2001.

[350] Z. Petrášek et al. **Precise measurement of diffusion coefficients using scanning fluorescence correlation spectroscopy**. *Biophysical Journal*, 2008.

[351] D. Waithe et al. **Optimized processing and analysis of conventional confocal microscopy generated scanning FCS data**. *Methods*, 2018.